INSTITUTO DE INVESTIGACIONES QUÍMICAS

Tesis Doctoral

Synthesis, reactivity and catalytic applications of Ir and Ru complexes based on lutidine-derived pincer ligands

Práxedes Sánchez Mellado

Sevilla, 2019

Synthesis, reactivity and catalytic applications of Ir and Ru complexes based on lutidine-derived pincer ligands

por

Práxedes Sánchez Mellado

Memoria presentada para optar al
Título de Doctor en Química

Fdo. Práxedes Sánchez Mellado

Directores

Andrés Suárez Escobar
Científico Titular del CSIC

Nuria Rendón Márquez
Profesora Titular de la
Universidad de Sevilla

A mis padres Victoria y Práxedes.

Y a mis abuelos Juanita y Luis, Carmen y Juan José.

Consideraciones generales

Los resultados presentados en esta Tesis Doctoral se enmarcan en una de las líneas de investigación del grupo *Organometallic Synthesis and Catalytic Applications* (*OSACA*) del Instituto de Investigaciones Químicas (CSIC - Universidad Sevilla), que tiene entre sus objetivos el estudio de nuevos sistemas metal-ligando y su aplicación en Catálisis Homogénea.

La presente Tesis Doctoral está estructurada en dos capítulos. En el Capítulo I se describe la síntesis y el estudio de la reactividad de complejos de paladio e iridio que incorporan ligandos pincer derivados de la lutidina de tipo CNP (C = carbeno *N*-heterocíclico, P = fosfina), así como diversas aplicaciones de éstos como catalizadores en reacciones de reducción. Este capítulo se encuentra dividido, a su vez, en dos secciones. En la primera de ellas, se describe la reactividad de los complejos de paladio e iridio basados en ligandos CNP^{Ph} que contienen sustituyentes fenilo en el grupo fosfino, y que han sido empleados como catalizadores en reacciones de hidrogenación de cetonas y de hidroboración de CO_2. En la segunda sección, se recogen los resultados obtenidos en el estudio de complejos de Ir que incorporan ligandos CNP^{tBu} que presentan en el grupo fosfino un sustituyente alquílico (*terc*-butilo), así como su aplicación en la hidrogenación quimioselectiva de aldehídos.

Finalmente, el Capítulo II está dedicado a la síntesis de complejos de rutenio basados en ligandos derivados de la lutidina de tipo pincer CNN(H) (N(H) = amina secundaria), el estudio de su reactividad ácido-base y frente al H_2, así como su aplicación como catalizadores en procesos de hidrogenación y deshidrogenación de *N*-heterociclos.

Con la finalidad de optar a la Mención Internacional en el título de Doctor (RD 99/2011; artículo 15), la presente Tesis Doctoral, con excepción de estas Consideraciones Generales, se ha redactado en inglés. Además, y como requisito imprescindible para dicha Mención, se realizó en el año 2017 una estancia de tres meses en el grupo de investigación del Prof. Karl Kirchner de la Universidad Técnica de Viena (TU Wien, Austria), financiada en el marco de la red europea COST "C-H Activation in Organic Synthesis". Durante dicha estancia, y gracias a la experiencia del grupo receptor, se exploró la coordinación de algunos de los ligandos preparados en el marco de esta Tesis Doctoral a metales de la primera serie de transición, y en particular a hierro y manganeso. Los resultados obtenidos en estas investigaciones no han sido incluidos en la presente memoria.

La resolución estructural de los compuestos presentados en esta memoria mediante difracción de rayos X de monocristal ha sido llevada a cabo por el Dr. Eleuterio Álvarez (Instituto de Investigaciones Químicas), de manera independiente a esta Tesis Doctoral. De manera similar, los cálculos DFT han sido realizados en nuestro grupo de investigación en colaboración con el Dr. Joaquín López-Serrano.

Parte de los resultados obtenidos durante la realización de esta Tesis Doctoral han sido publicados en revistas científicas del ámbito de la Química Inorgánica, Organometálica y la Catálisis, mientras que al menos dos artículos más se encuentran en proceso de redacción. Los artículos ya publicados se indican a continuación:

Synthesis, structure and reactivity of Pd and Ir complexes based on new lutidine-derived NHC/phosphine mixed pincer ligands. Práxedes Sánchez, Martín Hernández-Juárez, Eleuterio Álvarez, Margarita Paneque, Nuria Rendón, Andrés Suárez. *Dalton Trans.* **2016**, *45*, 16997. DOI: 10.1039/c6dt03652j

Hydroboration of carbon dioxide with catechol- and pinacolborane using an Ir– CNP pincer complex. Water influence on the catalytic activity*. Práxedes Sánchez, Martín Hernández-Juárez, Eleuterio Álvarez, Margarita Paneque, Nuria Rendón, Andrés Suárez. *Dalton Trans.* **2018**, *47*, 16766. DOI: 10.1039/c8dt03951h

Chapter I. Ir-CNP

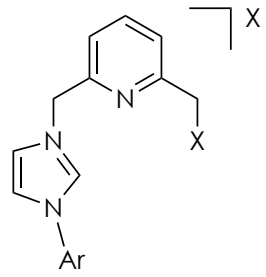

1a(Cl): Ar = Mes, X = Cl
1b(Cl): Ar = 3,5-Xyl, X = Cl
1b(Br): Ar = 3,5-Xyl, X = Br

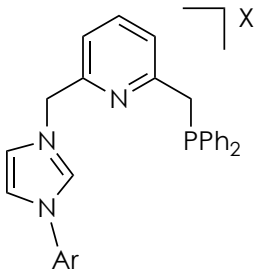

2a(Cl): Ar = Mes, X = Cl
2b(Cl): Ar = 3,5-Xyl, X = Cl
2b(Br): Ar = 3,5-Xyl, X = Br

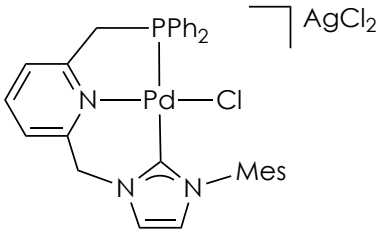

3

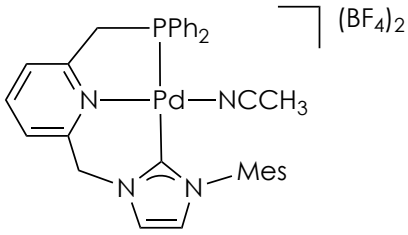

4

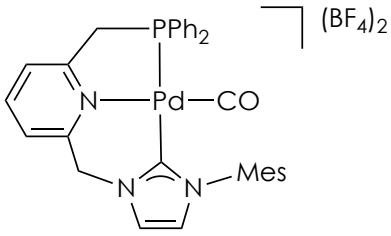

5

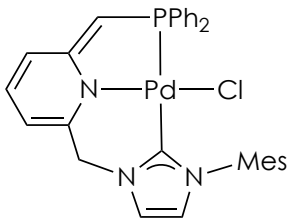

6

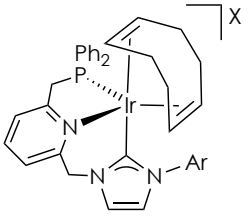

7a(Cl): Ar = Mes, X = Cl
7b(Cl): Ar = 3,5-Xyl, X = Cl
7b(Br): Ar = 3,5-Xyl, X = Br
7b(BAr$_F$): Ar = 3,5-Xyl, X = BAr$_F$

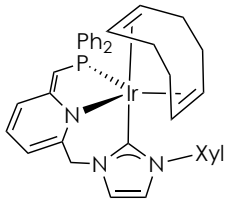

8

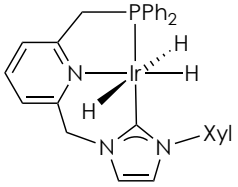

9

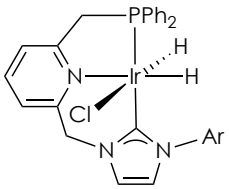

10a: Ar = Mes
10b: Ar = 3,5-Xyl

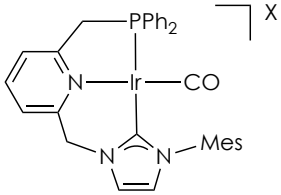

13(Cl): X = Cl
13(Bcat$_2$): X = Bcat$_2$
13(BAr$_F$): X = BAr$_F$

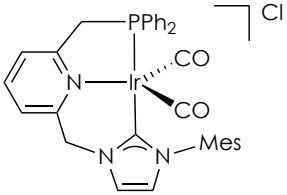

14

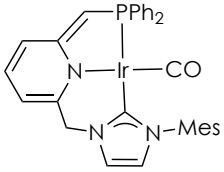

15a

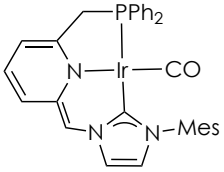

15b

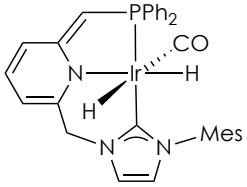

16

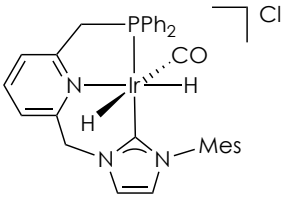

17

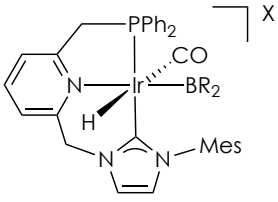

18(Bcat$_2$): R$_2$ = catecholate
19(BAr$_F$): R$_2$ = pinacolate

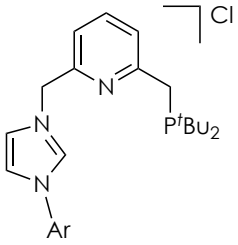

20a: Ar = Mes
20b: Ar = 3,5-Xyl

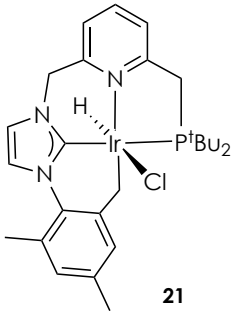

21

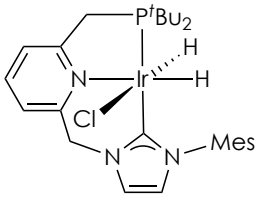

22a

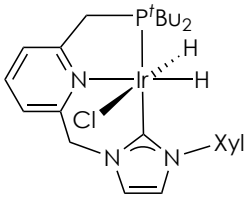

22b

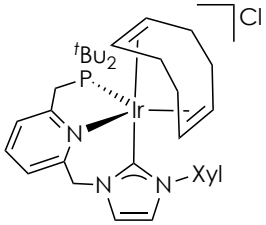

23

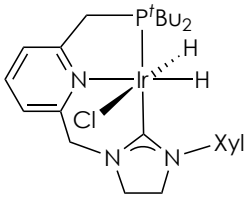

24

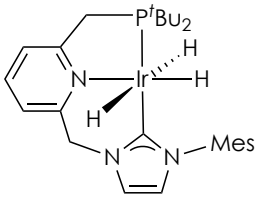

25a

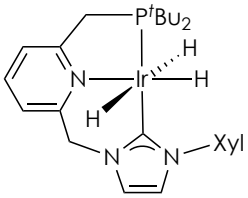

25b

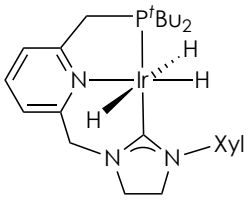

26

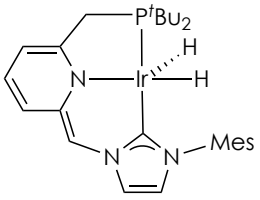

29

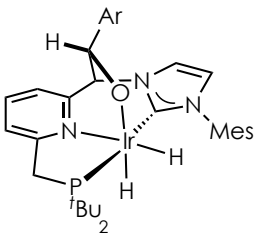

30a^{M}: Ar = Ph
30b^{M}: Ar = *p*-Br-Ph

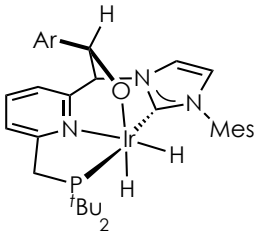

30a^{m}: Ar = Ph
30b^{m}: Ar = *p*-Br-Ph

Chapter II. Ru-CNN(H)

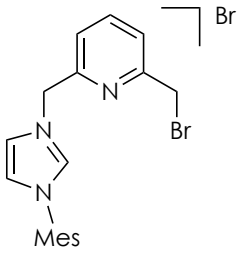

1a(Br)

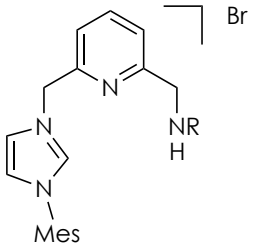

2a: R = ^{t}Bu
2b: R = CH_2Ph
2c: R = Ph

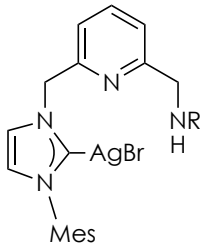

3a: R = ^{t}Bu
3b: R = CH_2Ph
3c: R = Ph

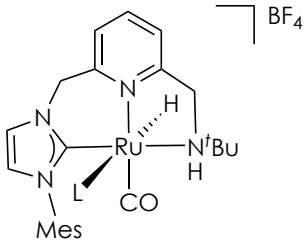

L = PPh_3

4a: R = ^{t}Bu
4b: R = CH_2Ph
4c: R = Ph

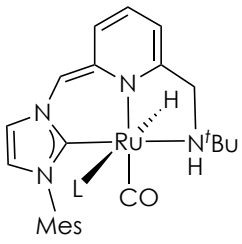

8: L = PPh_3

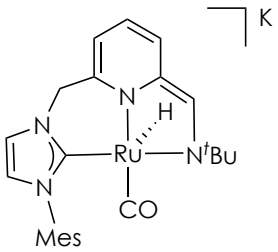

9

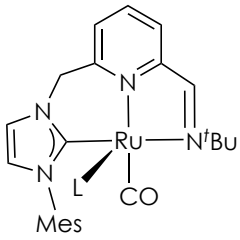

10: L = PPh_3

ABBREVIATIONS

ν	infrared stretching frequency of a bond (cm^{-1})
acac	acetylacetonate
COD	cycloocta-1,5-diene
DFT	Density Functional Theory
ESI	Electrospray Ionization (technique for mass spectrometry)
HRMS	High Resolution Mass Spectrometry
IR	infrared
KHMDS	potassium bis(trimethylsilyl)amide
2-MeTHF	2-methyltetrahydrofuran
MLC	metal-ligand cooperation
Mes	mesityl (2,4,6-$Me_3C_6H_2$)
NHC	*N*-heterocyclic carbene
ORTEP	Oak Ridge Thermal Ellipsoid Program (crystallographic representation)
r.t.	room temperature
S/C	substrate/catalyst ratio
THF	tetrahydrofuran, C_4H_8O
Tol	toluene
Xyl	3,5-xylyl (3,5-$Me_2C_6H_3$)
XNX	lutidine-derived pincer ligand with X donor flanking groups (X = phosphine, amine, NHC)
XNX*	deprotonated lutidine-derived pincer ligand

NMR Abbreviations

δ	chemical shift
COSY	correlation spectroscopy
C_q	quaternary carbon
EXSY	Exchange Spectroscopy
HSQC	^{1}H-^{13}C correlation spectroscopy (Heteronuclear Single Quantum Coherence)
HMBC	^{1}H-^{13}C correlation spectroscopy (Heteronuclear Multiple Bond Correlation)
NMR	Nuclear Magnetic Resonance
NOESY	nuclear Overhauser enhancement spectroscopy
ppm	parts per million
T_1	relaxation time
s	singlet
d	doublet
t	triplet
q	quartet
m	multiplet
br	broad
$^{n}J_{AB}$	coupling constant (Hz) between A and B nuclei separated by n bonds

General Introduction

Transition metal catalysis has been largely associated to metal-centered processes, such as oxidative addition, reductive elimination and insertion of unsaturated molecules, in which the ancillary ligands plays merely a spectator role modifying the steric and electronic properties of the metal to improve its reactivity.[1]

At variance with most transition metal catalysts, metalloenzymes possess functional groups as part of the first and second coordination spheres around the metal center that participate in the recognition and activation of substrates and in the stabilization of reaction intermediates, providing an efficient acceleration of the biological transformations.[2] For example, the [FeFe]-hydrogenase active site contains a secondary amino function that directly participates in the heterolytic splitting of the H_2 molecule coordinated to the Fe(II) center by accepting a proton (H^+) (Figure 1). The overall process takes place without an overall change of the metal oxidation states.

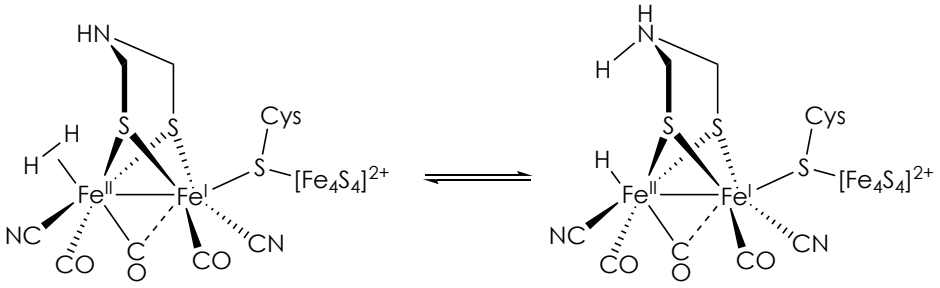

Figure 1. H_2 heterolysis by the [FeFe]-hydrogenase.

Inspired by Nature, metal complexes incorporating ligands containing Brønsted acidic/basic sites, which facilitate substrate binding and activation

[1] (a) P. W. N. M. van Leeuwen, *Homogeneous Catalysis: Understanding the Art*, Kluwer Academic, **2004**; (b) J. Hartwig, *Organotransition Metal Chemistry*, University Science Book, **2010**.
[2] M. D. Wodrich, X. Hu, *Nat. Rev. Chem.* **2017**, *2*, 0099; (b) D. Schilter, J. M. Camara, M. T. Huynh, S. Hammes-Schiffer, T. B. Rauchfuss, *Chem. Rev.* **2016**, *116*, 8693; (c) W. Lubitz, H. Ogata, O. Rüdiger, E. Reijerse, *Chem. Rev.* **2014**, *114*, 4081.

as in metalloenzymes, have also been explored, and their use has become a fundamental approach to the development of improved catalytic systems and novel reactions.[3] In these artificial catalysts, the ligand cooperates with the metal in the activation of a substrate, usually undergoing a reversible chemical transformation.

A prevailing metal-ligand cooperation (MLC) mode is based on the reversible metal-amine/metal-amide interconversion (Figure 2).[4] This approach was pioneered by the group of Noyori allowing for the development of hydrogenation, transfer hydrogenation and dehydrogenation catalysts that furnish unrivaled levels of catalytic activity and selectivity.[5] For example, $RuCl_2$(P-P)(N-N) complexes (P-P = chiral diphosphine, N-N = chiral primary diamine), in the presence of a base, catalyzes the hydrogenation of ketones with enantioselectivities of up to 99% *ee* using low catalyst loadings under mild reaction conditions (8 bar H_2, 28 ^oC, S/C up to 10^5).[6] The commonly accepted catalytic species is a dihydride complex, RuH_2(P-P)(N-N), generated by reaction of $RuCl_2$(P-P)(N-N) with H_2 and base (Figure 3).[7] This species transfers a hydride bound to Ru and a proton of the

[3] (a) H. Grützmacher, *Angew. Chem. Int. Ed.* **2008**, *47*, 1814; (b) J. R. Khusnutdinova, D. Milstein, *Angew. Chem. Int. Ed.* **2015**, *54*, 12236; (c) B. Askevold, H. W. Roesky, S. Schneider, *ChemCatChem* **2012**, *4*, 307.

[4] P. A. Dub, J. C. Gordon, *Nat. Rev. Chem.* **2018**, *2*, 396.

[5] B. Zhao, Z. Han, K. Ding, *Angew. Chem. Int. Ed.* **2013**, *52*, 4744.

[6] (a) T. Ohkuma, C. A. Sandoval, R. Srinivasan, Q. Lin, Y. Wei, K. Muñiz, R. Noyori, *J. Am. Chem. Soc.* **2005**, 8288; (b) T. Ohkuma, H. Ooka, T. Ikariya, R. Noyori, *J. Am. Chem. Soc.* **1995**, 10417; (c) T. Ohkuma, H. Doucet, T. Pham, K. Mikami, T. Korenaga, M. Terada, R. Noyori, *J. Am. Chem. Soc.* **1998**, 1086; (d) H. Doucet, T. Ohkuma, K. Murata, T. Yokozawa, M. Kozawa, E. Katayama, A. F. England, T. Ikariya, R. Noyori, *Angew. Chem. Int. Ed.* **1998**, 1703; (e) N. Arai, K. Suzuki, S. Sugizaki, H. Sorimachi, T. Ohkuma, *Angew. Chem. Int. Ed.* **2008**, *47*, 1770.

[7] (a) S. E. Clapham, A. Hadzovic, R. H. Morris, *Coord. Chem. Rev.* **2004**, *248*, 2201; (b) C. A. Sandoval, T. Ohkuma, K. Muñiz, R. Noyori, *J. Am. Chem. Soc.* **2003**, *125*, 13490; (c) K. Abdur-Rashid, S. E. Clapham, A. Hadzovic, J. N. Harvey, A. J. Lough, R. H. Morris, *J. Am. Chem. Soc.* **2002**, 15104; (d) R. Noyori, M. Yamakawa, S. Hashiguchi, *J. Org. Chem.* **2001**, 7931.

diamine ligand to the ketone through an outer-sphere mechanism.[8,9] Subsequent heterolytic splitting of H_2 assisted by the amido ligand leads to the initial dihydride Ru complex.

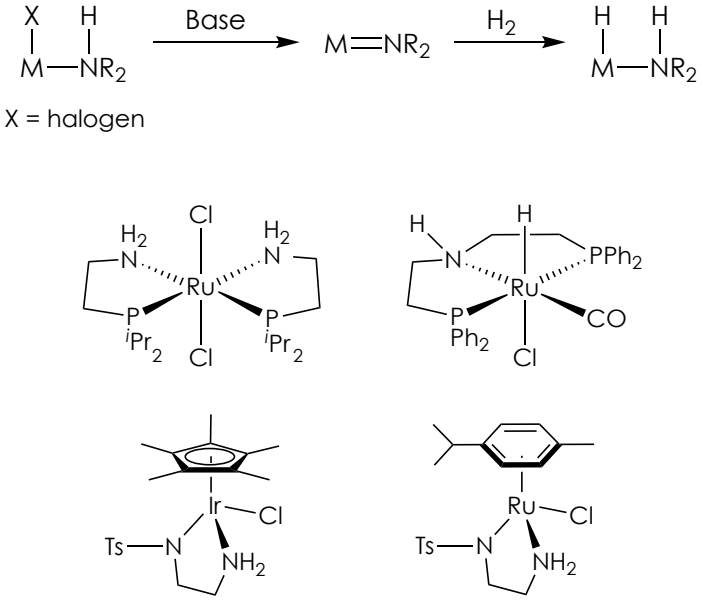

Figure 2. Metal-ligand cooperation based on metal-amine/metal-amide interconversion, and examples of catalysts based on this MLC mode.

[8] O. Eisenstein, R. H. Crabtree, *New J. Chem.* **2013**, *37*, 21.
[9] Proton-transfer from the amine ligand to the ketone has been recently questioned: ref. 4.

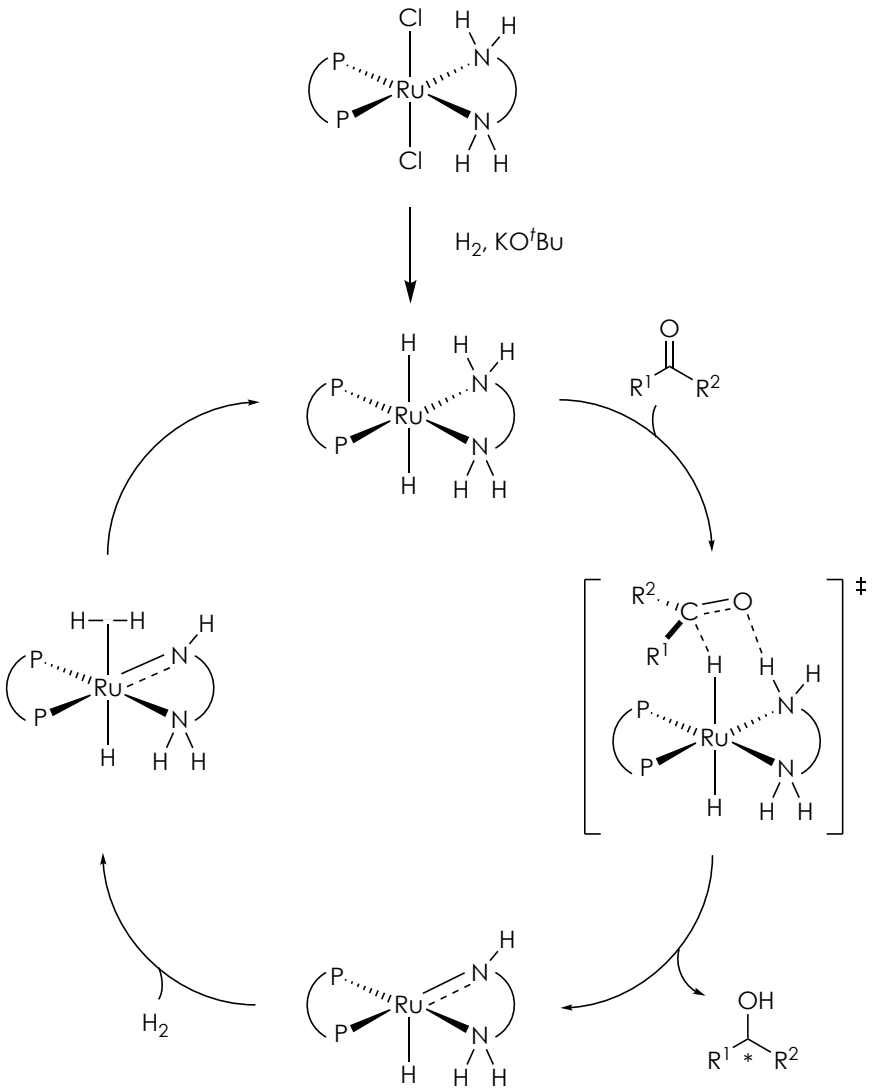

Figure 3. Commonly accepted mechanism of ketone hydrogenation catalyzed by $RuCl_2$(P-P)(N-N) complexes.

In addition to metal complexes featuring primary or secondary amine donors, metal-ligand systems based on other cooperation modes have also been developed.[10] One of such systems implies the

[10] (a) D. Gelman, S. Musa, *ACS Catal.* **2012**, *2*, 245; (b) S. Kuwata, T. Ikariya, *Chem. Commun.* **2014**, 14290; (c) C. Camp, J. Arnold, *Dalton Trans.* **2016**, *45*, 14462; (d) X. Tan, W. Zeng, X.

deprotonation/dearomatization of a lutidine-derived pincer ligand.[11] Particularly, metal complexes based on tridentate lutidine-derived PNP (with two phosphine donors as sidearms) and PNN (having a hemilabile *N*-donor flanking group) ligands have been extensively studied by the group of Milstein (Figure 4).[12] The methylene bridges of these derivatives are prone to deprotonation upon reaction with base, leading to the dearomatization of the pyridine moiety and the formation of an exocyclic double bond. The species thus formed are able to participate in the activation of a diversity of H-X (X = H,[13] C,[14,13a-b] O,[13d] N,[15] B,[16] S[17]) bonds with the concomitant rearomatization of the *N*-heterocyclic ring (Figure 5). Interestingly, in the context of this PhD Thesis, it is worth mentioning that H_2 activation by deprotonated lutidine-derived metal complexes has led to hydride complexes

---

Zhang, L. W. Chung, X. Zhang, *Chem. Commun.* **2018**, *54*, 535; (e) Y. Kashiwame, M. Watanabe, K. Araki, S. Kuwata, T. Ikariya, *Bull. Chem. Soc. Jpn.* **2011**, *84*, 251; (f) B. L. Conley, M. K. Pennington-Boggio, E. Boz, T. J. Williams, *Chem. Rev.* **2010**, *110*, 2294; (g) R. E. Rodríguez-Lugo, M. Trincado, M. Vogt, F. Tewes, G. Santiso-Quinones, H. Grützmacher, *Nat. Chem.* **2013**, *5*, 342.

[11] (a) J. I. van der Vlugt, J. N. H. Reek, *Angew. Chem. Int. Ed.* **2009**, *48*, 8832; (b) D. Milstein, *Phil. Trans. R. Soc. A* **2015**, *373*, 20140189; (c) C. Gunanathan, D. Milstein, *Acc. Chem. Res.* **2011**, *44*, 588.

[12] (a) C. Gunanathan, D. Milstein, *Top. Organomet. Chem.* **2011** *37*, 55; (b) T. Zell, D. Milstein, *Acc. Chem. Res.* **2015**, *48*, 1979; (c) D. Milstein, *Top. Catal.* **2010**, *53*, 915; (d) T. Zell, Y. Ben-David, D. Milstein, *Angew. Chem. Int. Ed.* **2014**, *53*, 4685.

[13] (a) E. Ben-Ari, G. Leitus, L. J. W. Shimon, D. Milstein, *J. Am. Chem. Soc.* **2006**, *128*, 15390; (b) L. Schwartsburd, M. A. Iron, L. Konstantinovski, Y. Diskin-Posner, G. Leitus, L. J. W. Shimon, D. Milstein, *Organometallics* **2010**, *29*, 3817; (c) R. Langer, G. Leitus, Y. Ben-David, D. Milstein, *Angew. Chem. Int. Ed.* **2011**, *50*, 2120; (d) M. Vogt, A. Nerush, Y. Diskin-Posner, Y. Ben-David, D. Milstein, *Chem. Sci.* **2014**, *5*, 2043; (e) J. Zhang, G. Leitus, Y. Ben-David, D. Milstein, *J. Am. Chem. Soc.* **2005**, *127*, 10840

[14] (a) A. Kumar, M. Feller, Y. Ben-David, Y. Diskin-Posner, D. Milstein, *Chem. Commun.* **2018**, *54*, 5365; (b) M. A. Iron, E. Ben-Ari, R. Cohena, D. Milstein, *Dalton Trans.*, **2009**, 9433.

[15] (a) E. Khaskin, M. A. Iron, L. J. W. Shimon, J. Zhang, D. Milstein, *J. Am. Chem. Soc.* **2010**, *132*, 8542; (b) M. Feller, Y. Diskin-Posner, L. J. W. Shimon, E. Ben-Ari, D. Milstein, *Organometallics* **2012**, *31*, 4083.

[16] A. Anaby, B. Butschke, Y. Ben-David, L. J. W. Shimon, G. Leitus, M. Feller, D. Milstein, *Organometallics* **2014**, *33*, 3716.

[17] J. I. van der Vlugt, M. Lutz, E. A. Pidko, D. Vogt, A. L. Spek, *Dalton Trans.* **2009**, 1016.

that have shown high levels of catalytic activity and selectivity in the hydrogenation of polar functionalities such as aldehydes,[18] ketones,[19,13c] esters,[20] amides,[21] ureas,[22] organic carbonates[23,20b] and CO_2.[24] Similarly, metal complexes based on deprotonated lutidine-derived PNP* and PNN* ligands are active catalysts in processes involving alcohol dehydrogenation. [13e, 21c-d,25]

---

[18] T. Zell, Y. Ben-David, D. Milstein, *Catal. Sci. Technol.* **2015**, *5*, 822.

[19] (a) R. Langer, M. A. Iron, L. Konstantinovski, Y. Diskin-Posner, G. Leitus, Y. Ben-David, D. Milstein, *Chem. Eur. J.* **2012**, *18*, 7196; (b) W. Li, J.-H. Xie, H. Lina, Q.-L. Zhou, *Green Chem.* **2012**, *14*, 2388; (c) Y. Yi, H. Liu, L.-P. Xiao, B. Wang, G. Song, *ChemSusChem* **2018**, *11*, 1474

[20] (a) J. Zhang, G. Leitus, Y. Ben-David, D. Milstein, *Angew. Chem. Int. Ed.* **2006**, *45*, 1113; (b) E. M. Krall, T. W. Klein, R. J. Andersen, A. J. Nett, R. W. Glasgow, D. S. Reader, B. C. Dauphinais, S. P. Mc Ilrath, A. A. Fischer, M. J. Carney, D. J. Hudson, N. J. Robertson, *Chem. Commun.* **2014**, *50*, 4884.

[21] (a) E. Balaraman, B. Gnanaprakasam, L. J. W. Shimon, D. Milstein, *J. Am. Chem. Soc.* **2010**, *132*, 16756; (b) J. Anand Garg, S. Chakraborty, Y. Ben-David, D. Milstein, *Chem. Commun.* **2016**, *52*, 5285; (c) P. Hu, E. Fogler, Y. Diskin-Posner, M. A. Iron, D. Milstein, *Nat. Commun.* **2015**, *6*, 6859; (d) P. Hu, Y. Ben David, D. Milstein, *Angew. Chem. Int. Ed.* **2016**, *55*, 1061.

[22] (a) E. Balaraman, Y. Ben-David, D. Milstein, *Angew. Chem. Int. Ed.* **2011**, *50*, 11702; (b) N. T. Fairweather, M. S. Gibson, H. Guan, *Organometallics* **2015**, *34*, 335.

[23] E. Balaraman, C. Gunanathan, J. Zhang, L. J. W. Shimon, D. Milstein, *Nat. Chem*. **2011**, *3*, 609.

[24] (a) R. Tanaka, M. Yamashita, K. Nozaki, *J. Am. Chem. Soc.* **2009** *131*, 14168; (b) R. Tanaka, M. Yamashita, L. W. Chung, K. Morokuma, K. Nozaki, *Organometallics* **2011**, *30*, 6742; (c) C. A. Huff, M. S. Sanford, *ACS Catal.* **2013**, *3*, 2412; (d) G. A. Filonenko, M. P. Conley, C. Copéret, M. Lutz, E. J. M. Hensen, E. A. Pidko, *ACS Catal.* **2013**, *3*, 2522; (e) G. A. Filonenko, R. van Putten, E. N. Schulpen, E. J. M. Hensen, E. A. Pidko, *ChemCatChem* **2014**, *6*, 1526; (f) R. Langer, Y. Diskin-Posner, G. Leitus, L. J. W. Shimon, Y. Ben David, D. Milstein, *Angew. Chem. Int. Ed.* **2011**, *50*, 9948.

[25] (a) C. Gunanathan, D. Milstein, *Science* **2013**, *341*, 1229712; (b) A. Kumar, N. A. Espinosa-Jalapa, G. Leitus, Y. Diskin-Posner, L. Avram, D. Milstein, *Angew. Chem. Int. Ed.* **2017**, *56*, 14992; (c) C. Gunanathan, L. J. W. Shimon, D. Milstein, *J. Am. Chem. Soc.* **2009**, *131*, 3146; (d) C. Gunanathan, D. Milstein, *Angew. Chem. Int. Ed.* **2008**, *47*, 8661; (e) J. Zhang, M. Gandelman, L. J. W. Shimon, H. Rozenberg, D. Milstein, *Organometallics* **2004**, *23*, 4026; (f) B. Gnanaprakasam, J. Zhang, D. Milstein, *Angew. Chem. Int. Ed.* **2010**, *49*, 1468; (g) M. Nielsen, A. Kammer, D. Cozzula, H. Junge, S. Gladiali, M. Beller, *Angew. Chem. Int. Ed.* **2011**, *50*, 9593; (h) B. Gnanaprakasam, E. Balaraman, Y. Ben-David, D. Milstein, *Angew. Chem. Int. Ed.* **2011**, *50*, 12240; (i) M. Nielsen, H. Junge, A. Kammer, M. Beller, *Angew. Chem. Int. Ed.* **2012**, *51*, 5711; (j) A. Mukherjee, A Nerush, G. Leitus, L. J. W. Shimon, Y. Ben David, N. A. Espinosa-Jalapa, D. Milstein, *J. Am. Chem. Soc.* **2016**, *138*, 4298; (k) J. O. Bauer, G. Leitus, Y. Ben-David, D. Milstein, *ACS Catal.* **2016**, *6*, 8415; (l) C. Gunanathan, Y. Ben-

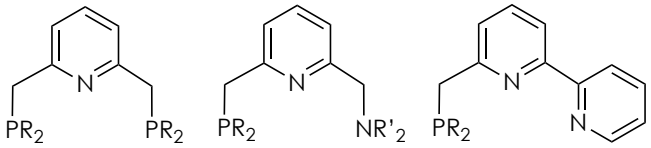

Figure 4. Relevant examples of lutidine-derived pincer ligands.

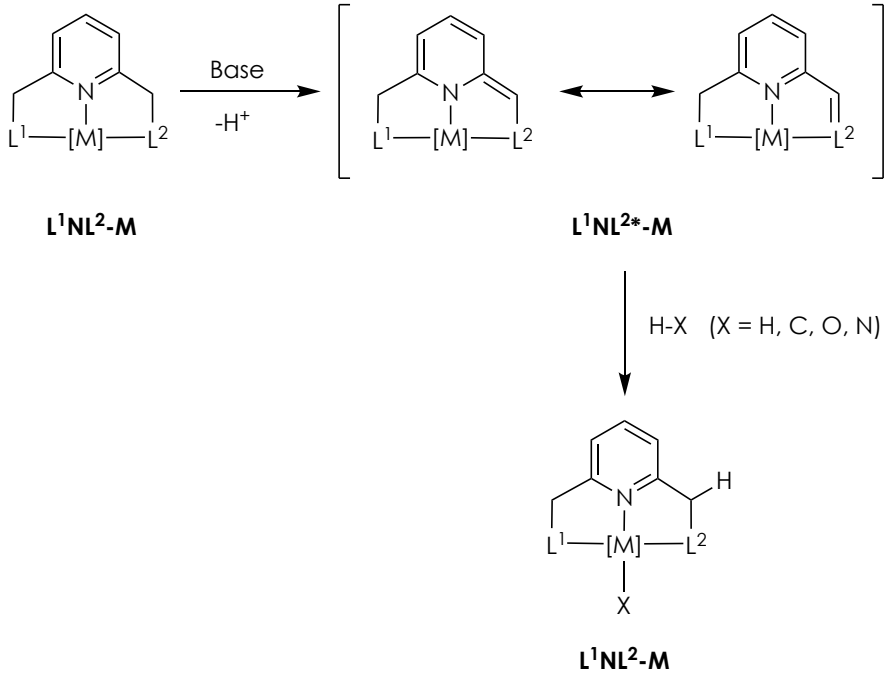

Figure 5. Ligand-assisted activation of H-X bonds by lutidine-derived complexes.

David, D. Milstein, *Science* **2007**, *317*, 790; (m) H. Zeng, Z. Guan, *J. Am. Chem. Soc.* **2011**, *133*, 1159; (n) B. Gnanaprakasam, D. Milstein, *J. Am. Chem. Soc.* **2011**, *133*, 1682; (o) D. Srimani, E. Balaraman, B. Gnanaprakasam, Y. Ben-David, D. Milstein, *Adv. Synth. Catal.* **2012**, *354*, 2403; (p) P. Hu, Y. Diskin-Posner, Y. Ben-David, D. Milstein, *ACS Catal.* **2014**, *4*, 2649; (q) E. Balaraman, E. Khaskin, G. Leitus, D. Milstein, *Nat. Chem.* **2013**, *5*, 122; (r) D. Srimani, Y. Ben-David, D. Milstein, *Angew. Chem. Int. Ed.* **2013**, *52*, 4012; (s) D. Srimani, Y. Ben-David, D. Milstein, *Chem. Commun.* **2013**, *49*, 6632; (t) P. Daw, S. Chakraborty, J. Anand Garg, Y. Ben-David, D. Milstein, *Angew. Chem. Int. Ed.* **2016**, *55*, 14373; (u) U. K. Das, Y. Ben-David, Y. Diskin-Posner, D. Milstein, *Angew. Chem. Int. Ed.* **2018**, *57*, 2179; (v) U. K. Das, Y. Ben-David, G. Leitus, Y. Diskin-Posner, D. Milstein, *ACS Catal.* **2019**, *9*, 479.

Furthermore, due to the presence of acidic (metal) and basic (deprotonated ligand) sites, the dearomatized metal complexes have been shown to exhibit frustrated Lewis pair (FLP) reactivity towards unsaturated molecules such as CO_2, [13d,21c,21d,24c,26] carbonyl compounds,[27] and nitriles[28] (Figure 6).

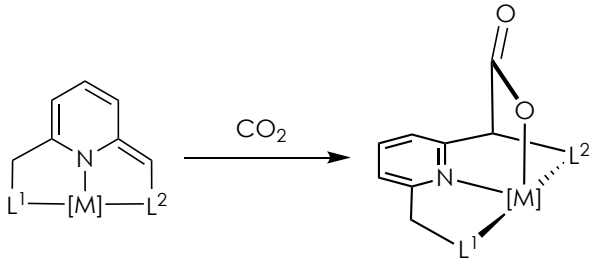

Figure 6. Example of the reactivity of deprotonated lutidine-derived metal complexes as frustrated Lewis pair with CO_2.

N-Heterocyclic carbenes (NHC) are strong σ-donors,[29] and substitution of phosphines by these ligands has resulted in superior catalysts for a number of catalytic reactions.[30] Therefore, an appealing modification of

---

[26] (a) M. Vogt, M. Gargir, M. A. Iron, Y. Diskin-Posner, Y. Ben-David, D. Milstein, *Chem. Eur. J.* **2012**, *18*, 9194; (b) A. Huff, J. W. Kampf, M. S. Sanford, *Organometallics* **2012**, *31*, 4643.

[27] (a) M. Montag, J. Zhang, D. Milstein, *J. Am. Chem. Soc.* **2012**, *134*, 10325; (b) C. A. Huff, J. W. Kampf, M. S. Sanford, *Chem. Commun.* **2013**, *49*, 7147.

[28] (a) M. Vogt, A. Nerush, M. A. Iron, G. Leitus, Y. Diskin-Posner, L. J. W. Shimon, Y. Ben-David, D. Milstein, *J. Am. Chem. Soc.* **2013**, *135*, 17004; (b) A. Nerush, M. Vogt, U. Gellrich, G. Leitus, Y. Ben-David, D. Milstein, *J. Am. Chem. Soc.* **2016**, *138*, 6985; (c) S. Perdriau, D. S. Zijlstra, H. J. Heeres, J. G. de Vries, E. Otten, *Angew. Chem. Int. Ed.* **2015**, *54*, 4236; (d) L. E. Eijsink, S. C. P. Perdriau, J. G. de Vries, E. Otten, *Dalton Trans.* **2016**, *45*, 16033.

[29] (a) *N-Heterocyclic Carbenes in Synthesis*; S. P. Nolan (Ed), Wiley-VCH, **2006**; (b) M. N. Hopkinson, C. Richter, M. Schedler, F. Glorius, *Nature* **2014**, *510*, 485; (c) S. P. Nolan, H. Clavier, *Chem. Soc. Rev.* **2010**, *39*, 3305.

[30] (a) R. H. Crabtree, *J. Organomet. Chem.* **2005**, *690*, 5451; (b) W. A. Herrmann, *Angew. Chem. Int. Ed.* **2002**, *41*, 1290; (c) G. C. Vougioukalakis, R. H. Grubbs, *Chem. Rev.* **2010**, *110*, 1746; (d) A. T. Normand, K. J. Cavell, *Eur. J. Inorg. Chem.* **2008**, 2781; (e) M.-T. Lee, C.-H. Hu, *Organometallics* **2004**, *23*, 976; (f) H. Díaz-Velazquez, F. Verpoort, *Chem. Soc. Rev.* **2012**, *41*, 7032.

lutidine-derived PNP and PNN pincer ligands resides in the replacement of the P-donors by NHCs since it might offer new opportunities for electronic and steric modification of the metal center, while retaining the Brønsted acid/base properties of the pyridylic moieties.

For example, Ru-CNN complexes containing either an hemilabile amine or pyridine fragment have been reported by the groups of Song[31] and Milstein,[32] respectively (Figure 7). These derivatives are very active catalysts in the hydrogenation of esters, even outperforming their Ru-PNN counterparts. Similarly, Iglesias and Sánchez have employed Ru-CNN complexes in the dehydrogenation of alcohols and in the transfer hydrogenation of ketones.[33]

[31] Y. Sun, C. Koehler, R. Tan, V. T. Annibale, D. Song, *Chem. Commun.* **2011**, *47*, 8349.
[32] (a) E. Fogler, E. Balaraman, Y. Ben-David, G. Leitus, L. J. W. Shimon, D. Milstein, *Organometallics* **2011**, *30*, 3826; (b) E. Balaraman, E. Fogler, D. Milstein, *Chem. Commun.* **2012**, *48*, 1111.
[33] C. del Pozo, M. Iglesias, F. Sánchez, *Organometallics* **2011**, *30*, 2180.

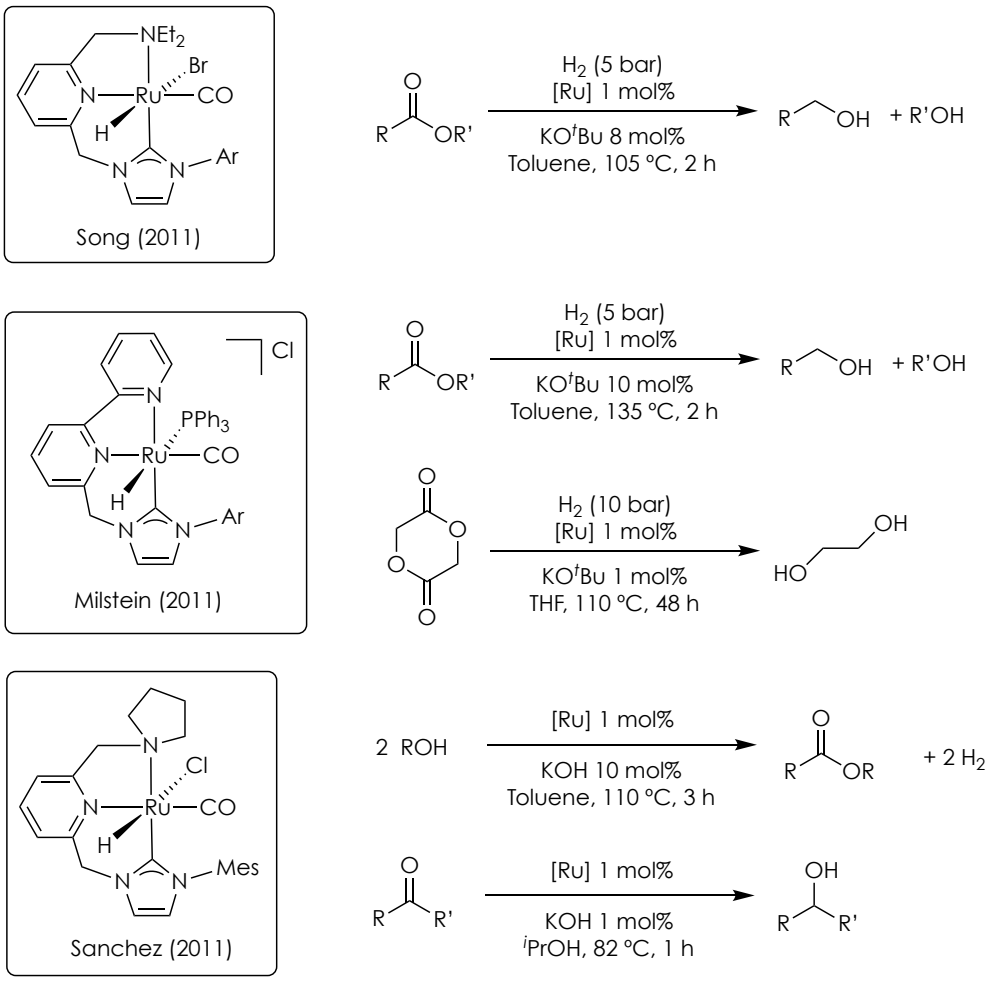

Figure 7. Catalytic applications of lutidine-derived Ru-CNN complexes.

Also of note, ruthenium complexes furnishing lutidine-derived CNC ligands have received a considerable attention in catalysis (Figure 8). While these derivatives exhibit a moderate activity in the dehydrogenation of alcohols[33] and in the hydrogenation of ethylene carbonate,[34] they are active

[34] X. Wu, L. Ji, Y. Ji, E. H. M. Elageed, G. Gao, *Catal. Commun.* **2016**, *85*, 57.

catalysts for ester hydrogenation providing to higher efficiencies than their Ru-PNP counterparts.[35]

Conversely, PNP-derived ruthenium complexes have been shown to be significantly more active in the hydrogenation of CO_2 to formates than the Ru-CNC derivatives.[24d,36] Mechanistic studies indicate that, as a consequence of the six-membered chelating ring, heterolytic H_2 cleavage by the deprotonated Ru-CNC* intermediates, that leads to catalytically active dihydride Ru-CNC species, takes place with much lower barriers than in the case of Ru-PNP*. However, catalysts deactivation by CO_2 addition to Ru-CNC* is also thermodynamically more favorable and occurs with only a slightly higher free energy barrier than the reaction with H_2.[36]

[35] G. A. Filonenko, E. Cosimi, L. Lefort, M. P. Conley, C. Copéret, M. Lutz, E. J. M. Hensen, E. A. Pidko, *ACS Catal.* **2014**, *4*, 2667.
[36] G. A. Filonenko, D. Smykowski, B. M. Szyja, G. Li, J. Szczygieł, E. J. M. Hensen, E. A. Pidko, *ACS Catal.* **2015**, *5*, 1145.

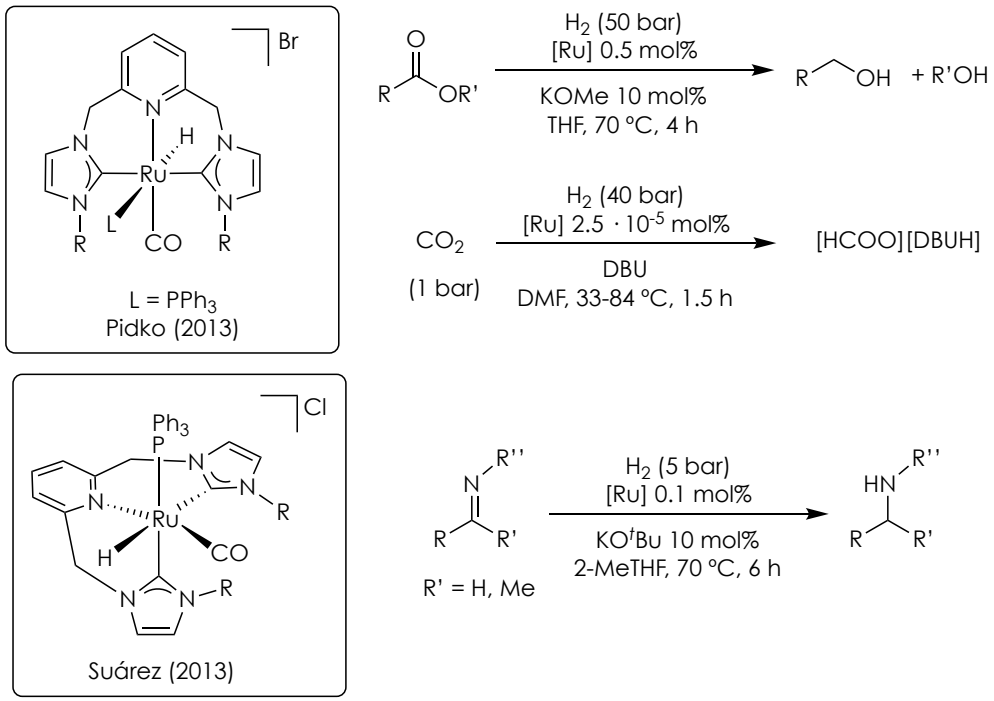

Figure 8. Catalytic applications of lutidine-derived Ru-CNC complexes.

Finally, our group has also previously synthesized Ru-CNC complexes that are active catalysts in the hydrogenation of imines.[37] The CNC ligands in these complexes adopt facial or meridional coordination modes depending on the size of the substituent of the NHC fragment due to the enlarge chelate rings in comparison to those of the PNP ligands.

Aiming to study new ligand architectures that may lead to improved catalytic systems, this PhD Thesis has focused on the synthesis of metal complexes containing lutidine-derived ligands with two non-equivalent donor groups,[38] a NHC and an additional flanking group such as phosphine or amine. Thus, in Chapter I, iridium and palladium complexes incorporating

[37] (a) M. Hernández-Juárez, M. Vaquero, E. Álvarez, V. Salazar, A. Suárez, *Dalton Trans.* **2013**, *42*, 351; (b) M. Hernández-Juárez, J. López-Serrano, P. Lara, J. P. Morales-Cerón, M. Vaquero, E. Álvarez, V. Salazar, A. Suárez, *Chem. Eur. J.* **2015**, *21*, 7540.
[38] M. Asay, D. Morales-Morales, *Dalton Trans.* **2015**, *44*, 17432.

CNP tridentate ligands with NHC and phosphine flanking donors are described. These derivatives have been examined in different reduction reactions including the hydrogenation of aldehydes and ketones, and the hydroboration of CO_2.

In Chapter II, ruthenium complexes incorporating CNN(H) (C = NHC; N(H) = secondary amine) ligands that combine two potential metal-ligand cooperation modes, metal-amine/metal-amido interconversion and lutidine deprotonation, have been prepared and their catalytic performances in the hydrogenation and acceptorless dehydrogenation of *N*-heterocycles explored.

1) (a) P. W. N. M. van Leeuwen, *Homogeneous Catalysis: Understanding the Art*, Kluwer Academic, **2004**; (b) J. Hartwig, *Organotransition Metal Chemistry*, University Science Book, **2010**.

2) M. D. Wodrich, X. Hu, *Nat. Rev. Chem.* **2017**, *2*, 0099; (b) D. Schilter, J. M. Camara, M. T. Huynh, S. Hammes-Schiffer, T. B. Rauchfuss, *Chem. Rev.* **2016**, *116*, 8693; (c) W. Lubitz, H. Ogata, O. Rüdiger, E. Reijerse, *Chem. Rev.* **2014**, *114*, 4081.

3) (a) H. Grützmacher, *Angew. Chem. Int. Ed.* **2008**, *47*, 1814; (b) J. R. Khusnutdinova, D. Milstein, *Angew. Chem. Int. Ed.* **2015**, *54*, 12236; (c) B. Askevold, H. W. Roesky, S. Schneider, *ChemCatChem* **2012**, *4*, 307.

4) P. A. Dub, J. C. Gordon, *Nat. Rev. Chem.* **2018**, *2*, 396.

5) B. Zhao, Z. Han, K. Ding, *Angew. Chem. Int. Ed.* **2013**, *52*, 4744.

6) (a) T. Ohkuma, C. A. Sandoval, R. Srinivasan, Q. Lin, Y. Wei, K. Muñiz, R. Noyori, *J. Am. Chem. Soc.* **2005**, 8288; (b) T. Ohkuma, H. Ooka, T. Ikariya, R. Noyori, *J. Am. Chem. Soc.* **1995**, 10417; (c) T. Ohkuma, H. Doucet, T. Pham, K. Mikami, T. Korenaga, M. Terada, R. Noyori, *J. Am. Chem. Soc.* **1998**, 1086; (d) H. Doucet, T. Ohkuma, K. Murata, T. Yokozawa, M. Kozawa, E. Katayama, A. F. England, T. Ikariya, R. Noyori, *Angew. Chem. Int. Ed.* **1998**, 1703; (e) N. Arai, K. Suzuki, S. Sugizaki, H. Sorimachi, T. Ohkuma, *Angew. Chem. Int. Ed.* **2008**, *47*, 1770.

7) (a) S. E. Clapham, A. Hadzovic, R. H. Morris, *Coord. Chem. Rev.* **2004**, *248*, 2201; (b) C. A. Sandoval, T. Ohkuma, K. Muñiz, R. Noyori, *J. Am. Chem. Soc.* **2003**, *125*, 13490; (c) K. Abdur-Rashid, S. E. Clapham, A. Hadzovic, J. N. Harvey, A. J. Lough, R. H. Morris, *J.*

Am. Chem. Soc. **2002**, 15104; (d) R. Noyori, M. Yamakawa, S. Hashiguchi, *J. Org. Chem.* **2001**, 7931.

8) O. Eisenstein, R. H. Crabtree, *New J. Chem.* **2013**, *37*, 21.

9) Proton-transfer from the amine ligand to the ketone has been recently questioned: ref. 4.

10) (a) D. Gelman, S. Musa, *ACS Catal.* **2012**, *2*, 245; (b) S. Kuwata, T. Ikariya, *Chem. Commun.* **2014**, 14290; (c) C. Camp, J. Arnold, *Dalton Trans.* **2016**, *45*, 14462; (d) X. Tan, W. Zeng, X. Zhang, L. W. Chung, X. Zhang, *Chem. Commun.* **2018**, *54*, 535; (e) Y. Kashiwame, M. Watanabe, K. Araki, S. Kuwata, T. Ikariya, *Bull. Chem. Soc. Jpn.* **2011**, *84*, 251; (f) B. L. Conley, M. K. Pennington-Boggio, E. Boz, T. J. Williams, *Chem. Rev.* **2010**, *110*, 2294; (g) R. E. Rodríguez-Lugo, M. Trincado, M. Vogt, F. Tewes, G. Santiso-Quinones, H. Grützmacher, *Nat. Chem.* **2013**, *5*, 342.

11) (a) J. I. van der Vlugt, J. N. H. Reek, *Angew. Chem. Int. Ed.* **2009**, *48*, 8832; (b) D. Milstein, *Phil. Trans. R. Soc. A* **2015**, *373*, 20140189; (c) C. Gunanathan, D. Milstein, *Acc. Chem. Res.* **2011**, *44*, 588.

12) (a) C. Gunanathan, D. Milstein, *Top. Organomet. Chem.* **2011** *37*, 55; (b) T. Zell, D. Milstein, *Acc. Chem. Res.* **2015**, *48*, 1979; (c) D. Milstein, *Top. Catal.* **2010**, *53*, 915; (d) T. Zell, Y. Ben-David, D. Milstein, *Angew. Chem. Int. Ed.* **2014**, *53*, 4685.

13) (a) E. Ben-Ari, G. Leitus, L. J. W. Shimon, D. Milstein, *J. Am. Chem. Soc.* **2006**, *128*, 15390; (b) L. Schwartsburd, M. A. Iron, L. Konstantinovski, Y. Diskin-Posner, G. Leitus, L. J. W. Shimon, D. Milstein, *Organometallics* **2010**, *29*, 3817; (c) R. Langer, G. Leitus, Y. Ben-David, D. Milstein, *Angew. Chem. Int. Ed.* **2011**, *50*, 2120; (d) M. Vogt, A. Nerush, Y. Diskin-Posner, Y. Ben-David, D. Milstein, *Chem.*

Sci. **2014**, *5*, 2043; (e) J. Zhang, G. Leitus, Y. Ben-David, D. Milstein, *J. Am. Chem. Soc.* **2005**, *127*, 10840

14) (a) A. Kumar, M. Feller, Y. Ben-David, Y. Diskin-Posner, D. Milstein, *Chem. Commun.* **2018**, *54*, 5365; (b) M. A. Iron, E. Ben-Ari, R. Cohena, D. Milstein, *Dalton Trans.*, **2009**, 9433.

15) (a) E. Khaskin, M. A. Iron, L. J. W. Shimon, J. Zhang, D. Milstein, *J. Am. Chem. Soc.* **2010**, *132*, 8542; (b) M. Feller, Y. Diskin-Posner, L. J. W. Shimon, E. Ben-Ari, D. Milstein, *Organometallics* **2012**, *31*, 4083.

16) A. Anaby, B. Butschke, Y. Ben-David, L. J. W. Shimon, G. Leitus, M. Feller, D. Milstein, *Organometallics* **2014**, *33*, 3716.

17) J. I. van der Vlugt, M. Lutz, E. A. Pidko, D. Vogt, A. L. Spek, *Dalton Trans.* **2009**, 1016.

18) T. Zell, Y. Ben-David, D. Milstein, *Catal. Sci. Technol.* **2015**, *5*, 822.

19) (a) R. Langer, M. A. Iron, L. Konstantinovski, Y. Diskin-Posner, G. Leitus, Y. Ben-David, D. Milstein, *Chem. Eur. J.* **2012**, *18*, 7196; (b) W. Li, J.-H. Xie, H. Lina, Q.-L. Zhou, *Green Chem.* **2012**, *14*, 2388; (c) Y. Yi, H. Liu, L.-P. Xiao, B. Wang, G. Song, *ChemSusChem* **2018**, *11*, 1474

20) (a) J. Zhang, G. Leitus, Y. Ben-David, D. Milstein, *Angew. Chem. Int. Ed.* **2006**, *45*, 1113; (b) E. M. Krall, T. W. Klein, R. J. Andersen, A. J. Nett, R. W. Glasgow, D. S. Reader, B. C. Dauphinais, S. P. Mc Ilrath, A. A. Fischer, M. J. Carney, D. J. Hudson, N. J. Robertson, *Chem. Commun.* **2014**, *50*, 4884.

21) (a) E. Balaraman, B. Gnanaprakasam, L. J. W. Shimon, D. Milstein, *J. Am. Chem. Soc.* **2010**, *132*, 16756; (b) J. Anand Garg, S. Chakraborty, Y. Ben-David, D. Milstein, *Chem. Commun.* **2016**, *52*, 5285; (c) P. Hu, E. Fogler, Y. Diskin-Posner, M. A. Iron, D. Milstein,

Nat. Commun. **2015**, *6*, 6859; (d) P. Hu, Y. Ben David, D. Milstein, *Angew. Chem. Int. Ed.* **2016**, *55*, 1061.

22) (a) E. Balaraman, Y. Ben-David, D. Milstein, *Angew. Chem. Int. Ed.* **2011**, *50*, 11702; (b) N. T. Fairweather, M. S. Gibson, H. Guan, *Organometallics* **2015**, *34*, 335.

23) E. Balaraman, C. Gunanathan, J. Zhang, L. J. W. Shimon, D. Milstein, *Nat. Chem*. **2011**, *3*, 609.

24) (a) R. Tanaka, M. Yamashita, K. Nozaki, *J. Am. Chem. Soc.* **2009** *131*, 14168; (b) R. Tanaka, M. Yamashita, L. W. Chung, K. Morokuma, K. Nozaki, *Organometallics* **2011**, *30*, 6742; (c) C. A. Huff, M. S. Sanford, *ACS Catal.* **2013**, *3*, 2412; (d) G. A. Filonenko, M. P. Conley, C. Copéret, M. Lutz, E. J. M. Hensen, E. A. Pidko, *ACS Catal.* **2013**, *3*, 2522; (e) G. A. Filonenko, R. van Putten, E. N. Schulpen, E. J. M. Hensen, E. A. Pidko, *ChemCatChem* **2014**, *6*, 1526; (f) R. Langer, Y. Diskin-Posner, G. Leitus, L. J. W. Shimon, Y. Ben-David, D. Milstein, *Angew. Chem. Int. Ed.* **2011**, *50*, 9948.

25) (a) C. Gunanathan, D. Milstein, *Science* **2013**, *341*, 1229712; (b) A. Kumar, N. A. Espinosa-Jalapa, G. Leitus, Y. Diskin-Posner, L. Avram, D. Milstein, *Angew. Chem. Int. Ed.* **2017**, *56*, 14992; (c) C. Gunanathan, L. J. W. Shimon, D. Milstein, *J. Am. Chem. Soc.* **2009**, *131*, 3146; (d) C. Gunanathan, D. Milstein, *Angew. Chem. Int. Ed.* **2008**, *47*, 8661; (e) J. Zhang, M. Gandelman, L. J. W. Shimon, H. Rozenberg, D. Milstein, *Organometallics* **2004**, *23*, 4026; (f) B. Gnanaprakasam, J. Zhang, D. Milstein, *Angew. Chem. Int. Ed.* **2010**, *49*, 1468; (g) M. Nielsen, A. Kammer, D. Cozzula, H. Junge, S. Gladiali, M. Beller, *Angew. Chem. Int. Ed.* **2011**, *50*, 9593; (h) B. Gnanaprakasam, E. Balaraman, Y. Ben-David, D. Milstein, *Angew.*

Chem. Int. Ed. **2011**, *50*, 12240; (i) M. Nielsen, H. Junge, A. Kammer, M. Beller, *Angew. Chem. Int. Ed.* **2012**, *51*, 5711; (j) A. Mukherjee, A. Nerush, G. Leitus, L. J. W. Shimon, Y. Ben-David, N. A. Espinosa-Jalapa, D. Milstein, *J. Am. Chem. Soc.* **2016**, *138*, 4298; (k) J. O. Bauer, G. Leitus, Y. Ben-David, D. Milstein, *ACS Catal.* **2016**, *6*, 8415; (l) C. Gunanathan, Y. Ben-David, D. Milstein, *Science* **2007**, *317*, 790; (m) H. Zeng, Z. Guan, *J. Am. Chem. Soc.* **2011**, *133*, 1159; (n) B. Gnanaprakasam, D. Milstein, *J. Am. Chem. Soc.* **2011**, *133*, 1682; (o) D. Srimani, E. Balaraman, B. Gnanaprakasam, Y. Ben-David, D. Milstein, *Adv. Synth. Catal.* **2012**, *354*, 2403; (p) P. Hu, Y. Diskin-Posner, Y. Ben-David, D. Milstein, *ACS Catal.* **2014**, *4*, 2649; (q) E. Balaraman, E. Khaskin, G. Leitus, D. Milstein, *Nat. Chem.* **2013**, *5*, 122; (r) D. Srimani, Y. Ben-David, D. Milstein, *Angew. Chem. Int. Ed.* **2013**, *52*, 4012; (s) D. Srimani, Y. Ben-David, D. Milstein, *Chem. Commun.* **2013**, *49*, 6632; (t) P. Daw, S. Chakraborty, J. Anand Garg, Y. Ben-David, D. Milstein, *Angew. Chem. Int. Ed.* **2016**, *55*, 14373; (u) U. K. Das, Y. Ben-David, Y. Diskin-Posner, D. Milstein, *Angew. Chem. Int. Ed.* **2018**, *57*, 2179; (v) U. K. Das, Y. Ben-David, G. Leitus, Y. Diskin-Posner, D. Milstein, *ACS Catal.* **2019**, *9*, 479.

26) (a) M. Vogt, M. Gargir, M. A. Iron, Y. Diskin-Posner, Y. Ben-David, D. Milstein, *Chem. Eur. J.* **2012**, *18*, 9194; (b) C. A. Huff, J. W. Kampf, M. S. Sanford, *Organometallics* **2012**, *31*, 4643.

27) (a) M. Montag, J. Zhang, D. Milstein, *J. Am. Chem. Soc.* **2012**, *134*, 10325; (b) C. A. Huff, J. W. Kampf, M. S. Sanford, *Chem. Commun.* **2013**, *49*, 7147.

28) (a) M. Vogt, A. Nerush, M. A. Iron, G. Leitus, Y. Diskin-Posner, L. J. W. Shimon, Y. Ben-David, D. Milstein, *J. Am. Chem. Soc.* **2013**, *135*,

17004; (b) A. Nerush, M. Vogt, U. Gellrich, G. Leitus, Y. Ben-David, D. Milstein, *J. Am. Chem. Soc.* **2016**, *138*, 6985; (c) S. Perdriau, D. S. Zijlstra, H. J. Heeres, J. G. de Vries, E. Otten, *Angew. Chem. Int. Ed.* **2015**, *54*, 4236; (d) L. E. Eijsink, S. C. P. Perdriau, J. G. de Vries, E. Otten, *Dalton Trans.* **2016**, *45*, 16033.

29) (a) *N-Heterocyclic Carbenes in Synthesis*; S. P. Nolan (Ed), Wiley-VCH, **2006**; (b) M. N. Hopkinson, C. Richter, M. Schedler, F. Glorius, *Nature* **2014**, *510*, 485; (c) S. P. Nolan, H. Clavier, *Chem. Soc. Rev.* **2010**, *39*, 3305.

30) (a) R. H. Crabtree, *J. Organomet. Chem.* **2005**, *690*, 5451; (b) W. A. Herrmann, *Angew. Chem. Int. Ed.* **2002**, *41*, 1290; (c) G. C. Vougioukalakis, R. H. Grubbs, *Chem. Rev.* **2010**, *110*, 1746; (d) A. T. Normand, K. J. Cavell, *Eur. J. Inorg. Chem.* **2008**, 2781; (e) M.-T. Lee, C.-H. Hu, *Organometallics* **2004**, *23*, 976; (f) H. Díaz-Velazquez, F. Verpoort, *Chem. Soc. Rev.* **2012**, *41*, 7032.

31) Y. Sun, C. Koehler, R. Tan, V. T. Annibale, D. Song, *Chem. Commun.* **2011**, *47*, 8349.

32) (a) E. Fogler, E. Balaraman, Y. Ben-David, G. Leitus, L. J. W. Shimon, D. Milstein, *Organometallics* **2011**, *30*, 3826; (b) E. Balaraman, E. Fogler, D. Milstein, *Chem. Commun.* **2012**, *48*, 1111.

33) C. del Pozo, M. Iglesias, F. Sánchez, *Organometallics* **2011**, *30*, 2180.

34) X. Wu, L. Ji, Y. Ji, E. H. M. Elageed, G. Gao, *Catal. Commun.* **2016**, *85*, 57.

35) G. A. Filonenko, E. Cosimi, L. Lefort, M. P. Conley, C. Copéret, M. Lutz, E. J. M. Hensen, E. A. Pidko, *ACS Catal.* **2014**, *4*, 2667.

36) G. A. Filonenko, D. Smykowski, B. M. Szyja, G. Li, J. Szczygieł, E. J. M. Hensen, E. A. Pidko, *ACS Catal.* **2015**, *5*, 1145.

37) (a) M. Hernández-Juárez, M. Vaquero, E. Álvarez, V. Salazar, A. Suárez, *Dalton Trans.* **2013**, *42*, 351; (b) M. Hernández-Juárez, J. López-Serrano, P. Lara, J. P. Morales-Cerón, M. Vaquero, E. Álvarez, V. Salazar, A. Suárez, *Chem. Eur. J.* **2015**, *21*, 7540.

38) M. Asay, D. Morales-Morales, *Dalton Trans.* **2015**, *44*, 17432.

Chapter I

Synthesis, reactivity and catalytic applications of M-CNP (M = Pd, Ir) complexes

I.1. Introduction

In the first Chapter of this PhD Thesis, the synthesis of a series of Pd and Ir complexes stabilized with new lutidine-derived pincer ligands incorporating non-equivalent phosphino and *N*-heterocyclic carbene flanking donor groups is described. Besides, the reactivity of the Ir complexes towards bases and H_2 has been investigated, as well as the catalytic performance in different processes such as the hydrogenation of ketones and aldehydes, and the hydroboration of CO_2.

I.1.1. H_2 activation by iridium pincer complexes

Dihydrogen activation is a key step in many catalytic reactions mediated by transition metal complexes, such as hydrogenation and hydroformylation.[1] The hydrogen atoms in the H_2 molecule are bound by a rather strong covalent bond (103 kcal/mol);[2] however, metal complexes are able to oxidatively add the H_2 molecule since the formation of two M-H bonds suffices for the breaking of the H-H bond (Scheme 1).[3] This process involves donation of the σ-bonding electrons of the hydrogen molecule on a vacant metal d orbital, and transfer of electrons from an occupied d orbital of the metal to the antibonding (σ*) orbital of dihydrogen (Figure 1). Moreover, if the latter interaction is not particularly strong, formation of a σ-dihydrogen intermediate complex can be expected.[4]

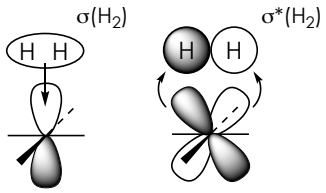

Figure 1. Orbital interactions in the H_2 activation by transition metal complexes.

In a (transient) σ-H_2 complex, heterolytic H-H activation may also occur. Due to the nonpolar and remarkably strong H-H bond, hydrogen gas

[1] J. F. Hartwig, *Organotransition Metal Chemistry: From Bonding to Catalysis*, University Science Books, **2010**.
[2] E. S. Wiedner, M. B. Chambers, C. L. Pitman, R. M. Bullock, A. J. M. Miller, A. M. Appel, *Chem. Rev.* **2016**, *116*, 8655.
[3] (a) G. J. Kubas, D. M. Heinekey, *Physical Inorganic Chemistry: Reactions, Processes, and Applications*, ed. A. Bakac, John Wiley & Sons, **2010**, *Ch. 5*; (b) M. A. Esteruelas, A. M. López, M. Oliván, *Chem. Rev.* **2016**, *116*, 8770.
[4] (a) G. J. Kubas, *Metal Dihydrogen and σ-Bond Complexes: Structure, Theory and Reactivity*; Kluwer, **2001**; (b) M. A. Esteruelas, L. A. Oro, *Chem. Rev.* **1998**, *98*, 577; (c) R. H. Crabtree, *Chem. Rev.* **2016**, *116*, 8750.

is a very weak acid (pK_a = 35, in H_2O). However, binding of H_2 to form a σ complex makes it a much better acid (pK_a < 20), facilitating deprotonation of the η^2-H_2 ligand by base and leading to the heterolytic cleavage of dihydrogen.[5] This deprotonation can be effected either by an external base or a basic moiety contained within a ligand of the complex in a *ligand-assisted process* (Scheme 1).

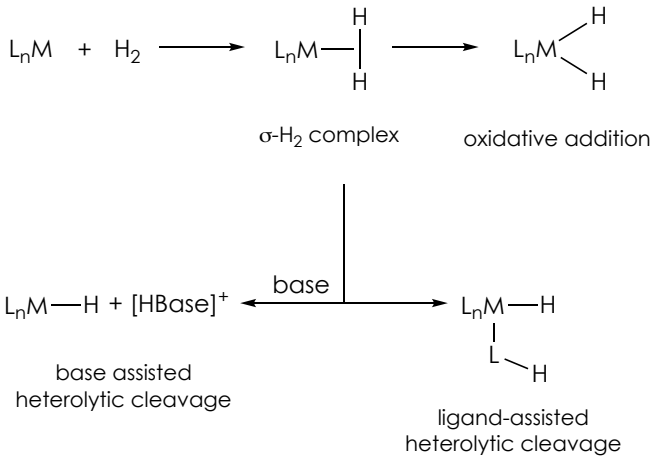

Scheme 1. Activation of H_2 by transition metal complexes.

Addition of H_2 to square-planar iridium complexes has been extensively studied, particularly with the Vaska's complex. Activation of H_2 by this derivative takes place by initial H_2 coordination to form a side-on bound σ-complex that undergoes a concerted oxidative addition to afford a *cis*-dihydride species (Scheme 2).[6] Similar steps have also been proposed for H_2 splitting by iridium pincer complexes.

[5] (a) P. G. Jessop, R. H. Morris, *Coord. Chem. Rev.* **1992**, *121*, 155; (b) D. M. Heinekey, W. J. Jr. Oldham, *Chem. Rev.* **1993**, *93*, 913.
[6] (a) P. P. Deutsch, R. Eisenberg, *Chem. Rev.* **1988**, *88*, 1147; (b) L. Vaska, *Acc. Chem. Res.* **1968**, *1*, 335.

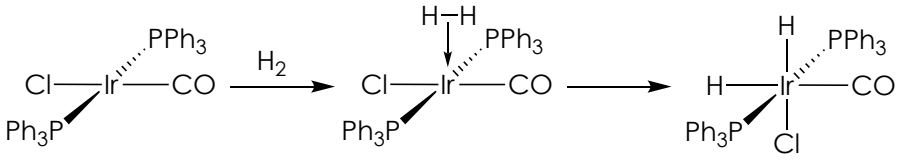

Scheme 2. H_2 activation by the Vaska´s complex.

For example, carbonyl iridium complexes containing anionic PCP and POCOP ligands reversibly add H_2 leading to *cis*-dihydride derivatives (Scheme 3).[7,8] The reversibility of this process has been attributed to the rigid square-planar geometry imposed by the pincer ligand since, as shown by theoretical calculations, electron density donation from the metal filled d orbital into the empty σ*(H-H) orbital is increased in square-planar d^8 complexes upon deviation from the ideal geometry.[9] Similarly, favorable H-H reductive elimination from cationic *cis*-dihydride iridium complexes incorporating a lutidine-derived PNP ligand has also been observed (Scheme 4).[10] Furthermore, H-H addition to Ir(POCOP)(CO) and Ir(PCP)(CO) complexes is significantly affected by the steric and electronic properties of the PR_2 groups. Thus, concerted oxidative addition of H_2 to sterically impeded Ir(POCOP^{tBu})(CO) and Ir(PCP^{tBu})(CO) complexes does not take place;[8,11] whereas the use of electron-withdrawing substituents affords the formation of *cis*-hydrides with both meridional and facially coordinated PCP ligands (Scheme 5).[12]

---

[7] B. Rybtchinski, Y. Ben-David, D. Milstein, *Organometallics* **1997**, *16*, 3786.
[8] J. M. Goldberg, S. D. T. Cherry, L. M. Guard, W. Kaminsky, K. I. Goldberg, D. M. Heinekey, *Organometallics* **2016**, *35*, 3546.
[9] (a) A. Dedieu, A. Strich, *Inorg. Chem.* **1979**, *18*, 2940; (b) J.-Y. Saillard, R. Hoffmann, *J. Am. Chem. Soc.* **1984**, *106*, 2006.
[10] S. M. Kloek, D. M. Heinekey, K. I. Goldberg, *Organometallics* **2006**, *25*, 3007.
[11] F. Liu, A. S. Goldman, *Chem. Commun.* **1999**, 655.
[12] J. J. Adams, N. Arulsamy, D. M. Roddick, *Organometallics* **2011**, *30*, 697.

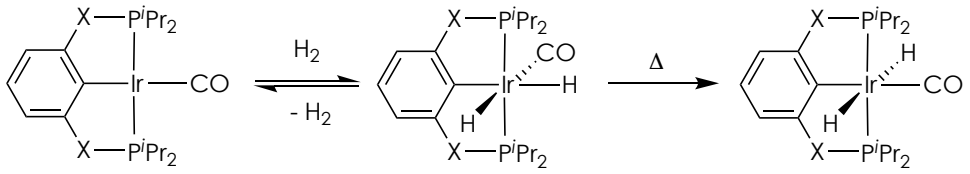

Scheme 3. H_2 activation by carbonyl Ir pincer complexes containing anionic PCP and POCOP ligands.

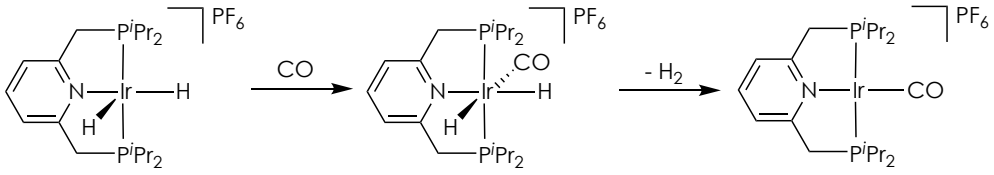

Scheme 4. H-H reductive elimination in a *cis*-$[IrH_2(PNP)(CO)]PF_6$ complex.

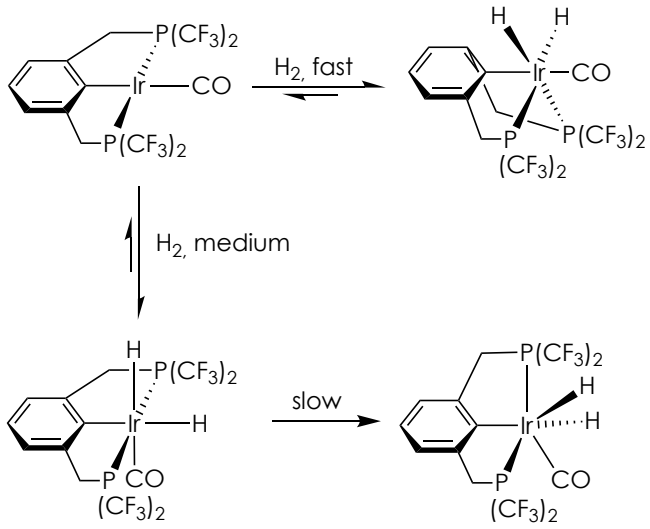

Scheme 5. H_2 addition to the $Ir(PCP^{CF3})(CO)$ complex.

Interestingly, upon heating, *cis*-IrH_2(POCOP)(CO) and *cis*-IrH_2(PCP)(CO) complexes isomerize to the thermodynamically more stable

trans derivatives (Scheme 3). While the higher stability of the *trans*-dihydride complexes in comparison to the *cis*-dihydrides is difficult to explain considering the high *trans* influence of the hydride ligands, the observed relative stability can be rationalized considering both steric and electronic factors. An axially coordinated CO ligand is sterically disfavored, whereas coordination of a hydride *trans* to the PCP aryl is more destabilizing than a carbonyl. Furthermore, different mechanisms have been proposed for this *cis-trans* isomerization, including: i) a non-dissociative trigonal twist of the pincer ligand in which the complex passes through a distorted octahedral intermediate (Scheme 6a),[13] and ii) a CO migratory insertion pathway involving a formyl derivative (Scheme 6b).[14]

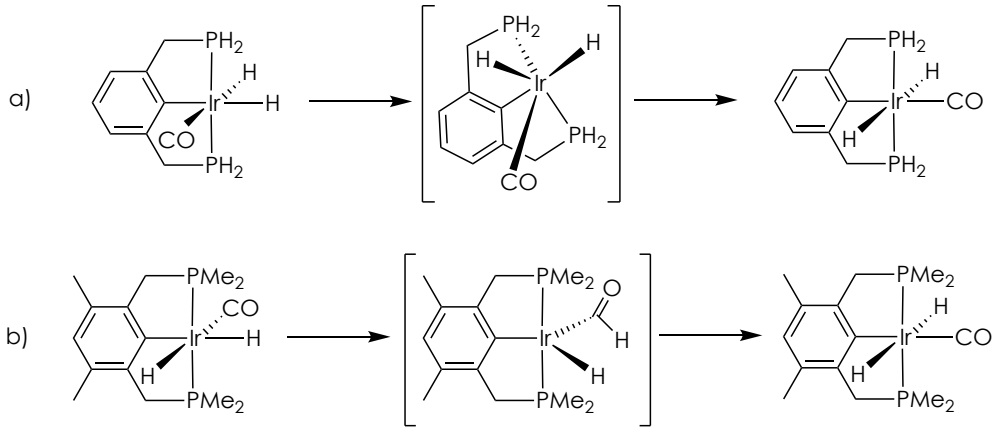

Scheme 6. Mechanisms for the *cis*/*trans* isomerization of dihydride Ir complexes.

Brookhart and coworkers observed that, while an Ir(I) methyl complex based on a bulky PONOP ligand did not activate H_2, addition of catalytic amounts of a weak acid, such as water, yielded a *trans*-dihydride species

[13] S. Li, M. B. Hall, *Organometallics* **1999**, *18*, 5682.
[14] T. T. Lekich, J. B. Gary, S. M. Bellows, T. R. Cundari, L. M. Guarda, D. M. Heinekey, *Dalton Trans.* **2018**, *47*, 16119

(Scheme 7).[15] Mechanistic studies revealed an acid-catalyzed pathway resulting in a dihydrogen-hydride complex that is deprotonated by the conjugate base in solution to give the *trans*-dihydride product. Proton-catalyzed H_2 activation leading to *trans*-dihydride complexes has also been shown for Ir(POCOP)(CO) and Ir(PCP)(CO) complexes, even in the case of ligands containing bulky P^{t}Bu$_2$ groups that were not capable of oxidatively activate H_2.[8]

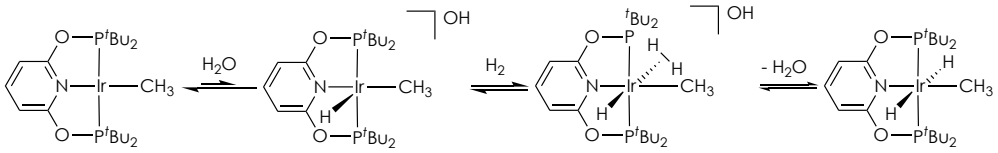

Scheme 7. Proton-catalyzed H_2 activation by PONOP-Ir complex.

Ligand-assisted heterolytic splitting of H_2 was first observed by Fryzuk and coworkers (Scheme 8).[16] The Ir(COE)[N(SiMe$_2$CH$_2$PPh$_2$)$_2$] complex under H_2 generates an iridium(III) trihydride, *fac*-IrH$_3$[HN(SiMe$_2$CH$_2$PPh$_2$)$_2$], that isomerizes to the *mer* isomer. Both isomers were found to be only stable in the presence of H_2, since H_2 elimination to yield the dihydrideamido complex IrH$_2$[N(SiMe$_2$CH$_2$PPh$_2$)$_2$] is favored. A related H_2 addition to Ir(III) methyl halide derivatives was also observed.

[15] M. Findlater, W. H. Bernskoetter, M. Brookhart, *J. Am. Chem. Soc.* **2010**, *132*, 4534.
[16] (a) M. D. Fryzuk, P. A. MacNeil, *Organometallics* **1983**, *2*, 682; (b) M. D. Fryzuk, P. A. MacNeil, S. J. Rettig, *Organometallics* **1985**, *4*, 1145; (c) M. D. Fryzuk, P. A. MacNeil, S. J. Rettig, *J. Am. Chem. Soc.* **1987**, *109*, 2803.

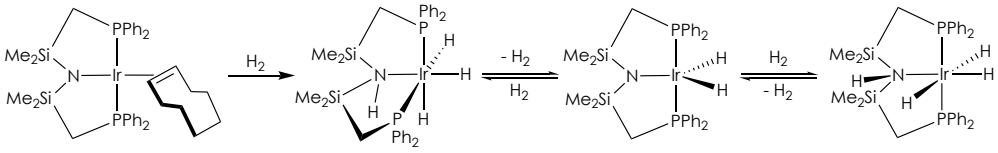

Scheme 8. Ligand-assisted heterolytic splitting of H_2 by an amido Ir complex.

Milstein *et al.* reported the generation of *trans*-dihydride complexes after exposure to H_2 of aryl and acetonyl Ir(I) complexes containing lutidine-derived PNP ligands (Scheme 9).[17,18] The proposed mechanism for the formation of these species accounts for the existence of an equilibrium of the initial Ir(I) complexes with their corresponding deprotonated hydride Ir(III)-PNP***** species, formed by a water-assisted proton transfer from a methylene arm of the pincer to the Ir center. Subsequent binding of H_2 to the vacant position *trans* to the hydrido ligand followed by transfer of hydrogen from the η^2-H_2 to the methyne carbon of the pincer bridge yields the *trans*-dihydride derivative.[19]

[17] E. Ben-Ari, G. Leitus, L. J. M. Shimon, D. Milstein, *J. Am. Chem. Soc.* **2006**, *128*, 15390.
[18] L. Schwartsburd, M. A. Iron, L. Konstantinovski, Y. Diskin-Posner, G. Leitus, L. J. W. Shimon, D. Milstein, *Organometallics* **2010**, *29*, 3817.
[19] M. A. Iron, E. Ben-Ari, R. Cohen, D. Milstein, *Dalton Trans.* **2009**, 9433.

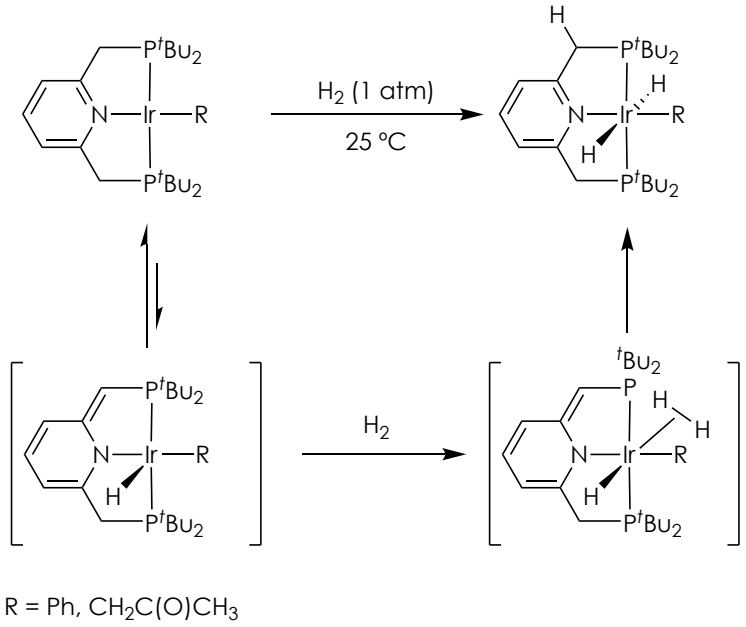

Scheme 9. Hydrogen activation by Ir-PNP pincer complexes.

Finally, a seemingly related ligand-assisted H_2 activation was reported for a dihydride Ir(III) complex containing a deprotonated lutidine-derived PNP* ligand. Exposure of this complex to hydrogen gas resulted in the formation of a trihydride IrH_3(PNP) species (Scheme 10).[20]

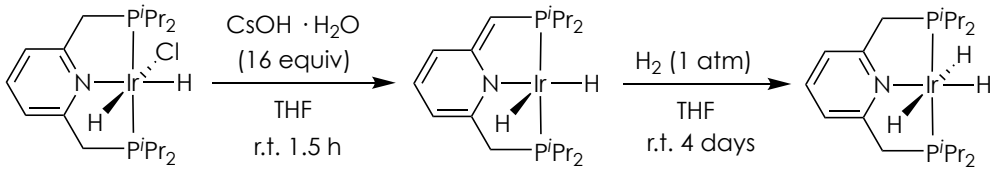

Scheme 10. Dihydrogen activation by an Ir-PNP* pincer complex.

[20] (a) R. Tanaka, M. Yamashita, K. Nozaki, *J. Am. Chem. Soc.* **2009**, *131*, 14168; (b) R. Tanaka, M. Yamashita, L. W. Chung, K. Morokuma, K. Nozaki, *Organometallics* **2011**, *30*, 6742.

I.1.2. Iridium catalysts based on proton-responsive pincer ligands for hydrogenation reactions

Hydrogenation reactions are important processes in chemical synthesis for the reduction of organic molecules.[21] At this respect, iridium metal complexes, particularly those based on proton-responsive ligands, have been widely employed as hydrogenation[22] and transfer hydrogenation[22,23] catalysts.

For example, Abdur-Rashid and coworkers examined the use of an iridium trihydride complex bearing a diethylamino-based PNP pincer ligand in the reduction of ketones and aldehydes using either H_2[24] or isopropanol[25] as reductants (Figure 2). Under 10 bar of H_2 in the presence of KO^{t}Bu, a range of aromatic, aliphatic and cyclic ketones were reduced to the corresponding alcohols at room temperature using S/C of up to 30,000. Interestingly, hydrogenation of benzalacetone and β-ionone that contain a conjugate olefin bond took place with full selectivity, whereas 50% hydrogenation of the C=C bond was observed in the reaction of 2-cyclohexen-1-one. On the other hand, lower catalyst loadings could be employed in the transfer hydrogenation reactions, although the reduction of benzalacetone gave the saturated alcohol as the sole product. An outer-sphere mechanism was proposed on the basis of the reactivity of the $IrClH_2$(PNP)

---

[21] (a) *Applied homogeneous catalysis with organometallic compounds*, 2nd Edn. B. Cornils, W. A. Herrmann (Eds.), VCH, **2002**; (b) *The handbook of homogeneous hydrogenation*, J. G. de Vries, C. J. Elsevier (Eds.), VCH, **2007**.
[22] (a) *Iridium complexes in organic synthesis*, L. A. Oro, C. Claver (Eds.), VCH, **2009**; (b) *Iridium Catalysis*, P. G. Andersson (Ed.), Springer, **2011**.
[23] D. Wang, D. Astruc, *Chem. Rev.* **2015**, *115*, 6621.
[24] X. Chen, W. Jia, R. Guo, T. W. Graham, M. A. Gullons, K. Abdur-Rashid, *Dalton Trans.* **2009**, 1407.
[25] Z. E. Clarke, P. T. Maragh, T. P. Dasgupta, D. G. Gusev, A. J. Lough, K. Abdur-Rashid, *Organometallics* **2006**, *25*, 4113.

complex with base, and of the resulting deprotonated derivative with H_2 (Figure 3).

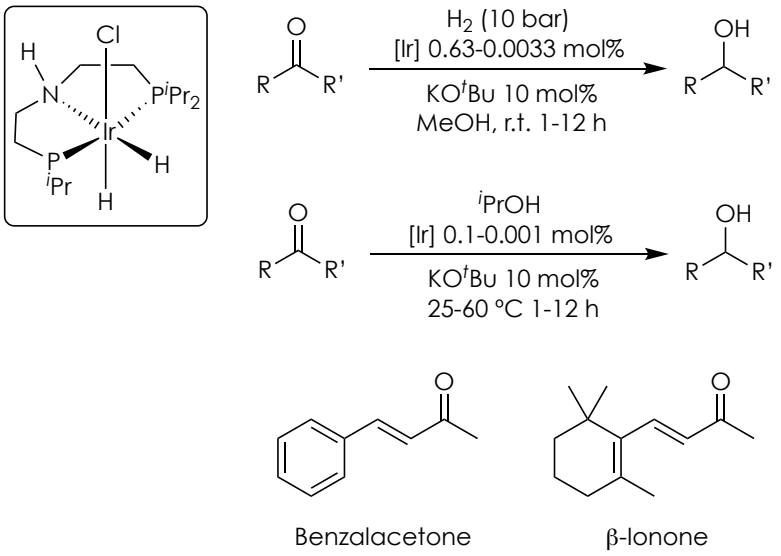

Figure 2. Hydrogenation and transfer hydrogenation of ketones using an Ir complex based on a diethylamino-derived PNP ligand.

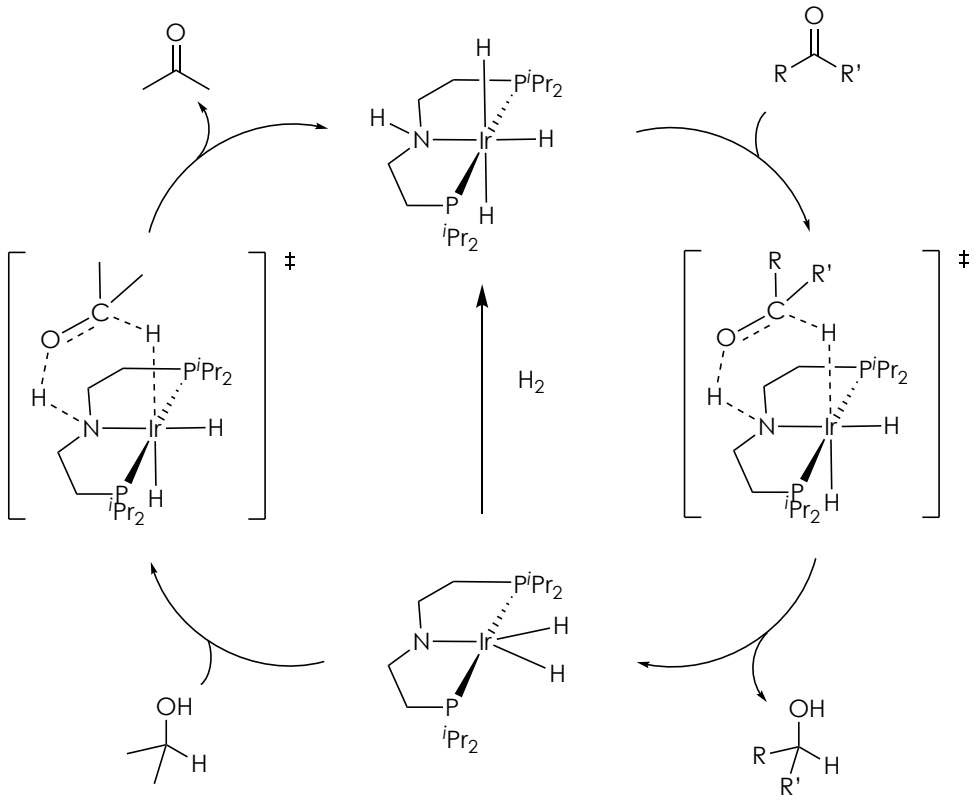

Figure 3. Proposed mechanisms for the hydrogenation and transfer hydrogenation of ketones using an Ir complex based on a diethylamino-derived PNP ligand.

Hydrogenation of esters is a more challenging process than that of ketones due to the reduced electrophilicity expected for the carbonyl carbon.[26] Although efficient catalytic systems have been developed for this transformation, only a limited number of iridium catalysts have been found to catalyze the conversion of esters to alcohols.[27] The Beller group studied the hydrogenation of esters to alcohols using iridium complexes containing a

[26] P. A. Dub, T. Ikariya, *ACS Catal.* **2012**, *2*, 1718.
[27] (a) J. Pritchard, G. A. Filonenko, R. van Putten, E. J. M. Hensen, E. A. Pidko, *Chem. Soc. Rev.* **2015**, *44*, 3808; (b) T. P. Brewster, N. M. Rezayee, Z. Culakova, M. S. Sanford, K. I. Goldberg, *ACS Catal.* **2016**, *6*, 3113.

diethylamino-derived PNP ligand (Figure 4).[28] Both $IrClH_2$(PNP) and IrH_3(PNP) complexes catalyzed the reduction of esters in the presence of base (NaOMe) under similar conditions (50 bar of H_2 and 130 ºC). Moreover, the IrH_3(PNP) catalyst was also found to catalyze the reduction process in the absence of base, although lower catalytic activities were achieved.

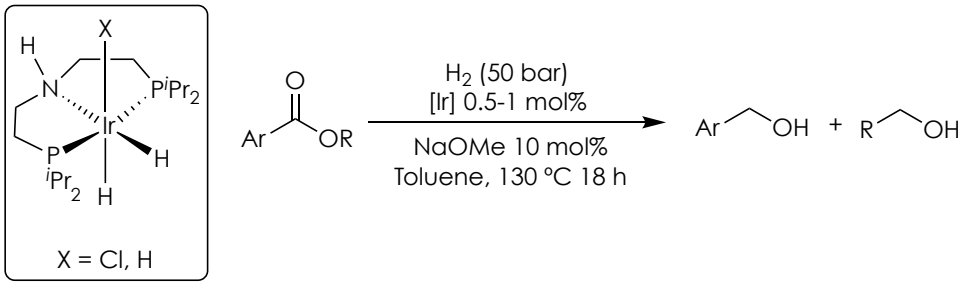

Figure 4. Hydrogenation of esters using a diethylamino-derived Ir-PNP complex.

Iridium complexes based on both lutidine- and diethylamino-derived PNP ligands have received attention as catalysts for the hydrogenation of CO_2 to formates. Under basic conditions (aqueous KOH), the Ir catalyst based on a lutidine-derived PNP ligand provided high catalytic activities, with TON and TOF values of up to $3.5\ 10^6$ and 150,000 h^{-1} respectively, for the formation of HCO_2K from CO_2 and H_2 (Figure 5).[20a] Under similar conditions, the Ir-PNP complex incorporating the alkyl pincer ligand provided maximum TON and TOF values of 348,000 and *ca.* 19,000 h^{-1}, respectively.[29]

Mechanistic studies for both catalytic systems support that the ligands are not directly involved in the catalytic process. The accepted mechanisms include the following steps: i) CO_2 insertion into the Ir-H bond to yield a

[28] K. Junge, B. Wendt, H. Jiao, M. Beller, *ChemCatChem* **2014**, *6*, 2810.
[29] T. J. Schmeier, G. E. Dobereiner, R. H. Crabtree, N. Hazari, *J. Am. Chem. Soc.* **2011**, *133*, 9274.

formate complex, ii) displacement of the coordinated formate by a H_2 molecule and, iii) deprotonation of the η^2-H_2 ligand by OH^- to regenerate the initial trihydride Ir complex (Figure 6).[30,20b] The main difference between the action modes of both catalysts resides in the rate determining step, which is the deprotonation of the Ir-H_2 for the lutidine-derived catalysts and the displacement of formate by H_2 for the diethylamino-derived system.

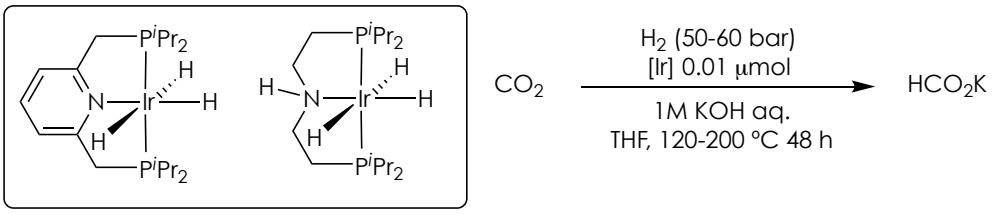

Figure 5. Ir-PNP catalysts for hydrogenation of CO_2

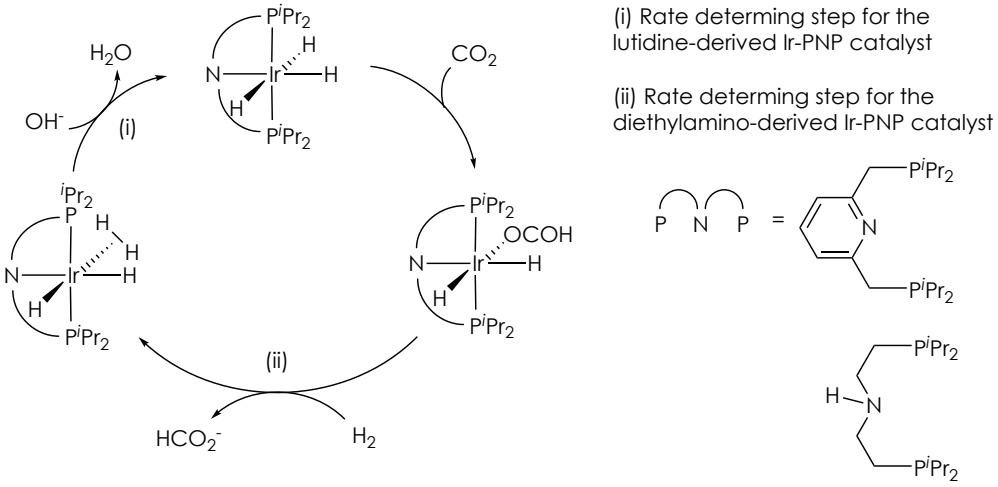

Figure 6. Catalytic cycles for the hydrogenation of CO_2 catalyzed by Ir-PNP complexes.

[30] (a) M. S. G. Ahlquist, *J. Mol. Catal. A: Chemical* **2010**, *324*, 3; (b) X. Yang, *ACS Catal.* **2011**, *1*, 849.

Lutidine-derived PNP-ligated Ir complexes have also been assayed in the hydrogenation of biomass-derived levulinic acid to γ-valerolactone, a platform chemical widely employed as solvent, synthetic intermediate and food additive (Figure 7).[31] The lutidine-derived PNP ligand conducted to a more efficient catalyst than other P-based tridentate ligands, leading to high yields of γ-valerolactone using low catalyst loadings (S/C up to 100,000; TON = 71,000).

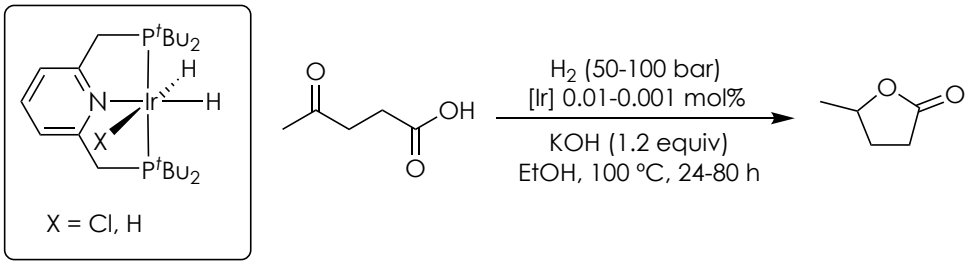

Figure 7. Hydrogenation of levulinic acid to γ-valerolactone catalyzed by a lutidine-derived Ir-PNP complex.

Finally, IrH_2Cl(PNP) and IrH_3(PNP) complexes bearing P-stereogenic lutidine-derived PNP ligands have been employed as catalysts in the asymmetric hydrogenation of ketones, olefins and quinoline (Figure 8).[32] Although good conversions were observed in these catalytic reactions, only low levels of optical induction were achieved.

[31] W. Li, J.-H. Xie, H. Lin, Q.-L. Zhou, *Green Chem.* **2012**, *14*, 2388.
[32] Z. Yang, X. Wei, D. Liu, Y. Liu, M. Sugiya, T. Imamoto, W. Zhang, *J. Organomet. Chem.* **2015**, *791*, 41.

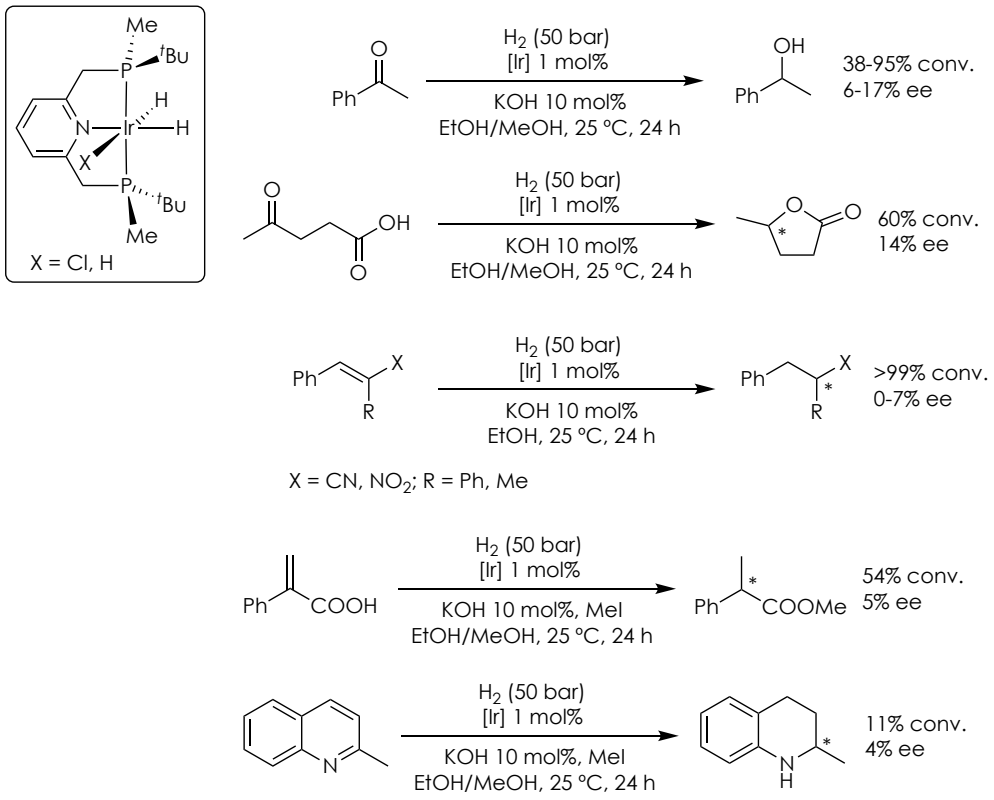

Figure 8. Examples of hydrogenation reactions performed with a chiral lutidine-derived Ir-PNP complex.

I.1.3. Hydroboration of CO_2 catalyzed by transition metal complexes

Carbon dioxide is the most convenient C1 carbon source for the synthesis of value added bulk and fine chemicals due to its renewable, economical, abundant and non-toxic nature.[33] Reactions involving the CO_2 molecule can be categorized into two main classes: i) non-redox processes, such as the synthesis of carbamates, carbonates, and urethanes,[33,34] and ii) reduction reactions to C1 products such as formic acid derivatives and MeOH equivalents.[35] While the former addition reactions are well-established processes, as exemplified by the industrial production of urea (Bosch−Meiser process),[36] efficient reduction of CO_2 still represents a formidable challenge due to the high thermodynamic and kinetic stability of this molecule.[37]

Catalytic hydrogenation is by far the most atom-economical alternative for the reduction of CO_2 to formates and methanol; however, it usually requires the use of harsh reaction conditions (high temperatures and H_2/CO_2 pressures).[37] Therefore, unsurprisingly, reactions of CO_2 with other reductants, such as hydrosilanes[38] and hydroboranes,[39] have also been widely

---

[33] (a) M. Aresta, *Carbon Dioxide as Chemical Feedstock*, Wiley-VCH, **2010**; (b) Q. Liu, L. P. Wu, R. Jackstell, M. Beller, *Nat. Commun.* **2015**, *6*, 5933; (c) A. M. Appel, J. E. Bercaw, A. B. Bocarsly, H. Dobbek, D. L. DuBois, M. Dupuis, J. G. Ferry, E. Fujita, R. Hille, P. J. A. Kenis, C. A. Kerfeld, R. H. Morris, C. H. F. Peden, A. R. Portis, S. W. Ragsdale, T. B. Rauchfuss, J. N. H. Reek, L. C. Seefeldt, R. K. Thauer, G. L. Waldrop, *Chem. Rev.* **2013**, *113*, 6621; (d) Y. Li, X. Cui, K. Dong, K. Junge, M. Beller, *ACS Catal.* **2017**, *7*, 1077.

[34] (a) J. Klankermayer, S. Wesselbaum, K. Beydoun, W. Leitner, *Angew. Chem. Int. Ed.* **2016**, *55*, 7296; (b) M. Aresta, A. Dibenedetto, A. Angelini, *Chem. Rev.* **2014**, *114*, 1709.

[35] C. Chauvier, T. Cantat, *ACS Catal.* **2017**, *7*, 2107.

[36] M. A. Benvenuto, *Industrial Chemistry*, De Gruyter, **2013**.

[37] (a) Y.-N. Li, R. Ma, L.-N. He, Z.-F. Diao, *Catal. Sci. Technol.* **2014**, *4*, 1498; (b) W.-H. Wang, Y. Himeda, J. T. Muckerman, G. F. Manbeck, E. Fujita, *Chem. Rev.* **2015**, *115*, 12936; (c) W. Wang, S. Wang, X. Ma, J. Gong, *Chem. Soc. Rev.* **2011**, *40*, 3703.

[38] F. J. Fernández-Álvarez, A. M. Aitani, L. A. Oro, *Catal. Sci. Technol.* **2014**, *4*, 611.

investigated since they allow for the use of milder reaction conditions. In addition, the reactivity of these reducing agents can be tuned by varying the silane or borane substituents, facilitating access to different C1 products including CO, MeOH and CH_4, as well as synthetically valuable formate and acetal derivatives.[40]

Hydroboration of CO_2 is promoted by diverse species including non-metal,[41] main group metal,[42] and transition metal catalysts,[43,44,45-59] which mediate the reduction of CO_2 to the formate, acetal or methoxide oxidation levels (Scheme 11).

---

[39] (a) C. C. Chong, R. Kinjo, *ACS Catal.* **2015**, *5*, 3238; (b) S. Bontemps, *Coord. Chem. Rev.* **2016**, *308*, 117.
[40] A. Tlili, E. Blondiaux, X. Frogneux, T. Cantat, *Green Chem.* **2015**, *17*, 157.
[41] (a) M.-A. Courtemanche, M.-A. Légaré, L. Maron, F.-G. Fontaine, *J. Am. Chem. Soc.* **2013**, *135*, 9326; (b) T. Wang, D. W. Stephan, *Chem. Eur. J.* **2014**, *20*, 3036; (c) Y. Yang, M. Xu, D. Song, *Chem. Commun.* **2015**, *51*, 11293; (d) A. Ramos, A. Antiñolo, F. Carrillo-Hermosilla, R. Fernández-Galán, A. Rodríguez-Diéguez, D. García-Vivó, *Chem. Commun.* **2018**, *54*, 4700; (e) S. C. Sau, R. Bhattacharjee, P. K. Vardhanapu, G. Vijaykumar, A. Datta, S. K. Mandal, *Angew. Chem. Int. Ed.* **2016**, *55*, 15147; (f) R. Declercq, G. Bouhadir, D. Bourissou, M.-A. Légaré, M.-A. Courtemanche, K. S. Nahi, N. Bouchard, F.-G. Fontaine, L. Maron, *ACS Catal.* **2015**, *5*, 2513; (g) M.-A. Courtemanche, M.-A. Légaré, L. Maron, F.-G. Fontaine, *J. Am. Chem. Soc.* **2014**, *136*, 10708; (h) C. Das Neves Gomes, E. Blondiaux, P. Thuéry, T. Cantat, *Chem. Eur. J.* **2014**, *20*, 7098; (i) T. Wang, D. W. Stephan, *Chem. Commun.* **2014**, *50*, 7007; (j) A. Tlili, A. Voituriez, A. Marinetti, P. Thuéry, T. Cantat, *Chem. Commun.* **2016**, *52*, 7553; (k) N. von Wolff, G. Lefèvre, J.-C. Berthet, P. Thuéry, T. Cantat, *ACS Catal.* **2016**, *6*, 4526; (l) G. Tuci, A. Rossin, L. Luconi, C. Pham-Huu, S. Cicchi, H. Ba, G. Giambastiani, *Catal. Sci. Technol.* **2017**, *7*, 5833.
[42] (a) M. D. Anker, M. Arrowsmith, P. Bellham, M. S. Hill, G. Kociok-Köhn, D. J. Liptrot, M. F. Mahon, C. Weetman, *Chem. Sci.* **2014**, *5*, 2826; (b) D. Mukherjee, S. Shirase, T. P. Spaniol, K. Mashima, J. Okuda, *Chem. Commun.* **2016**, *52*, 13155; (c) D. Mukherjee, H. Osseili, T. P. Spaniol, J. Okuda, *J. Am. Chem. Soc.* **2016**, *138*, 10790; (d) T. J. Hadlington, C. E. Kefalidis, L. Maron, C. Jones, *ACS Catal.* **2017**, *7*, 1853; (e) J. A. B. Abdalla, I. M. Riddlestone, R. Tirfoin, S. Aldridge, *Angew. Chem. Int. Ed.* **2015**, *54*, 5098.
[43] M. J. Sgro, D. W. Stephan, *Angew. Chem. Int. Ed.* **2012**, *51*, 11343.
[44] S. Bontemps, L. Vendier, S. Sabo-Etienne, *Angew. Chem. Int. Ed.* **2012**, *51*, 1671.
[45] R. Pal, T. L. Groy, R. J. Trovitch, *Inorg. Chem.* **2015**, *54*, 7506.

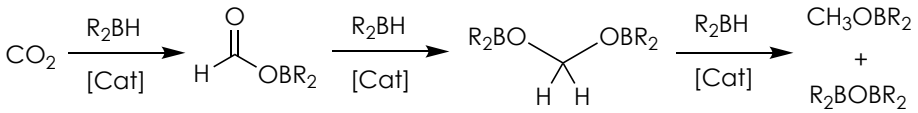

Scheme 11. Hydroboration of CO_2 to the formate, acetal and methoxide oxidation levels.

The accepted mechanism for the metal catalyzed hydroboration of CO_2 assumes the formation of metal-H species and involves three sequential catalytic cycles (Figure 9).[46] In the first cycle, CO_2 insertion into the catalyst M–H bond forms a metal-formate intermediate that upon interaction with a borane molecule yields borylformate, HCO_2BR_2. The subsequent reduction of formoxyborane implies the insertion into the catalyst M–H bond to produce formaldehyde[47] and, after interaction of the resulting M-OBR_2 intermediate with a new borane molecule, bis(boryl)oxide as by-product, R_2BOBR_2 (cycle II). Finally, formaldehyde can be reduced to CH_3OBR_2 by a third molecule of hydroborane (cycle III). In cycle II, the bis(boryl)acetal product can also be formed if β-alkoxy elimination from the M-OCH_2OBR_2 intermediate and reaction with HBR_2 occur. Therefore, as expected of a tandem catalytic process, a significant influence on the selectivity of both the catalyst and the nature of the borane, among other factors, is usually observed.[46c]

[46] (a) F. Huang, C. Zhang, J. Jiang, Z.-X. Wang, H. Guan, *Inorg. Chem.* **2011**, *50*, 3816; (b) F. Huang, Q. Wang, J. Guo, M. Wenb, Z.-X. Wang, *Dalton Trans.* **2018**, *47*, 4804; (c) M. R. Espinosa, D. J. Charboneau, A. Garcia de Oliveira, N. Hazari, *ACS Catal.* **2019**, *9*, 301.
[47] S. Bontemps, L. Vendier, S. Sabo-Etienne, *J. Am. Chem. Soc.* **2014**, *136*, 4419.

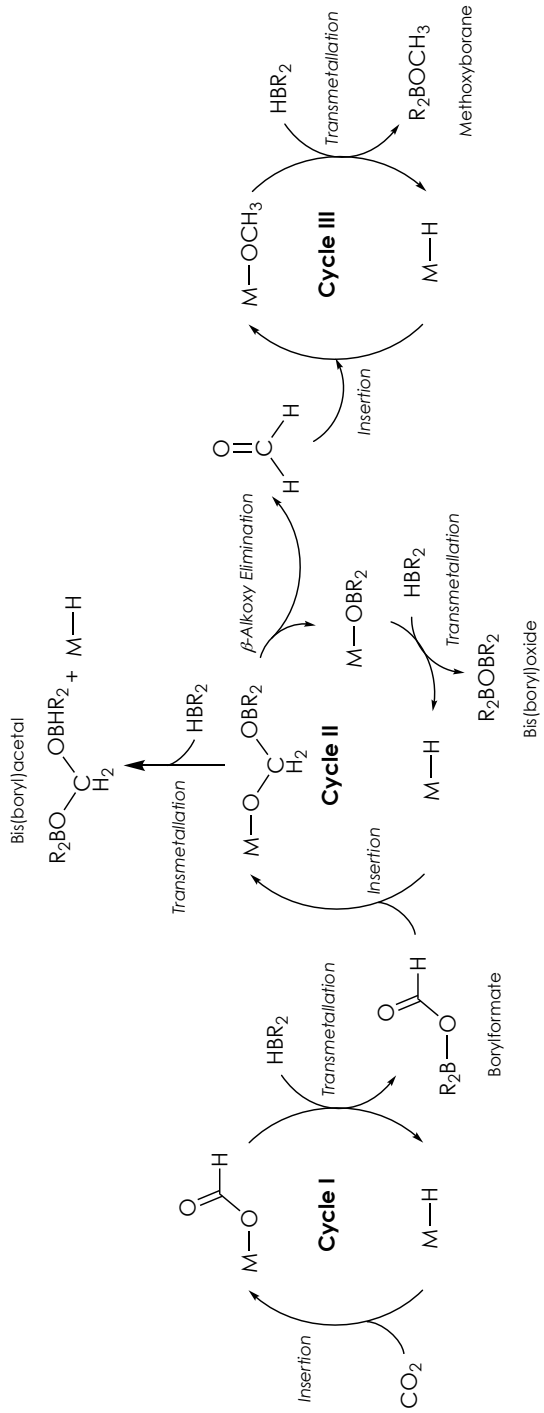

Figure 9. Mechanism for the metal-catalyzed hydroboration of CO_2.

Hydroboration of CO_2 with catecholborane catalyzed by transition-metal complexes usually proceeds to the methoxide reduction level (Figure 10). Among the different catalysts reported for this transformation, nickel and palladium pincer complexes have provided the highest catalytic activities, with TOF values of up to 1,780-2,400 h^{-1}.[48, 49, 50, 51, 52]

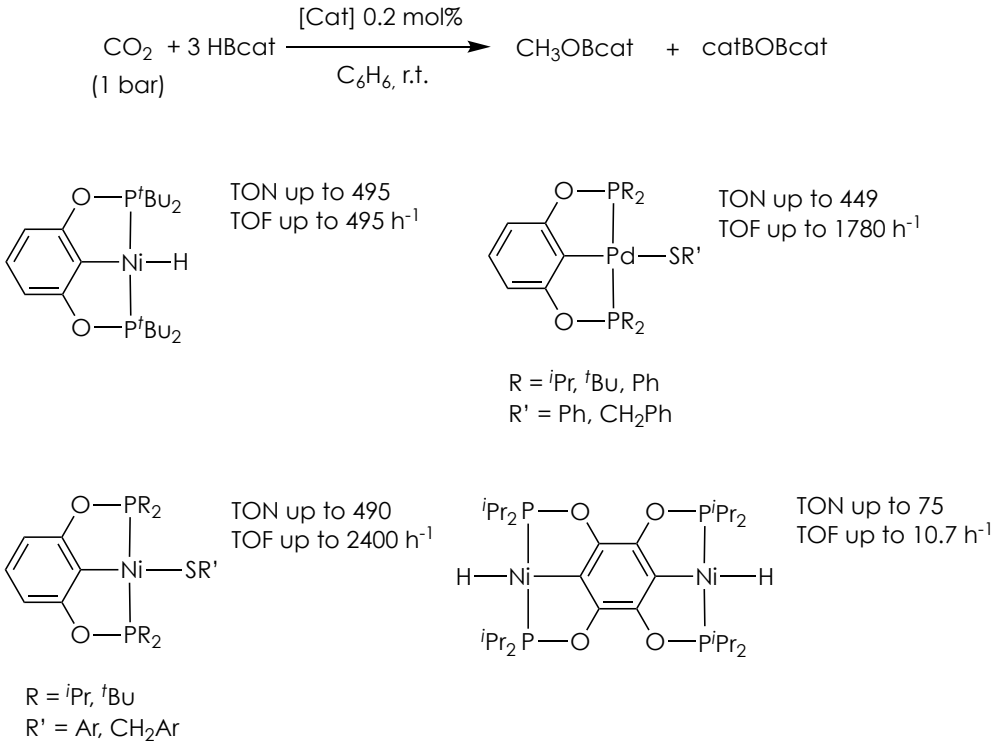

Figure 10. Ni and Pd pincer complexes employed in the hydroboration of CO_2 with HBcat.

---

[48] T. Liu, W. Meng, Q.-Q. Ma, J. Zhang, H. Li, S. Li, Q. Zhao, X. Chen, *Dalton Trans.* **2017**, *46*, 4504.
[49] Q.-Q. Ma, T. Liu, S. Li, J. Zhang, X. Chen, H. Guan, *Chem. Commun.* **2016**, *52*, 14262.
[50] (a) S. Chakraborty, J. Zhang, J. A. Krause, H. Guan, *J. Am. Chem. Soc.* **2010**, *132*, 8872; (b) S. Chakraborty, J. Zhang, Y. J. Patel, J. A. Krause, H. Guan, *Inorg. Chem.* **2013**, *52*, 37; (c) S. Chakraborty, Y. J. Patel, J. A. Krause, H. Guan, *Polyhedron* **2012**, *32*, 30.
[51] N. N. Wellala, H. T. Dong, J. A. Krause, H. Guan, *Organometallics* **2018**, *37*, 4031.
[52] J. Zhang, J. Chang, T. Liu, B. Cao, Y. Ding, X. Chen, *Catalysts* **2018**, *8*, 508.

Although CO_2 can also be reduced to methanol equivalents with less reactive boranes such as HBpin (pinacolborane) or 9-BBN (9-borabicyclo[3.3.1]nonane), selective reduction of CO_2 to the formate and acetal oxidation levels can be achieved by a proper selection of the catalyst. For example, Cu-NHC complexes have been found to be efficient catalysts for the selective hydroboration of CO_2 with HBpin to formoxyborane, which has been proven to serve as a formate source for synthetic purposes (Figure 11).[53,54,55] Similarly, ruthenium complexes based on lutidine-derived CNC ligands[56] and a Pd-PSiP pincer complex[57] provided high catalytic activities in the selective reduction of CO_2 to the formate level (Figure 11).

[53] R. Shintani, K. Nozaki, *Organometallics* **2013**, *32*, 2459.
[54] A. Burgun, R. S. Crees, M. L. Cole, C. J. Doonan, C. J. Sumby, *Chem. Commun.* **2014**, *50*, 11760.
[55] S. Bagherzadeh, N. P. Mankad, *J. Am. Chem. Soc.* **2015**, *137*, 10898.
[56] C. Koon Ng, J. Wu, T. S. Andy Hor, H.-K. Luo, *Chem. Commun.* **2016**, *52*, 11842.
[57] H.-W. Suh, L. M. Guard, N. Hazari, *Chem. Sci.* **2014**, *5*, 3859.

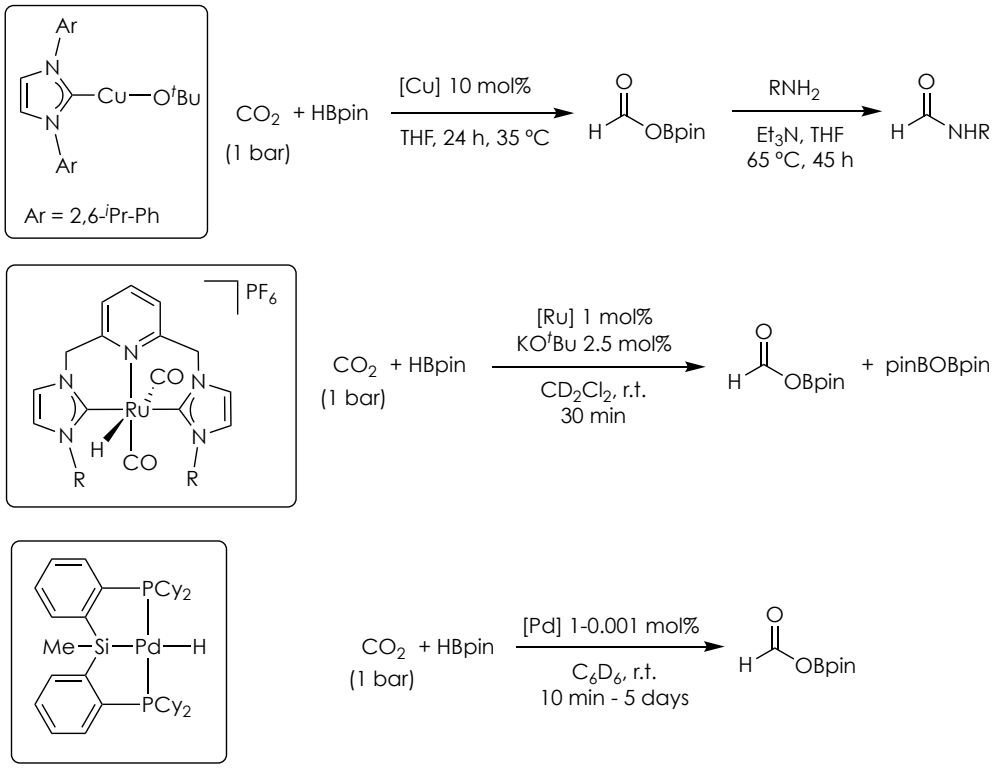

Figure 11. Examples of metal complexes for the hydroboration of CO_2 with HBpin, and synthetic applications of the resulting formoxyborane.

Acetal derivatives resulting from the partial reduction of CO_2 have been employed as methylene transfer reagents giving rise to the formation of new E-C bonds (E = N, C, O, P). At this respect, selective hydroboration of carbon dioxide to bis(boryl)acetal was carried out with HBpin using $[RuH_2(H_2)_2(PCyp_3)_2]$[47] and nickel-PSiP[58] complexes as catalyst, and with 9-BBN catalyzed by the $[Fe(H)_2(dmpe)_2]$ complex (dmpe = $Me_2PCH_2CH_2PMe_2$) (Figure 12).[59]

[58] L. J. Murphy, H. Hollenhorst, R. McDonald, M. Ferguson, M. D. Lumsden, L. Turculet, *Organometallics* **2017**, *36*, 3709.
[59] G. Jin, C. G. Werncke, Y. Escudié, S. Sabo-Etienne, S. Bontemps, *J. Am. Chem. Soc.* **2015**, *137*, 9563.

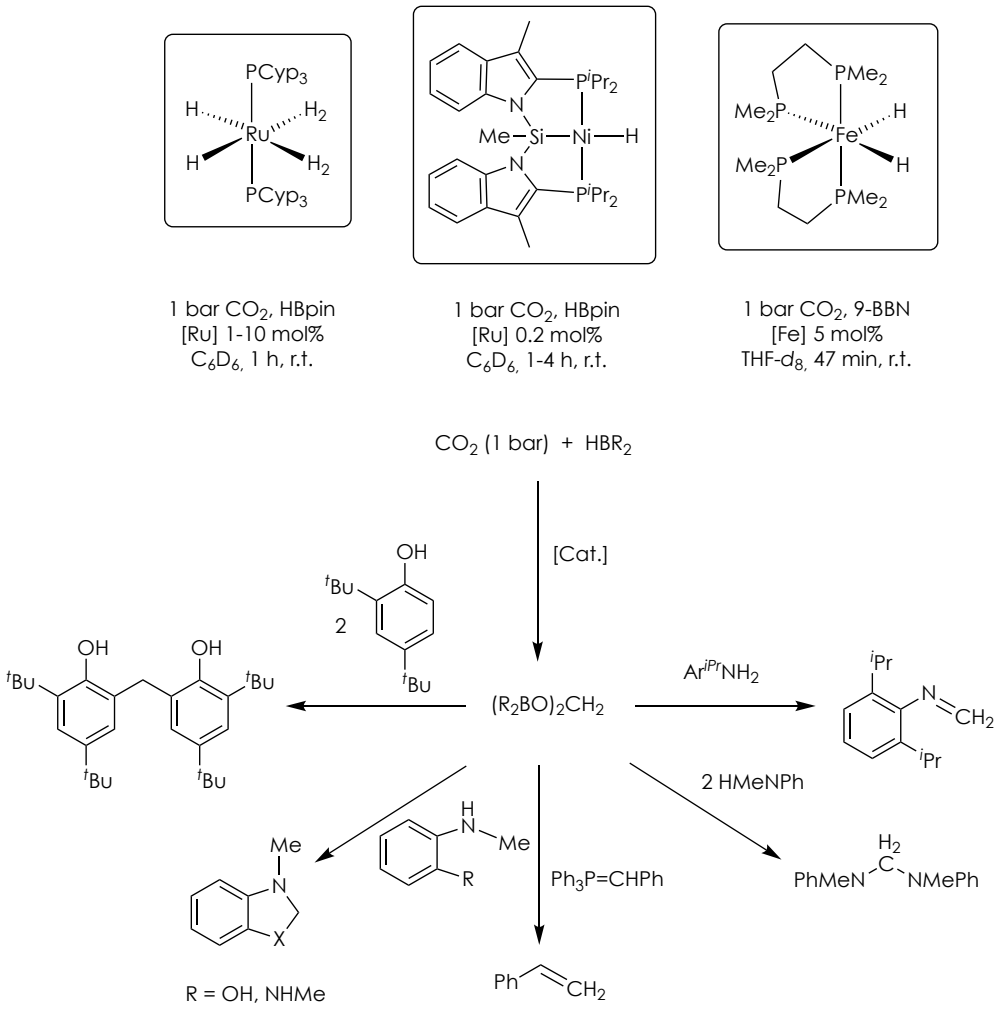

Figure 12. Catalysts used in the selective hydroboration of CO_2 with HBpin and 9-BBN to bis(boryl)acetal, and synthetic applications.

I.2. Results and discussion

I.2.1. General considerations

Pincer ligands having two inequivalent flanking donor groups provide a large electronic and steric diversity derived from the potential tuning of two different side donors.[60] However, a limited number of tridentate ligands incorporating significantly different strong σ-donating side donors, such as a phosphine and a NHC, have been reported, these being based on a 1,3-disubstituted phenyl ring backbone (**I**, Figure 1),[61] or a deprotonated picoline moiety (**II**).[62]

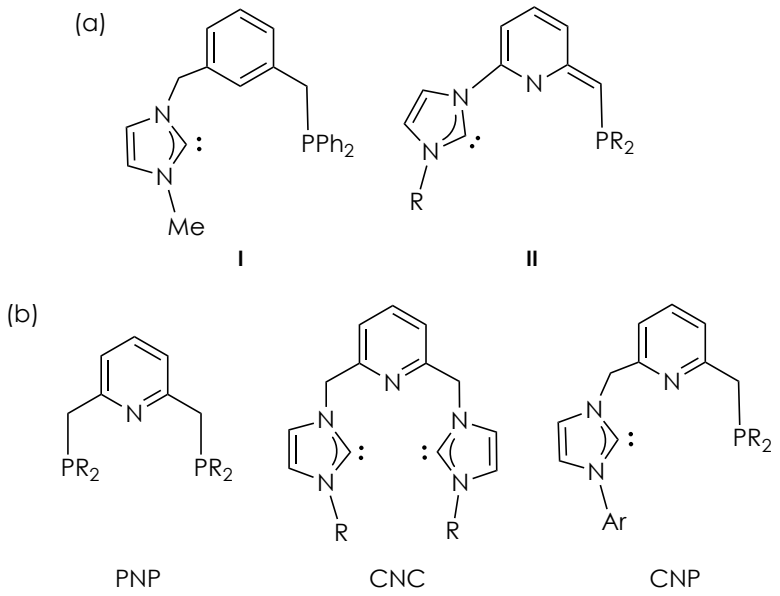

Figure 1. (a) Pincer ligands containing NHC and phosphine side donors (**I** and **II**), and (b) lutidine-derived PNP, CNC and CNP ligands.

[60] M. Asay, D. Morales-Morales, *Dalton Trans.* **2015**, *44*, 17432.
[61] X. Liu, P. Braunstein, *Inorg. Chem.* **2013**, *52*, 7367.
[62] (a) T. Simler, A. A. Danopoulos, P. Braunstein, *Chem. Commun.* **2015**, *51*, 10699; (b) T. Simler, P. Braunstein, A. A. Danopoulos, *Chem. Commun.* **2016**, *52*, 2717; (c) T. Simler, L. Karmazin, C. Bailly, P. Braunstein, A. A. Danopoulos, *Organometallics* **2016**, *35*, 903; (d) T. Simler, S. Choua, A. A. Danopoulos, P. Braunstein, *Dalton Trans.* **2018**, *47*, 7888.

In Chapter I, palladium and iridium complexes based on a new class of ligands having both NHC and phosphine side donors and a lutidine central fragment, CNP, have been investigated (Figure 1). A fundamental difference of these ligands with the previous picoline-based pincer derivatives **II** reported by Danopoulos, Braunstein *et al.* resides in the presence of a methylene linker between the pyridine and the NHC functionalities, which could be susceptible to deprotonation and enhances ligand flexibility. In addition, this ligand design allows for a direct comparison of the properties of lutidine-derived PNP and CNC ligands.

I.2.2. Synthesis, reactivity and catalytic applications of M-CNP^{Ph} (M = Pd, Ir) complexes

I.2.2.1. Synthesis of precursors of CNP^{Ph} ligands

In order to accomplish the synthesis of precursors of CNP^{Ph} ligands, the imidazolium salts **1** were prepared by prolonged heating of a solution of the corresponding 2,6-bis(halomethyl)pyridine and imidazole in toluene or THF (Scheme 1). Subsequent reaction of derivative **1a(Cl)** with diphenylphosphine in the presence of KO^{t}Bu furnished derivative **2a(Cl)** (Scheme 1). Alternatively, for the preparation of the salts **2b(Cl)** and **2b(Br)**, higher yields were obtained by using the diphenylphosphine–borane adduct for the introduction of the P-donor fragment, followed by treatment with MeOH under refluxing conditions to effect phosphine deprotection. Derivatives **2** were isolated with moderate to good yields (55-85%) as hygroscopic white or light brown solids.

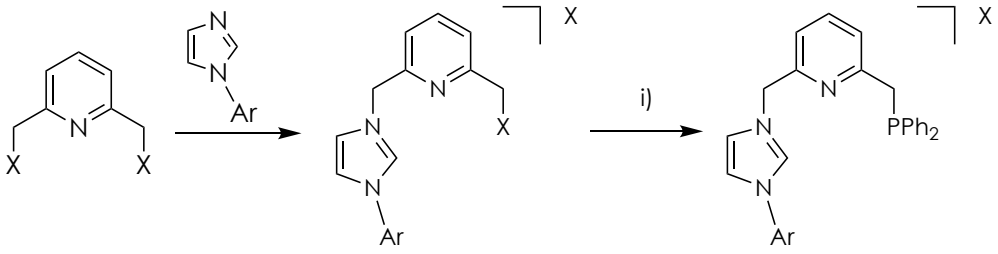

1a(Cl): Ar = Mes, X = Cl
1b(Cl): Ar = 3,5-Xyl , X = Cl
1b(Br): Ar = 3,5-Xyl , X = Br

2a(Cl): Ar = Mes, X = Cl
2b(Cl): Ar = 3,5-Xyl , X = Cl
2b(Br): Ar = 3,5-Xyl , X = Br

i) for **2a(Cl)**: PPh_2H + KO^tBu in MeCN/THF
for **2b(Cl)** and **2b(Br)**: $P(BH_3)Ph_2H$ + KO^tBu in MeCN/THF; then MeOH, reflux

Scheme 1. Synthesis of imidazolium salts **2**.

The CNP^{Ph} precursors **2** were characterized by NMR spectroscopy amd HRMS. In the ^1H NMR spectra, imidazolium salts **2** exhibit singlet signals at *ca.* 3.6 and 5.9 ppm, produced by the methylene CH_2P and CH_2N hydrogens, respectively. Moreover, the higher acidity of the imidazolium H-2 protons is reflected in a downfield resonance appearing at 10.3-11.3 ppm. The $^{31}P\{^1H\}$ NMR spectra of imidazolium salts **2** show a singlet resonance at *ca.* −11.7 ppm.

The solid state structure of **2a(Cl)** was determined by an X-ray diffraction study of a single crystal obtained by slow evaporation of a solution of this derivative in CH_2Cl_2 (Figure 2). Interestingly, a short distance between the imidazolium H-2 hydrogen and the chloride anion of 2.46 Å, smaller than the sum of the van der Waals radii (2.9-3.0 Å),[63] denotes the existence of a hydrogen bond, as also suggested by the downfield shifted resonance of the H-2 proton of **2a(Cl)** in the ^1H NMR experiment.

[63] R. S. Rowland, R. Taylor, *J. Phys. Chem.* **1996,** *100,* 7384.

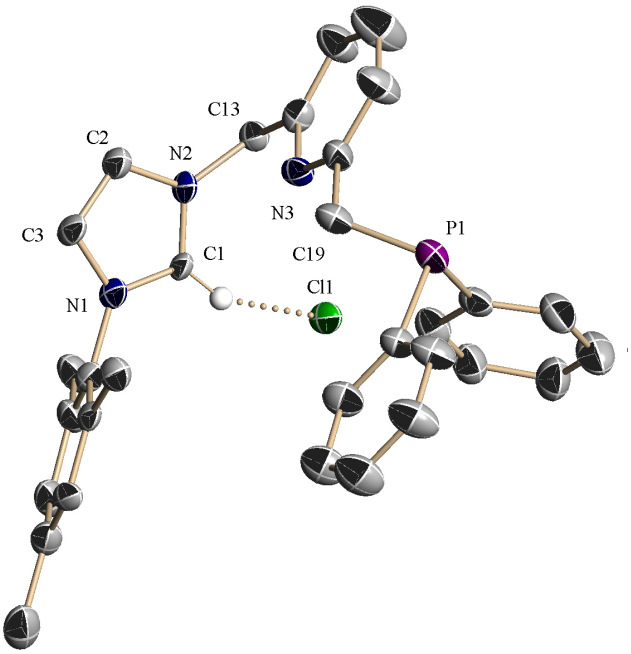

Figure 2. ORTEP drawing at 30% ellipsoid probability of **2a(Cl)**. Hydrogen atoms (except H-2) have been omitted for clarity.

I.2.2.2. Synthesis and reactivity of Pd-CNP^{Ph} complexes

To initially assess the coordination capability of the CNP^{Ph} ligands, the synthesis of a series of Pd-CNP^{Ph} complexes was investigated. Since *N*-heterocyclic carbene transfer with silver complexes to different metals is a well-established methodology for the preparation of metal-NHC derivatives under mild conditions,[64] salt **2a(Cl)** was made react with Ag_2O in CH_2Cl_2, followed by addition of $PdCl_2(MeCN)_2$ or $PdCl_2(COD)$, to yield complex **3** (Scheme 2).[65] Palladium derivative **3** has been fully characterized by NMR and elemental analysis. In the ^1H NMR spectrum (Table 1), two signals for the bridging methylenes are observed, appearing the CH_2P protons at 4.32 ppm as a doublet resonance ($^2J_{HP}$ = 11.3 Hz), whereas the CH_2N hydrogens produce a singlet at 6.05 ppm. The appearance in the $^{13}C\{^1H\}$ NMR spectrum of a doublet for the C-2 carbon of the NHC fragment at 166.4 ppm with a large $^2J_{CP}$ of 183 Hz, supports the *trans* disposition of the NHC and phosphine donors.

[64] (a) H. M. J. Wang, I. J. B. Lin, *Organometallics* **1998**, *17*, 972; (b) J. C. Garrison, W. J. Youngs, *Chem. Rev.* **2005**, *105*, 3978; (c) I. J. B. Lin, C. S. Vasam, *Coord. Chem. Rev.* **2007**, *251*, 642.
[65] N. Selander, K. J. Szabó, *Chem. Rev.* **2011**, *111*, 2048.

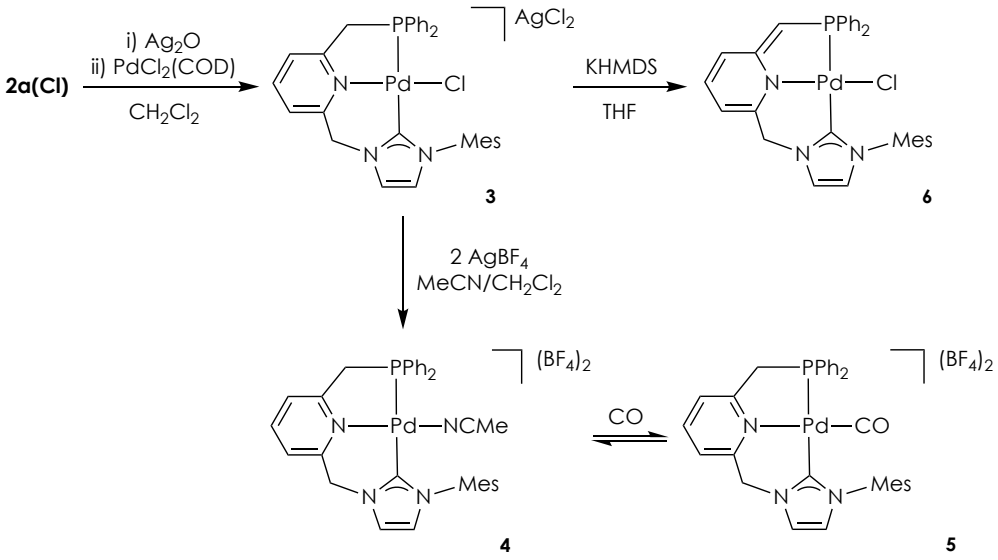

Scheme 2. Synthesis and reactivity of palladium complexes **3**-**6**.

Table 1. Selected NMR data for palladium complexes **3**-**6**.[a]

[Pd]	δ (^{31}P)	δ (^{1}H)		δ (^{13}C)		
		CH_2N	CH_2P / CHP	C-2 NHC	CO	MeCN
3	34.8	6.05	4.32 (d) (J_{HP} = 11.3)	166.4 (d) (J_{CP} = 183)	-	-
4	43.7	5.81	4.59 (d) (J_{HP} = 12.3)	163.1 (d) (J_{CP} = 161)	-	118.8 (br)
5	48.2	5.91	4.83 (d) (J_{HP} = 13.2)	164.8 (d) (J_{CP} = 142)	169.7 (d) (J_{CP} = 11)	-
6[b]	25.3	4.87	3.41 (s)	175.1 (d) (J_{CP} = 166)	-	-

[a] NMR spectra registered in CD_2Cl_2, unless otherwise noted. Chemical shifts (δ) are given in ppm. Coupling constants (*J*) are given in Hz. [b] NMR spectra registered in THF-d_8.

NMR data for complex **3** support the formation of a square-planar complex in which the CNP ligand is coordinated to the metal center as a pincer. A single crystal X-ray diffraction study of **3** confirmed the proposed structure (Figure 3). As anticipated, in the solid state the Pd atom shows a planar-square coordination sphere, as reflected in the values of the angles C(1)–Pd(1)–P(1) and N(3)–Pd(1)–Cl(1) of 168.65° and 175.03°, respectively. Moreover, the NHC–Pd–Py chelate ring presents a boat conformation as determined by the torsion angle C(14)–N(3)–Pd(1)–C(1) of 32.4°, whereas the 5-membered ring involving the phosphine donor has an envelope conformation with a C(18)–N(3)–Pd(1)–P(1) dihedral angle of 28.4°.

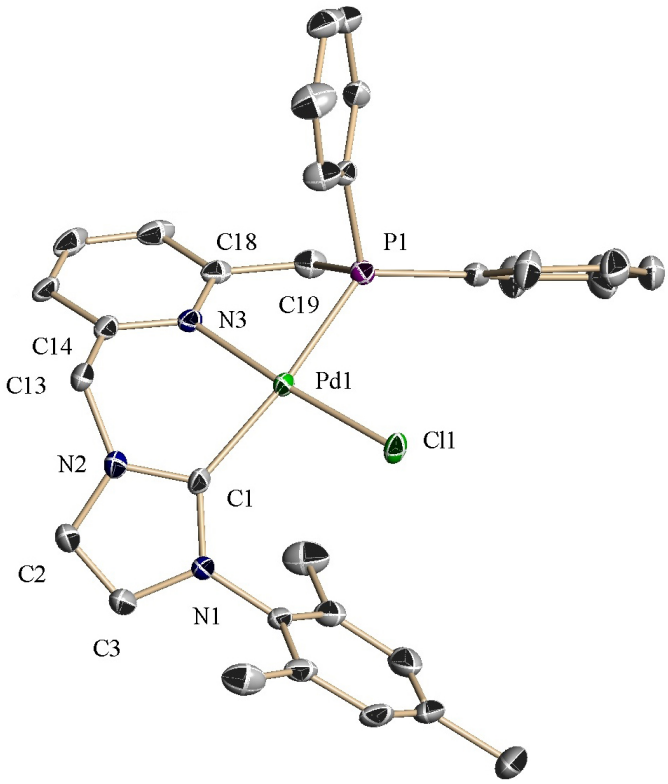

Bond lenghts (Å)		Angles (°)	
		C(1)–Pd(1)–P(1)	168.65(16)
Pd(1)–C(1)	2.038(6)	N(3)–Pd(1)–Cl(1)	175.03(14)
Pd(1)–N(3)	2.071(4)	P(1)–Pd(1)–Cl(1)	93.97(5)
Pd(1)–P(1)	2.2623(15)	P(1)–Pd(1)–N(3)	81.34(14)
Pd(1)–Cl(1)	2.2758(14)	C(1)–Pd(1)–Cl(1)	95.93(16)
		C(1)–Pd(1)–N(3)	88.6(2)

Figure 3. ORTEP drawing at 30% ellipsoid probability, and selected bond lengths (Å) and angles (°), of the cationic component of complex **3**. Hydrogen atoms and solvent molecules (CH_2Cl_2) have been omitted for clarity.

Halide abstraction from **3** with $AgBF_4$ in a CH_2Cl_2/MeCN solution mixture provided complex **4** (Scheme 2). This derivative was only stable in the presence of small amounts of MeCN, and therefore could not be isolated with analytical purity. Since the NMR data for this complex are similar to those of **3** (Table 1), with the exception of the presence of signals attributable to the MeCN ligand, an analogous structure can be anticipated.

Upon submitting the acetonitrile complex **4** to 1 bar of CO, ligand exchange occurred and partial transformation of **4** to the carbonyl complex **5** was observed. Interestingly, complexes **4** and **5** were in equilibrium, and CO removal produced the complete regeneration of **4**. In the $^{13}C\{^1H\}$ NMR spectrum of **5**, doublet signals at 169.7 (J_{CP} = 11 Hz) and 164.8 ppm (J_{CP} = 142 Hz) appear, which are assignable to the CO ligand and the C^2-NHC carbon, respectively.

To determine the acid/base reactivity of the Pd-CNP^{Ph} complexes, deprotonation of **3** was investigated.[66] Addition of KHMDS (1.1 equiv) to a suspension in THF-d_8 of **3** produced the selective deprotonation of the CNP^{Ph} ligand at the CH_2P arm yielding complex **6** as the sole observable product. In the ^1H NMR spectrum of **6**, the =CHP fragment appears as a singlet resonance at 3.41 ppm (integrating to 1H), whereas the methylene CH_2N produces a singlet at 4.87 ppm (integrating to 2H). Moreover, a significant upfield shift for the signals of the pyridine protons appearing in the range 5.55–6.46 ppm is observed, in accordance with the expected dearomatization of the ring.

[66] (a) J. I. van der Vlugt, M. A. Siegler, M. Janssen, D. Vogt, A. L. Spek, *Organometallics* **2009**, *28*, 7025; (b) M. Feller, E. Ben-Ari, M. A. Iron, Y. Diskin-Posner, G. Leitus, L. J. W. Shimon, L. Konstantinovski, D. Milstein, *Inorg. Chem.* **2010**, *49*, 1615; (c) W. D. Bailey, W. Kaminsky, R. A. Kemp, K. I. Goldberg, *Organometallics* **2014**, *33*, 2503.

I.2.2.3. Synthesis, reactivity and catalytic applications of olefin Ir-CNP^{Ph} complexes

I.2.2.3.a) Synthesis and structural features of olefin Ir-CNP^{Ph} complexes

Reactions of imidazolium salts **2** with [Ir(acac)(COD)] in CH_2Cl_2 yielded the cationic complexes **7** (Scheme 3). These olefin derivatives were isolated as yellow to orange solids that were stable in the solid state to the atmospheric conditions. Complexes **7** present very similar features in their NMR spectra. As exemplified with **7a(Cl)**, in the ^{1}H NMR spectrum (Figure 4) the CH_2P protons are non-equivalent and appear as an overlapped resonance at δ 3.45 and a doublet of doublets at 3.97 ppm ($^2J_{HH}$ = 14.8 Hz, $^2J_{HP}$ = 11.5 Hz); whereas the CH_2N bridge hydrogens produce two doublets at δ 5.56 and 7.12 ($^2J_{HH}$ = 14.0 Hz) (Figure 4). The olefinic protons cause two broad signals at 2.93 and 3.45 ppm, integrating for two protons each. In the $^{13}C\{^1H\}$ NMR spectrum, the C^2-NHC carbon originates a doublet at 164.5 ppm with a small J_{CP} coupling constant of 8 Hz, evidencing a *cis* arrangement of the phosphine and NHC donors, and therefore a *fac* coordination of the CNP^{Ph} ligand.

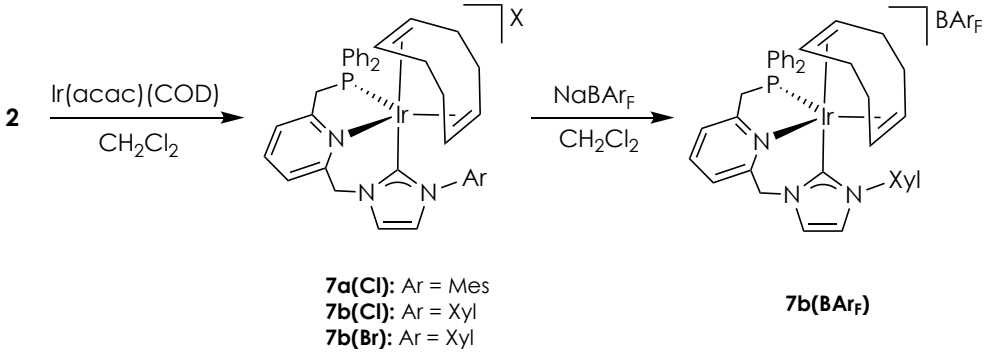

Scheme 3. Synthesis of cationic iridium complexes **7**.

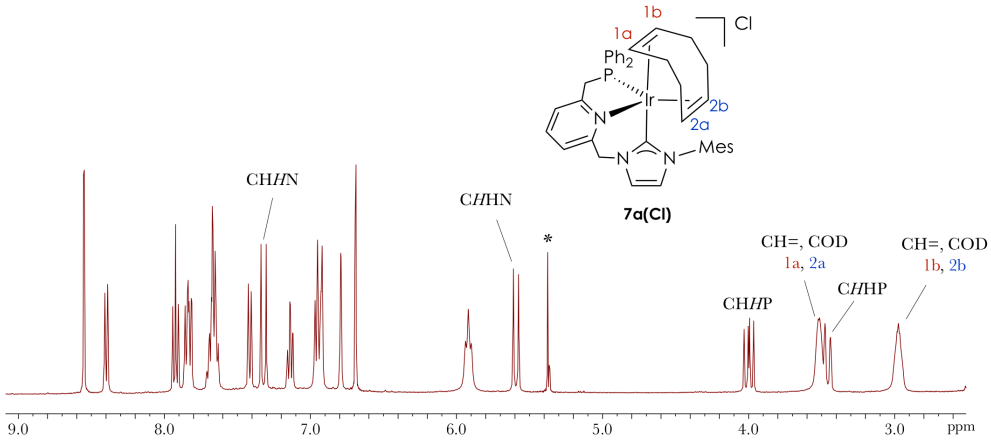

Figure 4. Region of the ^{1}H NMR spectrum (400 MHz, CD_2Cl_2) of complex **7a(Cl)** (* denotes residual CH_2Cl_2).

Since attempted crystallization of the above complexes did not yield X-ray quality crystals, anion exchange in complex **7b(Br)** was carried out by reaction with $NaBAr_F$ in CH_2Cl_2 (Scheme 3). The obtained complex **7b(BAr$_F$)** shows similar NMR data to those of **7b(Br)**, and its structure has been studied by single crystal X-ray diffraction (Figure 5). In the solid state, complex **7b(BAr$_F$)** is conveniently described as adopting a distorted trigonal bipyramidal geometry, despite the acute P–Ir–N(Py) bond angle of 75.98(8)°.

As anticipated, the CNP^{Ph} ligand coordinates in a facial mode; the NHC moiety ocuppies the apical position (P–Ir–C(NHC) = 95.61(10)º), and the pyridine and phosphine fragments are bound to the metal in the equatorial plane. In addition, the chelate ring involving the phosphine and pyridine fragments exhibits an envelope conformation (C(17)–N(3)–Ir(1)–P(1) = 29.5º), while the six-membered chelate ring containing the NHC donor adopts a boat-like conformation (C(13)–N(3)–Ir(1)–C(1) = −50.6º). The facial coordination of the CNP^{Ph} ligand, at variance with the *mer* arrangement showed by lutidine-derived PNP ligands, may be attributed to the larger flexibility of the six-membered Py–M–NHC chelate ring.[67] Moreover, this $C(NHC)_{ax}$–$N(Py)_{eq}$–P_{eq} coordination of the ligand differs significantly from previously reported pentacoordinated d^8 pincer complexes that usually exhibit an equatorial–axial–equatorial distribution of the ligand donors.[68,69,12] Finally, as observed with other pentacoordinated diolefin Ir complexes,[69] slightly longer distances from the metal to the C=C bond centroids for the alkene coordinated *trans* to the NHC than for the olefin placed in the meridional plane ($\Delta d_{(Ir\text{-centroid C=C})}$ = 0.14 Å) are observed.

[67] (a) M. Hernández-Juárez, M. Vaquero, E. Álvarez, V. Salazar, A. Suárez, *Dalton Trans.* **2013**, *42*, 351; (b) M. Hernández-Juárez, J. López-Serrano, P. Lara, J. P. Morales-Cerón, M. Vaquero, E. Álvarez, V. Salazar, A. Suárez, *Chem. Eur. J.* **2015**, *21*, 7540.

[68] G. A. Silantyev, O. A. Filippov, S. Musa, D. Gelman, N. V. Belkova, K. Weisz, L. M. Epstein, E. S. Shubina, *Organometallics* **2014**, *33*, 5964.

[69] (a) D. M. Roddick, D. Zargarian, *Inorg. Chim. Acta* **2014**, *422*, 251; (b) G. Mancano, M. J. Page, M. Bhadbhade, B. A. Messerle, *Inorg. Chem.* **2014**, *53*, 10159; (c) P. D. Newman, K. J. Cavell, A. J. Hallett, B. M. Kariuki, *Dalton Trans.* **2011**, *40*, 8807; (d) B. M. Kariuki, J. A. Platts, P. D. Newman, *Dalton Trans.* **2014**, *43*, 2971; (e) M. Iglesias, A. Iturmendi, P. J. Sanz Miguel, V. Polo, J. J. Pérez-Torrente, L. A. Oro, *Chem. Commun.* **2015**, *51*, 12431.

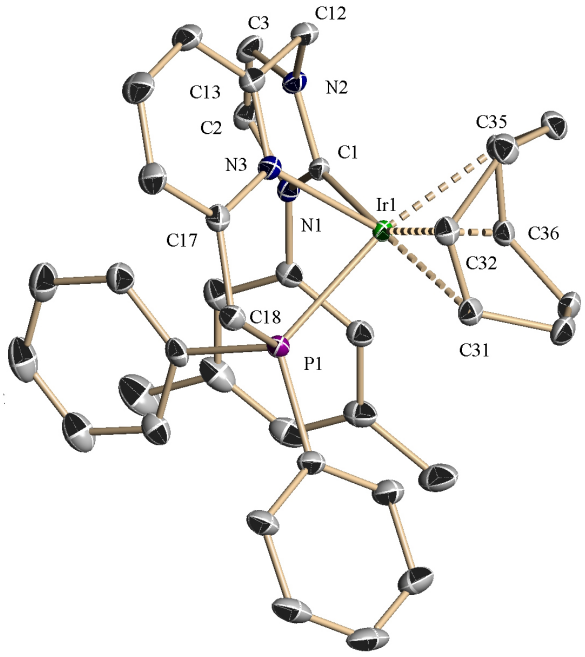

Bond lenghts (Å)		Angles (°)	
Ir(1)–C(1)	2.029(4)		
Ir(1)–N(3)	2.253(3)		
Ir(1)–P(1)	2.3412(9)	C(1)-Ir(1)-P(1)	95.61(10)
Ir(1)–C(31)	2.263(4)	N(3)–Ir(1)–P(1)	75.98(8)
Ir(1)–C(32)	2.217(4)	N(3)–Ir(1)–C(1)	81.07(13)
Ir(1)–C(35)	2.140(3)		
Ir(1)–C(36)	2.101(4)		

Figure 5. ORTEP drawing at 30% ellipsoid probability, and selected bond lengths (Å) and angles (°), of the cationic component of complex **7b(BAr$_F$)**. Hydrogen atoms and solvent molecules (CH_2Cl_2) have been omitted for clarity.

As mentioned above, the olefinic protons of the COD ligand in complexes **7** produce two broad signals (integrating for 2H each) in the ^{1}H NMR spectrum recorded at 25 ^{o}C, suggesting the existence of a dynamic behavior involving the cyclooctadiene rings. Moreover, ^{1}H–^{1}H COSY and ^{1}H–^{1}H NOESY experiments indicate that each signal is produced by protons of different olefinic moieties; i.e. the same resonance is produced by the H^{1b} and H^{2b} protons, while the H^{1a} and H^{2a} hydrogens originate another resonance (Figure 4). Therefore, the solution dynamics of the diolefin complexes **7** were studied by registering ^{1}H NMR spectra of complex **7a(Cl)** in the temperature range between 50 and −80 ^{o}C (Figure 6). The olefinic signals, appearing at 2.98 and 3.49 ppm at 25 ^{o}C, broaden upon lowering the temperature and eventually split at temperatures below −25 ^{o}C into two sets of two signals each, appearing at δ 2.23 (H^{2b}) and 3.39 (H^{1b}), and 2.86 (H^{2a}) and 3.90 (H^{1a}), respectively. A value of $\Delta G^{\ddagger}$ = 10.9 kcal mol^{-1} at the coalescence temperature (244 K) was estimated for the fluxional process.[70] The observed dynamic process can be attributed to olefin site exchange involving the decoordination of the C=C bond *trans* to the NHC fragment leading to a distorted tetrahedral intermediate **A**, followed by re-coordination of the free olefin moiety to the opposite side without lost of the *fac* coordination mode of the CNP ligand (Figure 7).

[70] J. Sandström, *Dynamic NMR Spectroscopy*, Academic Press, **1982**. Chap. 6.

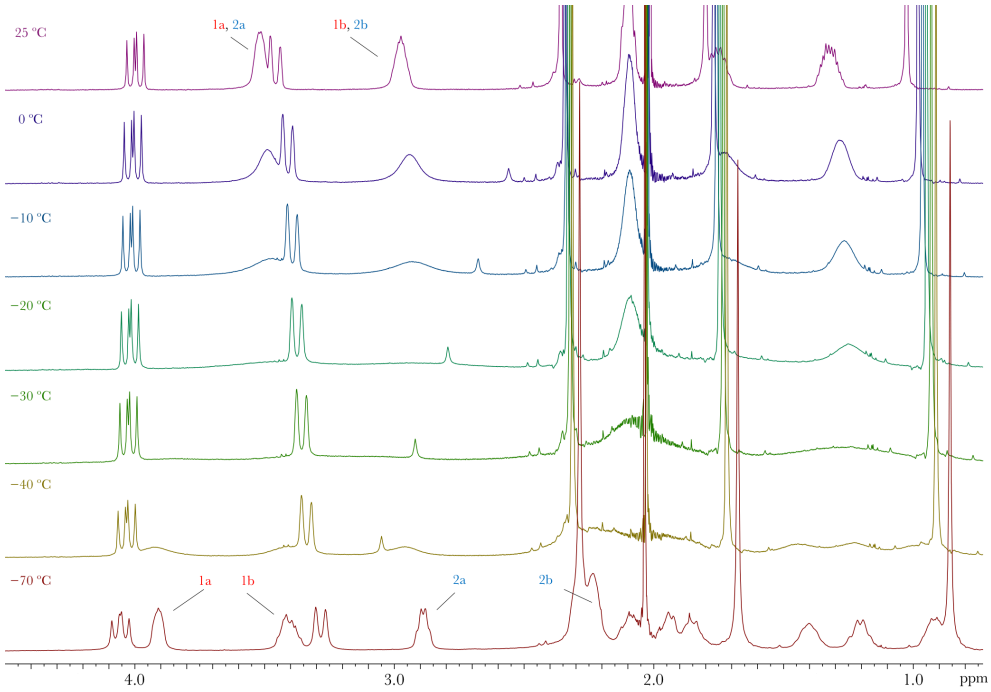

Figure 6. VT-^{1}H NMR spectra of **7a(Cl)** (400 MHz, CD_2Cl_2).

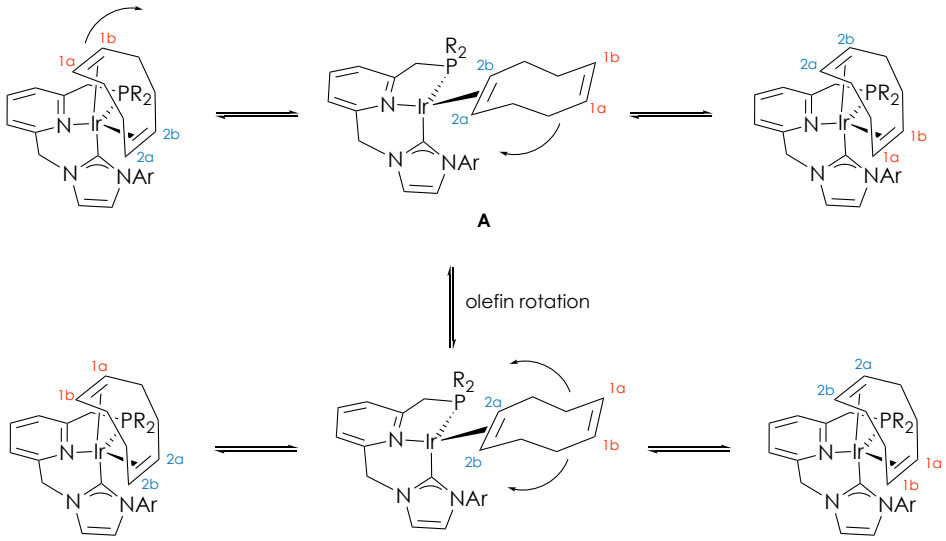

Figure 7. Proposed dynamic processes in solution operating in the cationic part of complexes **7** (positive charges have been supressed for clarity).

Moreover, the existence of additional fluxional processes with higher energy barriers was deduced from the ^{1}H-^{1}H EXSY spectrum of **7a(Cl)** registered at 50 ^{o}C (Figure 8). In this experiment, intense exchange cross-peaks between the signals of the olefinic protons appearing at 2.98 and 3.49 ppm are observed, in agreement with a dynamic behavior involving the rotation of the COD ligand after decoordination of one of the C=C bonds. Furthermore, the observation of strong correlation peaks between the resonances of the *o*-, *m*- and *p*- protons of one of the PPh groups with the aromatic protons of the other phenyl group, as well as between the signals of the methylene protons in each of the CH_2P and CH_2N arms, indicates that the CNP^{Ph} pincer in complexes **7** also undergoes structural changes, which could be assigned to a slow interconversion between the two enantiomeric forms of the complex. Previously, mirror-image isomer exchange involving a pseudo-Berry rotation has been observed for pentacoordinated pincer Ir

complexes containing diolefin ligands.[69b] However, this process in complexes **7** is unlikely due to the C(axial)–N(equatorial)–P(equatorial) arragement of the CNP^{Ph} ligand. Since, as discussed above, olefin decoordination seems facile, the observed fluxional process should involve the intermediacy of a square-planar structure **B** (Figure 9).

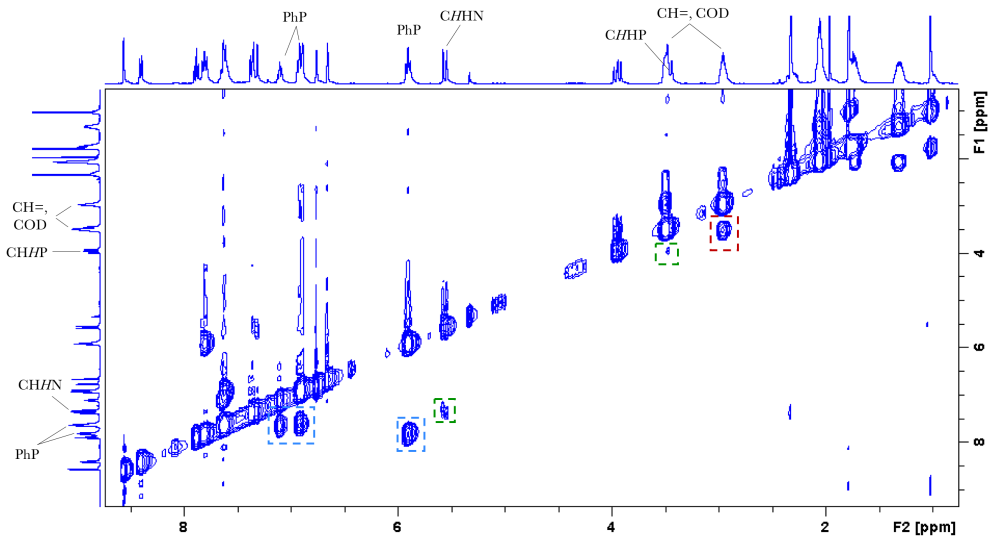

Figure 8. ^{1}H-^{1}H EXSY spectrum of **7a(Cl)** (400 MHz, CD_2Cl_2, 50 °C) Signals marked with the green squares: exchange cross-peaks due to CH_2P protons and exchange cross-peaks due to CH_2N protons. Signals marked with red squares: exchange cross-peaks due to olefinic protons. Signals marked with blue squares: exchange cross-peaks due to PPh_2 protons).

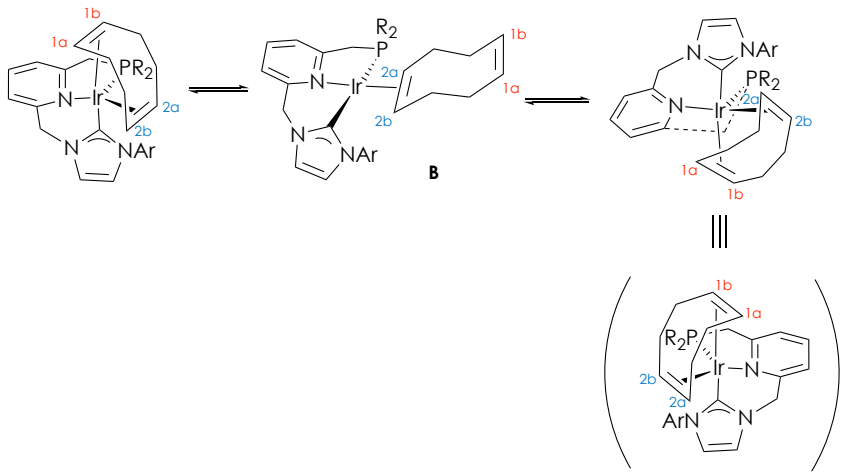

Figure 9. Proposed dynamic process with high barrier operating in the cationic part of complexes **7** (positive charges have been suppressed for clarity).

I.2.2.3.b) Reactivity with bases and H_2 of olefin Ir-CNP^{Ph} complexes

Deprotonation of the diolefin iridium complexes **7** was studied by adding KO^{t}Bu (1.1 equiv) to a THF-d_8 solution cooled to 0 ^{o}C of **7b(Br)** (Scheme 4).[17,18,20,71] Selective formation of a single species **8** was determined by NMR spectroscopy. In the ^{1}H NMR spectrum, the pyridine protons produce the characteristic high-field shifted resonances expected for the dearomatization of the central ring (5.6-6.4 ppm). Moreover, the appearance of a singlet at 3.86 ppm (integrating to 1H), assignable to the =CHP proton, and two mutually coupled doublets at 4.93 and 5.29 ppm ($^2J_{HH}$ = 13.6 Hz) (integrating to 1H each) due to the CH_2–NHC hydrogens, points to the selective deprotonation of the CH_2P arm of the pincer ligand. Furthermore, the C-2 NHC carbon appears as an overlapped doublet at 170.6 ppm in the ^{13}C{^{1}H} NMR spectrum. Although the J_{CP} value cannot be unambiguously calculated, a small value of 2 to 20 Hz is estimated, suggestive of a *cis* coordination of the phosphine and NHC donors. Further support for the inferred coordination mode was obtained from the observation of strong NOE contacts between the protons of the xylyl and PPh_2 groups of the CNP^{Ph} ligand in the ^{1}H-^{1}H NOESY experiment (Figure 10).

[71] M. Feller, E. Ben-Ari, Y. Diskin-Posner, R. Carmieli, L. Weiner, D. Milstein, *J. Am. Chem. Soc.* **2015**, *137*, 4634.

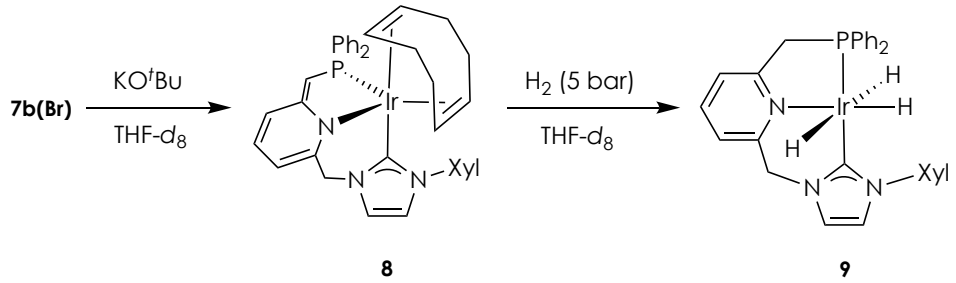

8 **9**

Scheme 4. Synthesis of **8**, and its reaction with H_2.

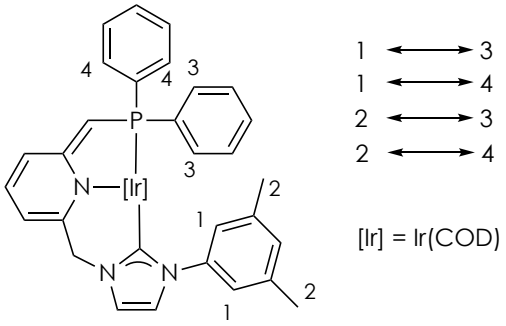

Figure 10. Selected cross-peaks observed in the ^{1}H-^{1}H NOESY spectrum of **8**.

To assess the ability of the deprotonated complex **8** to activate H_2 in a ligand-assisted process, a solution of **7b(Br)** and KO^{t}Bu in THF-d_8 was exposed to H_2 (5 bar) (Scheme 4). Analysis of the ^{1}H NMR spectrum of the resulting species leads to the formulation of **9** as a trihydride complex. In this experiment, the resonances produced by the Ir-H hydrogens appear as a doublet of doublets integrating for two protons at −9.98 ppm ($^2J_{HP}$ = 18.2 Hz, $^2J_{HH}$ = 4.8 Hz) due to the apical hydrido ligands, and a doublet of triplets for one proton at −19.64 ppm ($^2J_{HP}$ = 14.4 Hz) produced by the hydrogen *trans* to the pyridine. Moreover, the downfield shift of the resonances of the central ring of the pincer evidences the re-aromatization of the pyridine. In the ^{13}C{^{1}H} NMR spectrum, the carbenic carbon appears as a doublet at

176.9 ppm with a large $^{2}J_{CP}$ of 121 Hz, suggesting a mutually *trans* coordination of the flanking groups of the CNP^{Ph} ligand. Complex **9** was only stable under an atmosphere of H_2, and therefore could not be isolated. Interestingly, replacing the H_2 atmosphere by D_2 (4 bar) and heating to 60 °C for 4 h produces partial H/D scrambling of the hydrido ligands and the hydrogens of the methylene bridges of the pincer ligand (Scheme 5).

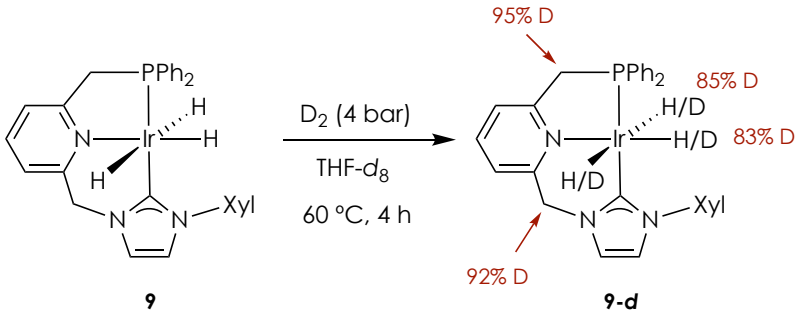

Scheme 5. Reaction with D_2 of **9**.

The olefin complexes **7(Cl)** cleanly reacted with H_2 giving rise to the formation of the dihydride derivatives **10** and cyclooctene (Scheme 6). The ^{1}H NMR spectrum of complex **10a** registers two doublets of doublets at −20.19 ($^{2}J_{HP}$ = 13.8 Hz, $^{2}J_{HH}$ = 7.0 Hz) and −23.30 ppm ($^{2}J_{HP}$ = 18.9 Hz), due to the hydrido ligands placed *trans* to the pyridine and *trans* to the chloride, respectively (Figure 11). The C-2 NHC appears at 172.9 ppm as a doublet signal with a large C-P coupling constant ($^{2}J_{CP}$ = 119 Hz) in the ^{13}C{^{1}H} NMR spectrum, permiting to propose a meridional coordination of the CNP^{Ph} ligand. Analogous spectroscopic data were found for **10b**.

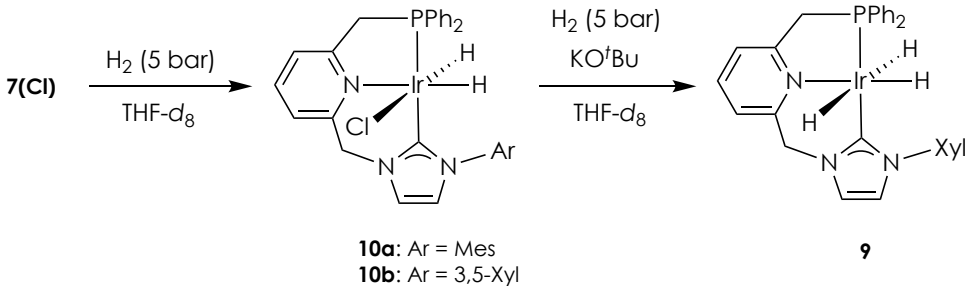

Scheme 6. Synthesis of the chlorodihydride complexes **10**, and reaction of **10b** with H_2 in the presence of KO^tBu.

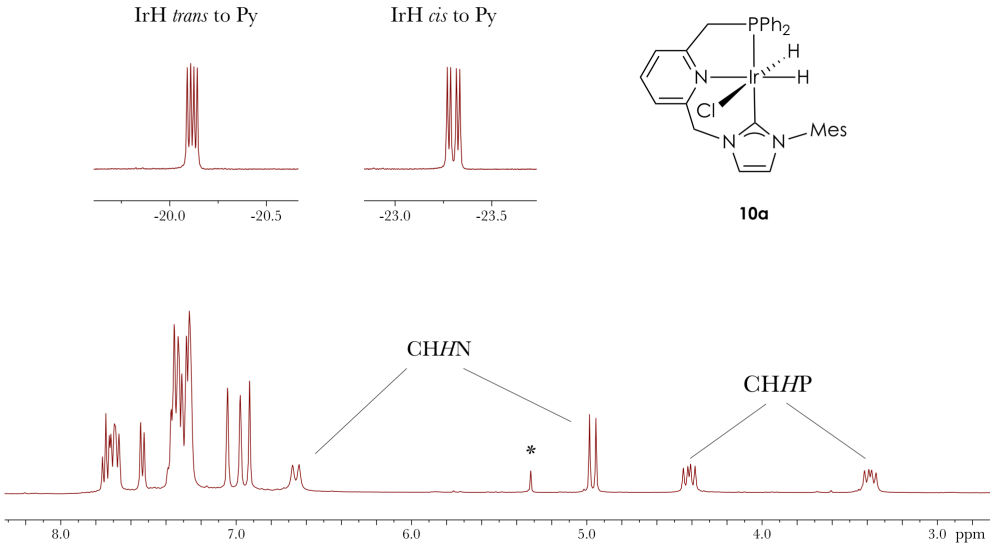

Figure 11. Regions of the ^1H NMR spectrum (CD_2Cl_2, 400 MHz) of complex **10a** (* denotes CH_2Cl_2).

Crystals of the complexes **10a** and **10b** adequate for X-ray diffraction studies were obtained from saturated CH_2Cl_2/hexane or THF solutions, respectively (Figures 12 and 13). In the solid state, these complexes are isostructural and show an octahedral geometry with a *cis* arrangement of the two hydrido ligands and the CNP^{Ph} pincer adopting a meridional

coordination, as defined in the structure of **10a** by the C(1)–Ir(1)–P(1) angle value of 166.5(3)°. In this complex, the torsion angle of −26.5(9)° for C(14)–N(3)–Ir(1)–C(1) denotes a boat-like conformation for the chelate ring incorporating the NHC arm, while the C(18)–N(3)–Ir(1)–P(1) dihedral angle of −14.9(8)° evidences an envelope conformation for the five membered chelate ring. Moreover, there exist short contacts (2.76 Å (**10a**) and 2.74 Å (**10b**)) between the axial hydrogens of the CH_2N arms and the chloride ligands suggestive of the existence of a weak hydrogen bond (sum of van der Waals radii of H and Cl: 2.9-3.0 Å).[63,72] This interaction is also manifested in the ^{1}H NMR spectra of **10a** and **10b** in the significant deshielding of the doublet resonances corresponding to the axial C*H*HN hydrogens (**10a**: δ_H = 6.70 ppm, $^2J_{HH}$ = 14.6 Hz; **10b**: δ_H = 6.53 ppm, $^2J_{HH}$ = 14.4 Hz)

[72] J. Reedijk, *Chem. Soc. Rev.* **2013**, *42*, 1776.

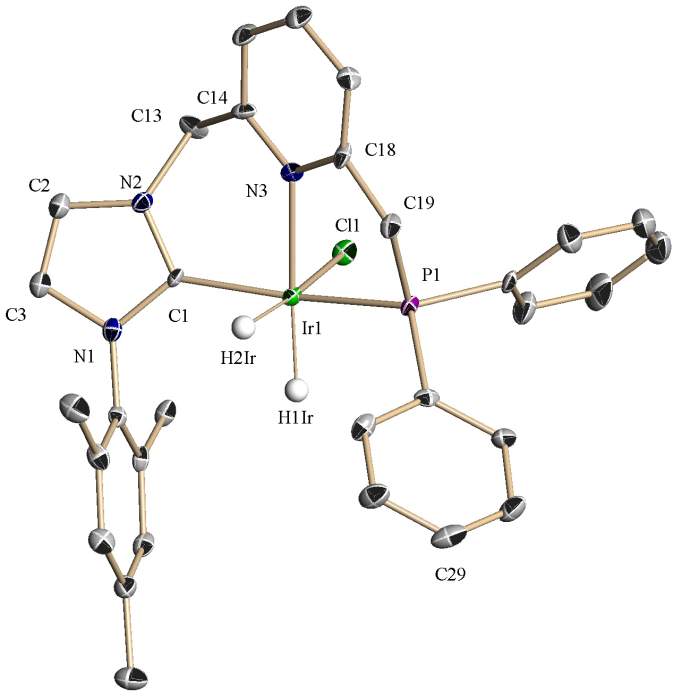

Bond lenghts (Å)		Angles (º)	
Ir(1)–C(1)	2.037(10)	C(1)–Ir(1)–P(1)	166.5(3)
Ir(1)–N(3)	2.192(9)	N(3)–Ir(1)– H(1)Ir	173.9
Ir(1)–P(1)	2.262(3)	P(1)–Ir(1)–H(1)Ir	92.7
Ir(1)–H(1)Ir	1.600	P(1)–Ir(1)–N(3)	82.2(3)
Ir(1)–H(2)Ir	1.599	C(1)–Ir(1)–H(1)Ir	95.4
Ir(1)–Cl(1)	2.509(3)	C(1)–Ir(1)–N(3)	89.0(4)

Figure 12. ORTEP drawing at 30% ellipsoid probability, and selected bond lengths (Å) and angles (º), of complex **10a**. Hydrogen atoms, except hydrido ligands, and solvent molecules (CH_2Cl_2) have been omitted for clarity.

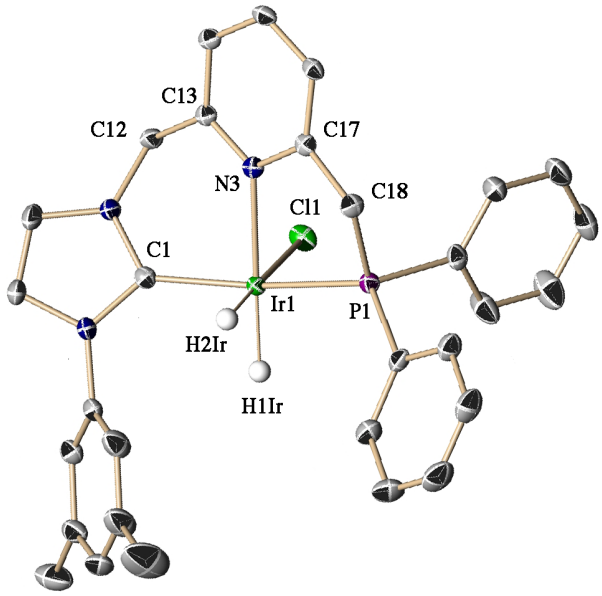

Bond lenghts (Å)		Angles (º)	
Ir(1)–C(1)	2.018(3)	C(1)–Ir(1)–P(1)	165.20(8)
Ir(1)–N(3)	2.186(2)	N(3)–Ir(1)– H(1)Ir	178.7(10)
Ir(1)–P(1)	2.2521(7)	P(1)–Ir(1)–H(1)Ir	97.8(11)
Ir(1)–H(1)Ir	1.591(17)	P(1)–Ir(1)–N(3)	81.92(6)
Ir(1)–H(2)Ir	1.574(17)	C(1)–Ir(1)–H(1)Ir	91.6(10)
Ir(1)–Cl(1)	2.5022(8)	C(1)–Ir(1)–N(3)	88.89(9)

Figure 13. ORTEP drawing at 30% ellipsoid probability, and selected bond lengths (Å) and angles (º), of complex **10b**. Hydrogen atoms, except hydrido ligands, and solvent molecules (THF) have been omitted for clarity.

Reversible H/D exchange of the hydrido ligands, albeit no deuteration of the methylene bridges of the CNP^{Ph} ligand, rapidly took place after exposure of a sample of **10a** in CD_2Cl_2 to deuterium gas (2 bar) at 45 °C (Scheme 7). Similarly, the same outcome was observed upon treating a sample of **10a** with CD_3OD for 24 h.

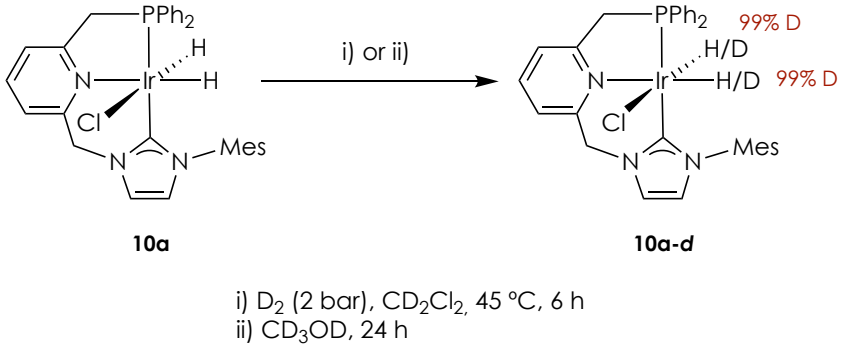

Scheme 7. Reactions with D_2 and CD_3OD of **10a**.

Finally, reaction of the chlorodihydride complex **10b** with H_2 (5 bar) in the presence of KO^tBu (1 equiv) in THF-d_8 produced the quantitative formation of the trihydride derivative **9**. This transformation likely involves a ligand-assisted H—H splitting (Scheme 6).

I.2.2.3.c) Hydrogenation of ketones catalyzed by Ir-CNP^{Ph} complexes

Iridium trihydride complexes analogous to derivative **9** based on lutidine-derived PNP ligands are active catalysts in hydrogenation reactions.[20] Therefore, since the trihydride complex **9** is readily obtained by reaction of **7b(Br)** with H_2 in the presence of base, the Ir–CNP^{Ph} complexes **7** were examined as catalyst precursors in the hydrogenation of ketones (Table 2).[24,73] In the presence of 15 mol% of KO^{t}Bu, complex **7a(Cl)** catalyzed the hydrogenation of acetophenone (**11a**) under 4 bar of H_2 at 30 °C in 2-methyltetrahydrofuran using 1.0 mol% of catalyst with 95% conversion after 16 h (entry 1). Catalyst loading could be decreased to 0.4 mol% by heating the reaction to 60 °C without a significant influence on the reaction rate (entry 2). Moreover, at this temperature, the pressure of H_2 could be reduced to 1 bar leading to full conversion of **11a** (entry 3). Finally, under the latter conditions, complex **7b(Cl)** was found to be slightly less active than its mesityl counterpart (entry 4).

[73] For selected examples of ketone hydrogenation catalyzed by Ir complexes with proton-responsive ligands: (a) L. Dahlenburg, R. Götz, *Eur. J. Inorg. Chem.* **2004**, 888; (b) C. S. Letko, Z. M. Heiden, T. B. Rauchfuss, *Eur. J. Inorg. Chem.* **2009**, 4927; (c) J. E. D. Martins, M. Wills, *Tetrahedron* **2009**, *65*, 5782; (d) J.-H. Xie, X.-Y. Liu, J.-B. Xie, L.-X. Wang, Q.-L. Zhou, *Angew. Chem. Int. Ed.* **2011**, *50*, 7329; (e) W. W. N. O, A. J. Lough, R. H. Morris, *Organometallics* **2012**, *31*, 2152.

Table 2. Hydrogenation of ketones catalyzed by Ir-CNP^{Ph} complexes.[a]

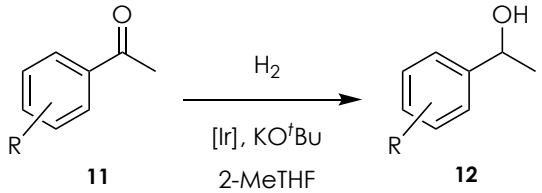

Entry	Ketone	Ir-CNP^{Ph}	T (°C)	Conv. (%)
1[b]	Acetophenone (**11a**)	**7a(Cl)**	30	95
2[b,c]			60	93
3			60	>99
4		**7b(Cl)**	60	98
5	4'-Methoxyacetophenone (**11b**)	**7a(Cl)**	80	96
6	4'-Chloroacetophenone (**11c**)			>99
7	2'-Bromoacetophenone (**11d**)			99
8	2'-Fluoroacetophenone (**11e**)			82
9	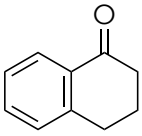 (**11f**)			89

[a] Reaction conditions, unless otherwise noted: 1 bar of H_2, 2-methyltetrahydrofuran, 1.0 mol% [Ir], 15 mol% KO^{t}Bu, 16 h. [S] = 0.1 M. Conversion was determined by ^{1}H NMR spectroscopy. [b] 4 bar of H_2. [c] 0.4 mol% [Ir].

Next, the hydrogenation of a series of substituted acetophenones was also studied using complex **7a(Cl)**. At 80 ^{o}C and under 1 bar of H_2, using 1.0 mol% of catalyst, *p*-methoxy-, *p*-chloro- and *o*-bromoacetophenone (**11b-11d**) were reduced with high conversions to their corresponding secondary alcohols **12b-12d** (entries 5-7). However, the hydrogenation of *o*-fluoroacetophenone (**11e**) was sluggisher (entry 8). Finally, under the same conditions, the reduction of α-tetralone (**11f**), a cyclic ketone, also proceeded with high conversion (entry 9).

The catalytic activity of complex **7a(Cl)** was also tested in the reduction of ketones using isopropanol as the hydrogen source (Table 3).[23,25] In these reactions, a small catalyst loading of 0.1 mol% was employed. Thus, acetophenone was reduced at 80 ^{o}C in 16 hours with 98% conversion (entry 1). The reduction of other acetophenones was also assayed and high conversions were achieved for the *p*-chloro and *o*-fluoro derivatives, whereas the *p*-methoxy- and *o*-bromoacetophenone were reduced with lower rates (entries 2-5). Finally, a low catalytic activity of **7a(Cl)** in the hydrogenation of α-tetralone with ^{i}PrOH was observed (entry 6).

Table 3. Transfer hydrogenation of ketones catalyzed by complex **7a(Cl)**.[a]

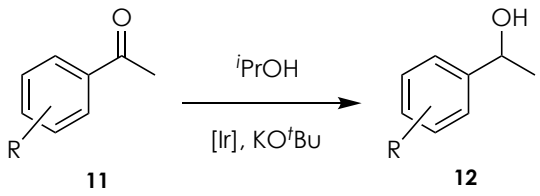

Entry	Ketone	Conv. (%)
1 [b]	Acetophenone (**11a**)	98
2	4'-Methoxyacetophenone (**11b**)	70
3	4'-Chloroacetophenone (**11c**)	95
4	2'-Bromoacetophenone (**11d**)	55
5	2'-Fluoroacetophenone (**11e**)	99
6	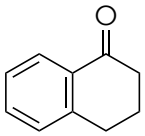 (**11f**)	6

[a] Reaction conditions, unless otherwise noted: *i*PrOH, 80 ºC, 0.1 mol% **7a(Cl)**, 15 mol% KO*t*Bu, [S] = 0.8 M. Reaction time: 16 h. Conversion was determined by ^{1}H NMR spectroscopy. [b] [S] = 1.2 M.

I.2.2.4. Synthesis, reactivity and catalytic applications of carbonyl Ir-CNP^{Ph} complexes

I.2.2.4.a) Synthesis and reactivity of carbonyl Ir-CNP^{Ph} complexes

The cyclooctadiene ligand in complexes **7** is readily displaced by carbon monoxide, as inferred from the reaction of **7a(Cl)** with CO in CH_2Cl_2 (Scheme 8). The ^{1}H NMR spectrum of the carbonyl complex **13(Cl)** evidences a planar coordination of the CNP^{Ph} since the methylene bridge of the phosphine arm appears as a doublet at 4.18 ppm ($^2J_{HP}$ = 10.0 Hz) and the CH_2N hydrogens produce a singlet at 6.11 ppm. Moreover, in the $^{13}C\{^1H\}$ NMR spectrum, the CO ligand appears at 177.2 ppm (d, $^2J_{CP}$ = 10 Hz), while the resonance for the C-2 NHC carbon is found at 178.1 ppm as a doublet signal with a large coupling constant of $^2J_{CP}$ = 99 Hz, further supporting the proposed mutually *trans* arragement of the carbene and the phosphino donor groups.

Complex **13(Cl)** allowed us to evaluate the donating properties of the new CNP^{Ph} ligands. The carbonyl ligand of **13(Cl)** absorbs in the IR spectrum at 1985 cm^{-1}, which is a higher frequency than that corresponding to the [Ir(PNP^{tBu})(CO)]PF_6 analogue complex (1964 cm^{-1}),[10,74] suggesting a lower electron density at the metal center in the Ir–CNP^{Ph} system.

[74] E. Ben-Ari, R. Cohen, M. Gandelman, L. J. W. Shimon, J. M. L. Martin, D. Milstein, *Organometallics* **2006**, *25*, 3190.

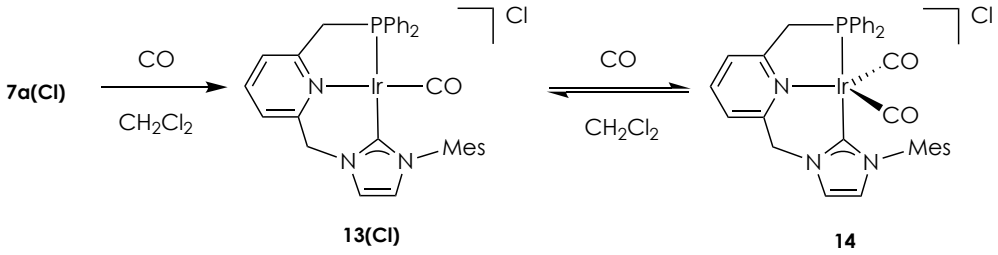

Scheme 8. Synthesis of complexes **13(Cl)** and **14**.

Interestingly, solutions in CH_2Cl_2 of complex **13(Cl)** exposed to CO produced in the IR spectrum two absorption bands at 1946 and 2021 cm^{-1}, in agreement with the coordination of a second CO molecule to the metal (Scheme 8).[12,69e,75] The dicarbonyl derivative **14** was characterized by NMR spectroscopy by pressurizing a solution of **13(Cl)** in CD_2Cl_2 with CO (1 bar). The presence in the ^1H NMR spectrum of a singlet signal at 6.09 ppm for the CH_2N arm, and a doublet at 4.29 ppm ($^2J_{HP}$ = 10.9 Hz) attributable to the CH_2P moiety, suggests the existence of a symmetry plane containing the CNP^{Ph}–Ir coordination plane. Moreover, in the $^{13}C\{^1H\}$ NMR spectrum a singlet at 177.4 ppm is observed for the CO ligands and a doublet at 161.3 ppm (J_{CP} = 94 Hz) is produced by the C-2 NHC carbon. These data support a meridional coordination of the CNP^{Ph} ligand,[12] at variance with the coordination geometry in the also pentacoordinated complexes **7**.

The carbonyl complexes **13(Cl)** and **14** exhibit a dynamic behavior in solution as deduced by registering their ^1H NMR spectra in the temperature range between 193 and 298 K (Figures 14 and 15). In the ^1H NMR spectra of **14**, at temperatures below 273 K, the doublet resonance at 4.29 ppm caused by the CH_2P bridge of the ligand broadens, and eventually splits into two doublets of doublets appearing at 4.50 ($^2J_{HH}$ = 10.5 Hz, $^2J_{HP}$ =

[75] (a) L. Vaska, *Science* **1966**, *152*, 769; (b) A. V. Polukeev, O. F. Wendt, *Organometallics* **2015**, *34*, 4262.

18.0 Hz) and 4.09 ppm ($^2J_{HH}$ = 10.5 Hz, $^2J_{HP}$ = 16.5 Hz) at 193 K. A similar behaviour is observed for the signal of the CH_2N arm, whereas the other resonances of the CNP^{Ph} ligand remain unchanged. An energy barrier ($\Delta G^{\ddagger}$) of 10.0 kcal mol^{-1} was estimated at the coalescence temperature (214 K) for the observed process.[70] Complex **13(Cl)** exhibits an analogous dynamic process, albeit signal splitting was not observed at the lowest temperature studied (193 K) indicating that the fluxional process has a lower barrier than that of **14**.

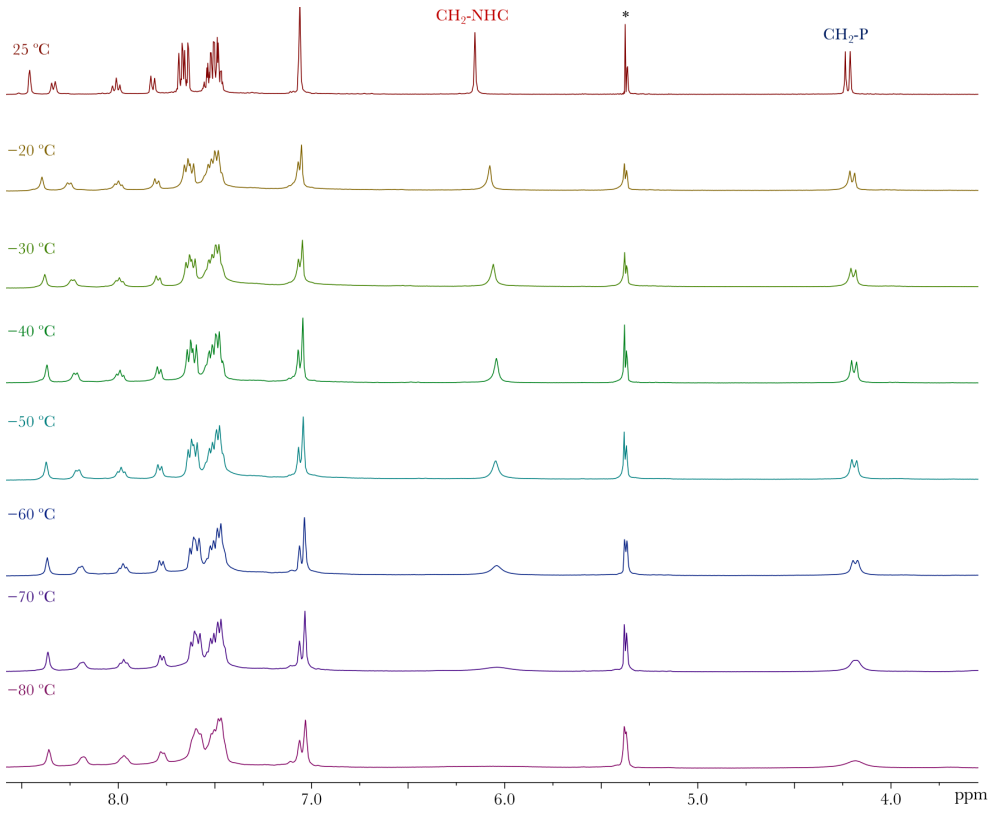

Figure 14. VT-^{1}H NMR spectra (CD_2Cl_2, 400 MHz) of **13(Cl)**.

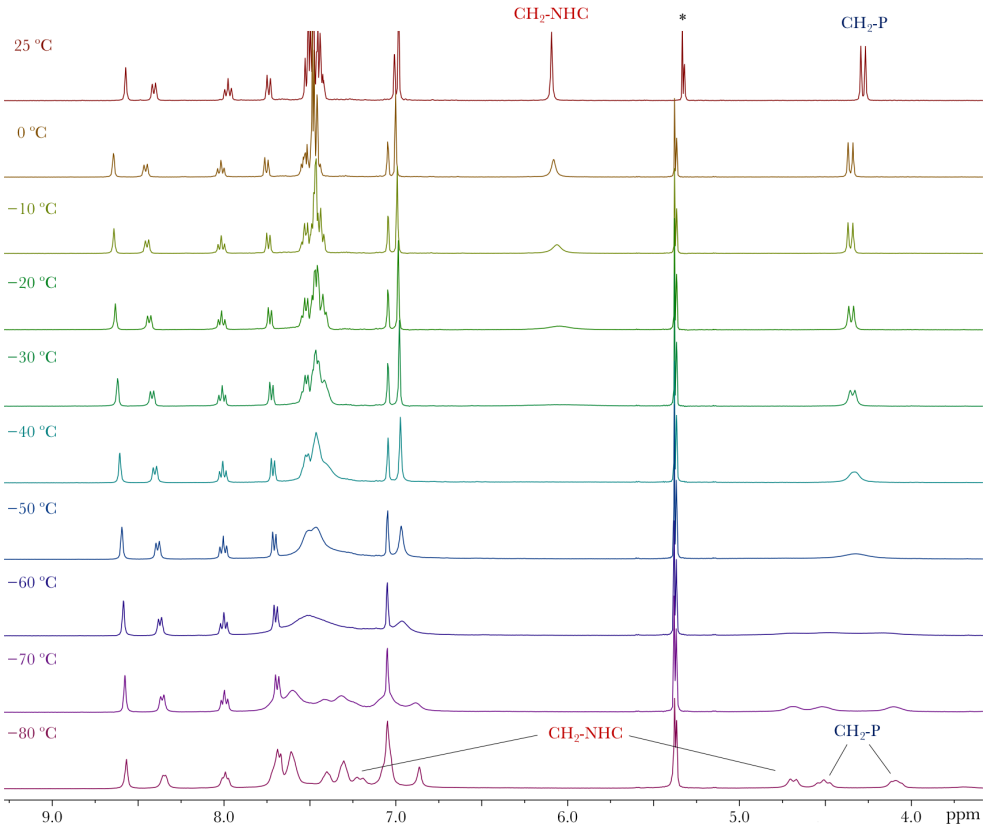

Figure 15. VT-^{1}H NMR spectra (CD_2Cl_2, 400 MHz) of **14**.

In square-planar Pd[76] and octahedral Ru complexes incorporating CNC ligands,[67b] similar dynamic processes have been assigned to the slow interconversion between the two twisted conformations adopted by the C^{2}(NHC)–M–N(Py) chelate rings of the pincer ligand. Consequently, the observed fluxionality in derivatives **13(Cl)** and **14** can be attributed to the equilibration of the two otherwise diastereotopic hydrogens of the CH_2P and CH_2-NHC methylene bridges (Figure 16).

[76] (a) S. Gründemann, M. Albrecht, J. A. Loch, J. W. Faller, R. H. Crabtree, *Organometallics* **2001**, *20*, 5485; (b) J. R. Miecznikowski, S. Gründemann, M. Albrecht, C. Mégret, E. Clot, J. W. Faller, O. Eisenstein, R. H. Crabtree, *Dalton Trans.* **2003**, 831.

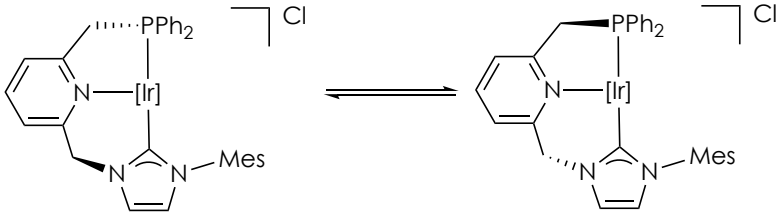

[Ir] = Ir(CO), **13(Cl)**; $Ir(CO)_2$, **14**

Figure 16. Interconversion between the limiting conformations of **13(Cl)** and **14**.

Deprotonation of the carbonyl derivative **13(Cl)** was brought about at room temperature with KO^{t}Bu in THF leading to the formation of an unseparable mixture of the deprotonated tautomeric species **15a** and **15b** (Scheme 9). These derivatives were isolated in good yield (70%) as a red solid that is sensitive to chlorinated solvents. The ratio between both species was determined by ^{1}H NMR spectroscopy and found to depend on the solvent. In THF-d_8, the mixture of **15a/15b** appeared in a 9:1 ratio (Figure 17), whereas a ratio of 8:2 was observed in C_6D_6. Moreover, the CH_2N bridge of the pincer ligand of complex **15a** appears in the ^{1}H NMR spectrum, registered in THF-d_8, as a singlet signal at 4.72 ppm (2H) and the methyne CHP arm produces a doublet resonance at 3.84 ppm ($^2J_{HP}$ = 1.9 Hz, 1H). On the other hand, complex **15b** shows the CHN pincer arm as a singlet peak at 6.17 ppm (1H) and the methylene CH_2P moiety as doublet signal at 3.51 ppm ($^2J_{HP}$ = 11.4 Hz, 2H). In agreement with the presence of dearomatized central rings, both complexes show the resonances corresponding to the pyridine derived fragments at upfield chemical shifts (6.30-5.37 ppm). In the $^{13}C\{^1H\}$ NMR spectrum, derivative **15a** exhibits the resonance produced by the carbene carbon as a doublet at 182.8 ppm (J_{CP} = 92 Hz) and that of the CO ligand at 182.0 ppm (d, J_{CP} = 10 Hz).

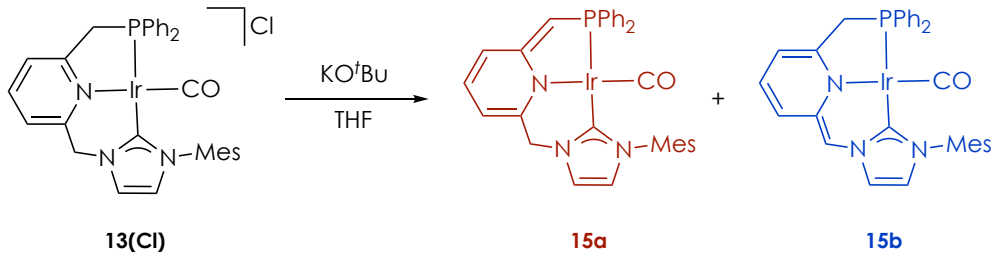

Scheme 9. Synthesis of complexes **15a** and **15b**.

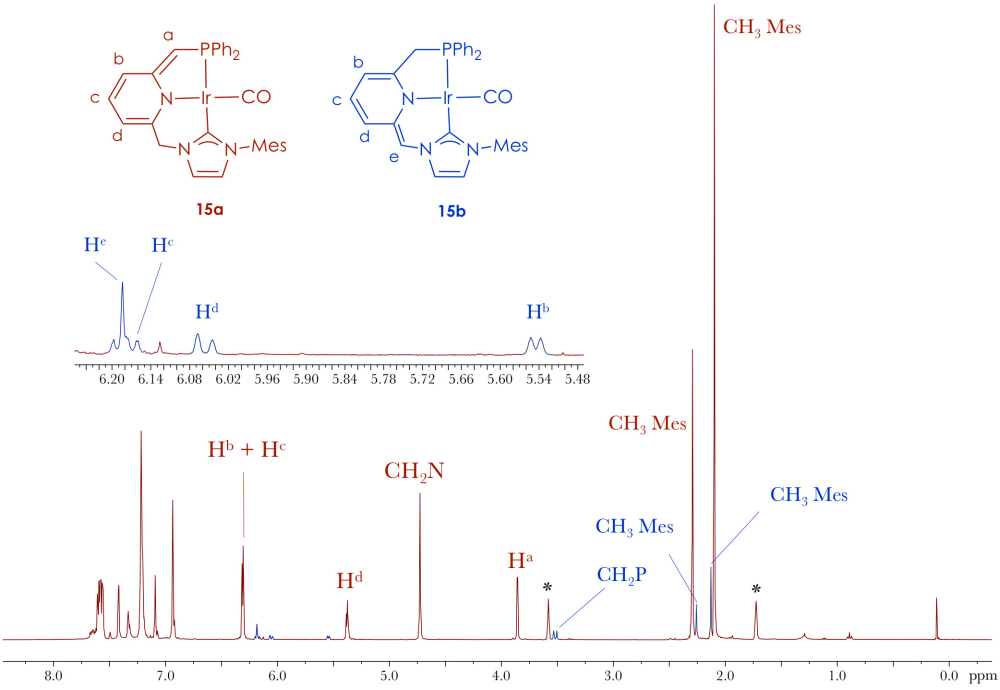

Figure 17. ^{1}H NMR spectrum (500 MHz) of the mixture of complexes **15a** and **15b** in THF-d_8.

In the IR spectrum of **15a/15b**, a band at 1938 cm^{-1} is observed. This value is similar to those of Ir(PCP)(CO) (ν_{CO} = 1920 cm^{-1}) and Ir(PNP^{tBu}*)(CO) (ν_{CO} = 1932 cm^{-1}) complexes,[7,77] and red shifted with respect to the absorption of **13(Cl)** (ν_{CO} = 1985 cm^{-1}).[18] The relatively low stretching frequency of the CO ligand reflects significant back-bonding from the metal to the π* orbital of the carbonyl, as expected for terminal carbonyls in electron-rich Ir(I) complexes.[7,77]

Cooling of a saturated solution of the mixture of complexes **15** in THF provided crystals of **15a** adequate for an X-ray diffraction study (Figure 18). Comparison of the C(18)-C(19) (1.37 Å) and C(19)-P(1) (1.74 Å) bond distances with the PyC=CP (1.39 Å) and CH-P (1.77 Å) lengths in the Ir(PNP^{tBu}*)(CO) complex corroborates the deprotonation of the methylene bridge of the phosphine arm.[78] Additionally, alternating C–C distances in the pyridine moiety evidence ring dearomatization as shown by the elongated C(18)–C(17) and C(16)–C(15) distances of 1.460 and 1.396 Å, and shortened C(17)–C(16) and C(15)–C (14) bond lengths of 1.343 and 1.378 Å, respectively (average C–C bond in the pyridine molecule: 1.38 Å) (Figure 18). Finally, the C(1)-Ir(1)-P(1) angle of 168.3(2)° indicates that the distorted square planar geometry remains despite the ligand deprotonation.

[77] (a) K. Krogh-Jespersen, M. Czerw, K. Zhu, B. Singh, M. Kanzelberger, N. Darji, P. D. Achord, K. B. Renkema, A. S. Goldman, *J. Am. Chem. Soc.* **2002**, *124*, 10797; (b) I. Göttker-Schnetmann, P. S. White, M. Brookhart, *Organometallics* **2004**, *23*, 1766.
[78] For the solid state structure of an analogous Ir(PNP*)(CO) complex: ref. 18.

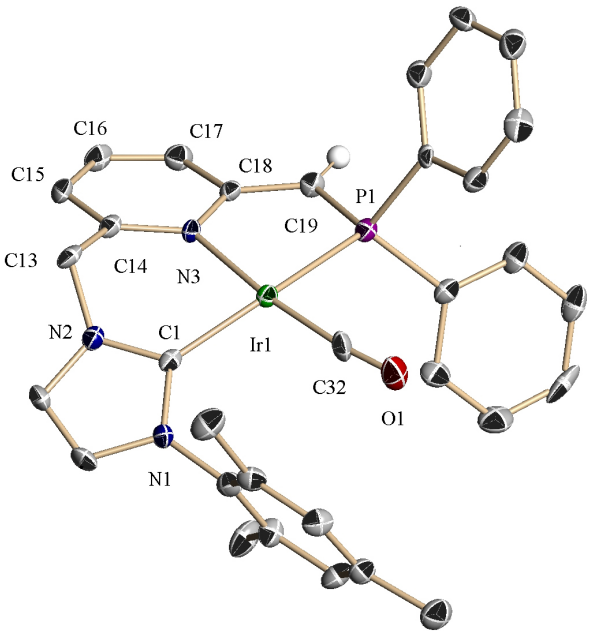

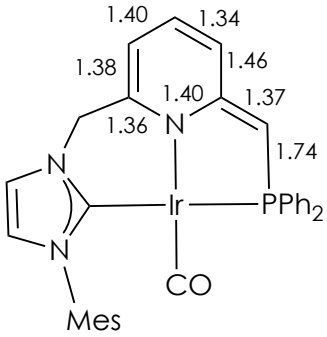

Bond lenghts (Å)		Angles (º)	
Ir(1)-C(1)	2.034(8)	C(1)-Ir(1)-P(1)	168.3(2)
Ir(1)-N(3)	2.127(5)	C(1)-Ir(1)-C(32)	97.2(3)
Ir(1)-P(1)	2.285(2)	C(32)-Ir(1)-N(3)	172.9(3)
Ir(1)-C(32)	1.818(8)	C(1)-Ir(1)-N(3)	89.7(2)
C(18)-C(19)	1.370(10)	P(1)-Ir(1)-N(3)	82.64(16)
P(1)-C(19)	1.743(7)	C(32)-Ir(1)-P(1)	90.3(2)

Figure 18. ORTEP drawing at 30% ellipsoid probability, and selected bond lengths (Å) and angles (º), of complex **15a**. All hydrogen atoms except the methyne proton and solvent molecule (THF) have been omitted for clarity.

As mentioned above, the ratio of complexes **15a** and **15b** in solution depends on the solvent, in strong agreement with the existence of an equilibrium between the tautomers. Further support for the proposed equilibrium was obtained from the ^{1}H-^{1}H EXSY spectrum of **15a/15b** in wet THF-d_8 registered at 25 ºC (Figure 19). Intense exchange cross-peaks were observed between the signals of the methyne and methylene fragments of **15a** and **15b** with those of water (red squares). Moreover, cross-peaks due to exchange between the hydrogens of the CHP and CH_2N bridges of **15a** (blue square), and the protons of the CHP and CH_2N moieties of **15a** with those of the CH_2P and CHN moieties of **15b**, respectively, were also detected (green squares). These observations indicate that interconversion between the tautomeric species **15a** and **15b** should take place both intra- and intermolecularly throught reversible protonation/deprotonation mediated by water acting as proton shuttle.[79]

[79] T. Cheisson, A. Auffrant, *Dalton Trans.* **2016**, *45*, 2069.

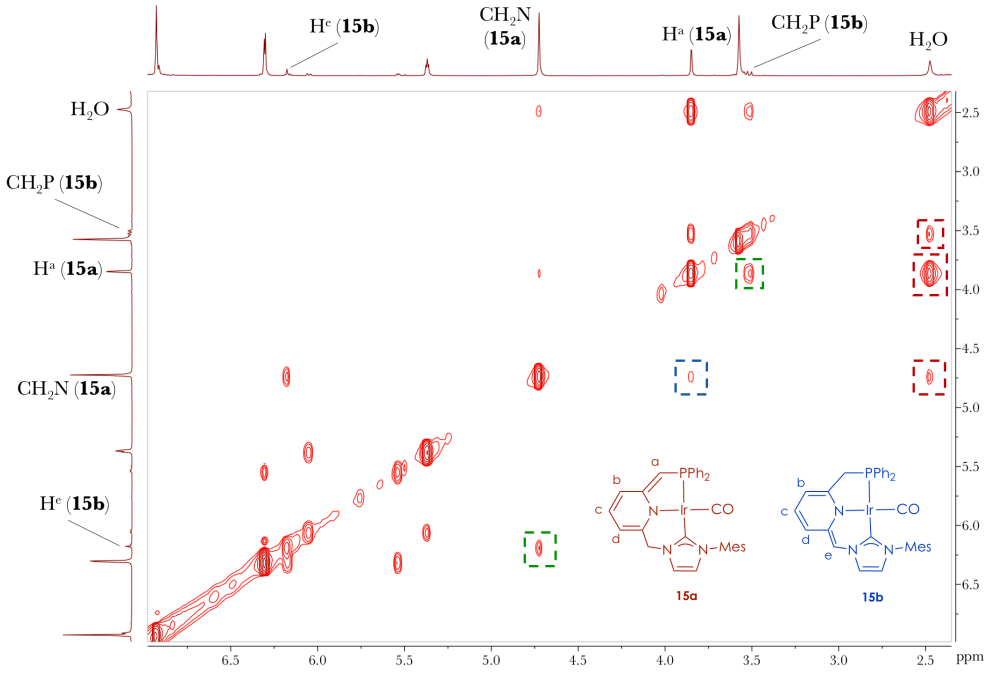

Figure 19. Region of the ^{1}H-^{1}H EXSY spectrum of **15a/15b** in wet THF-d_8 (500 MHz, 25 ºC).

I.2.2.4.b) Hydroboration of CO_2 catalyzed by carbonyl Ir-CNP^{Ph} complexes

The catalytic performance of complexes **15a/15b** in the hydroboration of CO_2 with catecholborane (HBcat) was explored. Reactions were carried out under 2 bar of CO_2 using 1.0 mol% of **15a/15b** in THF-d_8 at 30 ºC. Selective reduction of CO_2 to the methoxyborane derivative (CH_3OBcat) was confirmed by the appearance of a singlet at 3.81 ppm in the ^{1}H{^{11}B} NMR spectra of the catalytic reactions, and a broad signal in the ^{11}B NMR spectra at 22.5 ppm (Figures 20 and 21). Also, the concomitant formation of diboroxane, catBOBcat, was established by the precipitation of

a white solid after removal of THF-d_8 under vacuum and addition of C_6H_6. This precipitate produces in the ^1H NMR spectrum (THF-d_8) two multiplets centered at δ 6.83 and 6.93, and in the ^{11}B NMR experiment a broad signal at δ 16.5, which coincide with the literature spectroscopic data for catBOBcat.[80]

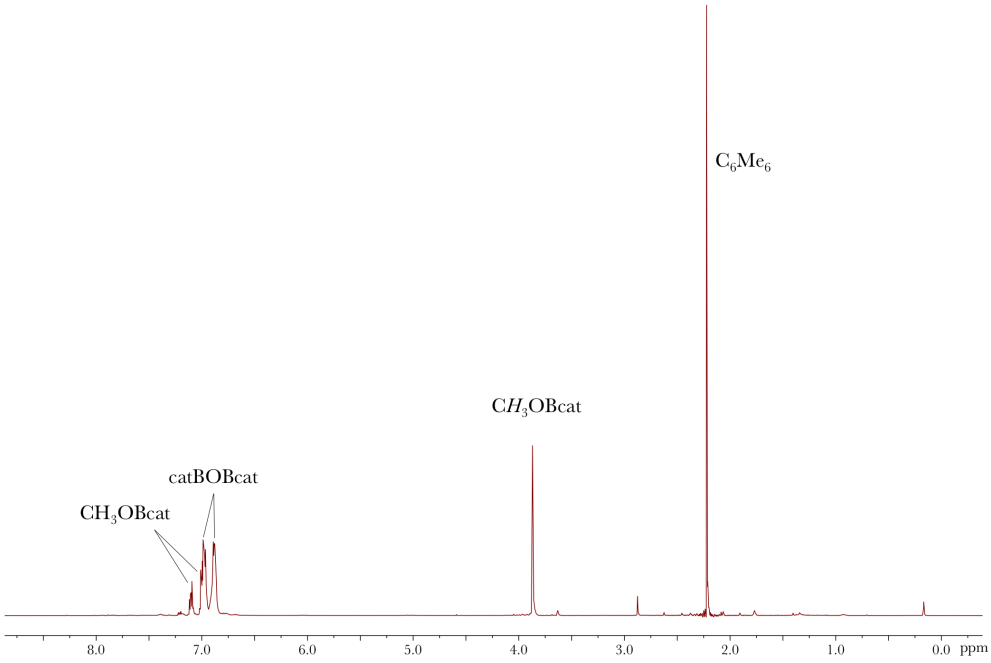

Figure 20. $^1H\{^{11}B\}$ NMR spectrum (400 MHz, THF-d_8) of the hydroboration of CO_2 with HBcat catalyzed by **15a/15b** (Table 4, entry 2).

[80] A. Lang, J. Knizek, H. Nöth, S. Schur, M. Thomann, *Z. Anorg. Allg. Chem.* **1997**, *623*, 901.

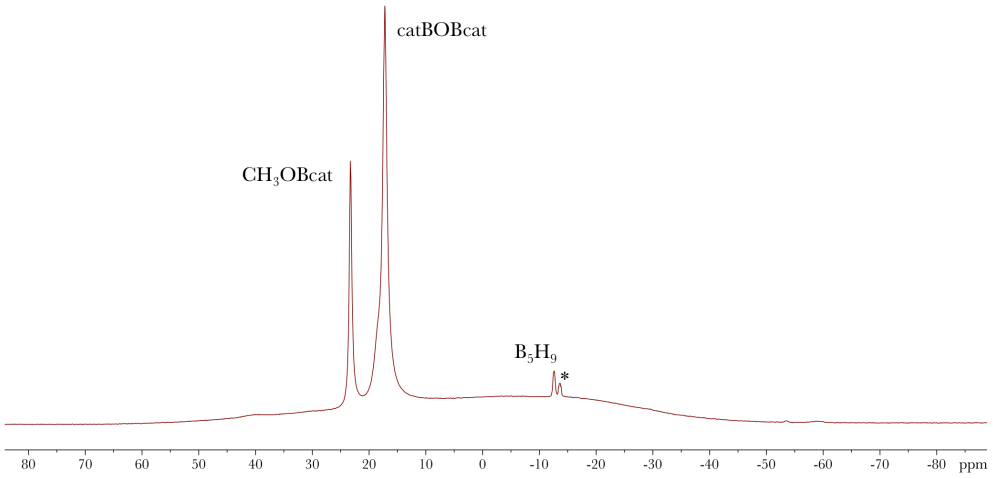

Figure 21. ^{11}B NMR spectrum (128 MHz, THF-d_8) of the hydroboration of CO_2 with HBcat catalyzed by **15a/15b** (Table 4, entry 2) (*, B_5H_9 and other boron species from commercial HBcat).

Initial catalytic reactions were found difficult to reproduce. Consequently, a detailed screening of the reaction parameters was carried out, evidencing that the presence of water has a significant influence on the reaction rate. Table 4 collects the results of the hydroboration of CO_2 with HBcat catalyzed by complexes **15a/15b** in the presence of variable amounts of water. While all the reactions proceeded to completion after prolongued reaction times, for a meaningful comparison of the catalytic activity, TON values were determined after 1.5 h.

Table 4. Hydroboration of CO_2 with HBcat catalyzed by carbonyl Ir-CNP^{Ph} complexes.[a]

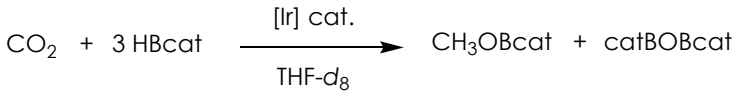

Entry	Catalyst	H_2O (mol%)	Yield (%)	TON
1	**15a/15b**	1	18	54
2		3	24	72
3		5	28	84
4		6	25	75
5[b]	**13(Cl)**	3	26	78

[a] Reaction conditions: 1.0 mol% [Ir], 2 bar CO_2, 30 °C, THF-d_8, [HBcat] = 0.5 M. Reaction time: 1.5 h, unless otherwise noted. Conversions were determined by $^1H\{^{11}B\}$ NMR spectroscopy using hexamethylbenzene as internal standard. TON values based on moles of B-H bonds reacted per mole catalyst: (mmol methoxyborane × 3)/(mmol Ir). [b] Reaction time: 16 h.

In the presence of 1 mol% of H_2O, formation of 18% of methoxyborane was observed (TON = 54; TOF = 36 h^{-1}) (entry 1). A gradual increase of the water content up to 5 mol% produced a faster transformation of CO_2 to methoxyborane, reaching up to 28% conversion (TON = 84; TOF = 56 h^{-1}) (entries 2 and 3). However, a further increase of the amount of water to 6 mol% led to a slight erosion in the catalytic activity (entry 4). It is interesting to note that complex **13(Cl)** was a poorer catalyst than **15a/15b** providing 78 turnovers after 16 h (entry 5).

Since a significant dependence on the hydroborane nature in the reaction rate and selectivity can be expected, the catalytic hydroboration of CO_2 with pinacolborane (HBpin) was also investigated. As in the case of the reactions with HBcat, a marked influence of the presence of water was noticed. Catalytic reactions were carried out with low catalyst loadings of 0.2 mol% of **15a/15b** and using 1 bar of CO_2 at 30 ºC (Table 5). Although, the use of pinacolborane in the hydroboration of CO_2 may proceed to the formate (HCO_2Bpin), acetal ($H_2C(OBpin)_2$) or methoxy (CH_3OBpin) derivatives, or mixtures thereof, formation of formoxyborane was found kinetically limiting (Figure 22 and 23).

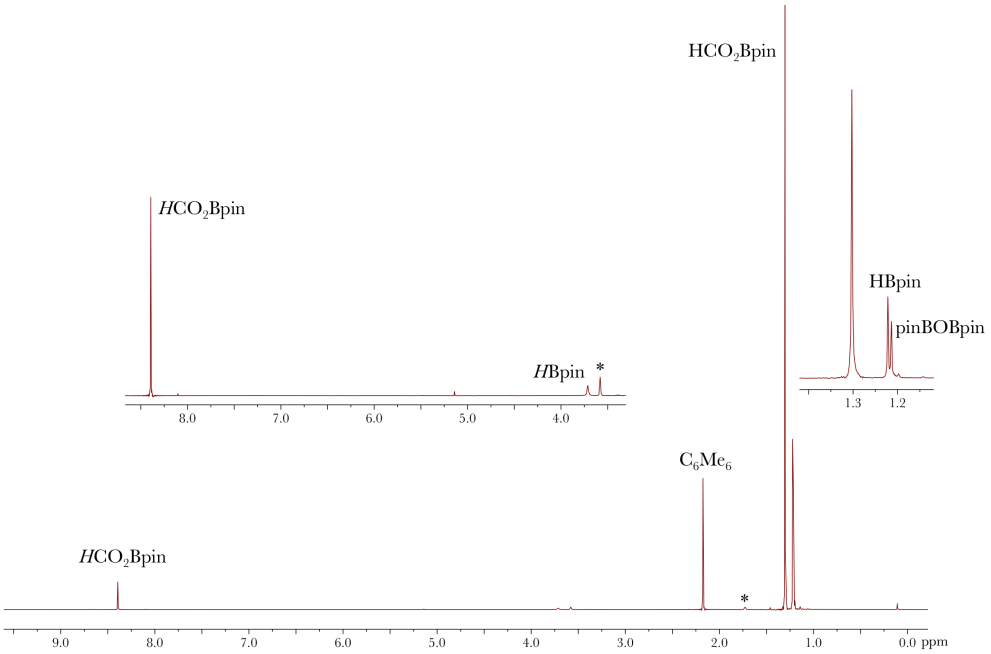

Figure 22. $^1H\{^{11}B\}$ NMR spectrum (400 MHz, THF-d_8) of the hydroboration of CO_2 with HBpin catalyzed by **15a/15b** (Table 5, entry 3) (reaction time: 10 min). (* solvent residual signals).

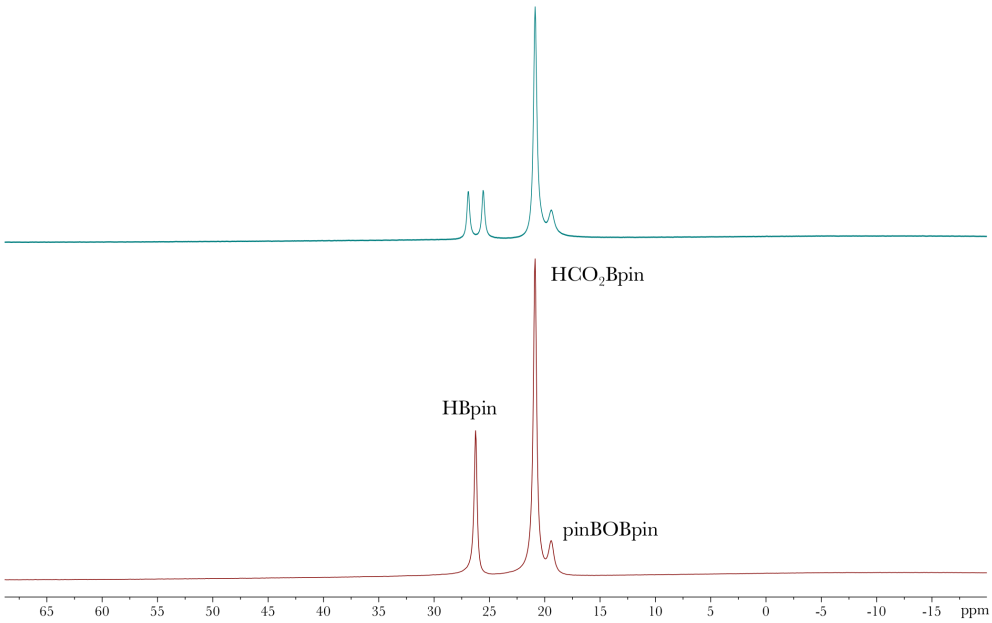

Figure 23. ^{11}B (top) and $^{11}B\{^1H\}$ (bottom) NMR spectra (128 MHz, THF-d_8) of the hydroboration of CO_2 with HBpin catalyzed by **15a/15b** (Table 5, entry 3) (reaction time: 10 min).

Table 5. Hydroboration of CO_2 with HBpin catalyzed by **15a/15b**.[a]

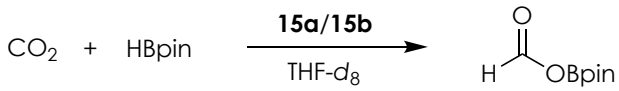

Entry	H_2O (mol%)	Yield (%)	TON
1	1	30	150
2	2	72	360
3	3	79	395
4	6	80	400
5	7	83	415
6[b]	3	74	740

[a] Reaction conditions, unless otherwise noted: 0.2 mol% **15a/15b**, 1 bar CO_2, 30 °C, THF-d_8, [HBpin] = 0.4 M. Reaction time: 20 min. Conversions were determined by $^1H\{^{11}B\}$ NMR spectroscopy using hexamethylbenzene as internal standard. TON values as determined from (mmol HCO_2Bpin)/(mmol Ir). [b] 0.1 mol% **15a/15b**. Reaction time: 1.0 h.

All the reactions proceeded to conversions of HBpin higher than 90%, although TON values were compared after a reaction time of 20 min. In the presence of 1 mol% of water, the formoxyborane derivative was obtained in 30% yield (TOF = 450 h^{-1}, entry 1), whereas upon sucessive additions of water up to 7 mol% a *ca.* three-fold rise of the catalytic activity was observed (TOF = 1,245 h^{-1}) (entries 2-5). It should be pointed out that in the presence of 7 mol% of water, the maximum theoretical yield of formoxyborane is 86% after taking into account the hydrolysis of pinacolborane to pinBOBpin.

Moreover, lower catalyst loadings were tested for this reaction. With 0.1 mol% of **15a/15b**, a 74% NMR yield of HCO_2Bpin after 1 h was obtained, which represents a notable TOF value of 740 h^{-1} (entry 6). Among the few catalysts that selectively perform the hydroboration of CO_2 to formoxyborane,[42c,53,54,56,57] only a palladium pincer complex reported by Hazari *et al.* provides faster reaction rates with low catalyst loadings (TOF >8,500 h^{-1} with 0.01 mol% Pd).[57]

I.2.2.4.c) Metal species formed under catalytic conditions

In an attempt to study the metal species formed under catalytic conditions, the hydroboration of CO_2 with HBcat in THF-d_8 using 20 mol% of **15a/15b** was investigated by NMR spectroscopy. After reaction completion, a single peak at 16.9 ppm was observed in the $^{31}P\{^1H\}$ NMR spectrum; whereas the ^1H NMR experiment showed the formation of a dihydride compound as deduced from the appearance of two doublets of doublets signals at −17.5 ($^2J_{HP}$ = 12 Hz, $^2J_{HH}$ = 2 Hz) and −8.3 ppm ($^2J_{HP}$ = 22 Hz, $^2J_{HH}$ = 2 Hz). To unequivocally identify this newly formed species, a solution of **15a/15b** in THF-d_8 was exposed to H_2 (5 bar) (Scheme 10), leading to the quantitative formation of a species, **16**, characterized in the ^1H NMR spectrum by two doublets of doublets appearing at δ −8.64 ($^2J_{HP}$ = 20.8 Hz, $^2J_{HH}$ = 1.5 Hz) and δ −16.59 ($^2J_{HP}$ = 11.3 Hz, $^2J_{HP}$ = 1.5 Hz). Derivative **16** contains a deprotonated CNP^{Ph} ligand as inferred from the appareance of a doublet at 3.93 ppm ($^2J_{HP}$ = 2.7 Hz), attributable to the =CHP linker, and an AX system composed of two doublets appearing at 5.01 and 4.70 ppm ($^2J_{HH}$ = 14.3 Hz) due to the CH_2N arm hydrogens. The

$^{13}C\{^{1}H\}$ NMR spectrum shows for the CO ligand a broad resonance at 176.5 ppm; while the C-2 NHC carbon appears at 162.7 ppm as a doublet with a large $^{2}J_{CP}$ of 92 Hz, indicative of a meridional coordination of the deprotonated CNP^{Ph} ligand. Finally, the $^{31}P\{^{1}H\}$ NMR spectrum presents a singlet at δ 8.8 ppm, making evident that the formation of complex **16** does not take place during the hydroboration reaction.

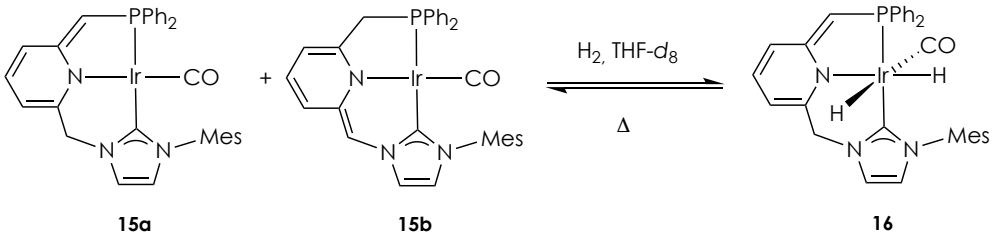

15a **15b** **16**

Scheme 10. Reaction of **15a/15b** with H_2.

Since derivative **15a** is structurally similar to carbonyl Ir complexes containing anionic PCP pincer ligands, it was deemed interesting to perform a detailed study of the reactivity of this species towards H_2. Solutions of **16** in THF-d_8 lose H_2 upon heating leading to the regeneration of the mixture of **15a** and **15b**. An analogous reversible dihydrogen addition has been observed for Ir(PCP)(CO) complexes,[7] what has been attributed to the rigid square-planar geometry of the Ir(I) complex that should disfavor oxidative addition of nonpolar substrates.[81] Moreover, upon heating to 60 °C a THF-d_8 solution of **16** under D_2 (1 bar), complete deuteration of the CH_2N and =CHP arms, as well as of the hydrido ligands, occurred. Furthermore, in the ^{1}H-^{1}H exchange spectroscopy (EXSY) spectrum (mixing time = 0.8 s) of **16** in wet THF-d_8 registered at 25 °C, intense exchange cross peaks are observed

[81] (a) A. Dedieu, A. Strich, *Inorg. Chem.* **1979**, *18*, 2940; (b) J.-Y. Saillard, R. Hoffmann, *J. Am. Chem. Soc.* **1984**, *106*, 2006.

between the signal corresponding to =CHP and water. These observations suggest a significant acidity of the CH_2/CH pincer bridges that can participate in exchange processes with the hydrido ligands.

In a further attempt to identify the species formed after the hydroboration of CO_2 mediated by complexes **15a/15b**, a THF-d_8 solution of the carbonyl complex **13(Cl)** was pressurized with 1 bar of H_2 (Scheme 11). Formation of the dihydride complex **17** was confirmed from the observation of resonances in the ^{1}H NMR spectrum appearing at −17.45 ppm (dd, $^2J_{HP}$ = 11.7 Hz, $^2J_{HH}$ = 1.6 Hz) attributable to the IrH *trans* to the pyridine moiety, and at −8.32 ppm (ddd, $^2J_{HP}$ = 22.2 Hz, $^2J_{HH}$ = 1.6 Hz, $^4J_{HH}$ = 1.6 Hz) caused by the hydrido ligand placed *cis* to the *N*-donor fragment that couples with the other IrH hydrogen and one of the hydrogens of the CH_2P bridge.[7,8,10] Meanwhile, the ^{31}P{^{1}H} NMR spectrum displayed a singlet signal at 16.9 ppm. Resonances in the ^{13}C{^{1}H} NMR spectrum of **17** include a singlet at 175.0 ppm, corresponding to the carbonyl ligand, and a doublet with a large J_{CP} of 100 Hz appearing at 156.9 ppm, due to the C-2 NHC carbon. Moreover, the IR spectrum shows two bands at 2338 and 2085 cm^{-1} for the Ir—H stretching and an absortion to 1987 cm^{-1} for the CO ligand. The NMR data of **17** is in agreement with the observed signals previously commented at the end of the catalytic reaction, and demonstrates that ligand protonation occurs under catalytic conditions. Complex **17** losses H_2 upon exposure to vacuum, regenerating complex **13(Cl)**.[81]

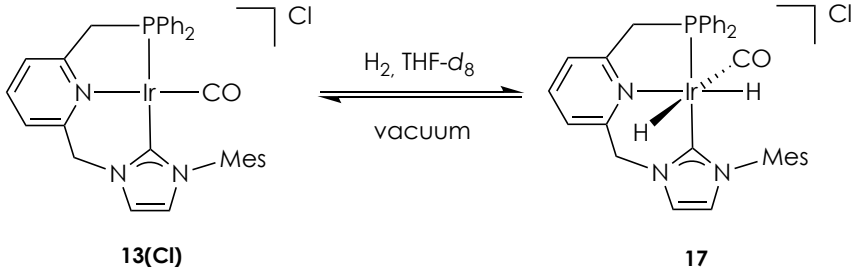

13(Cl) **17**

Scheme 11. Reversible H_2 addition to complex **13(Cl)**.

In addition, the solution obtained upon completion of the catalytic reaction between CO_2 and HBcat in the presence of 20 mol% of **15a/15b** was analyzed by ESI-MS. A peak at *m/z* 698 (relative intensity 100%) attributable to the cationic fragment $[IrH_2(CNP^{Ph})(CO)]^+$ (**17**$^+$) was detected in the ESI-MS positive mode spectrum (Figure 24). In the negative mode, a peak at *m/z* 227 (relative intensity 100%) that has been assigned to the arylspiroboronate ester $[Bcat_2]^-$ was observed (Figure 25). Formation of this anion, along with other boron species such as B_2cat_3 and BH_3, has been previously observed in the degradation of HBcat promoted by nucleophiles and metal complexes containing anionic ligands.[82] Similarly, although HBpin has been shown to be less prone to degradation than HBcat,[83] analysis of a

[82] (a) J. A. Melanson, C. M. Vogels, A. Decken, S. A. Westcott, *Inorg. Chem. Commun.*, **2010**, *13*, 1396; (b) G. M. Lee, C. M. Vogels, A. Decken, S. A. Westcott, *Eur. J. Inorg. Chem.* **2011**, 2433; (c) S. A. Westcott, T. B. Marder, R. T. Baker, J. C. Calabrese, *Can. J. Chem.* **1993**, *71*, 930; (d) S. A. Westcott, H. P. Blom, T. B. Marder, R. T. Baker, *J. Am. Chem. Soc.* **1992**, *114*, 8863; (e) S. A. Westcott, H. P. Blom, T. B. Marder, R. T. Baker, J. C. Calabrese, *Inorg. Chem.* **1993**, *32*, 2175; (f) S. Lachaize, K. Essalah, V. Montiel-Palma, L. Vendier, B. Chaudret, J.-C. Barthelat, S. Sabo-Etienne, *Organometallics* **2005**, *24*, 2935; (g) W. Clegg, M. R. J. Elsegood, A. J. Scott, T. B. Marder, C. Dai, N. C. Norman, N. L. Pickett, E. G. Robins, *Acta Crystallogr. Sect. C: Cryst. Struct. Commun.* **1999**, *55*, 733; (h) S. A. Westcott, N. J. Taylor, T. B. Marder, R. T. Baker, N. J. Jones, J. C. Calabrese, *J. Chem. Soc. Chem. Commun*. **1991**, 304; (i) J. Knizek, H. Nöth, *Eur. J. Inorg. Chem.* **2011**, 1888; (j) S. Harder, J. Spielmann, *J. Organomet. Chem.* **2012**, *698*, 7.

[83] (a) C. M. Crudden, Y. B. Hleba, A. C. Chen, *J. Am. Chem. Soc.* **2004**, *126*, 9200; (b) C. E. Tucker, J. Davidson, P. Knochel, *J. Org. Chem.* **1992**, *57*, 3482; (c) C. M. Crudden, D.

catalytic reaction with HBpin using 20 mol% of **15a/15b** by ESI-MS allowed for the detection of the cationic fragment $\mathbf{13}^+$ and the anion $[Bpin_2]^-$ (*m/z* 243; relative intensity 100%).[84] Formation of $[BR_2]^-$ anions could involve the nucleophilic attack of the hydroborane by the methyne carbon of the deprotonated CNP^{Ph}* ligand,[79] or a ligand-assisted B–H activation as shown by Milstein *et al.* for related Ru complexes.[85]

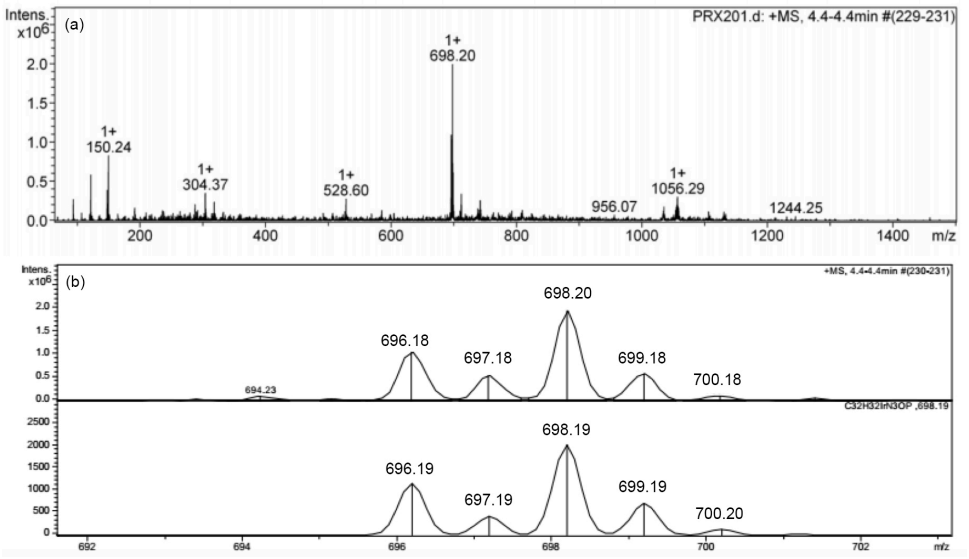

Figure 24. a) ESI-MS positive mode spectrum of the reaction of **15a/15b** with HBcat (5 equiv) under CO_2 (2 bar); b) experimental (top) and simulated (bottom) isotope patterns for *m/z* 698.

Edwards, *Eur. J. Org. Chem.* **2003**, 4695; (d) I. Beletskaya, A. Pelter, *Tetrahedron* **1997**, *53*, 4957.

[84] (a) J. Dale, *J. Chem. Soc.* **1961**, 922; (b) C. Kleeberg, A. G. Crawford, A. S. Batsanov, P. Hodgkinson, D. C. Apperley, M. S. Cheung, Z. Lin, T. B. Marder, *J. Org. Chem.* **2012**, *77*, 785; (c) W. G. Henderson, M. J. How, G. R. Kennedy, E. F. Mooney, *Carbohydr. Res.* **1973**, *28*, 1; (d) H. Wu, J. M. Garcia, F. Haeffner, S. Radomkit, A. R. Zhugralin, A. H. Hoveyda, *J. Am. Chem. Soc.* **2015**, *137*, 10585.

[85] A. Anaby, B. Butschke, Y. Ben-David, L. J. W. Shimon, G. Leitus, M. Feller, D. Milstein, *Organometallics* **2014**, *33*, 3716.

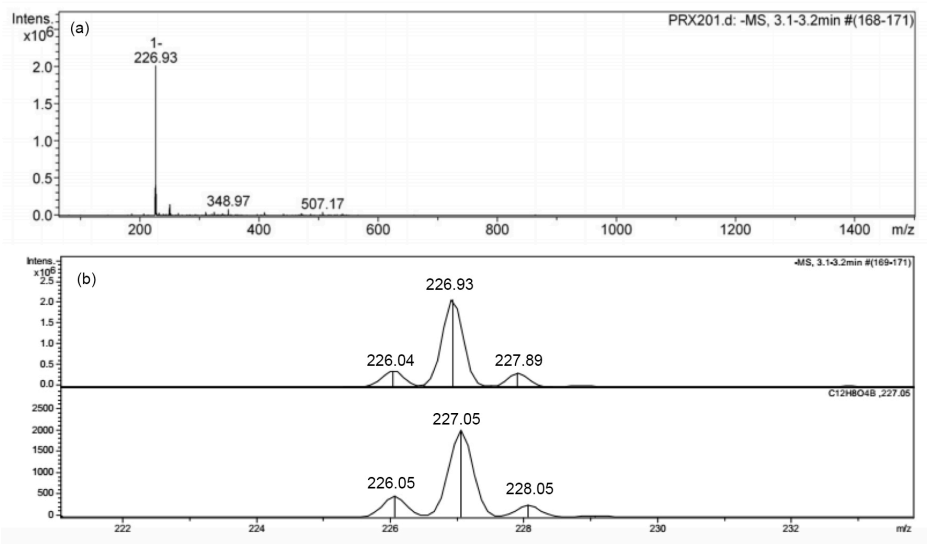

Figure 25. a) ESI-MS negative mode spectrum of the reaction of **15a/15b** with HBcat (5 equiv) under CO_2 (2 bar); b) experimental (top) and simulated (bottom) isotope patterns for *m/z* 227.

Since the reactions with HBcat are significantly slower than those with HBpin, the hydroboration of CO_2 (2 bar) with HBcat in THF-d_8 using 10 mol% of **15a/15b** was monitored by NMR spectroscopy. In the $^{31}P\{^1H\}$ NMR spectrum, a singlet resonance at 15.7 ppm was observed during the reaction course. The ^1H NMR spectrum revealed the formation of a hydride species, as inferred from the appearance of a doublet peak at −6.9 ppm ($^2J_{HP}$ = 21 Hz). To characterize this newly formed species, complex **13(Bcat$_2$)** was easily synthetized after anion exchange of **13(Cl)** with Li[Bcat$_2$][86] and reacted with HBcat (Scheme 12). Thus, addition of a slight excess of HBcat (1.5 equiv) to a THF-d_8 solution of **13(Bcat$_2$)** produced the quantitative formation of the borylhydride iridium complex **18(Bcat$_2$)**. Attempted

[86] M. I. Webb, N. R. Halcovitch, E. G. Bowes, G. M. Lee, M. J. Geier, C. M. Vogels, T. O'Neill, H. Li, A. Flewelling, A. Decken, C. A. Gray, S. A. Westcott, *J. Heterocycl. Chem.* **2014**, *51*, 157.

isolation of this derivative yielded mixtures of **13(Bcat$_2$)** and **17(Bcat$_2$)**, and therefore this complex was characterized spectroscopically. In the hydride region, the ^{1}H NMR spectrum of **18(Bcat$_2$)** shows the presence of a doublet resonance at −6.90 ppm ($^2J_{HP}$ = 21.1 Hz). The presence of the carbonyl ligand was confirmed in the IR spectrum by an absorption at 2005 cm^{-1}, and in the ^{13}C{^{1}H} NMR spectrum by a broad resonance at 176.8 ppm. In the latter experiment, the carbenic carbon produces a doublet at 154.3 ppm (J_{CP} = 96 Hz) evincing a *mer* coordination of the pincer ligand. Finally, the ^{11}B NMR spectrum shows in addition to the resonances at 22.5 (d, J_{BH} = 189 Hz) and 15.1 ppm due to HBcat and biscatecholborate, respectively, a singlet at 12.9 ppm, which was assigned to the boryl ligand (Figure 26).

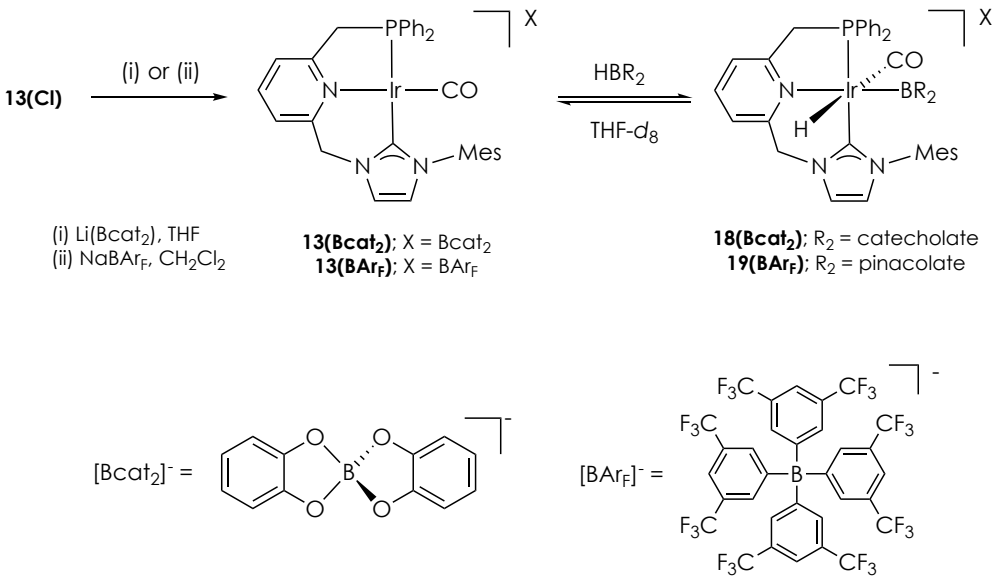

Scheme 12. Synthesis of **13(Bcat$_2$)** and **13(BAr$_F$)**, and reactions with boranes.

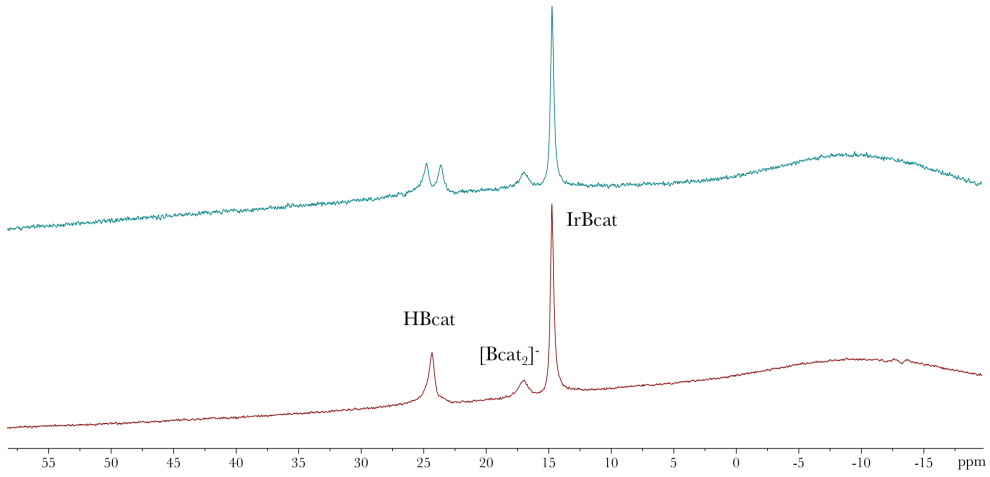

Figure 26. $^{11}B\{^{1}H\}$ (bottom) and ^{11}B NMR (top) spectra (160 MHz, THF-d_8) of the reaction of **13(Bcat$_2$)** with HBcat (1.2 equiv) to yield **18(Bcat$_2$)**.

While the above spectroscopic data support the proposed formulation for **18(Bcat$_2$)** as [Ir(*mer*-CNP^{Ph})(CO)H(Bcat)][(Bcat$_2$)], the two possible isomers resulting from the oxidative addition of HBcat to **13(Bcat$_2$)**, *i.e. trans* (**18-I**) or *cis* (**18-II**) coordination of the boryl ligand to the pyridine fragment, cannot be directly distinguished. However, from the comparison of the chemical shift of the resonance of the hydrido ligand of this compound with those of complex **17(Bcat$_2$)**, *cis* coordination of the Bcat moiety to the carbonyl ligand is suggested. Moreover, this ligand arrangement should be favored since the *trans* coordination of the two potentially π-accepting boryl and carbonyl ligands is prevented.[87] DFT calculations (B3LYP-D3, 6-31g(d,p)/SDD) of both complexes indicated that the proposed cationic species **18-I** is more stable by 3.2 kcal mol^{-1} than **18-II** (Figure 27).

[87] (a) H. Braunschweig, M. Colling, *Coord. Chem. Rev.* **2001**, *223*, 1; (b) J. Zhu, Z. Lin, T. B. Marder, *Inorg. Chem.* **2005**, *44*, 9384.

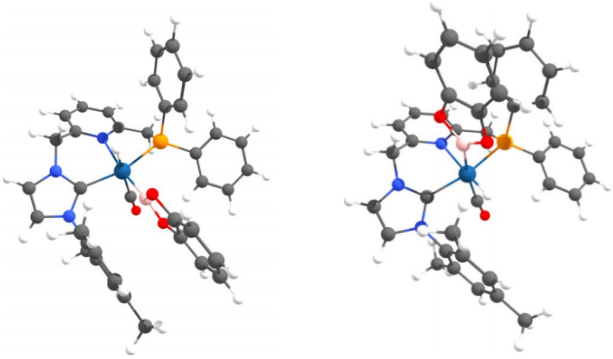

18-I **18-II**

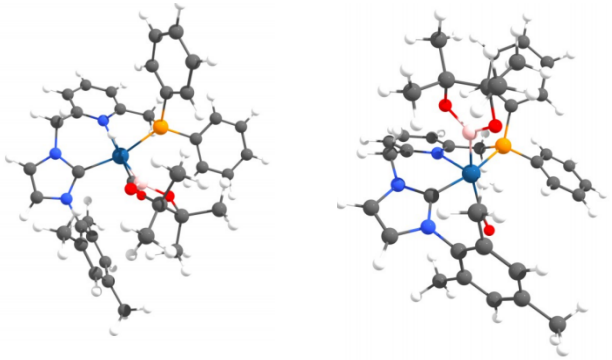

19-I **19-II**

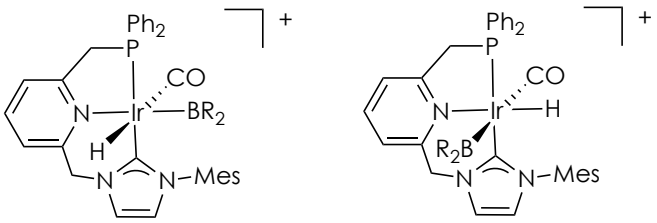

R_2 = catechol	**18-I** (0.0)	**18-II** (3.2)
R_2 = pinacol	**19-I** (3.5)	**19-II** (0.0)

Figure 27. Optimized structures and relative thermodynamic stability of the cationic fragments of **18-I** and **18-II**, and **19-I** and **19-II**. Data in parentheses are ΔG in THF (kcal mol^{-1}).

In the ^{1}H-^{1}H EXSY spectrum of the reaction mixture of **13(Bcat$_2$)** and HBcat in THF-d_8 registered at 25 ºC, exchange cross peaks were observed between the signals of the aromatic hydrogens corresponding to the [Bcat$_2$]$^-$ anion and those of free HBcat, indicative of the existence of a boron substituent scrambling process (Scheme 13). Upon registering the same experiment at 50 ºC, a cross-peak signal caused by the exchange between free HBcat and the hydrido ligand was also observed, further manifesting the reversibility of B–H oxidative addition by complex **13(Bcat$_2$)** (Figure 28).

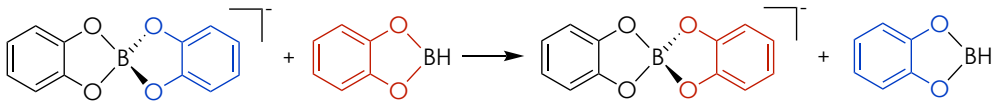

Scheme 13. Scrambling of boron substituents between HBcat and [Bcat$_2$]$^-$.

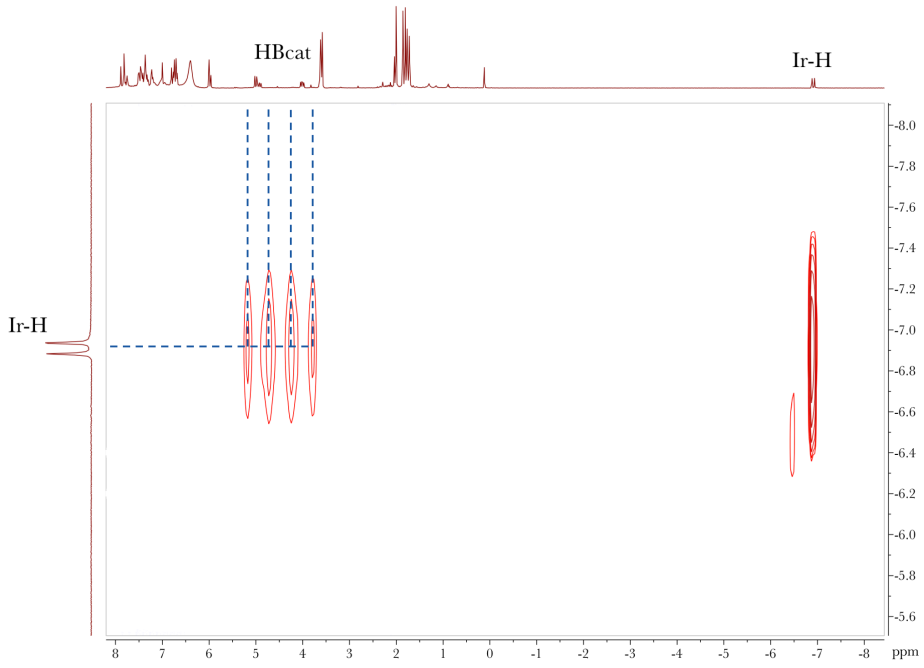

Figure 28. ^{1}H-^{1}H EXSY spectrum (400 MHz, THF-d$_8$, 328 K) of the reaction of **13(Bcat$_2$)** with HBcat (1.2 equiv) to yield **18(Bcat$_2$)** (mixing time = 800 ms).

Formation of analogous species to **18(Bcat$_2$)** with HBpin was examined by reacting complex **13(BAr$_F$)**, previously synthetized by treatment of **13(Cl)** with NaBAr$_F$, with an excess of HBpin (2.4 equiv) (Scheme 12). NMR data of the hydridoboryl iridium complex **19(BAr$_F$)** resemblance those of **18(Bcat$_2$)**, with the logical differences of the signals due to the boryl ligand and [BAr$_F$]$^-$, evincing the *cis* arrangement of the boryl and CO ligands. However, DFT calculations (B3LYP-D3, 6-31g(d,p)/SDD) showed a lower stability for **19-I** in comparison to **19-II** by 3.5 kcal mol^{-1}. Inspection of the optimized structure of **19-I** allow ascribing the reduced stability to the presence of non-stabilizing interactions between the more sterically demanding pinacol moiety with the substituents of the NHC and phosphine fragments (Figure 27). In addition, exchange cross-peaks between the resonances of the hydrido ligand of **19(BAr$_F$)** and those of the free borane were observed in the ^{1}H-^{1}H EXSY spectrum.

A likely mechanism for the hydroboration of CO_2 catalyzed by complexes **18(Bcat$_2$)** and **19(BAr$_F$)** would involve the insertion of CO_2 into the metal-H bond to yield formate species. However, no changes were noticed in the NMR spectra of solutions in THF-d_8 of **18(Bcat$_2$)** and **19(BAr$_F$)** upon exposure to CO_2 (2 bar). Therefore, in order to corroborate whether **18(Bcat$_2$)** and **19(BAr$_F$)** could participate in the reduction of CO_2 with boranes, the catalytic performance of complexes **13(Bcat$_2$)** and **13(BAr$_F$)** was examined. Under the reaction conditions of Table 4, entry 5, **13(Bcat$_2$)** provided in the hydroboration of CO_2 with HBcat a significantly low TOF of 6.8 h^{-1} (89% conv. after 13 h). Similarly, complex **13(BAr$_F$)** was also found to be an inefficient catalyst in the reduction of CO_2 with HBpin since negligible formation of the expected formoxyborane was observed (<5% conv. after 21 h). These observations support that **18(Bcat$_2$)** and **19(BAr$_F$)** are not significantly involved in the hydroboration of CO_2 using

15a/15b as catalytic precursors. Similar results have been previously observed in other metal catalyzed hydroborations. For instance, while $[IrCl(COE)_2]_2/PPh_3$ mixtures are active in the addition of HBcat to olefins, the isolated boryl iridium complexes generated from the reaction of this catalytic system and hydroboranes are poor catalysts.[82c] Also, while thiolate Ni and Pd pincer complexes have been shown to provide very active catalysts for the hydroboration of CO_2 to CH_3OBcat, the hydride species observed under catalytic conditions does not seem to be involved in the catalytic process.[48,49]

The level of reduction of CO_2 with HBpin can be controlled to some extent by an appropriate choice of the catalyst, leading to the formation of formate, acetal and methoxide derivatives.[39,47,53-54,56-59] The metal-catalyzed hydroboration of CO_2 to CH_3OBR_2 occurs in three successive steps.[46] The first one involves CO_2 insertion into the metal–H bond to yield a formate intermediate that upon interaction with a molecule of HBR_2 produces the formoxyborane derivative. Subsequent insertion of HCO_2BR_2 into the catalyst M–H bond produces formaldehyde, which is finally reduced to CH_3OBR_2 by a third molecule of HBR_2. Based on this mechanism, Hazari *et al.* have assumed that the high selectivity observed for a pincer Pd complex in the hydroboration of CO_2 with HBpin to formoxyborane is determined by the larger size of the pinacol fragment that prevents further reduction of HCO_2Bpin.[57] Furthermore, selective reduction of CO_2 to the formate level with HBpin has only been accomplished with metal based catalysts.[54,56-57] Therefore, since a highly selective CO_2 hydroboration with HBpin to formoxyborane takes place using **15a/15b**, it can be expected that metal species should be involved in the catalytic reactions. Furthermore, considering the degradation of the hydroboranes as well as the observed influence of water, it can be proposed that the catalytically active species are

iridium derivatives formed in low concentrations by reaction of **15a/15b** with hydroborane and water.

I.2.3. Synthesis of Ir-CNP^{tBu} complexes and catalytic applications in the hydrogenation of aldehydes

I.2.3.a) Synthesis of CNP^{tBu} ligand precursors

Di-*tert*-butylphosphino substituted imidazolium salts **20** were prepared by alkylation of di-*tert*-butylphosphine with **1(Cl)** in CH_2Cl_2, followed by the deprotonation of the resulting phosphonium salts **20·HCl** with phenethyldiethylamine ScavengePore resin (Scheme 14). Derivatives **20a** and **20b·HCl** were isolated with moderate purity (65-77% as determined by NMR), and used without further purification for the preparation of Ir-CNP^{tBu} complexes, as described in the following section.

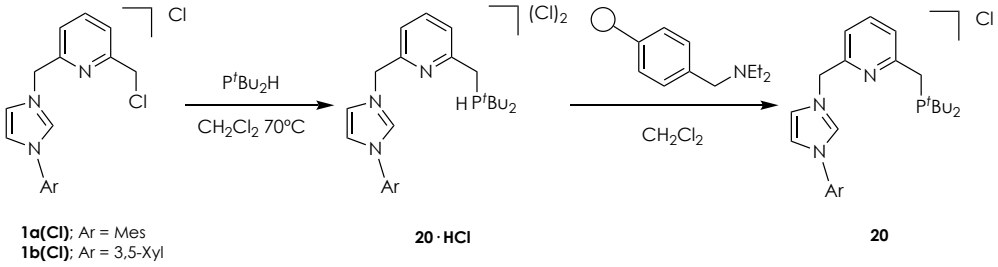

Scheme 14. Synthesis of CNP^{tBu} ligands precursors **20**.

Salts **20** were characterized by NMR spectroscopy and HRMS. In the $^{31}P\{^1H\}$ NMR spectrum, the imidazolium salt **20a** produces a broad resonance at 37.1 ppm. Meanwhile, in the ^1H NMR experiment, the methylene protons of the CH_2P and CH_2N arms appear as singlets at 3.04 (br) and 6.02 ppm, respectively, and the H-2 hydrogen of the imidazolium ring produces a broad resonance at 10.84 ppm. On the other hand, **20b·HCl** shows in the ^1H NMR spectrum a doublet signal at 4.01 ppm (J_{HP} = 12.1 Hz) and a singlet resonance at 6.06 ppm, corresponding to the methylene CH_2P

and CH_2N hydrogens; whereas a singlet is observed at 11.90 ppm caused by the H-2 hydrogen of the imidazolium moiety. Protonation of the phosphino group of **20b·HCl** is evidenced by the presence of a doublet resonance at 8.93 ppm with a large ^{1}H-^{31}P coupling of 495 Hz. This coupling value is also manifested in the ^{31}P NMR spectrum, where a doublet signal at 32.5 ppm ($^{1}J_{PH}$ = 490 Hz) is observed.

I.2.3.b) Synthesis and reactivity of Ir-CNP^{tBu} complexes

As shown with the carbene precursors **2** in Section I.2.2.3.a, the synthesis of Ir complexes containing CNP^{tBu} ligands was initially assayed by reaction of the imidazolium salt **20a** with Ir(acac)(COD), leading to the formation of the fully characterized complex **21** (Scheme 15). In the ^{1}H NMR spectrum, this derivative exhibits the resonances corresponding to the CH_2N methylene protons as a set of two mutually coupled doublets appearing at 7.03 and 4.86 ppm ($^{2}J_{HH}$ = 14.5 Hz), and the signals of the CH_2P hydrogens as two doublets of doublets at 3.54 ($^{2}J_{HH}$ = 16.5 Hz, $^{2}J_{HP}$ = 8.7 Hz) and 2.66 ppm ($^{2}J_{HH}$ = 16.5 Hz, $^{2}J_{HP}$ = 7.1 Hz) (Figure 29). More interestingly, there is a doublet signal in the hydride region at −24.5 ppm (J_{HP} = 17 Hz), and only two singlets (integrating for 3 H each) in the region expected for the methyl substitutents of the mesityl group. Meanwhile, two other resonances are observed at 3.92 (d, $^{2}J_{HH}$ = 11.6 Hz, 1H) and 2.88 ppm (dd, $^{2}J_{HH}$ = 11.6 Hz, $^{3}J_{HP}$ = 9.1 Hz, 1H) that exhibit cross-peak signals in the ^{1}H-^{13}C HSQC experiment with a broad resonance appearing at δ_C −9.6 ppm, suggestive of the presence of an Ir-C bond (Figure 30). Overall, these

data point to the metalation of one of the CH_3 groups of the mesityl fragment.[88]

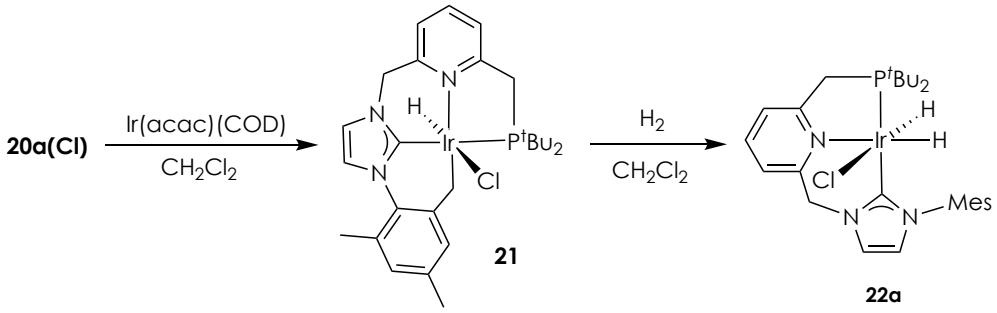

Scheme 15. Synthesis of Ir-CNP^{tBu} complexes **21** and **22a**.

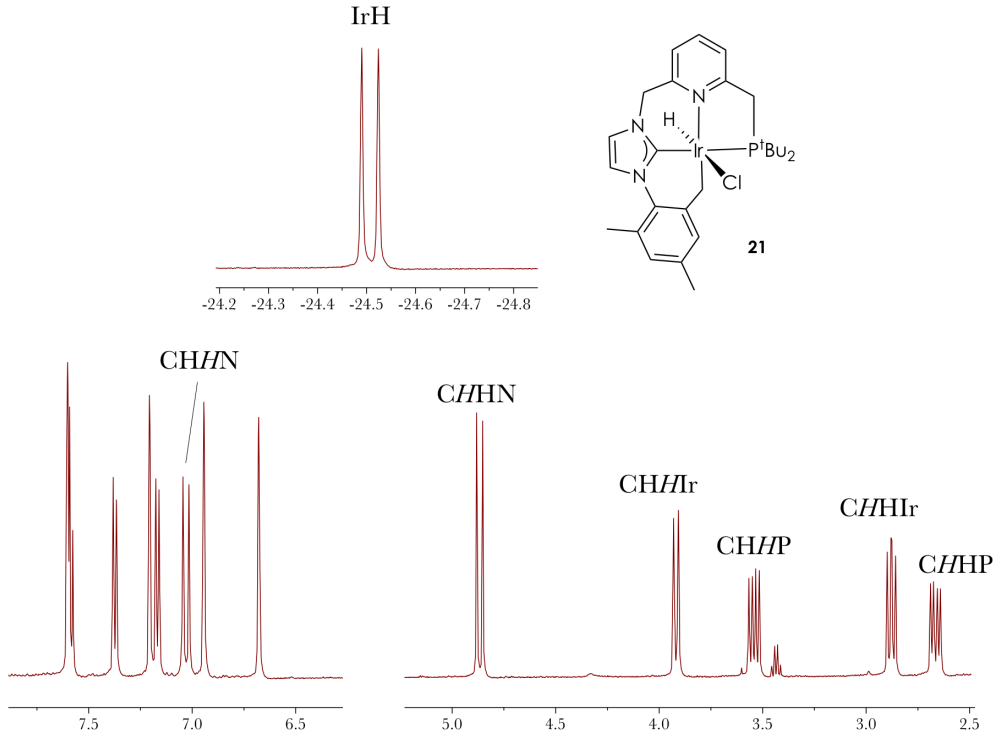

Figure 29. Selected regions of the ^{1}H NMR spectrum (300 MHz, CD_2Cl_2) of complex **21**.

[88] M. Albrecht, *Chem. Rev.* **2010**, *110*, 576.

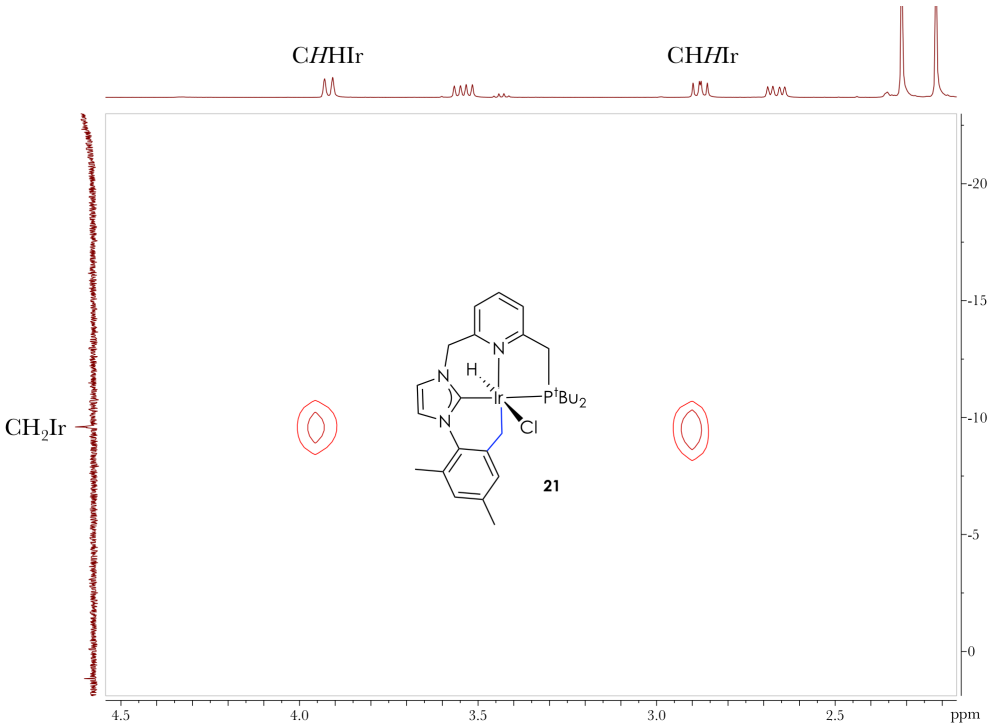

Figure 30. Region of the ^{1}H-^{13}C HSQC spectrum (400 MHz, CD_2Cl_2) of **21**.

The proposed structure of **21** was further confirmed by an X-ray diffraction study of the complex (Figure 31). In the solid state, this complex has a slightly distorted octahedral geometry with the metalated CNP^{tBu} ligand adopting a tetracoordinated planar coordination as indicated by the value of the angles C(1)–Ir(1)–P(1)=166.79(16)° and C(10)–Ir(1)–N(3)=172.79(16)°. Moreover, the existence of a hydrogen bond between the axial hydrogen of the CH_2N arm and the chloro ligand is evident from the value of the H···Cl distance of 2.6 Å, which is shorter than the sum of van der Waals radii of H and Cl (2.9-3.0 Å).[63,72] This interaction is also manifested in the significant deshielding of the doublet resonance corresponding to the C*H*HN axial hydrogen in the ^{1}H NMR spectrum (δ_H 7.07, $^{2}J_{HH}$ = 14.5 Hz) (Figure 29).

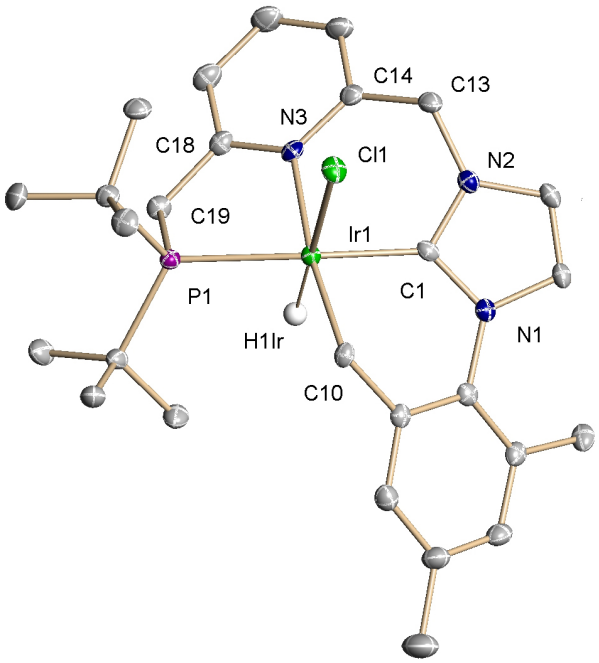

Bond lenghts (Å)		Angles (º)	
Ir(1)–C(1)	1.980(5)	C(1)–Ir(1)–P(1)	166.79(16)
Ir(1)–N(3)	2.139(4)	C(10)–Ir(1)– N(3)	172.79(16)
Ir(1)–P(1)	2.32271(12)	N(3)–Ir(1)–P(1)	82.24(11)
Ir(1)–C(10)	2.085(5)	C(1)–Ir(1)–N(3)	89.47(17)
Ir(1)–H(1)	1.589(19)	C(1)–Ir(1)–C(10)	83.44(18)
Ir(1)–Cl(1)	2.5616(11)	C(10)–Ir(1)–P(1)	104.97(13)

Figure 31. ORTEP drawing at 30% ellipsoid probability, and selected bond lengths (Å) and angles (º), of complex **21**. Hydrogen atoms, except the hydrido ligand, have been omitted for clarity.

The synthesis of the chlorodihydrido complex **22a**, an analogous derivative of **10a** containing the CNP^{tBu} ligand, was examined by exposing overnight a solution in CH_2Cl_2 heated to 65 ^oC of **21** to an atmosphere of H_2 (4 bar) (Scheme 15). The dihydride complex **22a** was obtained quantitatively as a yellow solid that was analytically and spectroscopically characterized. The ^1H NMR of **22a** spectrum exhibits a similar pattern to that of **10a** with the expected differences due to the substituents of the phosphino group. For example, the hydride region shows two doublets of doublets at −20.36 ($^2J_{HP}$ = 14.4 Hz, $^2J_{HH}$ = 6.5 Hz) and −24.89 ($^2J_{HP}$ = 17.2 Hz, $^2J_{HH}$ = 6.5 Hz) attributable to the IrH *trans* and *cis* to the pyridine fragment, respectively. As observed with complex **10a**, pressurization of a sample in CD_2Cl_2 of **22a** at room temperature with deuterium gas (3 bar) produced after 5 h the complete deuteration of the hydrido ligands. However, deuterium incorporation at the methylenes arms of the pincer was not observed even after prolongued heating of the sample to 50 ^oC for 72 h.

Conversely, reaction of the xylyl substituted derivative **20b** with Ir(acac)(COD) in CH_2Cl_2 produced the formation of the diolefin complex **23** (Scheme 16). This derivative was not isolated with analytical purity, although it could be spectroscopically characterized by NMR techniques. Complex **23** presents a similar ^1H NMR spectrum to that of **7b(Cl)**, with the expected differences due to the phosphine substituents. Moreover, at variance with complexes **7**, distinct sharp signals are observed for each olefinic hydrogen of the COD ligand in the ^1H NMR spectrum registered at room temperature. Also, the resonance of C-2 of the NHC ligand in the $^{13}C\{^1H\}$ NMR spectrum appears as a singlet at 181.4 ppm, suggesting a *cis* coordination of the NHC and phosphino donors.

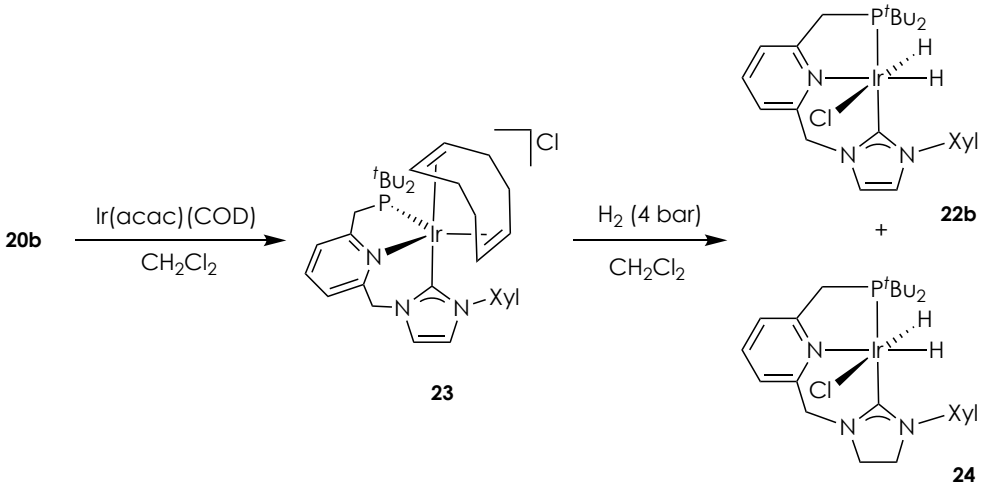

Scheme 16. Synthesis of Ir-CNP^{tBu} complexes **23**, **22b** and **24**.

As previously mentioned with Ir-CNP^{Ph} complexes **7**, the iridium complex **23** also readily reacts with H_2 (Scheme 16). However, in addition to the expected dihydride complex **22b**, hydrogenation of the imidazolylidene ligand fragment was also observed, leading to an unseparable mixture of **22b** and **24** in an 85:15 ratio, respectively. The addition of dihydrogen to the C=C double bond of the imidazolylidene moiety was readily deduced from the observation of new multiplet signals appearing at 3.91 (integrating to 2H), 4.05 and 4.30 ppm in the ^{1}H NMR spectrum, which are assignable to the –CH_2CH_2– linkage of the imidazolidinylidene donor. The hydrido ligands of **23** produce two doublet of doublets at –20.41 ($^2J_{HP}$ = 14.5 Hz, $^2J_{HH}$ = 5.9 Hz) and –24.40 ($^2J_{HP}$ = 17.8 Hz, $^2J_{HH}$ = 5.9 Hz) that correspond to the hydrogens coordinated *trans* and *cis* to the pyridine ring, respectively.

Hydrogenation of an imidazolylidene ligand has been previously observed in a related Ir-CNP system.[89]

In order to obtain trihydride Ir-CNP^{tBu} complexes that may serve as hydrogenation catalysts, complex **22a** was treated with an excess of NaH leading to the formation of the derivative **25a** (Scheme 17). Similarly, reaction of **22b** and **24** produced a mixture of the trihydride complexes **25b** and **26**, in an 8:2 ratio (Scheme 18). Complexes **25** show similar features in their NMR spectra to the trihydride Ir-CNP^{Ph} complex **9**. However, compound **25a** could be isolated as an analytically pure solid, and is stable in the solid state for extended periods of time. Complex **25a** reacts with chlorinated solvents leading to the dihydride derivative **22a**.

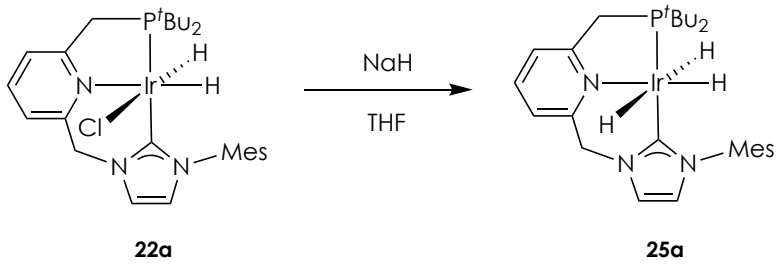

22a **25a**

Scheme 17. Synthesis of the trihydride Ir-CNP^{tBu} complex **25a**.

[89] M. Hernández-Juárez, J. López-Serrano, P. González-Herrero, N. Rendón, E. Álvarez, M. Paneque, A. Suárez, *Chem. Commun.* **2018**, *54*, 3843.

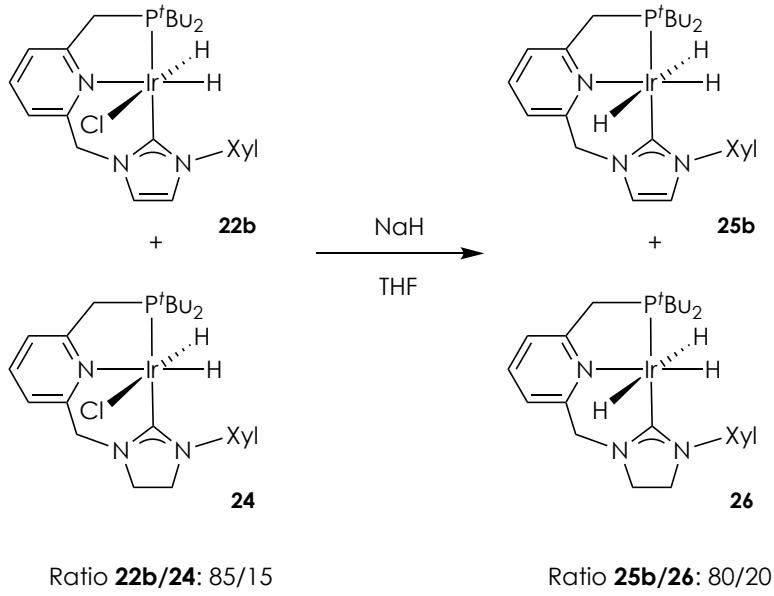

Scheme 18. Synthesis of the trihydride Ir-CNP^{tBu} complexes **25b** and **26**.

Complexes with three H atoms in the coordination sphere of the metal can exhibit two possible structures, i.e. those of a trihydride or a dihydrogen/hydride complex.[90] Therefore, to further confirm the trihydride formulation of the iridium complex **25a**, which could alternatively be described as a hydrido-dihydrogen σ-complex, T_1 values (spin-lattice relaxation time) were measured for both types of Ir-H hydrogens. Determination of T_1 values is an easy method, albeit not exempt of uncertainty since it can be affected by different factors, to differentiate between dihydride and σ-H_2 complexes since the rate of relaxation ($1/T_1$) depends on the inverse sixth power of the H-H distance.[4c,91] Dihydride

[90] (a) D. M. Heinekey, N. G. Payne, G. K. Schulte *J. Am. Chem. Soc.* **1988**, *110*, 2303; (b) D. M. Heinekey, J. M. Millar, T. F. Koetzle, N. G. Payne, K. W. Zilm, *J. Am. Chem. Soc.* **1990**, *112*, 909; (c) D. M. Heinekey, A. S. Hinkle, J. D. Close, *J. Am. Chem. Soc.* **1996**, *118*, 5353; (d) W. J. Oldham, A. S. Hinkle, D. M. Heinekey, *J. Am. Chem. Soc.* **1997**, *119*, 11028.

[91] (a) G. J. Kubas *Metal Dihydrogen and σ-Bond Complexes. Structure, Theroy and Reactivity*, Kluwer Academic/Plenum Publishers, **2001**, *Chap. 5*; (b) R. H. Crabtree, *Acc. Chem. Res.* **1990**, *23*, 95.

complexes are characterized by relaxation times of the order of 0.5 s, whereas σ-dihydrogen derivatives exhibit faster relaxations with T_1 values below 100 ms.[92] Since relaxation rates are temperature-dependent, it is necessary to find the temperature at which the maximum rate of relaxation ($T_{1,min}$) is observed. Figure 32 depicts a representation of T_1 values as a function of temperature for de Ir-H hydrogens of complex **25a** in toluene-d_8. $T_{1,min}$ values of *ca.* 0.5 s were observed confirming the trihydride formulation for complex **25a** (Table 6).

Table 6. T_1 values for Ir-H hydrogens of complex **25a** in toluene-d_8.

Temperature (K)	T_1 (ms) Ir-H at −10.14 ppm	T_1 (ms) Ir-H at −20.03 ppm
298.15	710	710
273.15	513	498
263.15	486	486
253.15	470	495
243.15	474	509

[92] D. G. Hamilton, R. H. Crabtree, *J. Am. Chem. Soc.* **1988**, *110*, 4126.

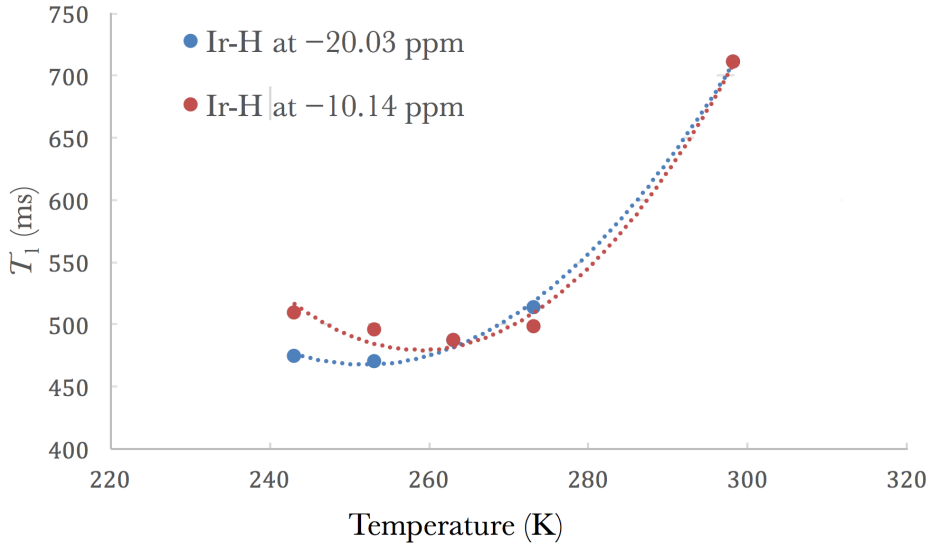

Figure 32. Representation of T_1 values of the Ir-H hydrogens *vs* temperature.

Deuteration studies were also performed with derivatives **25**. The trihydride derivative **25a** in toluene-d_8 underwent partial H/D exchange of the hydrido ligands and the methylene bridges in the presence of D_2 (5 bar; 20 h), suggestive of the reversible exchange of free D_2 with a η^2-H_2 ligand resulting from the intramolecular protonation of Ir-H by protons of the CNP^{tBu} methylene moieties (Figure 33).[93]

[93] (a) X. Yang, M. B. Hall, *J. Am. Chem. Soc.* **2010**, *132*, 120; (b) J. Li, Y. Shiota, K. Yoshizawa, *J. Am. Chem. Soc.* **2009**, *131*, 13584.

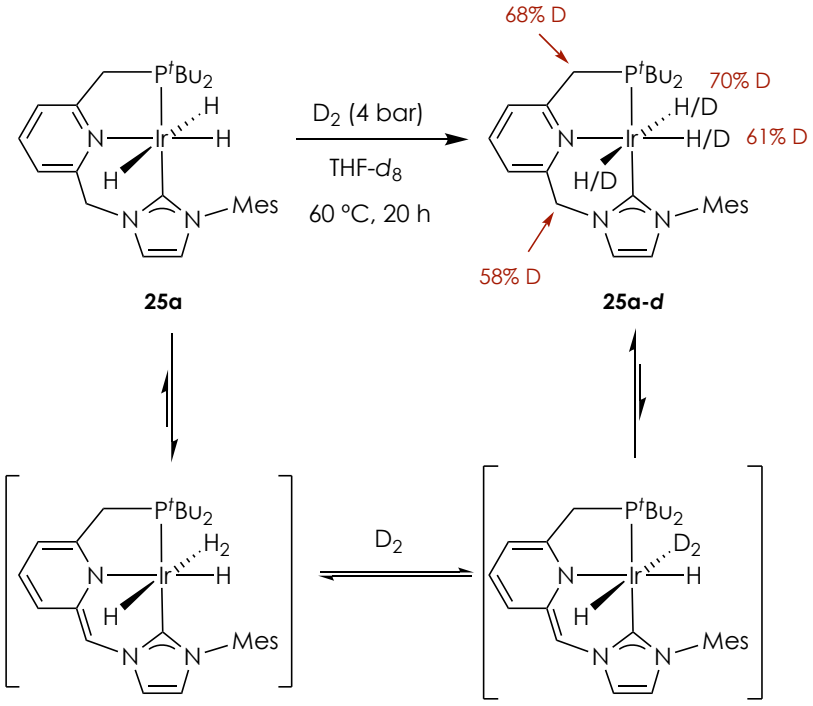

Figure 33. Deuteration of complex **25a** in toluene-d_8 with D_2 (5 bar), and proposed mechanism for H/D exchange (formation of a σ-H_2 complex after protonation by the CH_2-P bridge is also possible).

I.2.3.c) Hydrogenation of aldehydes catalyzed by Ir–CNP^{tBu} complexes

Trihydride complexes **25** and **26** were explored as catalysts in the chemoselective hydrogenation of aldehydes (Table 7).[94] Firstly, the catalytic performances in the hydrogenation of benzaldehyde (**27a**) (4 bar H_2, 25 ^oC) of complex **25a** and the mixture of **25b** and **26** were compared using catalyst loadings of 0.5 mol% (entries 1 and 2). Similar catalytic activities were observed for both systems. Using lower catalyst loadings (0.1 mol%) of **25a** and higher concentrations of substrate, benzaldehyde was hydrogenated with 96% conversion with a TOF of 40 h^{-1} (entry 3). Under these reaction conditions, the hydrogenation of a range of substituted aromatic aldehydes was investigated in order to assess the chemoselectivity and functional group tolerance of the catalyst. The reduction of substrates bearing *p*-bromo (**27b**) and *p*-fluoro (**27c**) substituents was accomplished with high conversions, and hydrogenolysis of the C-X bonds was not detected (entries 4 and 5). Also, 4-nitrobenzaldehyde (**27d**) was selectively hydrogenated to the corresponding alcohol without observable reduction of the nitro group (entry 6). Finally, *p*-trifluoromethyl-substituted benzaldehyde (**27e**) and vanillin (**27f**) were hydrogenated with 76% and >99% conversion, respectively (entries 7 and 8).

The selective hydrogenation of an aldehyde function in the presence of a C=C bond is an important step in the production of fragances, fine chemicals and pharmaceutical compounds.[95] Therefore, the reduction of a series of α,β-

[94] For selected examples of aldehyde hydrogenation catalyzed by Ir complexes: (a) I. Cano, L. M. Martínez-Prieto, L. Vendier, P. W. N. M. van Leeuwen, *Catal. Sci. Technol.* **2018**, *8*, 221; (b) X. Wu, C. Corcoran, S. Yang, J. Xiao, *ChemSusChem* **2008**, *1*, 71; (c) M. G. Manas, J. Graeupner, L. J. Allen, G. E. Dobereiner, K. C. Rippy, N. Hazari, R. H. Crabtree, *Organometallics* **2013**, *32*, 4501.

[95] (a) P. Gallezot, D. Richard, *Catal. Rev.: Sci. Eng.* **1998**, *40*, 81; (b) P. Mäki-Arvela, J. Hájek, T. Salmi, D. Y. Murzin, *Appl. Catal. A* **2005**, *292*, 1.

unsaturated aldehydes was examined using catalyst **25a**. High conversion and selectivity towards C=O hydrogenation was observed in the reduction with H_2 of *trans*-cinnamaldehyde (**27g**) under the previous optimized conditions (entry 9). Conversely, the hydrogenation of *trans*-2-hexenal (**27h**) was sluggish and required a higher catalyst loading (0.5 mol%) to achieve 88% conversion with a notable selectivity to the unsaturated alcohol (entry 10). The reduction of citronellal (**27i**), having a non-conjugated C=C bond, was also examined (entry 11). Alcohol (**28i**) was quantitatively obtained with a selectivity of 99%. Finally, citral, a 1:0.6 mixture of geranial (***cis*-27j**) and neral (***trans*-27j**), was reduced under the standard conditions to geraniol (***cis*-28j**) and nerol (***trans*-28j**) with no observable isomerization of the conjugated C=C bond and a selectivity of 96% (entry 12).

Table 7. Hydrogenation of aldehydes catalyzed by Ir-CNP^{tBu} complexes.[a]

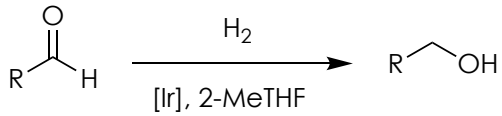

27 **28**

Entry	Aldehyde	[Ir]	Conv. (%)	Ratio unsaturated/saturated alcohol (%)
1[b]		**25a**	70	-
2[b]	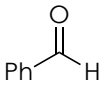 **27a**	**25b/26**	72	-
3		**25a**	96	-
4	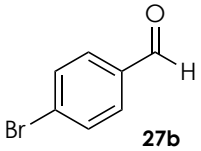 **27b**	**25a**	>99	-
5	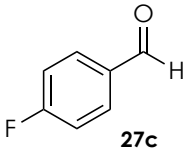 **27c**		96	-
6[c]	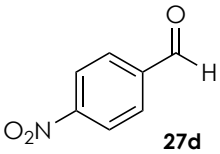 **27d**		>99	-
7	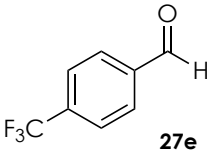 **27e**		76	-

Table 7(cont). Hydrogenation of aldehydes catalyzed by Ir-CNP^{tBu} complexes.[a]

Entry	Aldehyde	[Ir]	Conv. (%)	Ratio unsaturated/saturated alcohol (%)
8	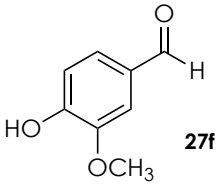 **27f**	**25a**	>99	-
9	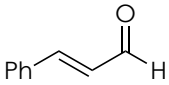 **27g**		>99	99:1
10[c,d]	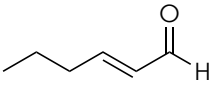 **27h**		84	88:12
11	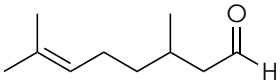 **27i**		>99	99:1
12[e]	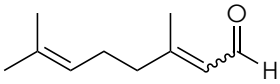 **27j** *cis*/*trans* = 1:0.6		>99[e]	96:4

[a] Reaction conditions, unless otherwise noted: 4 bar of H_2, 2-methyltetrahydrofuran, 0.1 mol% Ir-CNP^{tBu}, 25 °C, 24 h. [S] = 2.0 M. Conversion and selectivity towards the unsaturated alcohol were determined by ^{1}H NMR spectroscopy using mesitylene as internal standard. [b] 0.5 mol% Ir-CNP^{tBu}, [S] = 0.3 M, 6 h. [c] [S] = 1.0 M. [d] 0.5 mol% Ir-CNP^{tBu}. [e] Geranial/neral ratio = 1:0.6.

I.2.3.d) Mechanistic studies of the hydrogenation of aldehydes

The acid–base properties of the methylene bridges of lutidine derived ligands are relevant to the development of ligand-assisted reactions.[96] Hence, as previously studied with the Ir-CNP^{Ph} complexes, the reactivity of **22a** towards bases was investigated. Reaction of **22a** with KHMDS or KO^{t}Bu (1.5 equiv) in THF-d_8 resulted in the selective deprotonation of the CH_2N arm with formation of the pyridine dearomatized species **29** (Scheme 19). The ^{1}H NMR spectrum of **29** features a singlet resonance for the proton of the methyne CHN bridge at 6.44 ppm, and a doublet at 2.78 ppm ($^2J_{HP}$ = 8.9 Hz) caused by the CH_2P arm. Moreover, the expected dearomatization of the pyridine ring is reflected in the significant upfield shift of the resonances of the central ring hydrogens appearing in the range 6.2-4.9 ppm. In the $^{13}C\{^1H\}$ NMR spectrum, the carbenic carbon appears at 179.6 ppm as a doublet with a large J_{CP} coupling constant of 110 Hz, evincing a meridional coordination of the CNP^{tBu} ligand.

[96] (a) C. Gunanathan, D. Milstein, *Acc. Chem. Res.* **2011**, *44*, 588; (b) R. Khusnutdinova, D. Milstein, *Angew. Chem. Int. Ed.* **2015**, *54*, 12236.

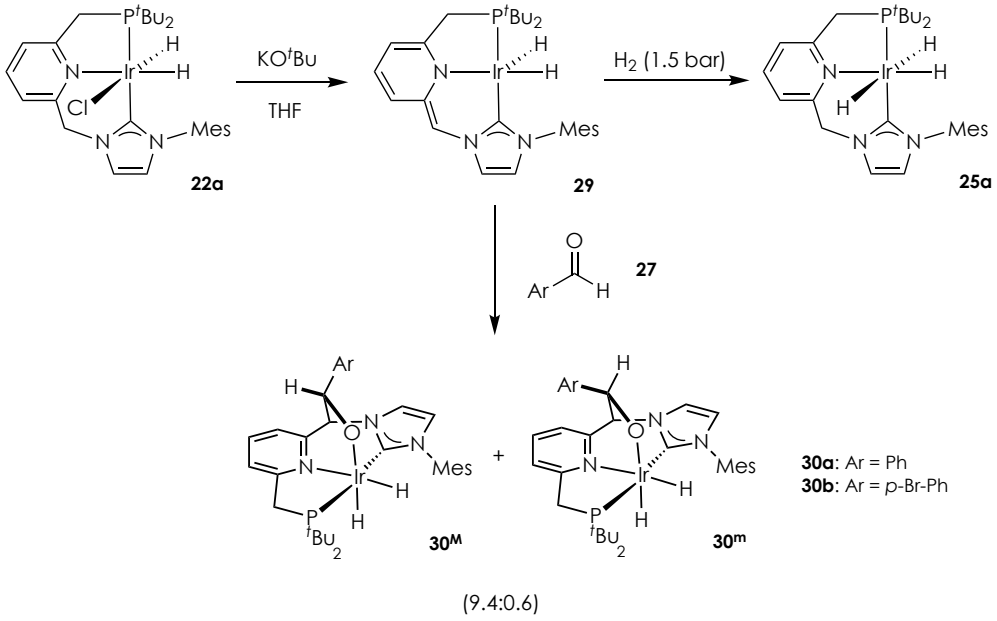

Scheme 19. Formation of complex **29**, and reactions with H_2 and aldehydes.

Interestingly, in the ^{1}H NMR spectrum of **29** the hydrido ligands are equivalent at temperatures above −50 °C producing a sharp doublet at −23.77 ppm ($^2J_{HP}$ = 11.3 Hz), indicative of a trigonal bipyramidal geometry of the complex, as previously observed for Ir(PCP)H_2 derivatives,[77,97] or a square pyramidal structure,[98] in which the pincer occupies the pyramid base and the hydrido ligands are rapidly exchanging. Furthermore, T_1 determinations in THF-d_8 shows a $T_{1,min}$ value of approximately 150 ms, in agreement with a IrH_2(CNP*) formulation for complex **29** (Figure 34, Table 8).

[97] (a) J.-F. Riehl, Y. Jean, O. Eisenstein, M. Pélissier, *Organometallics* **1992**, *11*, 729; (b) M. Gupta, C. Hagen, W. C. Kaska, R. E. Cramer, C. M. Jensen, *J. Am. Chem. Soc.* **1997**, *119*, 840; (c) K. Krogh-Jespersen, M. Czerw, M. Kanzelberger, A. S. Goldman, *J. Chem. Inf. Comput. Sci.* **2001**, *41*, 56; (d) S. Niu, M. B. Hall, *J. Am. Chem. Soc.* **1999**, *121*, 3992.
[98] A. V. Polukeev, R. Marcos, M. S. G. Ahlquist, O. F. Wendt, *Chem. Eur. J.* **2016**, *22*, 4078.

Table 8. T_1 values for Ir-H hydrogens of complex **29** in THF-d_8.

Temperature (K)	T_1 (ms)
298.15	385
273.15	260
263.15	213
253.15	160
243.15	157
233.15	163

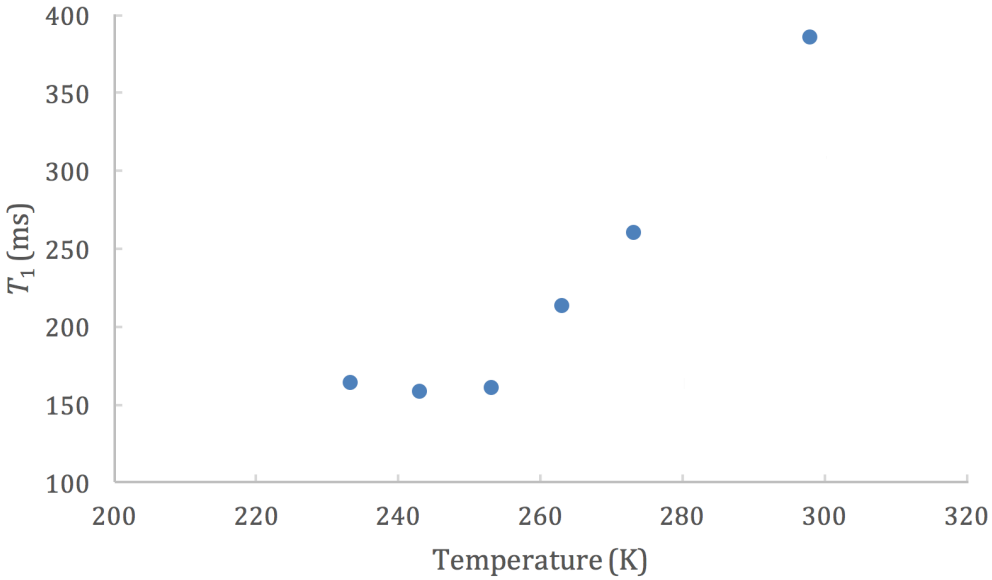

Figure 34. Representation of T_1 values of the Ir-H hydrogens of **29** *vs* temperature.

The ability of the deprotonated complex **29** to participate in ligand-assisted H-H activation was established after the observed formation of the trihydride derivative **25a** upon exposure of a solution of **29** in THF-d_8 to an atmosphere of H_2 (1.5 bar) (Scheme 19).

Complexes based on deprotonated lutidine-derived pincer ligands have been shown to exhibit FLP-type reactivity towards electrophiles such as CO_2, carbonyl compounds, nitriles and imines.[99,67b] Hence, formation of analogous species with aldehydes was investigated by addition of KHMDS to a 1:2 solution of **22a** and benzaldehyde in THF-d_8 (Scheme 19). In the hydride region, the ^{1}H NMR spectrum of the resulting solution demonstrates the formation of two new dihydride species, **30a^{M}** and **30a^{m}**, in a 9.4:0.6 ratio (Table 9). This ratio did not change further after prolonged standing of the solution at room temperature, suggesting that it represents the equilibrium product mixture (see below). The major complex, **30a^{M}**, produces two doublets of doublets at −19.39 ($^2J_{HP}$ = 14.2 Hz, $^2J_{HH}$ = 7.8 Hz) and −24.33 ppm ($^2J_{HP}$ = 18.2 Hz, $^2J_{HH}$ = 7.8 Hz); whereas the minor derivative also shows two doublet of doublets appearing at −20.06 ($^2J_{HP}$ = 13.7 Hz, $^2J_{HH}$ = 7.4 Hz) and −24.11 ppm ($^2J_{HP}$ = 18.5 Hz, $^2J_{HH}$ = 7.4 Hz). Moreover, the CHN methyne bridge of **30a^{M}** appears at 5.64 ppm as a singlet, and the resonances for the diasterotopic protons of the methylene CH_2P are shown as two doublet of doublets at 3.61 ($^2J_{HH}$ = 15.5 Hz, $^2J_{HP}$ = 8.9 Hz) and 2.95 ($^2J_{HH}$ = 15.5 Hz, $^2J_{HP}$ = 6.7 Hz) ppm. The presence of a intense cross-peak signal in the ^{1}H-^{1}H NOESY spectrum between one of the resonances corresponding to the CH_2P arm (δ 2.95 ppm) and one of the

[99] (a) M. Vogt, M. Gargir, M. A. Iron, Y. Diskin-Posner, Y. Ben-David, D. Milstein, *Chem. Eur. J.* **2012**, *18*, 9194; (b) C. A. Huff, J. W. Kampf, M. S. Sanford, *Organometallics* **2012**, *31*, 4643; (c) M. Montag, J. Zhang, D. Milstein, *J. Am. Chem. Soc.* **2012**, *134*, 10325; (d) C. A. Huff, J. W. Kampf, M. S. Sanford, *Chem. Commun.* **2013**, *49*, 7147; (e) C. A. Huff, M. S. Sanford, *ACS Catal.* **2013**, *3*, 2412; (f) G. A. Filonenko, M. P. Conley, C. Copéret, M. Lutz, E. J. M. Hensen, E. A. Pidko, *ACS Catal.* **2013**, *3*, 2522; (g) M. Vogt, A. Nerush, M. A. Iron, G. Leitus, Y. Diskin-Posner, L. J. W. Shimon, Y. Ben-David, D. Milstein, *J. Am. Chem. Soc.* **2013**, *135*, 17004; (h) M. Vogt, A. Nerush, Y. Diskin-Posner, Y. Ben-David, D. Milstein, *Chem. Sci.* **2014**, *5*, 2043; (i) G. A. Filonenko, E. Cosimi, L. Lefort, M. P. Conley, C. Copéret, M. Lutz, E. J. M. Hensen, E. A. Pidko, *ACS Catal.* **2014**, *4*, 2667.

hydrido ligands (δ −24.33 ppm) of the major isomer **30a^{M}** allows to assign the resonance appearing at lower field in the hydride region to the apical IrH hydrogen. In addition, pyridine aromatization in **30a^{M}** is inferred from the downfield shift of the aromatic protons appearing in the range 6.6-7.8 ppm.

Moreover, formation of the new carbon–carbon bond is proposed from the appearance of a singlet at 4.90 ppm corresponding to the alcoxide –C(Ph)H–O–Ir fragment, which exhibits an intense cross-peak with the resonance due to the CHN moiety in the ^{1}H-^{1}H NOESY spectrum. Furthermore, this signal is significantly shifted upfield with respect to the chemical shift of the carbonyl hydrogen of the free aldehyde (δ_H 10.01 ppm), as expected from a change in the sp^2 hybridization of the carbonyl carbon to sp^3. Further confirmation of the assignment of this signal was obtained from the existence of an exchange cross-peak in the ^{1}H-^{1}H EXSY spectrum with the resonance of the carbonyl proton of benzaldehyde (**27a**). Finally, the ^{13}C{^{1}H} NMR spectrum contains two signals at δ 75.4 and 76.8 ppm, attributable to the –C(Ph)H–O–Ir and the CHN carbons, respectively.

Table 9. Selected $^{31}P\{^{1}H\}$ and ^{1}H NMR data of complexes **30**.[a]

Complex	*M/m* ratio	δ (^{31}P)	δ (^{1}H)	
			IrH *trans* Py	IrH *cis* Py
30a^{M}	9.4:0.6	75.5	−19.39 (dd) $^{2}J_{HP}$ = 14.2, $^{2}J_{HH}$ = 7.8	−24.33 (dd) $^{2}J_{HP}$ = 18.2, $^{2}J_{HH}$ = 7.8
30a^{m}		76.1	−20.06 (dd) $^{2}J_{HP}$ = 13.7, $^{2}J_{HH}$ = 7.4	−24.11 (dd) $^{2}J_{HP}$ = 18.5, $^{2}J_{HH}$ = 7.4
30b^{M}	9.4:0.6	75.6	−19.35 (dd) $^{2}J_{HP}$ = 14.2, $^{2}J_{HH}$ = 7.8	−24.56 (dd) $^{2}J_{HP}$ = 18.4, $^{2}J_{HH}$ = 7.8
30b^{m}		76.1	−20.01 (dd) $^{2}J_{HP}$ = 14.0, $^{2}J_{HH}$ = 7.7	−24.34 (dd) $^{2}J_{HP}$ = 19.5, $^{2}J_{HH}$ = 7.7

[a] NMR spectra registered in THF-d_8. Chemical shifts (δ) are given in ppm. Coupling constants (*J*) are given in Hz. *M/m* ratios as determined by ^{1}H NMR spectroscopy.

Although only two isomers are observed, the reaction of benzaldehyde with a deprotonated IrH_2(CNP*) complex could, in principle, lead to four isomeric products (Figure 35). These include two pairs of regioisomers resulting from aldehyde coordination involving either the CHP or CHN arms, with each pair being a set of diastereomers that differs in the aldehyde coordinating face. The relative stabilities of these adducts were studied using DFT calculations (B3LYP-D3, 6-31g(d,p)/SDD). *Exo* coordination of benzaldehyde to the Ir-CNP* framework of **29** was found to be 0.89 kcal mol^{-1} more stable than binding of the aldehyde through the opposite face (*endo*), allowing to assign the major species **30a^{M}** to the **30a^{N,exo}** isomer. Moreover, adducts resulting from the coordination of benzaldehyde to the Ir-CNP* framework deprotonated at the phosphine arm are significantly disfavored, likely due to the higher steric hindrance caused by the bulky *t*Bu groups.

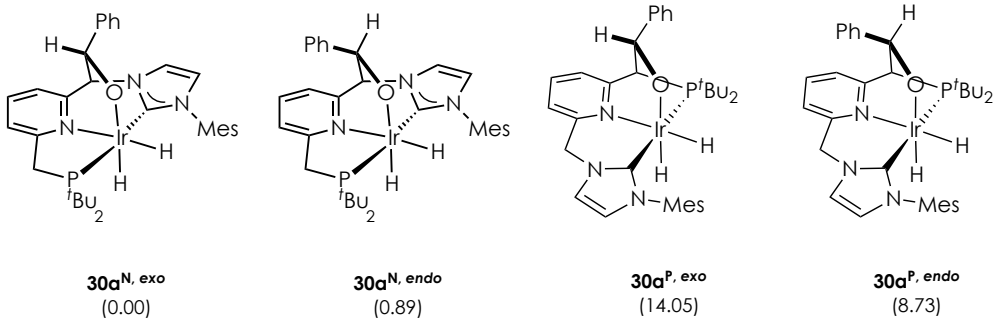

Figure 35. Relative thermodynamic stability of **30a^{N,exo}** and **30a^{N,endo}**, and **30a^{P,exo}** and **30a^{P,endo}**. Data in parenthesis are ΔG in THF (kcal mol^{-1}).

Reaction of **29** with *p*-bromobenzaldehyde (2.4 equiv) in THF-d_8 also resulted in the formation of two isomers, **30b^{M}** and **30b^{m}**, formed in 9.4:0.6 ratio (Scheme 19, Table 9). Interestingly, addition at room temperature of aldehyde **27a** (1.8 equiv) to the above solution gave within minutes a mixture of **30a^{M}** and **30b^{M}** (**30b^{M}/30a^{M}** ratio = 3), a further indication for the reversibility of the formation of the C-C and O-Ir bonds. Relative thermodynamic stabilities of complexes **30a^{M}** and **30b^{M}** were determined from the observed equilibrium **30a^{M}** + **27b** $\rightleftharpoons$ **30b^{M}** + **27a** by using ^{1}H NMR spectroscopy. From the calculated $^{298}K_{eq}$ = 7.2, a stability order of the adducts **30b^{M}** > **30a^{M}** was estimated, as expected from the higher electrophilicity of the carbonyl carbon of **27b**. Finally, monitoring by NMR spectroscopy of a sample of **30b** pressurized with 2 bar of H_2 allowed observing the gradual dissapareance of the resonances corresponding to the adducts **30b** and the aldehyde **27b**, and the simultaneous appareance of the signals expected for the trihydride complex **25a** and alcohol **28b**.

Aiming to elucidate the species participating in the hydrogenation of aldehydes catalyzed by Ir-CNP^{tBu} complexes, the reaction of the trihydride complex **25a** with benzaldehyde (4.0 equiv) in THF-d_8 was investigated by

NMR spectroscopy (Scheme 20). In the ^{1}H NMR spectrum, formation of **30aM** (90%) and an unknown minor species **31** (<10%) was observed, along with benzyl alcohol **28a** (1 equiv with respect to **30aM**). Complex **31** exhibits in the ^{1}H NMR experiment two doublets of doublets appearing at −19.81 ($^{2}J_{HP}$ = 17.1, $^{2}J_{HH}$ = 14.7 Hz) and −26.57 ppm ($^{2}J_{HP}$ = 17.1, $^{2}J_{HH}$ = 6.7 Hz) in the hydride region. Moreover, signals assignable to the CH_2P and CH_2N pincer bridges have also been observed, suggesting the re-protonation of the pincer ligand. While isolation of this derivative has not been possible due to its low concentration, we hypothesize that **31** is a η^1-acyl complex which formation is explained by a CNP*-assisted C-H activation of benzaldehyde.[17,18,100]

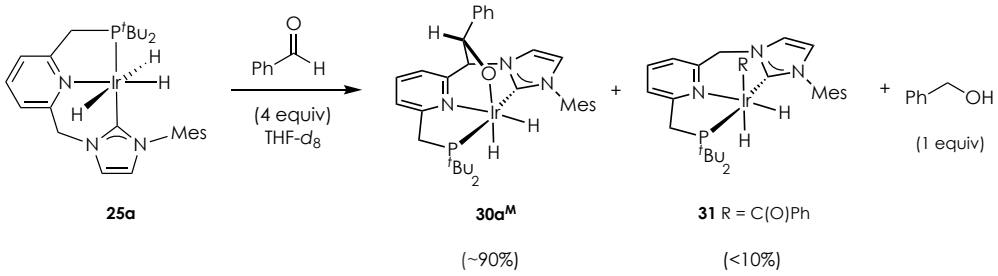

Scheme 20. Reaction of **25a** with benzaldehyde in THF-d_8.

On the other hand, monitoring of the hydrogenation of benzaldehyde catalyzed by 10 mol% of **25a** ($P(H_2)$ = 2 bar) showed **30a^{M}** and **31** as the only observable Ir species till complete transformation of benzaldehyde to benzyl alcohol took place and **25a** was regenerated.

[100] A. Kumar, M. Feller, Y. Ben-David, Y. Diskin-Posnerb, D. Milstein, *Chem. Commun.* **2018**, *54*, 5365.

Although further mechanistic studies are required, the assumption of a ligand-assisted mechanism for the hydrogenation of aldehydes catalyzed by $IrH_3(CNP^{tBu})$ complexes seems plausible on the basis of the experimental results commented above, albeit different pathways can be hypothetized (Figure 36). First, an outer-sphere mechanism involving simultaneous transfer of a hydrido ligand and a methylene proton from **25** to the aldehyde through a transition state **A‡** can be considered. Alternatively, a second reaction sequence could involve the initial insertion of the aldehyde into the Ir-H bond of complex **25** to yield the alcoxide intermediate **B**, followed by protonation of the alcoxy ligand by the acidic CH_2N hydrogens of the pincer leading to the pincer deprotonated derivative **C**. Both catalytic cycles would generate the deprotonated derivative **29**, which would activate a new molecule of H_2 to regenerate the catalytic species **25**. As shown above, complex **29** also reacts with aldehyde giving rise to the reversible formation of **30a**, which can be regarded as the catalyst resting state. Furthermore, although deprotonation of the P-arm of the CNP^{tBu} ligand has not been experimentally observed, participation of the CH_2P bridge in the catalytic process cannot be completely ruled out.

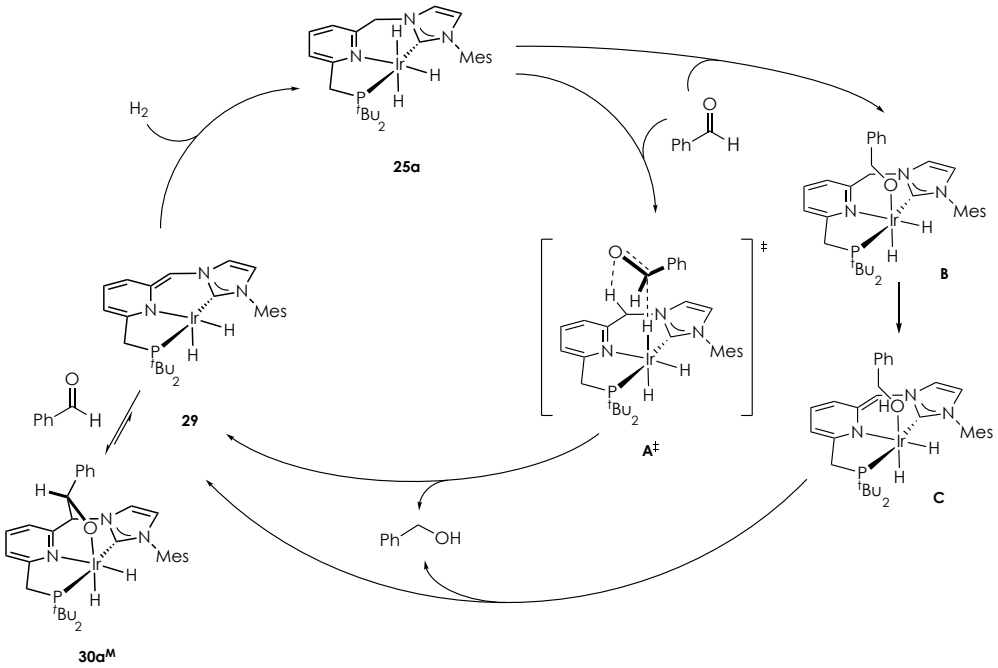

Figure 36. Proposed catalytic cycles for aldehyde hydrogenation catalyzed by trihydride Ir-CNP^{tBu} complexes.

In an attempt to obtain further information on the species participating in the catalytic process, particularly regarding the formation of **B**, a series of experiments were performed. Firstly, the hydrochloride iridium complex **22a** was reacted with sodium phenylmethanolate (8 equiv) in THF-d_8, affording a 45:55 mixture of the trihydrido complex **25a** and the adduct **30a^{M}** (Scheme 21). A similar outcome was observed when benzyl alcohol (10 equiv) was added at 0 ^{o}C to a THF-d_8 solution of **29**, previously generated *in situ* by reaction of **22a** with KHMDS. The resulting solution was found to contain by ^{1}H NMR spectroscopy a 1:1 mixture of the aldehyde adducts **30a** (**30a^{M}/30a^{m}** ratio = 2.3) and the trihydride complex **25a** (Scheme 22). These results suggest that provided an alcoxide derivative **B** is formed, rapid β-hydrogen elimination to yield the IrH_3(CNP^{tBu}) complex **25a** and

benzaldehyde should take place. It should be noted that a conventional alkoxide *β*-hydride elimination (a simple migratory deinsertion) taking place in the coordinatively saturated derivative **B** seems unlikely since an empty coordination site *cis* to the alkoxide ligand is required. However, other mechanisms have been invoked for this type of process in late transition metal alcoxides,[101,102] including full dissociation of the alcoxy ligand, followed by hydride transfer from the dissociated alkoxide to the metal center.[99c,103]

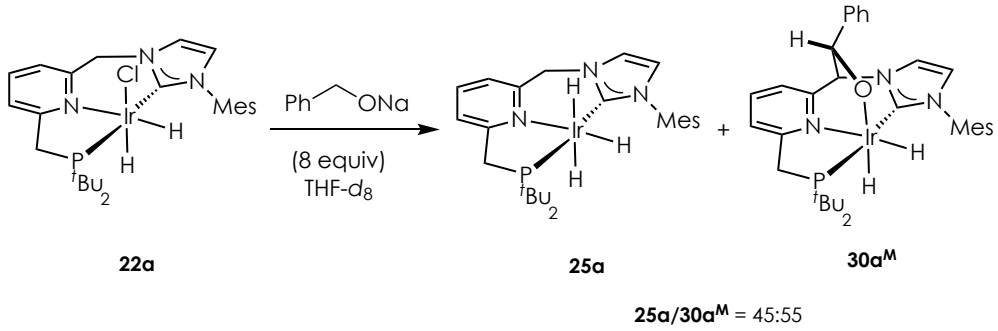

Scheme 21. Reaction of **22a** with sodium phenylmethanolate in THF-d_8.

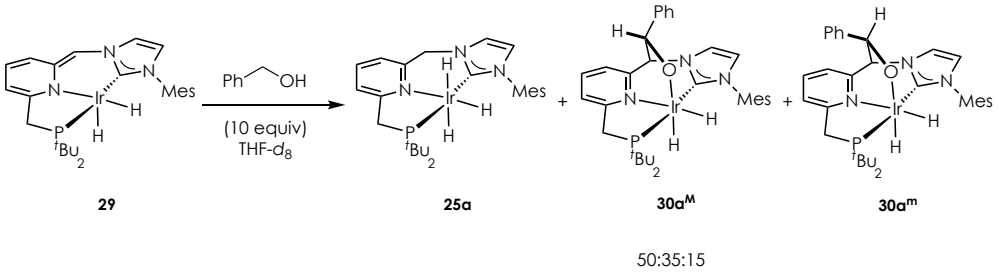

Scheme 22. Reaction of **29** with benzyl alcohol in THF-d_8 at 0 °C.

[101] R. Noyori, M. Yamakawa, S. Hashiguchi, *J. Org. Chem.* **2001**, *66*, 7931.
[102] (a) J. C. M. Ritter; R. G. Bergman, *J. Am. Chem. Soc.* **1997**, *119*, 2580. (b) J. C. M. Ritter; R. G. Bergman, *J. Am. Chem. Soc.* **1998**, *120*, 6826.
[103] (a) O. Blum, D. Milstein, *J. Organomet. Chem.* **2000**, *593−594*, 479; (b) C. M. Fafard, O. V. Ozerov, *Inorg. Chim. Acta* **2007**, *360*, 286; (c) N. A. Smythe, K. A. Grice, B. S. Williams, K. I. Goldberg, *Organometallics* **2009**, *28*, 277. (d) G. R. Fulmer, A. N. Herndon, W. Kaminsky, R. A. Kemp, K. I. Goldberg, *J. Am. Chem. Soc.* **2011**, *133*, 17713.

I.3. Experimental procedures

I.3.1. General considerations

All reactions and manipulations were performed under nitrogen or argon atmosphere, either in a Braun MBraun Unilab Pro glovebox or using standard Schlenk-type techniques.[104] All solvents were dried and distilled under nitrogen, using the following desiccants: sodium-benzophenone-ketyl for diethyl ether (Et_2O), tetrahydrofuran (THF) and 2-methyltetrahydrofuran (2-MeTHF); sodium for hexane, pentane and toluene; CaH_2 for dichloromethane (CH_2Cl_2) and acetonitrile (CH_3CN); and NaOMe for methanol (MeOH).[105] Microanalyses were performed by the Analytical Service of the Instituto de Investigaciones Químicas, using a Leco TruSpec Micro elemental analyzer. The NMR experiments were carried out on Bruker DPX-300, DRX-400, DRX-500 and Advance^{III}-400/R apparatous. The ^{1}H and ^{13}C spectra were referenced to external $SiMe_4$ using the residual proton peaks of the deuterated solvent as internal standards, while ^{31}P and ^{11}B were referenced to external 85% H_3PO_4 and $BF_3 \cdot Et_2O$, respectively. Spectral assignments were made by routine one- and two-dimensional experiments, including ^{1}H-^{1}H COSY, ^{1}H-^{1}H NOESY, ^{1}H-^{13}C HSQC, ^{1}H-^{13}C HMBC, $^{1}H\{^{31}P\}$ and $^{1}H\{^{11}B\}$ NMR spectroscopies. All NMR measurements were carried out at 25 ^{o}C, unless otherwise noted. High resolution mass spectra (HRMS) data were obtained using a ThermoFisher QExactive mass spectrometer at the Analytical Services of the Universidad de Sevilla (CITIUS). ESI-MS experiments were carried out in a Bruker Esquire 6000 apparatus by the Mass Spectrometry Service of the Instituto de

[104] D. F. Shriver, M. A. Dredzon, *The Manipulation of Air-Sensitive Compounds*, 2nd Edition; Wiley-Interscience, **1986**.
[105] D. D. Perrin, W. L. F. Armarego, *Purification of Laboratory Chemicals*, 2nd Edition; Pergamon Press, **1980**.

Investigaciones Químicas. Infrared spectra were recorded on a Bruker Tensor 27 spectrometer.

Ir(acac)(COD), [106] Li[Bcat$_2$][86] and Na[BAr$_F$] [107] were synthetized according to reported methods. The derivatives 1-(3,5-dimethylphenyl)- and 1-(2,4,6-trimethylphenyl)-1*H*-imidazole [108] were synthetized following previously reported methods. All other reagents were purchased from commercial suppliers and used as received.

[106] M. Rueping, R. M. Koenigs, R. Borrmann, J. Zoller, T. E. Weirich, J. Mayer, *Chem. Mater.* **2011**, *23*, 2008.
[107] N. A. Yakelis, R. G. Bergman, *Organometallics* **2005,** *24,* 3579.
[108] M. C. Perry, X. Cui, M. T. Powell, D.-R. Hou, J. H. Reibenspies, K. Burgess, *J. Am. Chem. Soc.* **2003**, *125*, 113.

I.3.2. Synthesis of imidazolium salts

1-[(6-(Chloromethyl)pyridin-2-yl)methyl]-3-mesityl-1*H*-imidazol-2-ium chloride, 1a(Cl)

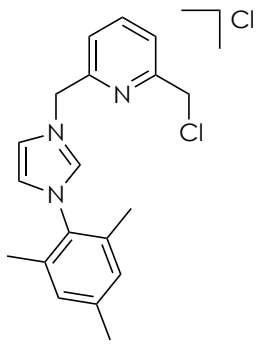

A solution of 2,6-bis(chloromethyl)pyridine (4.00 g, 22.7 mmol) and 1-mesityl-1*H*-imidazole (2.12 g, 11.4 mmol) in toluene (80 mL) was refluxed for 7 days. The resulting precipitate was filtered, washed with cold THF (2 × 20 mL) and pentane (3 × 20 mL), and dried under vacuum. Brown solid (2.91 g, 70%).

^{1}H NMR (400 MHz, $CDCl_3$): δ 10.56 (s, 1H, H arom Imid), 8.13 (s, 1H, H arom Imid), 8.06 (d, $^{3}J_{HH}$ = 7.7 Hz, 1H, H arom Py), 7.84 (dd, $^{3}J_{HH}$ = 7.7 Hz, $^{3}J_{HH}$ = 7.7 Hz, 1H, H arom Py), 7.48 (d, $^{3}J_{HH}$ = 7.7 Hz, 1H, H arom Py), 7.10 (s, 1H, H arom Imid), 6.99 (s, 2H, 2 H arom Mes), 6.24 (s, 2H, CH_2N), 4.63 (s, 2H, CH_2Cl), 2.33 (s, 3H, CH_3), 2.04 (s, 6H, 2 CH_3) ppm.

^{13}C{^{1}H} NMR (126 MHz, $CDCl_3$): δ 156.0 (C_q arom), 151.9 (C_q arom), 141.5 (C_q arom), 140.8 (CH arom), 138.9 (CH arom), 134.3 (2 C_q arom), 130.8 (C_q arom), 130.0 (2 CH arom), 125.1 (CH arom), 124.1 (CH arom),

124.0 (CH arom), 122.8 (CH arom), 52.3 (CH_2N), 45.1 (CH_2Cl), 21.2 (CH_3), 17.7 (2 CH_3) ppm.

HRMS (ESI): *m/z* calcd for $C_{19}H_{21}ClN_3$ [$(M-Cl)^+$]: 326.1424; found: 326.1411.

1-[(6-(Chloromethyl)pyridin-2-yl)methyl]-3-(3,5-xylyl)-1*H*-imidazol-2-ium chloride, 1b(Cl)

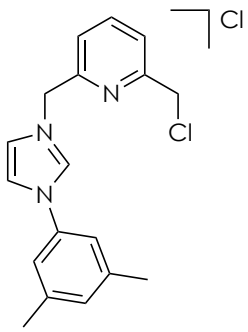

A solution of 2,6-bis(chloromethyl)pyridine (3.96 g, 22.5 mmol) and 1-xylyl-1*H*-imidazole (1.93 g, 11.2 mmol) in THF (20 mL) was heated to 45 °C for 7 days. The solution was concentrated to half of the initial volume by solvent evaporation, and Et_2O (10 mL) was added to precipitate the product. The solid was filtered, washed with Et_2O (2 × 10 mL) and pentane (3 × 5 mL) and dried under vacuum. White solid (2.21 g, 57%).

^{1}H NMR (400 MHz, $CDCl_3$): δ 11.09 (s, 1H, H arom Imid), 8.19 (d, $^3J_{HH}$ = 7.2 Hz, 1H, H arom Py), 8.09 (s, 1H, H arom Imid), 7.89 (dd, $^3J_{HH}$ = 8.0 Hz, $^3J_{HH}$ = 7.2 Hz, 1H, H arom Py), 7.54 (m, 2H, H arom Py + H arom Imid), 7.23 (s, 2H, 2 H arom Xyl), 7.11 (s, 1H, H arom Xyl), 6.10 (s, 2H, CH_2N), 4.69 (s, 2H, CH_2Cl), 2.36 (s, 6H, 2 CH_3) ppm.

^{13}C{^{1}H} NMR (101 MHz, $CDCl_3$): δ 156.1 (C_q arom), 151.7 (C_q arom), 140.9 (CH arom), 140.5 (2 C_q arom), 136.4 (CH arom), 134.3 (CH arom), 132.1 (CH arom), 125.2 (CH arom), 124.1 (C_q arom), 123.8 (CH arom), 120.3 (CH arom), 119.6 (2 CH arom), 52.7 (CH_2N), 45.4 (CH_2Cl), 21.4 (2

CH_3) ppm.

HRMS (ESI): *m/z* calcd for $C_{18}H_{19}ClN_3$ [$(M-Cl)^+$]: 312.1268; found: 312.1256.

1-[(6-(Bromomethyl)pyridin-2-yl)methyl]-3-(3,5-xylyl)-1*H*-imidazol-2-ium chloride, 1b(Br)

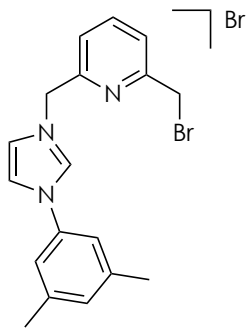

A solution of 1-xylyl-1*H*-imidazole (1.00 g, 5.8 mmol) and 2,6-bis(bromomethyl)pyridine (3.08 g, 11.6 mmol) in THF (40 mL) was stirred for 7 days at room temperature. The resulting precipitate was filtered, washed with cold THF (2 × 10 mL) and hexane (2 × 10 mL), and dried under vacuum. Light brown solid (2.00 g, 79%).

^{1}H NMR (500 MHz, CD_2Cl_2): δ 10.86 (s, 1H, H arom Imid), 7.98 (s, 1H, H arom Imid), 7.80 (d, $^{3}J_{HH}$ = 7.6 Hz, 1H, H arom Py), 7.75 (s, 1H, H arom Imid), 7.72 (dd, $^{3}J_{HH}$ = 7.7 Hz, $^{3}J_{HH}$ = 7.6 Hz, 1H, H arom Py), 7.42 (d, $^{3}J_{HH}$ = 7.6 Hz, 1H, H arom Py), 7.34 (s, 2H, 2 H arom Xyl), 7.12 (s, 1H, H arom Xyl), 5.98 (s, 2H, CH_2N), 4.51 (s, 2H, CH_2Br), 2.36 (s, 6H, 2 CH_3) ppm.

^{13}C{^{1}H} NMR (126 MHz, CD_2Cl_2): δ 157.4 (C_q arom), 152.9 (C_q arom), 141.0 (2 C_q arom), 138.9 (CH arom), 136.1 (CH arom), 134.7 (C_q arom), 132.0 (CH arom), 124.0 (CH arom), 123.9 (CH arom), 123.6 (CH arom), 120.7 (CH arom), 119.7 (2 CH arom), 53.9 (CH_2N), 34.0 (CH_2Br), 21.2 (2 CH_3) ppm.

HRMS (ESI): *m/z* calcd for $C_{18}H_{19}BrN_3$ [$(M-Br)^+$]: 356.0757; found: 356.0751.

1-[(6-(Diphenylphosphinomethyl)pyridin-2-yl)methyl]-3-mesityl-1*H*-imidazol-2-ium chloride, 2a(Cl)

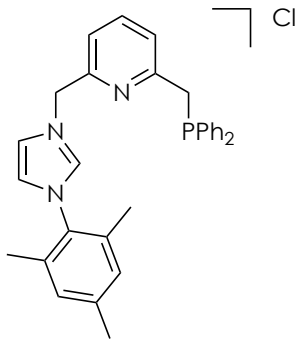

To a solution of PPh_2H (1.08 g, 5.8 mmol) in THF (10 mL) was added a solution of KO^tBu (0.650 g, 5.80 mmol) in THF (10 mL). The resulting mixture was stirred for 5 min, and added to a solution of **1a(Cl)** (2.00 g, 5.5 mmol) in MeCN (40 mL). The suspension was stirred overnight, and MeOH (15 mL) was added to quench the reaction. Solvent was evaporated, and the residue was extracted with CH_2Cl_2 (2 × 15 mL). The solid obtained after removal of the solvent was washed with Et_2O (3 × 20 mL) and pentane (3 × 20 mL), and dried under vacuum. Light brown solid (2.40 g, 85%).

^{1}H NMR (500 MHz, CD_2Cl_2): δ 10.30 (s, 1H, H arom Imid), 7.85 (s, 1H, H arom Imid), 7.60 (d, $^3J_{HH}$ = 7.5 Hz, 1H, H arom Py), 7.54 (dd, $^3J_{HH}$ = 7.6 Hz, $^3J_{HH}$ = 7.6 Hz, 1H, H arom Py), 7.36 (m, 4H, 4 H arom PPh), 7.28 (m, 6H, 6 H arom PPh), 7.12 (s, 1H, H arom Imid), 7.03 (d, $^3J_{HH}$ = 7.7 Hz, 1H, H arom Py), 7.01 (s, 2H, 2 H arom Mes), 5.94 (s, 2H, CH_2N), 3.59 (s, 2H, CH_2P), 2.33 (s, 3H, CH_3), 2.01 (s, 6H, 2 CH_3) ppm.

^{31}P{^{1}H} NMR (202 MHz, CD_2Cl_2): δ −11.7 ppm.

$^{13}C\{^{1}H\}$ NMR (126 MHz, CD_2Cl_2): δ 158.8 (d, J_{CP} = 8 Hz, C_q arom), 152.7 (C_q arom), 141.4 (C_q arom), 138.7 (d, J_{CP} = 3 Hz, CH arom), 138.5 (d, J_{CP} = 15 Hz, 2 C_q arom), 137.9 (CH arom), 134.7 (2 C_q arom), 133.0 (d, J_{CP} = 19 Hz, 4 CH arom), 131.2 (C_q arom), 129.9 (2 CH arom), 129.0 (2 CH arom), 128.7 (d, J_{CP} = 7 Hz, 4 CH arom), 124.0 (d, J_{CP} = 5 Hz, CH arom), 123.9 (CH arom), 122.7 (CH arom), 121.3 (d, J_{CP} = 2 Hz, CH arom), 53.7 (CH_2N), 38.3 (d, J_{CP} = 17 Hz, CH_2P), 21.1 (CH_3), 17.7 (2 CH_3) ppm.

HRMS (ESI): *m/z* calcd for $C_{31}H_{31}N_3P$ $[(M-Cl)^+]$: 476.2256; found: 476.2243.

1-[(6-(Diphenylphosphinomethyl)pyridin-2-yl)methyl]-3-(3,5-xylyl)-1*H*-imidazol-2-ium chloride, 2b(Cl)

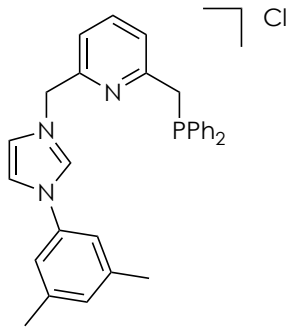

To a solution of $Ph_2P(BH_3)H$ (0.288 g, 1.44 mmol) in THF (10 mL) was added a solution of KO^{t}Bu (0.161 g, 1.44 mmol) in THF (5 mL). The mixture was stirred for 10 min, and added to a suspension of **1b(Cl)** (0.500 g, 1.44 mmol) in MeCN (10 mL). The resulting mixture was stirred overnight, and MeOH (10 mL) was added to quench the reaction. Solvent was evaporated under vacuum, and the residue was extracted with CH_2Cl_2 (3 × 10 mL). Solvent removal followed by washings with Et_2O (2 × 10 mL) yielded a light orange solid which should correspond to the borane adduct of **2b(Cl)**. This solid was dissolved in MeOH (10 mL), and the solution was transferred to a Fisher–Porter vessel and heated to 75 °C for 24 h. Volatiles were removed under vacuum, and MeOH (10 mL) was newly added and the previous procedure repeated. The resulting solid was washed with toluene (2 × 5 mL) and Et_2O (3 × 5 mL) to give an off-white solid (0.444 g, 62%).

^{1}H NMR (400 MHz, CD_2Cl_2): δ 11.28 (s, 1H, H arom Imid), 7.74 (d, $^3J_{HH}$ = 7.6 Hz, 1H, H arom Py), 7.64 (dd, $^3J_{HH}$ = 7.7 Hz, $^3J_{HH}$ = 7.7 Hz, 1H, H arom Py), 7.55 (d, $^3J_{HH}$ = 1.1 Hz, 1H, H arom Imid), 7.44 (m, 4H, 4 H

arom), 7.36 (m, 7H, 7 H arom), 7.29 (s, 2H, 2 H arom Xyl), 7.21 (s, 1H, H arom Xyl), 7.12 (d, $^{3}J_{HH}$ = 7.8 Hz, 1H, H arom Py), 5.91 (s, 2H, CH_2N), 3.69 (s, 2H, CH_2P), 2.45 (s, 6H, 2 CH_3) ppm.

$^{31}P\{^{1}H\}$ NMR (121 MHz, CD_2Cl_2): δ −11.8 ppm.

$^{13}C\{^{1}H\}$ NMR (101 MHz, CD_2Cl_2): δ 159.0 (d, J_{CP} = 8 Hz, C_q arom), 152.6 (C_q arom), 141.0 (2 C_q arom), 138.5 (d, J_{CP} = 15 Hz, 2 C_q arom), 138.0 (CH arom), 136.6 (CH arom), 134.9 (C_q arom), 133.0 (d, J_{CP} = 19 Hz, 4 CH arom), 131.9 (CH arom), 129.1 (2 CH arom), 128.7 (d, J_{CP} = 7 Hz, 4 CH arom), 124.2 (d, J_{CP} = 5 Hz, CH arom), 123.7 (CH arom), 121.8 (CH arom), 120.2 (CH arom), 119.7 (2 CH arom), 54.0 (CH_2N), 38.3 (d, J_{CP} = 16 Hz, CH_2P), 21.3 (2 CH_3) ppm.

HRMS (ESI): *m/z* calcd for $C_{30}H_{29}N_3P$ [$(M-Cl)^+$]: 462.2094; found: 462.2082.

1-[(6-(Diphenylphosphinomethyl)pyridin-2-yl)methyl]-3-(3,5-xylyl)-1*H*-imidazol-2-ium bromide, 2b(Br)

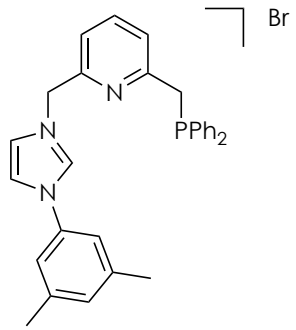

Derivative **2b(Br)** was synthetized from **1b(Br)** as described above for **2b(Cl)**. White solid (0.693 g, 55%).

^{1}H NMR (500 MHz, CD_2Cl_2): δ 10.77 (s, 1H, H arom Imid), 7.65 (d, $^{3}J_{HH}$ = 7.6 Hz, 1H, H arom Py), 7.61 (s, 1H, H arom Imid), 7.56 (m, 2H, H arom Py + H arom Imid), 7.38 (m, 4H, 4 H arom PPh), 7.32 (s, 2H, 2 H arom Xyl), 7.29 (m, 6H, 6 H arom PPh), 7.13 (s, 1H, H arom Xyl), 7.07 (d, $^{3}J_{HH}$ = 7.6 Hz, 1H, H arom Py), 5.84 (s, 2H, CH_2N), 3.62 (s, 2H, CH_2P), 2.37 (s, 6H, 2 CH_3) ppm.

^{31}P{^{1}H} NMR (202 MHz, CD_2Cl_2): δ −11.7 ppm.

^{13}C{^{1}H} NMR (125 MHz, CD_2Cl_2): δ 159.0 (d, J_{CP} = 8 Hz, C_q arom), 152.3 (C_q arom), 141.0 (2 C_q arom), 138.4 (d, J_{CP} = 15 Hz, 2 C_q arom), 137.9 (CH arom), 135.9 (CH arom), 134.8 (C_q arom), 132.9 (d, J_{CP} = 19 Hz, 4 CH arom), 131.9 (CH arom), 129.1 (2 CH arom), 128.7 (d, J_{CP} = 7 Hz, 4 CH arom), 124.2 (d, J_{CP} = 5 Hz, CH arom), 123.9 (CH arom), 121.6 (CH arom), 120.3 (CH arom), 119.7 (2 CH arom), 54.0 (CH_2N), 38.3 (d, J_{CP} = 16 Hz,

CH_2P), 21.3 (2 CH_3) ppm.

HRMS (ESI): *m/z* calcd for $C_{30}H_{29}N_3P$ [$(M-Br)^+$]: 462.2099; found: 462.2089.

1-[(6-(Di-*tert*-butylphosphinomethyl)pyridin-2-yl)methyl]-3-mesityl-1*H*-imidazol-2-ium chloride, 20a

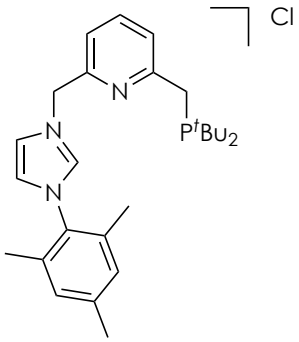

A solution of **1a(Cl)** (0.800 g, 2.21 mmol) and ^{t}Bu$_2$PH (1.29 g, 8.80 mmol) in CH_2Cl_2 (20 mL) was heated to 65 ºC for 6 days. The solvent was evaporated, and the residue was washed with THF (15 mL) and dried under vacuum. Phenethyl diethylamine ScavengePore resin (3.500 g; base loading: 0.66 mmol/g) was added to a solution of the solid in THF (30 mL), and the mixture was stirred for 30 min, and filtered. The solution was brought to dryness, and the residue was washed with Et_2O (15 mL). CH_2Cl_2 was added and the formed solution was stirred for 1 h. The solvent was evaporated and the solid was washed with Et_2O (15 mL), and dried under vacuum (0.509 g). The compound was obtained with a purity of 77% as determined by ^{1}H NMR spectroscopy, and used for the synthesis of the Ir complex **21** without further purification.

^{1}H NMR (400 MHz, CD_2Cl_2): δ 10.84 (s, 1H, H arom Imid), 8.07 (s, 1H, H arom), 7.65 (m, 2H, 2 H arom), 7.40 (m, 1H, H arom), 7.15 (m, 1H, H arom), 7.04 (m, 2H, 2 H arom Mes), 6.02 (s, 2H, CH_2N), 3.04 (br, 2H, CH_2P), 2.34 (s, 3H, CH_3), 2.07 (s, 6H, 2 CH_3), 1.11 (d, $^3J_{HP}$ = 11.0 Hz, 18H, 2 $C(CH_3)_3$) ppm.

$^{31}P\{^{1}H\}$ NMR (162 MHz, CD_2Cl_2): δ 37.1 (br) ppm.

$^{13}C\{^{1}H\}$ NMR (101 MHz, CD_2Cl_2): δ 163.2 (C_q arom), 159.2 (C_q arom), 152.5 (C_q arom), 139.4 (CH arom), 138.0 (CH arom), 134.8 (2 C_q arom), 131.4 (C_q arom), 130.1 (2 CH arom), 124.5 (CH arom), 123.9 (CH arom), 122.7 (CH arom), 121.1 (CH arom), 53.8 (overlapped with the residual solvent signal, CH_2N), 36.5 (d, J_{CP} = 59 Hz, 2 $C(CH_3)_3$), 32.2 (d, J_{CP} = 19 Hz, CH_2P), 29.7 (d, J_{CP} = 12 Hz, 2 $C(CH_3)_3$), 21.2 (CH_3), 17.8 (2 CH_3) ppm.

HRMS (ESI): *m/z* calcd for $C_{27}H_{39}N_3P$ $[(M-Cl)^+]$: 436.2882; found: 436.2869.

Hydrochloride of the 1-[(6-(di-*tert*-butylphosphinomethyl)pyridin-2-yl)methyl]-3-mesityl-1*H*-imidazol-2-ium chloride, 20b·HCl

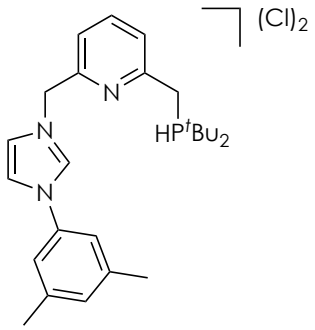

A solution of **1b(Cl)** (0.700 g, 2.00 mmol) and ^{t}Bu$_2$PH (1.170 g, 8.00 mmol) in CH_2Cl_2 (10 mL) was heated to 65 °C for 6 days. The solvent was evaporated, and the resulting solid was washed with THF (15 mL) and dried under vacuum giving rise to a light brown solid (0.883 g). The compound was obtained with a purity of 65% as determined by ^{1}H NMR spectroscopy, and used without further purification for the synthesis of the iridium complex **23**.

^{1}H NMR (400 MHz, CD_2Cl_2): δ 11.90 (s, 1H, H arom Imid), 8.93 (d, $^1J_{HP}$ = 495 Hz, 1H, PH), 8.89 (s, 1H, H arom Imid), 7.99 (d, $^3J_{HH}$ = 7.6 Hz, 1H, H arom Py), 7.78 (m, 2H, H arom Py + H arom Imid), 7.71 (d, $^3J_{HH}$ = 7.8 Hz, 1H, H arom Py), 7.52 (s, 2H, 2 H arom Xyl), 7.18 (s, 1H, H arom Xyl), 6.06 (s, 2H, CH_2N), 4.01 (d, $^2J_{HP}$ = 12.1 Hz, 2H, CH_2P), 2.44 (s, 6H, 2 CH_3), 1.47 (d, $^3J_{HP}$ = 16.0 Hz, 18H, 2 $C(CH_3)_3$) ppm.

^{31}P{^{1}H} NMR (162 MHz, CD_2Cl_2): δ 32.5 (br) ppm.

$^{13}C\{^{1}H\}$ NMR (101 MHz, CD_2Cl_2): δ 153.0 (C_q arom), 152.5 (d, J_{CP} = 7 Hz, C_q arom), 140.7 (2 C_q arom), 139.3 (CH arom), 137.1 (CH arom), 134.5 (C_q arom), 131.4 (CH arom), 125.0 (CH arom), 124.8 (d, J_{CP} = 6 Hz, CH arom), 123.2 (CH arom), 119.7 (CH arom), 119.0 (2 CH arom), 52.7 (CH_2N), 32.8 (d, J_{CP} = 33 Hz, 2 $C(CH_3)_3$), 27.3 (2 $C(CH_3)_3$), 24.2 (d, J_{CP} = 41 Hz, CH_2P), 21.0 (2 CH_3) ppm.

HRMS (ESI): *m/z* calcd for $C_{26}H_{37}N_3P$ $[(M-HCl-Cl)^+]$: 422.2725; found: 422.2718.

I.3.3. Synthesis of Pd-CNP^{Ph} complexes

[Pd(C^{Mes}NP^{Ph})Cl](AgCl$_2$) (3)

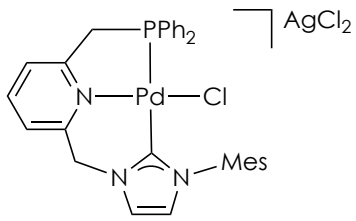

To a solution of **2a(Cl)** (0.100 g, 0.20 mmol) in CH_2Cl_2 (7 mL) was added Ag_2O (0.049 g, 0.21 mmol). The suspension was stirred for 24 h, and then filtered. To the resulting solution was added $PdCl_2$(cod) (0.057 g, 0.20 mmol). After stirring for 4 h, solvent was removed under vacuum, and the residue was washed with Et_2O (2 × 5 mL), extracted with CH_2Cl_2 (2 × 5 mL), and crystallized from a CH_2Cl_2/toluene solvent mixture. Pale yellow solid (0.096 g, 60%).

Anal. calcd (%) for $C_{31}H_{30}AgCl_3N_3PPd$: C 46.8; H 3.8; N 5.3; found: C 47.2; H 3.7; N 4.8.

^{1}H NMR (500 MHz, CD_2Cl_2): δ 8.30 (d, $^3J_{HH}$ = 7.6 Hz, 1H, H arom Py), 8.21 (s, 1H, H arom NHC), 8.05 (dd, $^3J_{HH}$ = 7.5 Hz, $^3J_{HH}$ = 7.5 Hz, 1H, H arom Py), 7.92 (d, $^3J_{HH}$ = 7.6 Hz, 1H, H arom Py), 7.73 (dd, $^3J_{HP}$ = 12.1 Hz, $^3J_{HH}$ = 8.1 Hz, 4H, 4 H arom PPh), 7.58 (t, $^3J_{HH}$ = 7.5 Hz, 2H, 2 H arom PPh), 7.50 (m, 4H, 4 H arom PPh), 7.03 (s, 2H, 2 H arom Mes), 6.95 (s, 1H, H arom NHC), 6.05 (s, 2H, CH_2N), 4.32 (d, $^2J_{HP}$ = 11.3 Hz, 2H, CH_2P), 2.39 (s, 3H, CH_3), 2.17 (s, 6H, 2 CH_3) ppm.

^{31}P{^{1}H} NMR (121 MHz, CD_2Cl_2): δ 34.8 ppm.

$^{13}C\{^{1}H\}$ NMR (126 MHz, CD_2Cl_2): δ 166.4 (d, J_{CP} = 183 Hz, C-2 NHC), 161.9 (d, J_{CP} = 7 Hz, C_q arom), 155.1 (C_q arom), 142.1 (CH arom), 139.6 (C_q arom), 135.8 (C_q arom), 135.5 (2 C_q arom), 133.3 (d, J_{CP} =11 Hz, 4 CH arom), 132.7 (2 CH arom), 129.7 (d, J_{CP} = 12 Hz, 4 CH arom), 129.0 (2 CH arom), 126.6 (d, J_{CP} = 46 Hz, 2 C_q arom), 126.4 (CH arom), 125.4 (d, J_{CP} = 10 Hz, CH arom), 124.0 (d, J_{CP} = 5 Hz, CH arom), 123.4 (d, J_{CP} = 5 Hz, CH arom), 55.2 (CH_2N), 41.7 (d, J_{CP} = 28 Hz, CH_2P), 21.3 (CH_3), 18.6 (2 CH_3) ppm.

MS (ESI, CH_2Cl_2): *m*/*z* 616 ([$(M-AgCl_2)^+$], 100).

[Pd(C^{Mes}NP^{Ph})(MeCN)](BF$_4$)$_2$ (4)

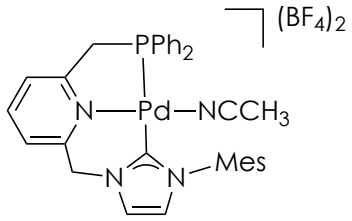

A mixture of palladium complex **3** (0.041 g, 0.06 mmol) and $AgBF_4$ (0.025 g, 0.13 mmol) in CH_2Cl_2/MeCN (3:1) (4 mL) was stirred in the dark for 2 h. The suspension was brought to dryness, and CH_2Cl_2 (4 mL) was added. The resulting suspension was filtered through a short pad of celite, and volatiles were removed under reduced pressure to yield a yellow solid (0.038 g, 85%). This complex is stable in solution in the presence of a slight amount of MeCN. Satisfactory elemental analysis for complex **4** could not be obtained presumably due to easy loss of MeCN.

^{1}H NMR (CD_2Cl_2, 400 MHz): δ 8.09 (td, $^3J_{HH}$ = 7.8 Hz, $^5J_{HP}$ = 1.3 Hz, 1H, H arom), 7.96 (m, 2H, 2 H arom), 7.88 (m, 1H, H arom), 7.78 (m, 1H, H arom), 7.76 (d, $^3J_{HH}$ = 1.5 Hz, 1H, H arom NHC), 7.74 (m, 1H, H arom), 7.73 (d, $^3J_{HH}$ = 1.5 Hz, 1H, H arom NHC), 7.68 (m, 2H, 2 H arom), 7.60 (m, 4H, 4 H arom), 7.13 (m, 3H, 3 H arom), 5.81 (s, 2H, CH_2N), 4.59 (d, $^2J_{HP}$ = 12.3 Hz, 2H, CH_2P), 2.37 (s, 3H, CH_3), 2.22 (s, 6H, 2 CH_3), 2.17 (br s, 3H, CH_3CN) ppm.

^{31}P{^{1}H} NMR (CD_2Cl_2, 162 MHz): δ 43.7 ppm.

^{13}C{^{1}H} NMR (CD_2Cl_2, 101 MHz): δ 163.1 (d, J_{CP} = 161 Hz, C-2 NHC), 163.0 (d, J_{CP} = 7 Hz, C_q arom), 155.1 (C_q arom), 143.5 (CH arom), 140.9 (C_q arom), 135.8 (2 C_q arom), 134.5 (C_q arom), 133.9 (d, J_{CP} = 3 Hz, 2 CH arom), 133.3 (d, J_{CP} = 12 Hz, 4 CH arom), 130.5 (d, J_{CP} = 12 Hz, 4 CH

arom), 129.7 (2 CH arom), 126.5 (d, J_{CP} = 12 Hz, CH arom), 126.4 (CH arom), 124.2 (d, J_{CP} = 5 Hz, CH arom), 123.7 (d, J_{CP} = 5 Hz, CH arom), 123.6 (d, J_{CP} = 51 Hz, 2 C_q arom), 118.8 (br, CH_3CN), 55.3 (CH_2N), 40.4 (d, J_{CP} = 30 Hz, CH_2P), 21.1 (CH_3), 18.2 (2 CH_3), 2.4 (br, CH_3CN) ppm.

[Pd(C^{Mes}NP^{Ph})(CO)](BF$_4$)$_2$ (5)

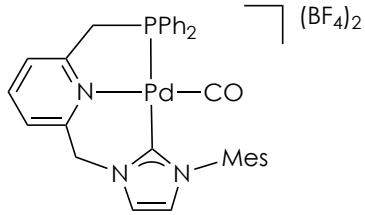

A J.Young valved NMR tube containing a solution of palladium complex **4** (0.020 g, 0.03 mmol) in CD_2Cl_2 (0.7 mL) was pressurized with 2 bar of CO. Formation of complex **5** (aprox. 45%) was determined by NMR analysis. The complex is only stable under CO atmosphere. NMR spectroscopy characterization of complex **5** was effected in admixture with **4**.

^{1}H NMR (CD_2Cl_2, 400 MHz): δ 8.14 (dd, $^3J_{HH}$ = 7.7 Hz, $^3J_{HH}$ = 7.7 Hz, 1H, H arom Py), 8.03 (d, $^3J_{HH}$ = 7.9 Hz, 1H, H arom Py), 7.95 (m, 1H, H arom), 7.91 (m, 1H, H arom), 7.82-7.60 (m, 10H, 10 H arom), 7.29 (s, 1H, H arom NHC), 7.13 (s, 2H, 2 H arom Mes), 5.91 (s, 2H, CH_2N), 4.83 (d, $^2J_{HP}$ = 13.2 Hz, 2H, CH_2P), 2.36 (s, 3H, CH_3), 2.18 (s, 6H, 2 CH_3) ppm.

^{31}P{^{1}H} NMR (CD_2Cl_2, 162 MHz): δ 48.2 ppm.

^{13}C{^{1}H} NMR (CD_2Cl_2, 101 MHz): δ 169.7 (d, J_{CP} = 11 Hz, CO), 164.8 (d, J_{CP} = 142 Hz, C-2 NHC), 162.3 (d, J_{CP} = 6 Hz, C_q arom), 154.2 (C_q arom), 144.3 (CH arom), 142.1 (C_q arom), 136.4 (2 C_q arom), 134.4 (m, 2 CH arom + C_q arom), 133.4 (d, J_{CP} = 12 Hz, 4 CH arom), 130.6 (d, J_{CP} = 12 Hz, 4 CH arom), 130.1 (2 CH arom), 126.5 (d, J_{CP} = 12 Hz, CH arom), 126.3 (CH arom), 124.4 (d, J_{CP} = 4 Hz, CH arom), 124.0 (d, J_{CP} = 4 Hz, CH arom), 123.3 (d, J_{CP} = 55 Hz, 2 C_q arom), 55.1 (CH_2N), 41.2 (d, J_{CP} = 31 Hz, CH_2P), 21.2 (CH_3), 17.9 (2 CH_3) ppm.

Complex 6

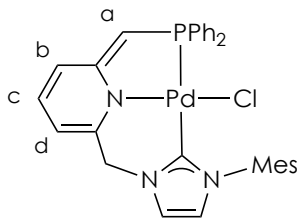

To a suspension of **3** (0.025 g, 0.04 mmol) in THF (2 mL) was added KHMDS (0.007 g, 0.04 mmol). The mixture was stirred for 30 min, and solvent was evaporated under reduced pressure. The residue was washed with Et_2O (2 × 2 mL) and extracted with THF (2 × 2 mL). Solvent removal under vacuum provided complex **6** as an orange solid (0.020 g, 85%). An analytical pure sample of **6** could not be obtained due to significant decomposition of the complex during purification.

^{1}H NMR (400 MHz, THF-d_8): δ 7.71 (m, 4H, 4 H arom Ph), 7.44 (s, 1H, H arom NHC), 7.22 (m, 6H, 6 H arom Ph), 6.98 (s, 1H, H arom NHC), 6.87 (s, 2H, 2 H arom Mes), 6.46 (ddd, $^3J_{HH}$ = 8.9 Hz, $^3J_{HH}$ = 6.4 Hz, $^5J_{HP}$ = 2.8 Hz, 1H, H^c), 6.30 (d, $^3J_{HH}$ = 8.7 Hz, 1H, H^b), 5.55 (d, $^3J_{HH}$ = 6.3 Hz, 1H, H^d), 4.87 (s, 2H, CH_2N), 3.41 (s, 1H, H^a), 2.30 (s, 3H, CH_3), 2.08 (s, 6H, 2 CH_3) ppm.

^{31}P{^{1}H} NMR (162 MHz, THF-d_8): δ 25.3 ppm.

^{13}C{^{1}H} NMR (126 MHz, THF-d_8): δ 175.1 (d, J_{CP} = 166 Hz, C-2 NHC), 174.8 (d, J_{CP} = 26 Hz, C_q arom), 150.0 (C_q arom), 138.7 (C_q arom), 137.9 (C_q arom), 137.4 (d, J_{CP} = 8 Hz, 2 C_q arom), 136.2 (2 C_q arom), 133.3 (d, J_{CP} = 11 Hz, 4 CH arom), 132.7 (C^c), 129.6 (2 CH arom), 129.0 (2 CH arom), 128.2 (d, J_{CP} = 11 Hz, 4 CH arom), 123.4 (d, J_{CP} = 5 Hz, CH arom), 121.2

(d, J_{CP} = 4 Hz, CH arom), 117.0 (d, J_{CP} = 21 Hz, C^{b}), 102.9 (C^{d}), 63.3 (d, J_{CP} = 66 Hz, C^{a}), 56.9 (CH_2N), 21.2 (CH_3), 18.6 (2 CH_3) ppm.

I.3.4. Synthesis of olefin Ir-CNP^{Ph} complexes

[Ir(C^{Mes}NP^{Ph})(COD)]Cl (7a(Cl))

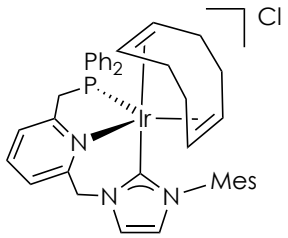

A solution of **2a(Cl)** (0.769 g, 1.50 mmol) in CH_2Cl_2 (8 mL) was added to a solution of Ir(acac)(COD) (0.600 g, 1.50 mmol) in CH_2Cl_2 (8 mL). The resulting solution was stirred overnight. Solvent was evaporated, and the solid was recrystallized from cold THF and washed with Et_2O (2 × 10 mL) and pentane (2 × 10 mL). Yellow solid (0.682 g, 56%).

^{1}H NMR (400 MHz, CD_2Cl_2): δ 8.46 (s, 1H, H arom NHC), 8.33 (d, $^3J_{HH}$ = 7.5 Hz, 1H, H arom Py), 7.88 (dd, $^3J_{HH}$ = 7.5 Hz, $^3J_{HH}$ = 7.5 Hz, 1H, H arom Py), 7.79 (dd, $^3J_{HP}$ = 8.5 Hz, $^3J_{HH}$ = 8.5 Hz, 2H, 2 H arom PPh), 7.62 (m, 3H, 3 H arom), 7.38 (d, $^3J_{HH}$ = 7.5 Hz, 1H, H arom Py), 7.12 (d, $^2J_{HH}$ = 14.0 Hz, 1H, C*H*HN), 7.08 (t, $^3J_{HH}$ = 7.5 Hz, 1H, H arom), 6.89 (m, 3H, 3 H arom), 6.75 (s, 1H, H arom), 6.65 (s, 1H, H arom NHC), 5.87 (dd, $^3J_{HP}$ = 8.0 Hz, $^3J_{HH}$ = 8.0 Hz, 2H, 2 H arom PPh), 5.56 (d, $^2J_{HH}$ = 14.0 Hz, 1H, C*H*HN), 3.97 (dd, $^2J_{HH}$ = 14.8 Hz, $^2J_{HP}$ = 11.5 Hz, 1H, C*H*HP), 3.45 (m, 3H, 2 CH= COD + C*H*HP), 2.93 (br, 2H, 2 CH= COD), 2.31 (s, 3H, CH_3), 2.05 (br, 4H, 4 C*H*H COD), 1.75 (s, 3H, CH_3), 1.71 (br, 2H, 2 C*H*H COD), 1.28 (br, 2H, 2 C*H*H COD), 0.98 (s, 3H, CH_3) ppm.

^{31}P {^{1}H} NMR (162 MHz, CD_2Cl_2): δ 16.9 ppm.

$^{13}C\{^{1}H\}$ NMR (126 MHz, CD_2Cl_2): δ 164.4 (d, J_{CP} = 8 Hz, C-2 NHC), 160.1 (d, J_{CP} = 4 Hz, C_q arom), 158.5 (d, J_{CP} = 6 Hz, C_q arom), 139.5 (CH arom + C_q arom), 137.7 (C_q arom), 136.8 (d, J_{CP} = 18 Hz, C_q arom), 135.9 (C_q arom), 135.3 (C_q arom), 134.0 (CH arom), 133.8 (CH arom), 131.6 (d, J_{CP} = 2 Hz, CH arom), 130.3 (d, J_{CP} =10Hz, 2 CH arom), 130.1 (d, J_{CP} = 2 Hz, CH arom), 130.1 (d, J_{CP} = 39 Hz, C_q arom), 129.3 (d, J_{CP} = 10 Hz, 2 CH arom), 129.2 (d, J_{CP} = 8 Hz, 2 CH arom), 128.8 (d, J_{CP} = 10 Hz, 2 CH arom), 125.0 (d, J_{CP} = 5 Hz, CH arom), 124.7 (CH arom), 124.3 (CH arom), 123.6 (d, J_{CP} = 2 Hz, CH arom), 63.5 (br, 4 CH= COD), 59.5 (CH_2N), 44.3 (d, J_{CP} = 29 Hz, CH_2P), 37.7 (d, J_{CP} = 6 Hz, 2 CH_2 COD), 28.8 (br, 2 CH_2 COD), 21.0 (CH_3), 18.0 (CH_3), 17.5 (CH_3) ppm.

MS (ESI, CH_2Cl_2): *m/z* 776 ([$(M-Cl)^+$], 100). Fragmentation of ion *m/z* = 776: 666 ([$(M-HCl-C_8H_{12})^+$], 100).

HRMS (ESI): *m/z* calcd for $C_{39}H_{42}N_3IrP$ [$(M-Cl)^+$]: 776.2746; found: 776.2740.

[Ir(C^{Xyl}NP^{Ph})(COD)]Cl (7b(Cl))

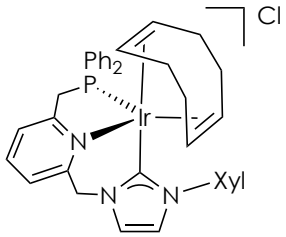

To a solution of Ir(acac)(COD) (0.269 g, 0.67 mmol) in CH_2Cl_2 (5 mL) was added a solution of **2b(Cl)** (0.335 g, 0.67 mmol) in CH_2Cl_2 (8 mL), and the reaction mixture was stirred for 4 h. After solvent evaporation, the solid was extracted with CH_3CN (5 mL). The solvent was removed under vacuum, and the resulting solid was washed with toluene (3 × 3 mL) and Et_2O (3 × 5 mL), and dried under vacuum. Orange-yellow solid (0.412 g, 77%).

Anal. calcd (%) for $C_{38}H_{40}ClIrN_3P \cdot CH_2Cl_2$: C 53.1, H 4.8, N 4.8; found: C 53.4, H 5.0, N 4.75.

^{1}H NMR (400 MHz, CD_2Cl_2): δ 8.42 (d, $^3J_{HH}$ = 4.0 Hz, 1H, H arom NHC), 8.32 (d, $^3J_{HH}$ = 8.0 Hz, 1H, H arom Py), 7.90 (dd, $^3J_{HH}$ = 8.0 Hz, $^3J_{HH}$ = 8.0 Hz, 1H, H arom Py), 7.83 (ddd, $^3J_{HP}$ = 10.4 Hz, $^3J_{HH}$ = 8.0 Hz, $^4J_{HH}$ = 1.6 Hz, 2H, 2 H arom PPh), 7.63 (m, 3H, 3 H arom PPh), 7.51 (d, $^3J_{HH}$ = 8.0 Hz, 1H, H arom Py), 7.20 (d, $^2J_{HH}$ = 12.0 Hz, 1H, C*H*HN), 7.05 (td, $^3J_{HH}$ = 7.6 Hz, $^5J_{HP}$ = 1.2 Hz, 1H, H arom PPh), 6.84 (d, $^3J_{HH}$ = 4.0 Hz, 1H, H arom NHC), 6.83 (s, 1H, H arom Xyl), 6.76 (m, 2H, 2 H arom PPh), 6.53 (s, 2H, 2 H arom Xyl), 5.59 (d, $^2J_{HH}$ = 12.0 Hz, 1H, C*H*HN), 5.43 (dd, $^3J_{HH}$ = 7.7 Hz, $^3J_{HH}$ = 7.7 Hz, 2H, 2 H arom PPh), 4.19 (dd, $^2J_{HH}$ = 15.6 Hz, $^2J_{HP}$ = 11.6, 1H, C*H*HP), 3.46 (br, 2H, 2 CH= COD), 3.35 (dd, $^2J_{HH}$ = 15.6 Hz,

$^{2}J_{HP}$ = 3.2 Hz, 1H, C*H*HP), 2.96 (br, 2H, 2 CH= COD), 2.32 (m, 4H, 4 C*H*H COD), 2.12 (s, 6H, 2 CH_3), 1.94 (m, 2H, 2 C*H*H COD), 1.39 (m, 2H, 2 C*H*H COD) ppm.

$^{31}P\{^{1}H\}$ NMR (162 MHz, CD_2Cl_2): δ 19.9 ppm.

$^{13}C\{^{1}H\}$ NMR (126 MHz, CD_2Cl_2): δ 164.5 (d, J_{CP} = 8 Hz, C-2 NHC), 160.3 (d, J_{CP} = 4 Hz, C_q arom), 159.0 (d, J_{CP} = 6 Hz, C_q arom), 139.5 (2 C_q arom), 139.2 (C_q arom), 138.4 (CH arom), 135.2 (d, J_{CP} = 25 Hz, C_q arom), 134.4 (d, J_{CP} = 13 Hz, 2 CH arom), 131.8 (d, J_{CP} = 2 Hz, CH arom), 129.6 (CH arom), 129.4 (m, 3 CH arom), 129.2 (d, J_{CP} = 10 Hz, 2 CH arom), 129.0 (d, J_{CP} = 8 Hz, 2 CH arom), 128.5 (d, J_{CP} = 47 Hz, C_q arom), 124.6 (d, J_{CP} = 4 Hz, CH arom), 124.1 (CH arom), 123.4 (d, J_{CP} = 2 Hz, CH arom), 122.1 (2 CH arom), 121.8 (CH arom), 66.1 (br, 4 CH= COD), 59.1 (CH_2N), 44.7 (d, J_{CP} = 27 Hz, CH_2P), 38.4 (d, J_{CP} = 6Hz, 2 CH_2 COD), 28.3 (2 CH_2 COD), 21.3 (2 CH_3) ppm.

[Ir(C^{Xyl}NP^{Ph})(COD)]Br (7b(Br))

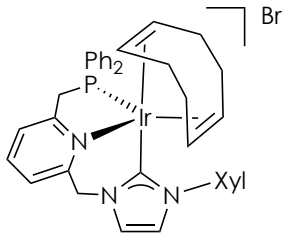

A solution of Ir(acac)(COD) (0.368 g, 0.92 mmol) in CH_2Cl_2 was added a solution of **2b(Br)** (0.500 g, 0.92 mmol) in CH_2Cl_2, and the mixture was stirred overnight. Solvent was evaporated, and the residue was extracted with CH_3CN (5 mL). The solution was brought to dryness, and the resulting solid was washed with toluene (7 mL) and Et_2O (7 mL). Pale orange solid (0.238 g, 31%).

Anal. calcd (%) for $C_{38}H_{40}BrIrN_3P$: C 54.2, H 4.8, N 5.0; found: C 54.4, H 5.0, N 4.7.

^{1}H NMR (400 MHz, CD_2Cl_2): δ 8.28 (d, $^3J_{HH}$ = 7.7 Hz, 1H, H arom Py), 8.26 (d, $^3J_{HH}$= 1.5 Hz, 1H, H arom NHC), 7.92 (dd, $^3J_{HH}$= 7.7 Hz, $^3J_{HH}$ = 7.7 Hz, 1H, H arom Py), 7.83 (dd, $^3J_{HP}$ = 8.9 Hz, $^3J_{HH}$= 8.9 Hz, 2H, 2 H arom PPh), 7.64 (m, 3H, 3 H arom PPh), 7.49 (d, $^3J_{HH}$= 7.8 Hz, 1H, H arom Py), 7.09 (t, $^3J_{HH}$= 7.5 Hz, 1H, H arom PPh), 6.91 (d, $^2J_{HH}$ = 14.1 Hz, 1H, C*H*HN), 6.88 (d, $^3J_{HH}$ = 1.5 Hz, 1H, H arom NHC), 6.85 (s, 1H, H arom Xyl), 6.79 (dd, $^3J_{HH}$ = 6.6 Hz, $^3J_{HH}$ = 6.6 Hz, 2H, 2 H arom PPh), 6.53 (s, 2H, 2 H arom Xyl), 5.65 (d, $^2J_{HH}$ = 14.1 Hz, 1H, C*H*HN), 5.45 (dd, $^3J_{HH}$ = 8.4 Hz, $^3J_{HH}$= 8.4 Hz, 2H, 2 H arom PPh), 4.17 (dd, $^2J_{HH}$ = 15.6 Hz, $^2J_{HP}$ = 11.6 Hz, 1H, C*H*HP), 3.49 (br, 2H, 2 CH= COD), 3.36 (dd, $^2J_{HH}$ = 15.6 Hz, $^2J_{HP}$ = 2.1 Hz, 1H, C*H*HP), 2.98 (br, 2H, 2 CH= COD), 2.35 (br, 4H, 2 CH_2

COD), 2.14 (s, 6H, 2 CH_3), 1.92 (br, 2H, CH_2 COD), 1.42 (br, 2H, CH_2 COD) ppm.

$^{31}P\{^1H\}$ NMR (162 MHz, CD_2Cl_2): δ 20.0 ppm.

$^{13}C\{^1H\}$ NMR (101 MHz, CD_2Cl_2): δ 164.8 (d, J_{CP} = 8 Hz, C-2 NHC), 160.4 (d, J_{CP} = 3 Hz, C_q arom), 158.8 (d, J_{CP} = 6 Hz, C_q arom), 139.6 (CH arom), 139.2 (C_q arom), 138.5 (2 C_q arom), 135.3 (d, J_{CP} = 25 Hz, C_q arom), 134.5 (d, J_{CP} = 13 Hz, 2 CH arom), 131.9 (CH arom), 129.8 (CH arom), 129.7 (CH arom), 129.5 (d, J_{CP} = 9 Hz, 2 CH arom), 129.3 (d, J_{CP} =10 Hz, 2 CH arom), 129.1 (d, J_{CP} = 8 Hz, 2 CH arom), 128.6 (d, J_{CP} = 43 Hz, C_q arom), 124.7 (d, J_{CP} = 4 Hz, CH arom), 123.8 (CH arom), 123.4 (CH arom), 122.3 (2 CH arom), 122.2 (CH arom), 66.0 (br, 4 CH= COD), 59.4 (CH_2N), 44.7 (d, J_{CP} = 28 Hz, CH_2P), 38.5 (d, J_{CP} = 6 Hz, 2 CH_2 COD), 28.4 (2 CH_2 COD), 21.4 (2 CH_3) ppm.

MS (ESI, CH_2Cl_2): *m/z* 762 ($[(M-Br)^+]$, 100). Fragmentation of ion *m/z* = 762: 654 ($[(M-Br-C_8H_{12})^+]$, 100).

[Ir(C^{Xyl}NP^{Ph})(COD)](BAr$_F$) (7b(BAr$_F$))

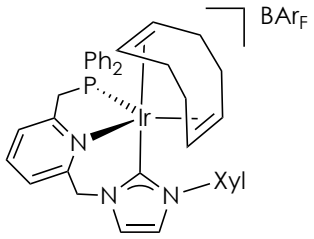

A solution of **7b(Br)** (0.100 g, 0.12 mmol) in CH_2Cl_2 (5 mL) was added to a solution of $NaBAr_F$ (0.105 g, 0.12 mmol) in CH_2Cl_2 (5 mL). The resulting suspension was stirred for 4 h. The precipitate was filtered off, and the solvent was removed under vacuum to yield complex **7b(BAr$_F$)** as an orange solid (0.164 g, 85%). Crystals of complex **7b(BAr$_F$)** suitable for X-ray diffraction analysis were grown by layering pentane over a CH_2Cl_2 solution of the complex.

Anal. calcd (%) for $C_{70}H_{52}BF_{24}IrN_3P$: C 51.7, H 3.2, N 2.6; found: C 51.6, H 3.2, N 2.5.

^{1}H NMR (500 MHz, CD_2Cl_2): δ 7.86 (dd, $^3J_{HH}$ = 7.6 Hz, $^3J_{HH}$ = 7.6 Hz, 1H, H arom Py), 7.81 (dd, $^3J_{HH}$ = 8.5 Hz, $^3J_{HP}$ = 6.7 Hz, 2H, 2 H arom PPh), 7.76 (s, 8H, 8 H arom BAr$_F$), 7.66 (m, 4H, 3 H arom PPh + H arom Py), 7.58 (s, 4H, 4 H arom BAr$_F$), 7.48 (d, $^3J_{HH}$ = 7.7 Hz, 1H, H arom Py), 7.33 (d, $^3J_{HH}$ = 2.0 Hz, 1H, H arom NHC), 7.11 (t, $^3J_{HH}$ = 7.5 Hz, 1H, H arom PPh), 6.95 (d, $^3J_{HH}$ = 2.0 Hz, 1H, H arom NHC), 6.93 (s, 1H, H arom Xyl), 6.82 (ddd, $^3J_{HH}$ = 8.1 Hz, $^3J_{HH}$ = 8.1 Hz, $^4J_{HP}$ = 1.9 Hz, 2H, 2 H arom PPh), 6.49 (s, 2H, 2 H arom Xyl), 5.86 (d, $^2J_{HH}$ = 14.2 Hz, 1H, C*H*HN), 5.48 (dd, $^3J_{HH}$ = 8.7 Hz, $^3J_{HP}$ = 8.7 Hz, 2H, 2 H arom PPh), 5.44 (d, $^2J_{HH}$ = 14.2 Hz, 1H, C*H*HN), 4.16 (dd, $^2J_{HH}$ = 15.6 Hz, $^2J_{HP}$ = 11.3 Hz, 1H, C*H*HP),

3.55 (br, 2H, 2 CH= COD), 3.39 (dd, $^{2}J_{HH}$ = 15.6 Hz, $^{2}J_{HP}$ = 3.0 Hz, 1H, C*H*HP), 3.02 (br, 2H, 2 CH= COD), 2.39 (m, 4H, 4 C*H*H COD), 2.16 (s, 6H, 2 CH_3), 1.95 (m, 2H, 2 C*H*H COD), 1.49 (m, 2H, 2 C*H*H COD) ppm.

$^{31}P\{^{1}H\}$ NMR (202 MHz, CD_2Cl_2): δ 20.3 ppm.

$^{13}C\{^{1}H\}$ NMR (125 MHz, CD_2Cl_2): δ 166.1 (d, J_{CP} = 8 Hz, C-2 NHC), 162.2 (q, J_{CB} = 50 Hz, 4 BC_q arom BAr_F), 161.5 (d, J_{CP} = 3 Hz, C_q arom), 157.5 (d, J_{CP} = 6 Hz, C_q arom), 139.7 (CH arom), 139.0 (d, J_{CP} = 10 Hz, C_q arom), 139.0 (2 C_q arom), 135.3 (m, 8 CH arom BAr_F), 135.1 (overlapped, C_q arom), 134.5 (d, J_{CP} = 14 Hz, 2 CH arom), 132.2 (d, J_{CP} = 2 Hz, CH arom), 130.5 (CH arom), 130.1 (d, J_{CP} = 2 Hz, CH arom), 129.7 (d, J_{CP} = 10 Hz, 2 CH arom), 129.5 (d, J_{CP} =10 Hz, 2 CH arom), 129.3 (d, J_{CP} = 8 Hz, 2 CH arom), 129.3 (q, J_{CF} = 32 Hz, 8 C_q arom BAr_F), 128.2 (d, J_{CP} = 38 Hz, C_q arom), 125.3 (d, J_{CP} = 5 Hz, CH arom), 124.8 (q, J_{CF} = 272 Hz, 8 CF_3), 123.4 (CH arom), 122.6 (2 CH arom), 122.2 (CH arom), 122.0 (CH arom), 117.9 (m, 4 CH arom BAr_F), 66.2 (br, 4 CH= COD), 60.7 (CH_2N), 44.7 (d, J_{CP} = 28 Hz, CH_2P), 38.3 (d, J_{CP} = 6 Hz, 2 CH_2 COD), 28.6 (2 CH_2 COD), 21.4 (2 CH_3) ppm.

MS (ESI, CH_2Cl_2): *m/z* 762 ([(*M*− $C_{32}H_{12}BF_{24})^{+}$], 100). Fragmentation of ion *m/z* = 762: 654 ([(*M*− $C_{32}H_{12}BF_{24}$−$C_8H_{12})^{+}$], 100).

I.3.5. Reactivity of complexes 7 towards KO^{t}Bu and H_2

Complex 8

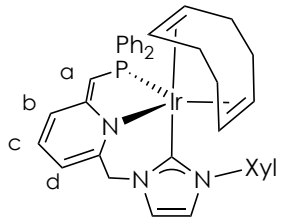

In a J.Young valved NMR tube, a suspension of **7b(Br)** (0.030 g, 0.036 mmol) in THF-d_8 (0.7 mL) cooled to 0 ^{o}C was treated with KO^{t}Bu (0.004 g, 0.039 mmol), inmediately forming a dark red solution that was analyzed by NMR spectroscopy.

^{1}H NMR (400 MHz, THF-d_8, 273 K): δ 7.98 (ddd, $^3J_{HH}$ = 7.9 Hz, $^3J_{HP}$ = 7.9 Hz, $^4J_{HH}$ = 1.6 Hz, 2H, 2 H arom PPh), 7.50 (d, $^3J_{HH}$ = 2.0 Hz, 1H, H arom NHC), 7.45 (m, 3H, 3 H arom PPh), 7.22 (d, $^3J_{HH}$= 2.0 Hz, 1H, H arom NHC), 7.00 (s, 2H, 2 H arom Xyl), 6.92 (td, $^3J_{HH}$= 7.4 Hz, $^5J_{HP}$ = 1.5 Hz, 1H, H arom PPh), 6.81 (ddd, $^3J_{HH}$= 7.7 Hz, $^3J_{HH}$= 7.7 Hz, $^4J_{HP}$ = 1.4 Hz, 2H, 2 H arom PPh), 6.79 (s, 1H, H arom Xyl), 6.65 (dd, $^3J_{HH}$= 7.5 Hz, $^3J_{HP}$ = 7.5 Hz, 2 H, 2 H arom PPh), 6.39 (ddd, $^3J_{HH}$= 8.5 Hz, $^3J_{HH}$= 6.3 Hz, $^5J_{HP}$ = 1.9 Hz, 1H, H^c), 5.98 (d, $^3J_{HH}$ = 8.6 Hz, 1H, H^b), 5.58 (d, $^3J_{HH}$= 6.2 Hz, 1H, H^d), 5.29 (d, $^2J_{HH}$ = 13.6 Hz, 1H, C*H*HN), 4.93 (d, $^2J_{HH}$ = 13.6 Hz, 1H, C*H*HN), 3.86 (s, 1H, H^a), 3.09 (br, 2H, 2 CH= COD), 2.62 (br, 2H, 2 CH= COD), 2.16 (s, 6H, 2 CH_3), 2.04 (br, 4H, 4 C*H*H COD), 1.89 (br, 2H, 2 CH*H* COD), 1.66 (br, 2H, 2 C*H*H COD) ppm.

^{31}P{^{1}H} NMR (162 MHz, THF-d_8, 273 K): δ 17.7 ppm.

$^{13}C\{^{1}H\}$ NMR (101 MHz, THF-d_8, 273 K): δ 170.6 (m, C-2 NHC + C_q arom), 153.6 (d, J_{CP} = 6 Hz, C_q arom), 148.8 (d, J_{CP} = 15 Hz, C_q arom), 140.8 (C_q arom), 138.5 (2 C_q arom), 136.8 (d, J_{CP} = 53 Hz, C_q arom), 134.0 (d, J_{CP} = 10 Hz, 2 CH arom), 131.4 (d, J_{CP} = 2 Hz, C^c), 130.3 (d, J_{CP} = 11 Hz, 2 CH arom), 129.2 (m, 2 CH arom), 128.4 (d, J_{CP} = 8 Hz, 2 CH arom), 128.3 (d, J_{CP} = 8 Hz, 2 CH arom), 127.1 (CH arom), 122.6 (2 CH arom), 122.0 (CH arom), 121.9 (CH arom), 114.2 (d, J_{CP} = 14 Hz, C^b), 100.3 (C^d), 76.5 (d, J_{CP} = 59 Hz, C^a), 61.6 (CH_2N), 37.3 (br d, J_{CP} = 3 Hz, 2 CH_2 COD), 30.7 (br, 2 CH_2 COD), 21.5 (2 CH_3) ppm. Signals for the four olefinic carbons could not be identified probably due to significant line broadening.

$IrH_3(C^{Xyl}NP^{Ph})$ (9)

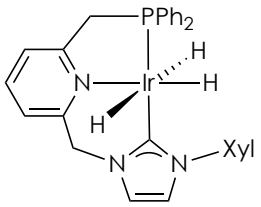

In a J.Young valved NMR tube, a suspension of **7b(Br)** (0.030 g, 0.04 mmol) in THF-d_8 (0.7 mL) was treated with KO^{t}Bu (0.004 g, 0.04 mmol). The NMR tube was charged with 5 bar of H_2, and the solution was analyzed by NMR spectroscopy.

Alternatively, in a J.Young valved NMR tube, a suspension cooled to −20 °C of **10b** (0.012 g, 0.02 mmol) in THF-d_8 (0.7 mL) was treated with KO^{t}Bu (0.002 g, 0.02 mmol). Immediately, the NMR tube was charged with 5 bar of H_2, and the resulting solution was analyzed by NMR spectroscopy.

^{1}H NMR (400 MHz, THF-d_8): δ 7.78 (dd, $^3J_{HP}$ = 8.5 Hz, $^3J_{HH}$ = 8.5 Hz, 4H, 4 H arom PPh), 7.82 (s, 2H, 2 H arom), 7.50 (dd, $^3J_{HH}$ = 7.6 Hz, $^3J_{HH}$ = 7.6 Hz, 1H, H arom Py), 7.35 (m, 2H, 2 H arom), 7.24 (m, 6H, 6 H arom), 7.11 (m, 1H, H arom), 7.07 (s, 1H, H arom NHC), 6.94 (s, 1H, H arom NHC), 5.18 (s, 2H, CH_2N), 3.98 (d, $^2J_{HP}$ = 10.0 Hz, 2H, CH_2P), 2.38 (s, 6H, 2 CH_3), −9.98 (dd, $^2J_{HP}$ = 18.2 Hz, $^2J_{HH}$ = 4.8 Hz, 2H, IrH *cis* to Py), −19.64 (dt, $^2J_{HP}$ = 14.4 Hz, $^2J_{HH}$ = 4.8 Hz, 1H, IrH *trans* to Py) ppm.

^{31}P{^{1}H} NMR (162 MHz, THF-d_8): δ 30.9 ppm.

^{13}C{^{1}H} NMR (101 MHz, THF-d_8): δ 176.9 (d, J_{CP} = 121 Hz, C-2 NHC), 164.7 (d, J_{CP} = 6 Hz, C_q arom), 155.9 (C_q arom), 143.0 (C_q arom), 139.1 (d, J_{CP} = 42 Hz, 2 C_q arom), 137.2 (2 C_q arom), 134.3 (d, J_{CP} = 13 Hz, 4 CH

arom), 134.1 (CH arom), 129.4 (2 CH arom), 128.2 (CH arom), 127.8 (d, J_{CP} = 10 Hz, 4 CH arom), 125.5 (2 CH arom), 121.3 (CH arom), 121.1 (d, J_{CP} = 9 Hz, CH arom), 120.5 (CH arom), 120.1 (d, J_{CP} = 4 Hz, CH arom), 59.9 (CH_2N), 49.2 (d, J_{CP} = 34 Hz, CH_2P), 21.2 (2 CH_3) ppm.

$IrH_2Cl(C^{Mes}NP^{Ph})$ (10a)

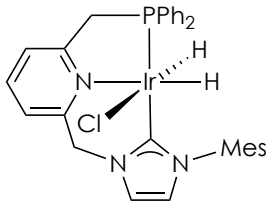

In a Fisher–Porter vessel, a solution of **7a(Cl)** (0.120 g, 0.15 mmol) in CH_2Cl_2 (8 mL) was pressurized with 2 bar of H_2 and stirred overnight. The system was depressurized, solvent was evaporated and the residue was washed with Et_2O (2 × 10 mL) and pentane (2 × 10 mL). Yellow solid (0.083 g, 80%). Crystals of complex **10a** suitable for X-ray diffraction analysis were grown by layering hexane over a CH_2Cl_2 solution.

Anal. calcd (%) for $C_{31}H_{32}ClIrN_3P$: C 52.8, H 4.6, N 5.9; found: C 52.9, H 4.7, N 5.4.

^{1}H NMR (400 MHz, CD_2Cl_2): δ 7.79 (dd, $^3J_{HH}$ = 7.8 Hz, $^3J_{HH}$ = 7.8 Hz, 1H, H arom Py), 7.73 (dd, $^3J_{HP}$ = 10.6 Hz, $^3J_{HH}$ = 7.9 Hz, 2H, 2 H arom PPh), 7.57 (d, $^3J_{HH}$ = 7.8 Hz, 1H, H arom Py), 7.40 (m, 6H, 6 H arom), 7.33 (m, 4H, 4 H arom), 7.09 (s, 1H, H arom NHC), 7.02 (s, 1H, H arom Mes), 6.97 (s, 1H, H arom Mes), 6.70 (d, $^2J_{HH}$ = 14.6 Hz, 1H, C*H*HN), 4.96 (d, $^2J_{HH}$ = 14.6 Hz, 1H, C*H*HN), 4.41 (dd, $^2J_{HH}$ = 16.3 Hz, $^2J_{HP}$ = 10.4 Hz, 1H, C*H*HP), 3.38 (dd, $^2J_{HH}$ = 16.3 Hz, $^2J_{HP}$ = 9.5 Hz, 1H, C*H*HP), 2.40 (s, 3H, CH_3), 2.20 (s, 3H, CH_3), 1.92 (s, 3H, CH_3), −20.19 (dd, $^2J_{HP}$ = 13.8 Hz, $^2J_{HH}$ = 7.0 Hz, 1H, IrH *trans* to Py), −23.30 (dd, $^2J_{HP}$ = 18.9 Hz, $^2J_{HH}$ = 7.0 Hz, 1H, IrH *cis* to Py) ppm.

^{31}P{^{1}H} NMR (162 MHz, CD_2Cl_2): δ 26.8 ppm.

$^{13}C\{^{1}H\}$ NMR (101 MHz, CD_2Cl_2): δ 172.9 (d, J_{CP} =119 Hz, C-2 NHC), 164.8 (d, J_{CP} = 6 Hz, C_q arom), 156.1 (C_q arom), 138.6 (C_q arom), 138.2 (C_q arom), 136.9 (C_q arom), 136.5 (CH arom), 135.7 (d, J_{CP} = 50 Hz, C_q arom), 135.4 (C_q arom), 134.7 (d, J_{CP} = 13 Hz, 2 CH arom), 132.4 (d, J_{CP} =11 Hz, 2 CH arom), 130.5 (d, J_{CP} = 2 Hz, CH arom), 129.5 (CH arom), 129.2 (CH arom), 128.6 (CH arom), 128.3 (d, J_{CP} =10 Hz, 2 CH arom), 128.0 (d, J_{CP} = 9 Hz, 2 CH arom), 122.7 (CH arom), 122.3 (d, J_{CP} = 9 Hz, CH arom), 121.2 (d, J_{CP} = 4 Hz, CH arom), 120.4 (d, J_{CP} = 4 Hz, CH arom), 56.7 (CH_2N), 47.1 (d, J_{CP} = 33 Hz, CH_2P), 21.3 (CH_3), 18.9 (CH_3), 18.5 (CH_3) ppm. Signals for one quaternary aromatic carbon could not be identified.

IR (Nujol): 2139 cm^{-1} (ν_{IrH}).

$IrH_2Cl(C^{Xyl}NP^{Ph})$ (10b)

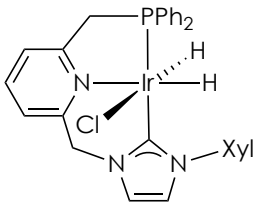

In a Fisher–Porter vessel, a solution of **7b(Cl)** (0.100 g, 0.12 mmol) in CH_2Cl_2 (5 mL) was pressurised with 5 bar of H_2 and heated to 50 °C. After 16 h, the system was cooled to room temperature and depressurized. The solvent was evaporated and the residue was washed with Et_2O (3 × 3 mL) and pentane (3 × 3 mL). Pale yellow solid (0.073 g, 85%).

^{1}H NMR (400 MHz, CD_2Cl_2): δ 7.85 (m, 2H, 2 H arom PPh), 7.74 (dd, $^3J_{HH}$ = 8.0 Hz, $^3J_{HH}$ = 8.0 Hz, 1H, H arom Py), 7.56 (d, $^3J_{HH}$ = 8.0 Hz, 1H, H arom Py), 7.47 (m, 4H, 4 H arom), 7.36 (m, 4H, 4 H arom), 7.29 (m, 3H, 3 H arom), 7.24 (d, $^3J_{HH}$ = 1.5 Hz, 1H, H arom NHC), 7.18 (m, 1H, H arom), 7.11 (s, 1H, H arom), 6.53 (d, $^2J_{HH}$ = 14.4 Hz, 1H, C*H*HN), 4.96 (d, $^2J_{HH}$ = 14.8 Hz, 1H, C*H*HN), 4.49 (dd, $^2J_{HH}$ = 16.4 Hz, $^2J_{HP}$ = 10.4 Hz, 1H, C*H*HP), 3.54 (dd, $^2J_{HH}$ = 16.6 Hz, $^2J_{HP}$ = 10.0 Hz, 1H, C*H*HP), 2.44 (s, 6H, 2 CH_3), −19.73 (dd, $^2J_{HP}$ = 16.6 Hz, $^2J_{HH}$ = 7.2 Hz, 1H, IrH *trans* to Py), −23.24 (dd, $^2J_{HP}$ = 18.8 Hz, $^2J_{HH}$ = 7.2 Hz, 1H, IrH *cis* to Py) ppm.

^{31}P{^{1}H} NMR (162 MHz, CD_2Cl_2): δ 27.7 ppm.

^{13}C{^{1}H} NMR (101 MHz, CD_2Cl_2): δ 172.4 (d, J_{CP} = 122 Hz, C-2 NHC), 164.9 (d, J_{CP} = 5 Hz, C_q arom), 155.8 (C_q arom), 141.9 (C_q arom), 138.5 (2 C_q arom), 136.8 (2 CH arom), 136.3 (d, J_{CP} = 52 Hz, C_q arom), 134.6 (d, J_{CP} = 12 Hz, 2 CH arom), 134.2 (d, J_{CP} = 38 Hz, C_q arom), 132.9 (d, J_{CP} = 11

Hz, 2 CH arom), 130.7 (d, J_{CP} = 2 Hz, CH arom), 129.8 (d, J_{CP} = 1 Hz, CH arom), 128.6 (d, J_{CP} = 10 Hz, 2 CH arom), 128.2 (d, J_{CP} = 9 Hz, 2 CH arom), 125.7 (2 CH arom), 122.7 (CH arom), 122.6 (d, J_{CP} = 9.0 Hz, CH arom), 121.5 (d, J_{CP} = 4 Hz, CH arom), 121.4 (d, J_{CP} = 5 Hz, CH arom), 57.1 (CH_2N), 46.3 (d, J_{CP} = 32 Hz, CH_2P), 21.6 (2 CH_3) ppm.

HRMS (ESI): *m/z* calcd for $C_{30}H_{30}N_3IrP$ $[(M-Cl)^+]$: 656.1801; found: 656.1794.

I.3.6. Synthesis of carbonyl Ir-CNP^{Ph} complexes

[Ir(C^{Mes}NP^{Ph})(CO)]Cl (13(Cl))

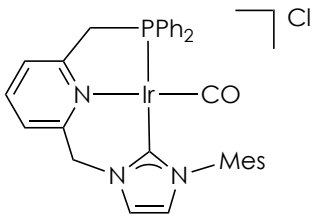

A solution of **7a(Cl)** (0.080 g, 0.10 mmol) in CH_2Cl_2 (10 mL) was bubbled with CO for 5 min, and the solvent was evaporated. The resulting solid was washed with Et_2O (2 × 10 mL) and pentane (2 × 10 mL), and crystallized from THF. Orange solid (0.048 g, 70%).

Anal. calcd (%) for $C_{32}H_{30}ClIrN_3OP$: C 52.6, H 4.1, N 5.75; found: C 52.2, H 4.6, N 5.5.

^{1}H NMR (300 MHz, CD_2Cl_2): δ 8.41 (s, 1H, H arom NHC), 8.28 (d, $^3J_{HH}$ = 7.5 Hz, 1H, H arom Py), 7.97 (dd, $^3J_{HH}$ = 7.6 Hz, $^3J_{HH}$ = 7.6 Hz, 1H, H arom Py), 7.77 (d, $^3J_{HH}$ = 7.7 Hz, 1H, H arom Py), 7.61 (ddd, $^3J_{HP}$ = 11.8 Hz, $^3J_{HH}$ = 7.7 Hz, $^4J_{HH}$ = 0.6 Hz, 4H, 4 H arom PPh), 7.46 (m, 6H, 6 H arom PPh), 7.02 (m, 3H, 2 H arom Mes + H arom NHC), 6.11 (s, 2H, CH_2N), 4.18 (d, $^2J_{HP}$ = 10.0 Hz, 2H, CH_2P), 2.34 (s, 3H, CH_3), 2.12 (s, 6H, 2 CH_3) ppm.

^{31}P{^{1}H} NMR (162 MHz, CD_2Cl_2): δ 45.7 ppm.

^{13}C{^{1}H} NMR (126 MHz, CD_2Cl_2): δ 178.1 (d, J_{CP} = 99 Hz, C-2 NHC), 177.2 (d, J_{CP} = 10 Hz, CO), 164.7 (d, J_{CP} = 7 Hz, C_q arom), 156.5 (C_q arom), 141.4 (CH arom), 140.1 (C_q arom), 136.3 (2 C_q arom), 135.7 (C_q arom),

133.2 (d, J_{CP} = 12 Hz, 4 CH arom), 131.9 (d, J_{CP} = 2Hz, 2 CH arom), 130.3 (d, J_{CP} = 53 Hz, 2 C_q arom), 129.4 (d, J_{CP} = 11 Hz, 4 CH arom), 129.2 (2 CH arom), 125.4 (CH arom), 124.4 (d, J_{CP} = 10 Hz, CH arom), 123.6 (d, J_{CP} = 3 Hz, CH arom), 122.0 (d, J_{CP} = 3 Hz, CH arom), 54.6 (CH_2N), 42.7 (d, J_{CP} = 31 Hz, CH_2P), 21.2 (CH_3), 18.5 (2 CH_3) ppm.

IR (Nujol): 1985 cm^{-1} (ν_{CO}).

[Ir(C^{Mes}NP^{Ph})(CO)](Bcat$_2$) (13(Bcat$_2$))

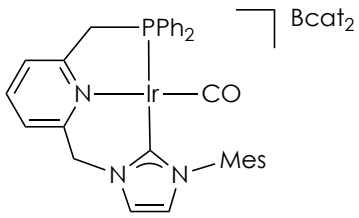

A solution of **13(Cl)** (0.100 g, 0.14 mmol) and Li[Bcat$_2$] (0.035 g, 0.15 mmol) in MeCN (8 mL) was stirred for 1 h. The suspension was filtered, and solvent was removed under reduced pressure. The residue was extracted with CH_2Cl_2 (2 × 10 mL), and the solution was brought to dryness. The resulting solid was washed with pentane (2 × 8 mL) and dried under vacuum. Complex **13(Bcat$_2$)** was obtained as an orange solid (0.073 g, 58%).

^{1}H NMR (500 MHz, CD_2Cl_2): δ 7.79 (dd, $^3J_{HH}$ = 7.7 Hz, $^3J_{HH}$ = 7.7 Hz, 1H, H arom Py), 7.65 (d, $^3J_{HH}$ = 7.7 Hz, 1H, H arom Py), 7.59 (m, 6H, 6 H arom), 7.52 (m, 2H, 2 H arom), 7.44 (m, 4H, 4 H arom), 7.04 (s, 2H, 2 H arom Mes), 7.01 (s, 1H, H arom NHC), 6.55 (m, 8H, B(cat)$_2$), 5.42 (s, 2H, CH_2N), 4.09 (d, $^2J_{HP}$ = 10.1 Hz, 2H, CH_2P), 2.36 (s, 3H, CH_3), 2.13 (s, 6H, 2 CH_3) ppm.

^{31}P{^{1}H} NMR (202 MHz, CD_2Cl_2): δ 45.4 ppm.

^{11}B{^{1}H} NMR (96 MHz, CD_2Cl_2): δ 14.4 ppm.

^{13}C{^{1}H} NMR (125 MHz, CD_2Cl_2): δ 178.6 (d, J_{CP} = 98 Hz, C-2 NHC), 177.1 (d, J_{CP} = 9 Hz, CO), 165.0 (d, J_{CP} = 7 Hz, C_q arom), 155.3 (C_q arom), 152.3 (4 C_q arom B(cat)$_2$), 141.5 (CH arom), 140.3 (C_q arom), 136.3 (2 C_q arom), 135.6 (C_q arom), 133.2 (d, J_{CP} = 12 Hz, 4 CH arom), 132.0 (2 CH arom), 130.2 (d, J_{CP} = 54 Hz, 2 C_q arom), 129.5 (d, J_{CP} = 11 Hz, 4 CH

arom), 129.3 (2 CH arom), 124.7 (d, J_{CP} = 10 Hz, CH arom), 124.6 (CH arom), 122.8 (CH arom), 122.5 (CH arom), 118.2 (4 CH arom $B(cat)_2$), 108.7 (4 CH arom $B(cat)_2$), 55.5 (CH_2N), 42.6 (d, J_{CP} = 31 Hz, CH_2P), 21.3 (CH_3), 18.5 (2 CH_3) ppm.

IR (Nujol): 1973 cm^{-1} (ν_{CO}).

HRMS (ESI): *m/z* calcd for $C_{32}H_{30}IrN_3OP$ [$(M-Bcat_2)^+$]: 696.1750; found: 696.1743.

[Ir(C^{Mes}NP^{Ph})(CO)](BAr$_F$) (13(BAr$_F$))

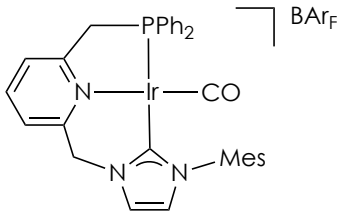

A solution of **13(Cl)** (0.096 g, 0.13 mmol) and Na[BAr$_F$] (0.116 g, 0.13 mmol) in CH_2Cl_2 (7 mL) was stirred for 2 h. The suspension was filtered, and solvent was removed under reduced pressure. The resulting solid was washed with pentane (2 × 10 mL), and dried under vacuum. Complex **13(BAr$_F$)** was obtained as an orange solid (0.186 g, 91%).

Anal. calcd (%) for $C_{64}H_{42}BF_{24}IrN_3OP$: C 49.3; H 2.7; N 2.7; found: C 49.2; H 2.9; N 2.8.

^{1}H NMR (500 MHz, CD_2Cl_2): δ 7.95 (dd, $^3J_{HH}$ = 7.7 Hz, $^3J_{HH}$ = 7.7 Hz, 1H, H arom Py), 7.76 (s, 8H, 8 H arom BAr$_F$), 7.72 (d, $^3J_{HH}$ = 7.8 Hz, 1H, H arom Py), 7.63 (m, 4H, 4 H arom), 7.59 (s, 4H, 4 H arom BAr$_F$), 7.51 (m, 7H, 7 H arom), 7.44 (dd, $^3J_{HH}$ = 1.8 Hz, $^5J_{HP}$ = 0.8 Hz, 1H, H arom NHC), 7.17 (d, $^3J_{HH}$ = 1.8 Hz, 1H, H arom NHC), 7.09 (s, 2H, 2 H arom Mes), 5.39 (s, 2H, CH_2N), 4.14 (d, $^2J_{HP}$ = 10.1 Hz, 2H, CH_2P), 2.40 (s, 3H, CH_3), 2.16 (s, 6H, 2 CH_3) ppm.

^{31}P{^{1}H} NMR (202 MHz, CD_2Cl_2): δ 45.6 ppm.

^{11}B{^{1}H} NMR (96 MHz, CD_2Cl_2): δ −6.6 ppm.

^{13}C{^{1}H} NMR (125 MHz, CD_2Cl_2): δ 179.3 (d, J_{CP} = 99 Hz, C-2 NHC), 176.4 (d, J_{CP} = 10 Hz, CO), 165.9 (d, J_{CP} = 7 Hz, C_q arom), 162.2 (q, J_{CB} =

50 Hz, 4 BC_q arom BAr_F), 154.9 (C_q arom), 141.5 (CH arom), 140.8 (C_q arom), 136.1 (2 C_q arom), 135.2 (m, 8 CH arom BAr_F), 133.2 (d, J_{CP} = 12 Hz, 4 CH arom), 132.3 (2 CH arom), 129.6 (overlapped, 2 C_q arom), 129.6 (d, J_{CP} = 11 Hz, 4 CH arom), 129.5 (2 CH arom), 129.3 (q, J_{CF} = 32 Hz, 8 C_q arom BAr_F), 125.0 (q, J_{CF} = 272 Hz, 8 CF_3), 124.9 (d, J_{CP} = 10 Hz, CH arom), 123.9 (CH arom), 123.3 (CH arom), 121.8 (CH arom), 117.9 (m, 4 CH arom BAr_F), 56.3 (CH_2N), 43.1 (d, J_{CP} = 31 Hz, CH_2P), 21.3 (CH_3), 18.5 (2 CH_3) ppm. Signal for one quaternary aromatic carbon could not be identified.

IR (Nujol): 1979 cm^{-1} (ν_{CO}).

[Ir(C^{Mes}NP^{Ph})(CO)$_2$]Cl (14)

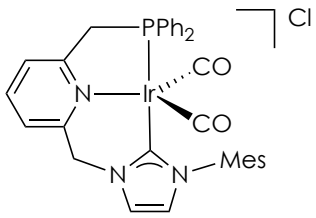

In a J.Young valved NMR tube, a solution of **13(Cl)** (0.011 g, 0.01 mmol) in CD_2Cl_2 (0.7 mL) was pressurized with 1 bar of CO. The solution was analyzed by NMR spectroscopy.

^{1}H NMR (400 MHz, CD_2Cl_2): δ 8.57 (d, $^3J_{HH}$ = 0.8 Hz, 1H, H arom NHC), 8.41 (d, $^3J_{HH}$ = 7.5 Hz, 1H, H arom Py), 7.98 (dd, $^3J_{HH}$ = 7.6 Hz, $^3J_{HH}$ = 7.6 Hz, 1H, H arom Py), 7.74 (d, $^3J_{HH}$ = 7.7 Hz, 1H, H arom Py), 7.47 (m, 10H, 10 H arom PPh), 7.01 (d, $^3J_{HH}$ = 0.8 Hz, 1H, H arom NHC), 6.98 (s, 2H, 2 H arom Mes), 6.09 (s, 2H, CH_2N), 4.29 (d, $^2J_{HP}$ = 10.9 Hz, 2H, CH_2P), 2.32 (s, 3H, CH_3), 2.03 (s, 6H, 2 CH_3) ppm.

^{31}P{^{1}H} NMR (162 MHz, CD_2Cl_2): δ 26.8 ppm.

^{13}C{^{1}H} NMR (126 MHz, CD_2Cl_2): δ 177.4 (CO), 161.5 (C_q arom), 161.3 (d, J_{CP} = 94 Hz, C-2 NHC), 155.1 (C_q arom), 140.5 (CH arom), 140.2 (C_q arom), 136.1 (2 C_q arom), 135.7 (C_q arom), 132.5 (d, J_{CP} = 12 Hz, 4 CH arom), 131.1 (2 CH arom), 129.5 (d, J_{CP} = 11 Hz, 4 CH arom), 129.4 (d, J_{CP} = 55 Hz, 2 C_q arom), 129.4 (2 CH arom), 125.2 (CH arom), 124.4 (CH arom), 124.0 (d, J_{CP} = 9 Hz, CH arom), 122.8 (CH arom), 56.7 (CH_2N), 44.9 (d, J_{CP} = 37 Hz, CH_2P), 21.2 (CH_3), 18.1 (2 CH_3) ppm.

IR (CH_2Cl_2): 1946 (ν_{CO}), 2021 (ν_{CO}) cm^{-1}.

Complexes 15a/15b

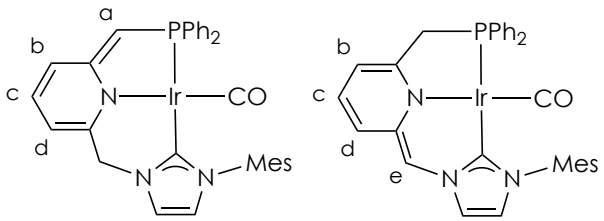

15a **15b**

To a solution of **13(Cl)** (0.075 g, 0.10 mmol) in THF (5 mL) was added a solution of KO^{t}Bu (0.013 g, 0.11 mmol) in THF (5 mL) giving rise to a red solution. The mixture was stirred for 2 h, and solvent was evaporated under reduced pressure. The residue was extracted with toluene (2 × 10 mL), and volatiles were removed under vacuum. The solid obtained was washed with pentane (2 × 10 mL), and dried under vacuum to give the mixture of complexes **15a** and **15b** as a red solid (0.050 g, 70%). The **15a/15b** ratio in THF-d_8 is 9:1. Crystals of **15a** suitable for X-ray diffraction analysis were grown from a saturated solution of **15a** and **15b** in THF.

Anal. calcd (%) for $C_{32}H_{29}IrN_3OP$: C 55.3, H 4.2, N 6.0; found: C 55.1, H 4.6, N 6.1.

IR (Nujol): 1938 cm^{-1} (ν_{CO}).

*NMR spectroscopy data of complex **15a***

^{1}H NMR (500 MHz, THF-d_8): δ 7.57 (m, 4H, 4 H arom PPh), 7.41 (s, 1H, H arom NHC), 7.20 (m, 6H, 6 H arom PPh), 7.09 (s, 1H, H arom NHC), 6.92 (s, 2H, 2 H arom Mes), 6.30 (m, 2H, H^b + H^c), 5.37 (dd, $^3J_{HH}$ = 3.7 Hz, $^3J_{HH}$ = 3.7 Hz, 1H, H^d), 4.72 (s, 2H, CH_2N), 3.84 (d, $^2J_{HP}$ = 1.9 Hz, 1H, H^a), 2.28

(s, 3H, CH_3), 2.09 (s, 6H, 2 CH_3) ppm.

$^{31}P\{^1H\}$ NMR (202 MHz, THF-d_8): δ 28.3 ppm.

$^{13}C\{^1H\}$ NMR (125 MHz, THF-d_8): δ 182.8 (d, J_{CP} = 92 Hz, C-2 NHC), 182.0 (d, J_{CP} = 10 Hz, CO), 156.3 (d, J_{CP} = 24 Hz, C_q arom), 150.8 (d, J_{CP} = 1 Hz, C_q arom), 140.6 (d, J_{CP} = 58 Hz, 2 C_q arom), 139.6 (C_q arom), 137.5 (C_q arom), 136.9 (2 C_q arom), 132.9 (d, J_{CP} = 11 Hz, 4 CH arom), 131.9 (d, J_{CP} = 2 Hz, C^c), 129.4 (2 CH arom), 129.3 (d, J_{CP} = 2 Hz, 2 CH arom), 128.3 (d, J_{CP} = 10 Hz, 4 CH arom), 121.8 (d, J_{CP} = 3 Hz, CH arom), 121.1 (d, J_{CP} = 3 Hz, CH arom), 117.8 (d, J_{CP} = 19 Hz, C^b), 101.7 (C^d), 69.1 (d, J_{CP} = 69 Hz, C^a), 57.3 (CH_2N), 21.2 (CH_3), 18.6 (2 CH_3) ppm.

*NMR spectroscopy data of complex **15b***

^1H NMR (500 MHz, THF-d_8): δ 7.64 (m, 4H, 4 H arom PPh), 7.49 (s, 1H, H arom NHC), 7.32 (m, 6H, 6 H arom PPh), 7.06 (s, 1H, H arom NHC), 6.91 (s, 2H, 2 H arom Mes), 6.17 (s, 1H, H^e), 6.17 (d, $^3J_{HH}$ = 8.7 Hz, $^3J_{HH}$ = 6.3 Hz, 1H, H^c), 6.05 (d, $^3J_{HH}$ = 8.9 Hz, 1H, H^d), 5.53 (d, $^3J_{HH}$ = 6.1 Hz, 1H, H^b), 3.51 (d, $^2J_{HP}$ = 11.4 Hz, 1H, CH_2P), 2.25 (s, 3H, CH_3), 2.12 (s, 6H, 2 CH_3) ppm.

$^{31}P\{^1H\}$ NMR (202 MHz, THF-d_8): δ 33.3 ppm.

Complex 16

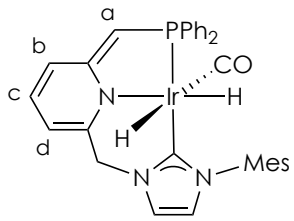

In a J.Young-valved NMR tube, a solution of **15a/15b** (0.010 g, 0.014 mmol) in THF-d_8 (0.5 mL) was charged with 5 bar of H_2 for 24 h. The solvent was evaporated and the residue was dried under vacuum. Orange-dark solid (9.5 g, 95%). Satisfactory elemental analysis for complex **16** could not be obtained.

^{1}H NMR (500 MHz, THF-d_8): δ 7.58 (m, 3H, 3 H arom), 7.41 (dd, J_{HP} = 10.1 Hz, $^3J_{HH}$ = 7.6 Hz, 2H, 2 H arom), 7.19 (m, 7H, 7 H arom), 7.06 (m, 2H, 2 H arom), 6.56 (dd, $^3J_{HH}$ = 8.8 Hz, $^3J_{HH}$ = 6.2 Hz, 1H, H^c), 6.43 (d, $^3J_{HH}$ = 8.8 Hz, 1H, H^b), 5.71 (d, $^3J_{HH}$ = 6.2 Hz, 1H, H^d), 5.01 (d, $^2J_{HH}$ = 14.1 Hz, 1H, C*H*HN), 4.70 (d, $^2J_{HH}$ = 14.3 Hz, 1H, C*H*HN), 3.93 (d, $^2J_{HP}$ = 2.7 Hz, 1H, H^a), 2.43 (s, 3H, CH_3), 2.03 (s, 3H, CH_3), 1.95 (s, 3H, CH_3), −8.64 (dd, $^2J_{HP}$ = 20.8 Hz, $^2J_{HH}$ = 1.5 Hz, 1H, IrH *cis* to Py), −16.59 (dd, $^2J_{HP}$ = 11.3 Hz, $^2J_{HH}$ = 1.6 Hz, 1H, IrH *trans* to Py) ppm.

^{31}P{^{1}H} NMR (202 MHz, THF-d_8): δ 8.8 ppm.

^{13}C{^{1}H} NMR (125 MHz, THF-d_8): δ 176.5 (br m, CO), 174.7 (d, J_{CP} = 19 Hz, C_q arom), 162.7 (d, J_{CP} = 92 Hz, C-2 NHC), 150.3 (C_q arom), 145.0 (d, J_{CP} = 50 Hz, C_q arom), 140.7 (d, J_{CP} = 71 Hz, C_q arom), 139.2 (C_q arom), 138.4 (C_q arom), 136.7 (C_q arom), 136.0 (C_q arom), 134.7 (d, J_{CP} = 11 Hz, 2 CH arom), 132.0 (d, J_{CP} = 2 Hz, C^c), 131.4 (d, J_{CP} = 12 Hz, 2 CH arom),

129.5 (CH arom), 129.3 (CH arom), 129.0 (CH arom), 128.6 (CH arom), 128.0 (d, J_{CP} = 10 Hz, 2 CH arom), 127.8 (d, J_{CP} = 11 Hz, 2 CH arom), 122.0 (CH arom), 121.8 (d, J_{CP} = 3 Hz, CH arom), 115.3 (d, J_{CP} = 18 Hz, C^{b}), 102.0 (C^{d}), 66.6 (d, J_{CP} = 78 Hz, C^{a}), 60.3 (CH_2N), 21.2 (CH_3), 18.7 (CH_3), 18.4 (CH_3) ppm.

IR (Nujol): 2140 (ν_{IrH}), 2068 (ν_{IrH}), 1956 (ν_{CO}) cm^{-1}.

[IrH$_2$(C^{Mes}NP^{Ph})(CO)]Cl (17)

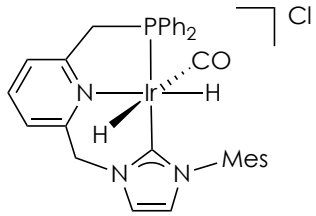

In a J.Young valved NMR tube, a solution of **13(Cl)** (0.050 g, 0.07 mmol) in CD_2Cl_2 (0.5 mL) was charged with 5 bar of H_2. The resulting solution was analyzed by NMR spectroscopy. Complex **17** losses hydrogen upon exposure to vacuum.

^{1}H NMR (500 MHz, CD_2Cl_2): δ 8.45 (s, 1H, H arom NHC), 8.29 (d, $^3J_{HH}$ = 6.4 Hz, 1H, H arom Py), 7.99 (dd, $^3J_{HH}$ = 7.3 Hz, $^3J_{HH}$ = 6.6 Hz, 1H, H arom Py), 7.82 (d, $^3J_{HH}$ = 6.4 Hz, 1H, H arom Py), 7.60 (dd, $^3J_{HP}$ = 12.8 Hz, $^3J_{HH}$ = 7.7 Hz, 2H, 2 H arom PPh), 7.51 (dd, $^3J_{HH}$ = 7.6 Hz, J_{HP} = 6.3 Hz, 1H, H arom PPh), 7.40 (m, 5H, 5 H arom PPh), 7.27 (m, 2H, 2 H arom PPh), 7.12 (d, $^2J_{HH}$ = 15.4 Hz, 1H, C*H*HN), 7.07 (s, 1H, H arom NHC), 7.05 (s, 2H, 2 H arom Xyl), 4.89 (d, $^2J_{HH}$ = 15.3 Hz, 1H, C*H*HN), 4.82 (dd, $^2J_{HH}$ = 17.1 Hz, $^2J_{HP}$ = 12.5 Hz, 1H, C*H*HP), 3.63 (dd, $^2J_{HH}$ = 17.1 Hz, $^2J_{HP}$ = 10.2 Hz, 1H, C*H*HP), 2.42 (s, 3H, CH_3), 2.01 (s, 3H, CH_3), 1.86 (s, 3H, CH_3), −8.32 (ddd, $^2J_{HP}$ = 22.2 Hz, $^2J_{HH}$ = 1.6 Hz, $^4J_{HH}$ = 1.6 Hz, 1H, IrH *cis* to Py), −17.45 (dd, $^2J_{HP}$ = 11.7 Hz, $^2J_{HH}$ = 1.6 Hz, 1H, IrH *trans* to Py) ppm.

^{31}P{^{1}H} NMR (202 MHz, CD_2Cl_2): δ 16.9 ppm.

^{13}C{^{1}H} NMR (125 MHz, CD_2Cl_2): δ 175.0 (CO), 163.4 (d, J_{CP} = 3 Hz, C_q arom), 156.9 (d, J_{CP} = 100 Hz, C-2 NHC), 155.8 (C_q arom), 140.3 (CH arom), 139.6 (C_q arom), 136.8 (C_q arom), 135.7 (C_q arom), 135.5 (C_q arom),

134.9 (d, J_{CP} = 12 Hz, 2 CH arom), 134.4 (d, J_{CP} = 49 Hz, C_q arom), 132.3 (d, J_{CP} = 2 Hz, CH arom), 131.3 (d, J_{CP} = 2 Hz, CH arom), 130.4 (d, J_{CP} = 11 Hz, 2 CH arom), 130.1 (d, J_{CP} = 63 Hz, C_q arom), 129.5 (d, J_{CP} = 10 Hz, 2 CH arom), 129.4 (CH arom), 129.2 (CH arom), 129.1 (d, J_{CP} = 12 Hz, 2 CH arom), 125.7 (CH arom), 124.1 (d, J_{CP} = 3 Hz, CH arom), 123.4 (d, J_{CP} = 10 Hz, CH arom), 121.8 (d, J_{CP} = 3 Hz, CH arom), 58.1 (CH_2N), 46.1 (d, J_{CP} = 37 Hz, CH_2P), 21.3 (CH_3), 18.4 (CH_3), 18.2 (CH_3) ppm.

MS (ESI, CH_2Cl_2/MeCN): *m/z* 698 ([($M-Cl^+$)], 100).

IR (CD_2Cl_2): 2338 (ν_{IrH}), 2085 (ν_{IrH}), 1987 (ν_{CO}) cm^{-1}.

[IrH(Bcat)(C^{Mes}NP^{Ph})(CO)](Bcat$_2$) (18(Bcat$_2$))

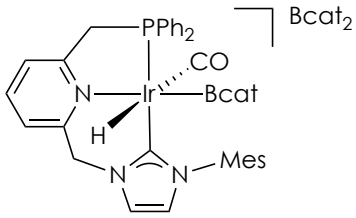

In a J.Young-valved NMR tube, a solution of **13(Bcat$_2$)** (0.035 g, 0.04 mmol) in THF-d_8 (0.5 mL) was treated with HBcat (5.0 μL, 0.05 mmol). Complete conversion of **13(Bcat$_2$)** into **18(Bcat$_2$)** was determined by NMR spectroscopy. Complex **18(Bcat$_2$)** was spectroscopically characterized in admixture with HBcat.

^{1}H NMR (500 MHz, THF-d_8): δ 7.91 (d, $^3J_{HH}$ = 1.1 Hz, 1H, H arom NHC), 7.86 (d, $^3J_{HH}$ = 7.9 Hz, 1H, H arom Py), 7.82 (dd, $^3J_{HH}$ = 7.8 Hz, $^3J_{HH}$ = 7.8 Hz, 1H, H arom Py), 7.74 (d, $^3J_{HH}$ = 7.4 Hz, 1H, H arom Py), 7.48 (m, 4H, 4 H arom), 7.36 (m, 4H, 4 H arom), 7.24 (m, 2H, 2 H arom), 7.05 (d, $^3J_{HH}$ = 1.1 Hz, 1H, H arom NHC), 6.82 (s, 1H, H arom Mes), 6.76 (m, 2H, 2 H arom IrBcat), 6.70 (m, 2H, 2 H arom IrBcat), 6.39 (br m, 8H, 8 H arom Bcat$_2$), 6.00 (d, $^2J_{HH}$ = 15.7 Hz, 1H, C*H*HN), 5.97 (s, 1H, H arom Mes), 5.01 (dd, $^2J_{HH}$ = 17.3 Hz, $^2J_{HP}$ = 12.5 Hz, 1H, C*H*HP), 5.00 (d, $^2J_{HH}$ = 15.7 Hz, 1H, C*H*HN), 3.98 (dd, $^2J_{HH}$ = 17.1 Hz, $^2J_{HP}$ = 10.2 Hz, 1H, C*H*HP), 2.01 (s, 3H, CH_3), 1.86 (s, 3H, CH_3), 1.81 (s, 3H, CH_3), −6.90 (d, $^2J_{HP}$ = 21.1 Hz, 1H, IrH) ppm.

^{31}P{^{1}H} NMR (202 MHz, THF-d_8): δ 15.7 ppm.

^{11}B NMR (96 MHz, THF-d_8): δ 15.1 (br, Bcat$_2$), 12.9 (IrBcat) ppm.

$^{13}C\{^{1}H\}$ NMR (101 MHz, THF-d_8): δ 176.8 (br, CO), 162.0 (C_q arom), 155.1 (C_q arom), 154.3 (d, J_{CP} = 96 Hz, C-2 NHC), 153.3 (4 C_q arom $Bcat_2$), 151.0 (2 C_q arom IrBcat), 141.3 (CH arom), 140.1 (C_q arom), 136.2 (C_q arom), 135.8 (C_q arom), 135.2 (C_q arom), 133.7 (d, J_{CP} = 11 Hz, 2 CH arom), 132.4 (d, J_{CP} = 11 Hz, 2 CH arom), 132.2 (CH arom), 131.9 (CH arom), 131.8 (d, J_{CP} = 50 Hz, C_q arom), 130.0 (d, J_{CP} = 11 Hz, 2 CH arom), 129.9 (CH arom), 129.4 (CH arom), 129.2 (d, J_{CP} = 62 Hz, C_q arom), 129.1 (d, J_{CP} = 12 Hz, 2 CH arom), 125.0 (CH arom), 124.9 (CH arom), 124.7 (d, J_{CP} = 10 Hz, CH arom), 123.9 (CH arom), 121.4 (2 CH arom IrBcat), 118.0 (4 CH arom $Bcat_2$), 111.3 (2 CH arom IrBcat), 108.7 (4 CH arom $Bcat_2$), 59.1 (CH_2N), 46.1 (d, J_{CP} = 39 Hz, CH_2P), 21.3 (CH_3), 18.6 (CH_3), 17.6 (CH_3) ppm.

IR (CH_2Cl_2): 2101 (ν_{IrH}), 2005 (ν_{CO}) cm^{-1}.

[IrH(Bpin)(C^{Mes}NP^{Ph})(CO)](BAr$_F$) (19(BAr$_F$))

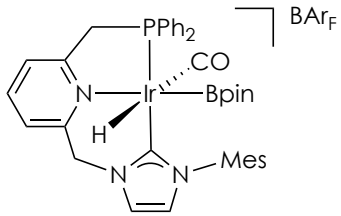

In a J.Young valved NMR tube, a solution of **13(BAr$_F$)** (0.023 g, 0.015 mmol) in THF-d_8 (0.5 mL) was treated with HBpin (5.3 μL, 0.036 mmol). Complete conversion of **13(BAr$_F$)** into **19(BAr$_F$)** was determined by NMR spectroscopy. Complex **19(BAr$_F$)** was spectroscopically characterized in admixture with HBpin.

^{1}H NMR (400 MHz, THF-d_8): δ 8.03 (dd, $^3J_{HH}$ = 7.7 Hz, $^3J_{HH}$ = 7.7 Hz, 1H, H arom Py), 7.79 (s, 8H, 8 H arom BAr$_F$), 7.73 (m, 2H, 2 H arom), 7.68 (d, $^3J_{HH}$ = 7.7 Hz, 1H, H arom Py), 7.61 (m, 2H, 2 H arom), 7.57 (s, 4H, 4 H arom BAr$_F$), 7.45 (m, 8H, 8 H arom), 7.25 (s, 1H, H arom), 7.06 (s, 1H, H arom), 7.01 (s, 1H, H arom), 5.79 (d, $^2J_{HH}$ = 15.8 Hz, 1H, C*H*HN), 5.19 (d, $^2J_{HH}$ = 15.8 Hz, 1H, C*H*HN), 4.86 (dd, $^2J_{HH}$ = 16.9 Hz, $^2J_{HP}$ = 12.5 Hz, 1H, C*H*HP), 3.83 (dd, $^2J_{HH}$ = 17.1 Hz, $^2J_{HP}$ = 10.4 Hz, 1H, C*H*HP), 2.33 (s, 3H, CH_3), 2.12 (s, 3H, CH_3), 2.05 (s, 3H, CH_3), 0.74 (s, 6H, 2 CH_3 IrBpin), 0.71 (s, 6H, 2 CH_3 IrBpin), −6.81 (d, $^2J_{HP}$ = 22.1 Hz, 1H, IrH) ppm.

^{31}P{^{1}H} NMR (162 MHz, THF-d_8): δ 18.1 ppm.

^{11}B NMR (128 MHz, THF-d_8): δ 23.2 (br, IrBpin), −4.6 (BAr$_F$) ppm.

^{13}C{^{1}H} NMR (101 MHz, THF-d_8): δ 178.0 (br, CO), 162.6 (q, J_{CB} = 50 Hz, 4 BC_q arom BAr$_F$), 162.4 (C_q arom), 156.8 (d, J_{CP} = 102 Hz, C-2 NHC),

155.6 (C_q arom), 140.8 (CH arom), 139.8 (C_q arom), 137.2 (C_q arom), 135.9 (C_q arom), 135.4 (m, 8 CH arom BAr_F), 133.8 (d, J_{CP} = 11 Hz, 2 CH arom), 132.1 (m, 2 CH arom), 132.0 (CH arom), 131.8 (CH arom), 129.8 (m, 4 CH arom + 8 C_q arom BAr_F), 128.8 (d, J_{CP} = 11 Hz, 2 CH arom), 125.2 (q, J_{CF} = 272 Hz, 8 CF_3), 125.0 (CH arom), 123.6 (CH arom), 123.4 (CH arom), 123.3 (CH arom), 118.0 (m, 4 CH arom BAr_F), 82.8 (2 C_q IrBpin), 59.7 (CH_2N), 47.3 (d, J_{CP} = 37 Hz, CH_2P), 24.9 (overlapped with solvent signal, 2 CH_3 IrBpin), 20.9 (CH_3), 18.9 (CH_3), 18.8 (CH_3) ppm. Signals for three quaternary aromatic carbons could not be detected due to significant spectrum complexity.

IR (CH_2Cl_2): 2089 (ν_{IrH}), 1993 (ν_{CO}) cm^{-1}.

I.3.7. Synthesis of Ir-CNP^{tBu} complexes

Complex 21

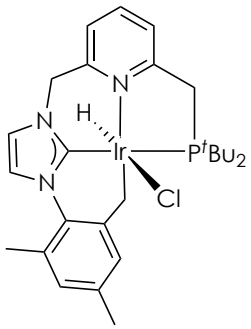

A dichloromethane (25 mL) solution of **20a** (0.700 g, 1.38 mmol) and Ir(acac)(COD) (0.495 g, 1.24 mmol) was stirred for 3 days. The formed yellow precipitate was filtered, washed with Et_2O (2 × 10 mL) and pentane (2 × 10 mL), and dried under vacuum. Light yellow solid (0.431 g, 47%). Crystals of **21** suitable for X-ray diffraction analysis were grown from a saturated solution of the complex in CH_2Cl_2.

Anal. calcd (%) for $C_{27}H_{38}ClIrN_3P$: C 48.9, H 5.8, N 6.3; found: C 49.0, H 5.9, N 6.1.

^{1}H NMR (500 MHz, CD_2Cl_2): δ 7.64 (s, 1H, H arom NHC), 7.63 (dd, $^3J_{HH}$ = 7.8 Hz, $^3J_{HH}$ = 7.8 Hz, 1H, H arom Py), 7.41 (d, $^3J_{HH}$ = 7.8 Hz, 1H, H arom Py), 7.24 (s, 1H, H arom NHC), 7.20 (d, $^3J_{HH}$ = 7.8 Hz, 1H, H arom Py), 7.07 (d, $^2J_{HH}$ = 14.5 Hz, 1H, C*H*HN), 6.98 (s, 1H, H arom Mes), 6.71 (s, 1H, H arom Mes), 4.90 (d, $^2J_{HH}$ = 14.5 Hz, 1H, C*H*HN), 3.95 (d, $^2J_{HH}$ = 11.3 Hz, 1H, C*H*HIr), 3.58 (dd, $^2J_{HH}$ = 16.5 Hz, $^2J_{HP}$ = 8.7 Hz, 1H, C*H*HP), 2.91 (dd, $^2J_{HH}$ = 11.2 Hz, $^3J_{HP}$ = 9.1 Hz, 1H, CH*H*Ir), 2.70 (dd, $^2J_{HH}$ = 16.5 Hz, $^2J_{HP}$ = 7.2 Hz, 1H, C*H*HP), 2.35 (s, 3H, CH_3), 2.25 (s, 3H, CH_3), 1.40 (d, $^3J_{HP}$ = 12.4 Hz, 9H, C(CH_3)$_3$), 1.34 (d, $^3J_{HP}$ = 12.5 Hz, 9H, C(CH_3)$_3$),

−24.47 (d, $^{2}J_{HP}$ = 17.0 Hz, 1H, IrH) ppm.

$^{31}P\{^{1}H\}$ NMR (202 MHz, CD_2Cl_2): δ 54.6 ppm.

$^{13}C\{^{1}H\}$ NMR (125 MHz, CD_2Cl_2): δ 176.1 (d, J_{CP} = 118 Hz, C-2 NHC), 166.9 (d, J_{CP} = 5 Hz, C_q arom), 156.3 (C_q arom), 151.4 (C_q arom), 136.5 (C_q arom), 135.7 (CH arom), 135.2 (C_q arom), 128.0 (CH arom), 127.7 (C_q arom), 127.2 (CH arom), 122.6 (CH arom), 121.7 (d, J_{CP} = 7 Hz, CH arom), 119.8 (d, J_{CP} = 4 Hz, CH arom), 119.6 (d, J_{CP} = 4 Hz, CH arom), 56.9 (CH_2N), 40.0 (d, J_{CP} = 23 Hz, CH_2P), 38.0 (d, J_{CP} = 9 Hz, $C(CH_3)_3$), 33.2 (d, J_{CP} = 20 Hz, $C(CH_3)_3$), 30.8 (d, J_{CP} = 4 Hz, $C(CH_3)_3$), 29.0 (d, J_{CP} = 5 Hz, $C(CH_3)_3$), 22.2 (CH_3 Mes), 20.9 (CH_3 Mes), −9.6 (br, CH_2Ir) ppm.

IR (Nujol): 2214 cm^{-1} (ν_{IrH}).

$IrH_2Cl(C^{Mes}NP^{tBu})$ (22a)

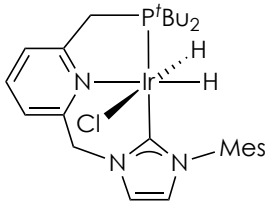

In a Fisher–Porter vessel, a solution of **21** (0.120 g, 0.18 mmol) in CH_2Cl_2 (20 mL) was pressurized with 4 bar of H_2 and heated to 65 °C overnight. The system was depressurized, solvent was evaporated and the residue was washed with pentane (2 × 10 mL). Yellow solid (0.115 g, 96%).

Anal. calcd (%) for $C_{27}H_{40}ClIrN_3P$: C 48.8, H 6.1, N 6.3; found: C 49.0, H 5.8, N 6.4.

^{1}H NMR (400 MHz, CD_2Cl_2): δ 7.69 (dd, $^3J_{HH}$ = 7.8 Hz, $^3J_{HH}$ = 7.8 Hz, 1H, H arom Py), 7.46 (d, $^3J_{HH}$ = 7.8 Hz, 1H, H arom Py), 7.30 (m, 2H, H arom Py + H arom NHC), 7.03 (s, 1H, H arom Mes), 6.95 (d, $^2J_{HH}$ = 14.4 Hz, 1H, C*H*HN), 6.92 (s, 1H, H arom Mes), 6.88 (s, 1H, H arom NHC), 4.92 (d, $^2J_{HH}$ = 14.4 Hz, 1H, C*H*HN), 3.58 (dd, $^2J_{HH}$ = 16.5 Hz, $^2J_{HP}$ = 8.7 Hz, 1H, C*H*HP), 2.78 (dd, $^2J_{HH}$ = 16.5 Hz, $^2J_{HP}$ = 7.6 Hz, 1H, C*H*HP), 2.37 (s, 3H, CH_3), 2.18 (s, 3H, CH_3), 1.92 (s, 3H, CH_3), 1.25 (d, $^3J_{HP}$ = 12.6 Hz, 9H, $C(CH_3)_3$), 1.20 (d, $^3J_{HP}$ = 12.5 Hz, 9H, $C(CH_3)_3$), –20.36 (dd, $^2J_{HP}$ = 14.4 Hz, $^2J_{HH}$ = 6.5 Hz, 1H, IrH *trans* to Py), –24.89 (dd, $^2J_{HP}$ = 17.2 Hz, $^2J_{HH}$ = 6.5 Hz, 1H, IrH *cis* to Py) ppm.

^{31}P{^{1}H} NMR (122 MHz, CD_2Cl_2): δ 64.8 ppm.

^{13}C{^{1}H} NMR (101 MHz, CD_2Cl_2): δ 173.2 (d, J_{CP} = 115 Hz, C-2 NHC), 167.0 (d, J_{CP} = 4 Hz, C_q arom), 156.4 (C_q arom), 138.4 (C_q arom), 138.2 (C_q

arom), 136.7 (C_q arom), 135.8 (CH arom), 135.4 (C_q arom), 128.9 (CH arom), 128.3 (CH arom), 122.1 (CH arom), 121.5 (d, J_{CP} = 8 Hz, CH arom), 121.0 (d, J_{CP} = 3 Hz, CH arom), 119.8 (d, J_{CP} = 4 Hz, CH arom), 56.5 (CH_2N), 39.4 (d, J_{CP} = 23 Hz, *C*(CH_3)), 38.1 (d, J_{CP} = 10 Hz, CH_2P), 32.4 (d, J_{CP} = 24 Hz, *C*(CH_3)), 30.6 (d, J_{CP} = 3 Hz, 3 C(*C*H_3)), 29.1 (d, J_{CP} = 4 Hz, 3 C(*C*H_3)), 21.3 (CH_3), 18.8 (CH_3), 18.1 (CH_3) ppm.

IR (Nujol): 2235 (ν_{IrH}), 2141 (ν_{IrH}) cm^{-1}.

[Ir(C^{Xyl}NP^{tBu})(COD)]Cl (23)

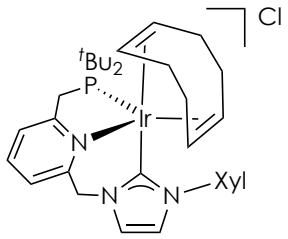

Dichloromethane (8 mL) was added to a mixture of **20b·HCl** (0.155 g, 0.31 mmol) and phenethyldiethylamine ScavengePore resin (0.850 g; base loading: 0.66 mmol/g), and the suspension was stirred for 1 h. The mixture was filtered through a short pad of celite and solvent was evaporated. A solution of Ir(acac)(COD) (0.125 g, 0.31 mmol) in THF (5 mL) was added to the residue, and the mixture was stirred overnight. The solvent was evaporated, and the resulting solid was washed with pentane (2 × 5 mL), and dried under vacuum to give complex **23** as a yellow solid (0.078 g, 32%).

^{1}H NMR (400 MHz, THF-d_8): δ 7.85 (s, 2H, 2 H arom Xyl), 7.65 (dd, $^{3}J_{HH}$ = 7.7 Hz, $^{3}J_{HH}$ = 7.7 Hz, 1H, H arom Py), 7.48 (d, $^{3}J_{HH}$ = 7.6 Hz, 1H, H arom Py), 7.43 (d, $^{3}J_{HH}$ = 2.2 Hz, 1H, H arom NHC), 7.39 (d, $^{3}J_{HH}$ = 7.8 Hz, 1H, H arom Py), 7.31 (d, $^{3}J_{HH}$ = 2.2 Hz, 1H, H arom NHC), 7.09 (s, 1H, H arom Xyl), 5.97 (d, $^{2}J_{HH}$ = 14.6 Hz, 1H, C*H*HN), 5.68 (d, $^{2}J_{HH}$ = 14.6 Hz, 1H, C*H*HN), 4.62 (m, 1H, CH= COD), 4.48 (m, 1H, CH= COD), 3.11 (m, 2H, 2 C*H*HP), 2.74 (m, 1H, CH= COD), 2.43 (s, 6H, 2 CH_3), 2.27 (m, 1H, CH= COD), 2.16 (m, 2H, C*H*H COD), 1.94 (m, 2H, C*H*H COD), 1.63 (m, 1H, C*H*H COD), 1.41 (m, 3H, C*H*H COD), 1.20 (d, $^{3}J_{HP}$ = 10.6 Hz, 9H, $C(CH_3)_3$), 1.17 (d, $^{3}J_{HP}$ = 10.6 Hz, 9H, $C(CH_3)_3$) ppm.

^{31}P{^{1}H} NMR (162 MHz, THF-d_8): δ 36.5 ppm.

$^{13}C\{^{1}H\}$ NMR (101 MHz, THF-d_8): δ 181.4 (C-2 NHC), 162.9 (d, J_{CP} = 14 Hz, C_q arom), 156.2 (C_q arom), 141.0 (C_q arom), 138.7 (2 C_q arom), 137.2 (CH arom), 129.3 (CH arom), 123.4 (3 CH arom), 122.4 (CH arom), 121.6 (CH arom), 120.7 (CH arom), 82. 9 (CH= COD), 82.5 (CH= COD), 56.8 (CH_2N), 52.0 (CH= COD), 51.7 (CH= COD), 33.8 (d, J_{CP} = 58 Hz, CH_2P), 32.3 (m, 2 $C(CH_3)_3$), 30.0 (m, 2 $C(CH_3)_3$ + 4 CH_2 COD), 21.1 (2 CH_3) ppm.

HRMS (ESI): *m/z* calcd for $C_{34}H_{48}IrN_3P$ $[(M-Cl)^+]$: 722.3215; found: 722.3202.

Complexes 22b and 24

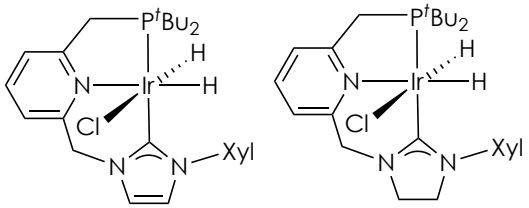

22b **24**

In a Fisher–Porter vessel, a solution of **23** (0.120 g, 0.18 mmol) in CH_2Cl_2 (20 mL) was pressurized with 4 bar of H_2, and heated to 65 °C overnight. The system was depressurized, solvent was evaporated, and the residue was washed with pentane (2 × 10 mL). Yellow solid (0.115 g, 96%). The compounds **22b** and **24** were obtained in an approximated ratio of 85:15.

*NMR spectroscopy and HRMS data for complex **22b***

^{1}H NMR (500 MHz, CD_2Cl_2): δ 7.70 (dd, $^3J_{HH}$ = 7.7 Hz, $^3J_{HH}$ = 7.7 Hz, 1H, H arom Py), 7.47 (d, $^3J_{HH}$ = 7.8 Hz, 1H, H arom Py), 7.28 (m, 3H, 2 H arom Xyl + H arom Py), 7.23 (d, $^3J_{HH}$ = 1.7 Hz, 1H, H arom NHC), 7.17 (d, $^3J_{HH}$ = 1.7 Hz, 1H, H arom NHC), 7.08 (s, 1H, H arom Xyl), 6.94 (d, $^2J_{HH}$ = 14.4 Hz, 1H, C*H*HN), 4.87 (d, $^2J_{HH}$ = 14.4 Hz, 1H, C*H*HN), 3.64 (dd, $^2J_{HH}$ = 16.7 Hz, $^2J_{HP}$ = 8.7 Hz, 1H, C*H*HP), 2.89 (dd, $^2J_{HH}$ = 16.6 Hz, $^2J_{HP}$ = 7.8 Hz, 1H, C*H*HP), 2.39 (s, 6H, 2 CH_3), 1.33 (d, $^3J_{HP}$ = 12.4 Hz, 9H, C(CH_3)$_3$), 1.27 (d, $^3J_{HP}$ = 12.7 Hz, 9H, C(CH_3)$_3$), –20.13 (dd, $^2J_{HP}$ = 14.7 Hz, $^2J_{HH}$ = 6.3 Hz, 1H, IrH *trans* to Py), –24.67 (dd, $^2J_{HP}$ = 17.4 Hz, $^2J_{HH}$ = 6.3 Hz, 1H, IrH *cis* to Py) ppm.

$^{31}P\{^{1}H\}$ NMR (162 MHz, THF-d_8): δ 64.6 ppm.

$^{13}C\{^{1}H\}$ NMR (101 MHz, THF-d_8): δ 172.2 (d, J_{CP} = 115 Hz, C-2 NHC), 166.7 (C_q arom), 156.9 (C_q arom), 142.7 (C_q arom), 137.6 (2 C_q arom), 136.3 (CH arom), 128.9 (CH arom), 125.8 (2 CH arom), 122.5 (m, 2 CH arom), 121.7 (CH arom), 120.6 (CH arom), 55.8 (CH_2N), 39.3 (d, J_{CP} = 23 Hz, $C(CH_3)_3$), 38.2 (d, J_{CP} = 11 Hz, CH_2P), 33.0 (d, J_{CP} = 24 Hz, $C(CH_3)_3$), 31.0 ($C(CH_3)_3$), 29.6 ($C(CH_3)_3$), 21.2 (2 CH_3) ppm.

HRMS (ESI): *m/z* calcd for $C_{26}H_{38}IrN_3P$ [$(M-Cl)^+$]: 616.2433; found: 616.2420.

*NMR spectroscopy and HRMS data for complex **24***

^{1}H NMR (500 MHz, CD_2Cl_2): δ 7.67 (dd, $^{3}J_{HH}$ = 7.6 Hz, $^{3}J_{HH}$ = 7.6 Hz, 1H, H arom Py), 7.43 (d, $^{3}J_{HH}$ = 7.8 Hz, 1H, H arom Py), 7.32 (s, 1H, H arom Xyl), 7.19 (m, 3H, 3 H arom), 6.36 (d, $^{2}J_{HH}$ = 14.6 Hz, 1H, C*H*HN), 4.30 (m, 1H, C*H*H NHC), 4.17 (d, $^{2}J_{HH}$ = 14.7 Hz, 1H, C*H*HN), 4.05 (m, 1H, C*H*H NHC), 3.91 (m, 2H, 2 C*H*H NHC), 3.61 (overlapped m, 1H, C*H*HP), 2.88 (overlapped m, 1H, C*H*HP), 2.34 (s, 6H, 2 CH_3), 1.29 (d, $^{3}J_{HP}$ = 12.0 Hz, 9H, $C(CH_3)_3$), 1.22 (d, $^{3}J_{HP}$ = 12.8 Hz, 9H, $C(CH_3)_3$), −20.41 (dd, $^{2}J_{HP}$ = 14.5 Hz, $^{2}J_{HH}$ = 5.9 Hz, 1H, IrH *trans* to Py), −24.40 (dd, $^{2}J_{HP}$ = 17.8 Hz, $^{2}J_{HH}$ = 5.9 Hz, 1H, IrH *cis* to Py) ppm.

$^{31}P\{^{1}H\}$ NMR (162 MHz, THF-d_8): δ 64.2 ppm.

HRMS (ESI): *m/z* calcd for $C_{26}H_{40}IrN_3P$ [$(M-Cl)^+$]: 618.2584; found: 618.2563.

$IrH_3(C^{Mes}NP^{tBu})$ (25a)

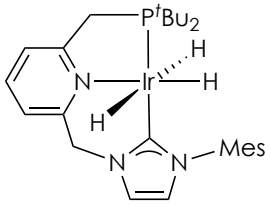

Tetrahydrofuran (8 mL) was added to a mixture of complex **22a** (0.095 g, 0.14 mmol) and NaH (0.070 g, 2.9 mmol), and the resulting suspension was heated to 40 ºC for 2 days. The solid was filtered off, and the solvent was evaporated. The obtained solid was washed with pentane (2 × 8 mL), and dried under vacuum. Yellow solid (0.079 g, 88%).

Anal. calcd (%) for $C_{27}H_{41}ClIrN_3P$: C 51.4, H 6.6, N 6.7; found: C 51.4, H 6.5, N 6.8.

^{1}H NMR (500 MHz, C_6D_6): δ 6.83 (m, 3H, 2 H arom Mes + H arom Py), 6.60 (d, $^3J_{HH}$ = 7.5 Hz, 1H, H arom Py), 6.56 (s, 1H, H arom NHC), 6.40 (d, $^3J_{HH}$ = 7.3 Hz, 1H, H arom Py), 6.34 (s, 1H, H arom NHC), 4.72 (s, 2H, CH_2N), 3.03 (d, $^2J_{HP}$ = 7.9 Hz, 2H, CH_2P), 2.30 (s, 6H, 2 CH_3), 2.11 (s, 3H, CH_3), 1.29 (d, $^3J_{HP}$ = 12.0 Hz, 18H, 2 $C(CH_3)_3$), −10.14 (dd, $^2J_{HP}$ = 15.6 Hz, $^2J_{HH}$ = 5.4 Hz, 2H, 2 IrH), −20.03 (dt, $^2J_{HP}$ = 13.8 Hz, $^2J_{HH}$ = 5.4 Hz, 1H, IrH) ppm.

^{31}P{^{1}H} NMR (202 MHz, C_6D_6): δ 76.3 ppm.

^{13}C{^{1}H} NMR (126 MHz, C_6D_6): δ 178.8 (d, J_{CP} = 113 Hz, C-2 NHC), 166.8 (d, J_{CP} = 5 Hz, C_q arom), 154.7 (C_q arom), 138.9 (C_q arom), 137.2 (C_q arom), 136.4 (2 C_q arom), 132.1 (CH arom), 128.9 (2 CH arom), 120.0 (CH arom), 119.8 (d, J_{CP} = 8 Hz, CH arom), 119.1 (d, J_{CP} = 4 Hz, CH arom),

118.6 (d, J_{CP} = 3 Hz, CH arom), 59.8 (CH_2N), 41.0 (d, J_{CP} = 19 Hz, CH_2P), 33.2 (d, J_{CP} = 17 Hz, 2 *C*(CH_3)), 29.9 (d, J_{CP} = 5 Hz, 6 C(*C*H_3)), 21.2 (CH_3), 19.6 (2 CH_3) ppm.

IR (Nujol): 2101 cm^{-1} (ν_{IrH}).

Complexes 25b and 26

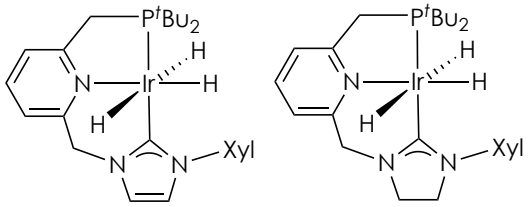

25b **26**

Tetrahydrofuran (8 mL) was added to an 85:15 mixture of complexes **22b** and **24** (0.078 g) and NaH (0.057 g, 2.39 mmol), and the solution was stirred overnight at room temperature. The suspension was filtered through a short pad of celite, and solvent was evaporated. The obtained yellow solid was washed with pentane (2 x 8 mL), and dried under vacuum (0.079 g, 88%). Compounds **25b** and **26** were obtained in an 80:20 ratio.

Anal. calcd (%) for 0.8 $C_{26}H_{39}IrN_3P$ + 0.2 $C_{26}H_{41}IrN_3P$: C 50.6, H 6.4, N 6.8; found: C 50.2, H 6.8, N 6.5.

*NMR spectroscopy data for complex **25b***

^{1}H NMR (400 MHz, THF-d_8): δ 7.81 (s, 2H, 2 H arom Xyl), 7.56 (dd, $^3J_{HH}$ = 7.6 Hz, $^3J_{HH}$ = 7.6 Hz, 1H, H arom Py), 7.33 (d, $^3J_{HH}$ = 8.1 Hz, 1H, H arom Py), 7.29 (s, 1H, H arom NHC), 7.22 (d, $^3J_{HH}$ = 7.5 Hz, 1H, H arom Py), 7.18 (s, 1H, H arom NHC), 6.88 (s, 1H, H arom Xyl), 5.13 (s, 2H, CH_2N), 3.35 (d, $^2J_{HP}$ = 8.1 Hz, 2H, CH_2P), 2.34 (s, 6H, 2 CH_3), 1.31 (d, $^3J_{HP}$ = 12.0 Hz, 18H, 2 $C(CH_3)_3$), −10.62 (dd, $^2J_{HP}$ = 16.0 Hz, $^2J_{HH}$ = 5.1 Hz, 2H, 2 IrH), −20.37 (dt, $^2J_{HP}$ = 14.6 Hz, $^2J_{HH}$ = 5.0 Hz, 1H, IrH) ppm.

^{31}P{^{1}H} NMR (162 MHz, THF-d_8): δ 77.3 ppm.

$^{13}C\{^{1}H\}$ NMR (101 MHz, THF-d_8): δ 177.8 (d, J_{CP} = 113 Hz, C-2 NHC), 166.3 (d, J_{CP} = 5 Hz, C_q arom), 154.5 (C_q arom), 142.6 (C_q arom), 136.2 (2 C_q arom), 132.7 (CH arom), 127.1 (CH arom), 124.8 (2 CH arom), 119.6 (m, 2 CH arom), 119.2 (d, J_{CP} = 4 Hz, CH arom), 119.1 (CH arom), 59.3 (CH_2N), 40.3 (d, J_{CP} = 20 Hz, CH_2P), 32.6 (d, J_{CP} = 17 Hz, 2 *C*(CH_3)), 29.1 (d, J_{CP} = 5 Hz, 6 C(*C*H_3)), 20.3 (2 CH_3) ppm.

IR (Nujol): ν = 2106 cm^{-1} (ν_{IrH}).

*NMR spectroscopy data for complex **26***

^{1}H NMR (400 MHz, THF-d_8): δ 7.78 (s, 2H, 2 H arom Xyl), 7.53 (dd, $^{3}J_{HH}$ = 7.5 Hz, $^{3}J_{HH}$ = 7.5 Hz, 1H, H arom Py), 7.39 (d, $^{3}J_{HH}$ = 7.4 Hz, 1H, H arom Py), 7.12 (d, $^{3}J_{HH}$ = 7.5 Hz, 1H, H arom Py), 6.68 (s, 1H, H arom Xyl), 4.57 (s, 2H, CH_2N), 3.99 (m, 2H, 2 C*H*H NHC), 3.76 (m, 2H, 2 C*H*H NHC), 3.35 (d, $^{2}J_{HP}$ = 8.1 Hz, 2H, CH_2P), 2.28 (s, 6H, 2 CH_3), 1.23 (d, $^{3}J_{HP}$ = 12.9 Hz, 18H, 2 C(CH_3)$_3$), −10.56 (dd, $^{2}J_{HP}$ = 17.6 Hz, $^{2}J_{HH}$ = 5.0 Hz, 2H, 2 IrH), −20.65 (dt, $^{2}J_{HP}$ = 14.2 Hz, $^{2}J_{HH}$ = 5.0 Hz, 1H, IrH) ppm.

$^{31}P\{^{1}H\}$ NMR (162 MHz, THF-d_8): δ 76.5 ppm.

Complex 29

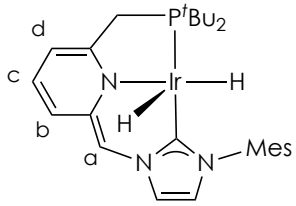

In a J.Young valved NMR tube, a solution of **22a** (0.020 g, 0.030 mmol) in THF-d_8 (0.5 mL) was treated with KHMDS (0.006 g, 0.030 mmol). The resulting solution was immediately analyzed by NMR spectroscopy.

^{1}H NMR (400 MHz, THF-d_8): δ 7.49 (s, 1H, H arom NHC), 7.09 (s, 1H, H arom NHC), 6.96 (s, 2H, 2 H arom Mes), 6.44 (s, 1H, H^a), 6.22 (m, 2H, H^b + H^c), 4.92 (d, $^3J_{HH}$ = 5.3 Hz, 1H, H^d), 2.78 (d, $^2J_{HP}$ = 8.9 Hz, 2H, CH_2P), 2.32 (s, 3H, CH_3), 1.99 (s, 6H, 2 CH_3), 1.15 (d, $^3J_{HP}$ = 12.6 Hz, 18H, 2 C(CH_3)$_3$), –23.77 (d, $^2J_{HP}$ = 11.3 Hz, 2H, 2 IrH) ppm.

^{31}P{^{1}H} NMR (162 MHz, THF-d_8): δ 74.4 ppm.

^{13}C{^{1}H} NMR (101 MHz, THF-d_8): δ 179.6 (d, J_{CP} = 110 Hz, C-2 NHC), 166.4 (d, J_{CP} = 8 Hz, C_q arom), 141.9 (C_q arom), 139.7 (C_q arom), 137.9 (C_q arom), 136.7 (2 C_q arom), 129.1 (2 CH arom), 126.9 (CH Py), 120.4 (CH arom + CH Py), 117.4 (CH arom), 98.6 (C^a), 97.2 (d, J_{CP} = 11 Hz, C^d), 35.0 (d, J_{CP} = 20 Hz, CH_2P), 34.7 (d, J_{CP} = 21 Hz, 2 *C*(CH_3)), 29.3 (d, J_{CP} = 5 Hz, 6 C(*C*H_3)), 21.0 (CH_3), 18.0 (2 CH_3) ppm.

Complex 30a^{M}

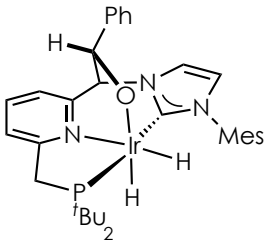

In a J.Young valved NMR tube, a solution of **22a** (0.020 g, 0.030 mmol) in THF-d_8 (0.5 mL) was treated with KHMDS (0.008 g, 0.039 mmol) and benzaldehyde (6.0 μL, 0.060 mmol). The resulting solution was analyzed by NMR spectroscopy.

^{1}H NMR (500 MHz, THF-d_8): δ 7.74 (t, $^{3}J_{HH}$ = 7.6 Hz, 1H, H arom), 7.62 (t, $^{3}J_{HH}$ = 7.4 Hz, 1H, H arom), 7.53 (m, 1H, H arom), 7.43 (m, 2H, 2 H arom), 7.04 (m, 2H, 2 H arom), 6.91 (m, 2H, 2 H arom), 6.80 (s, 1H, H arom), 6.75 (s, 1H, H arom), 6.59 (s, 1H, H arom), 5.64 (s, 1H, CHN), 4.90 (s, 1H, CHOIr), 3.61 (d, $^{2}J_{HH}$ = 15.5 Hz, $^{2}J_{HP}$ = 8.9 Hz, 1H, C*H*HP), 2.95 (dd, $^{2}J_{HH}$ = 15.5 Hz, $^{2}J_{HP}$ = 6.7 Hz, 1H, C*H*HP), 2.28 (s, 3H, CH_3), 2.21 (s, 3H, CH_3), 1.74 (s, 3H, CH_3), 1.23 (d, $^{3}J_{HP}$ = 12.1 Hz, 9H, $C(CH_3)_3$), 1.05 (d, $^{3}J_{HP}$ = 12.1 Hz, 9H, $C(CH_3)_3$), −19.39 (dd, $^{2}J_{HP}$ = 14.2 Hz, $^{2}J_{HH}$ = 7.8 Hz, 1H, IrH *trans* to Py), −24.33 (dd, $^{2}J_{HP}$ = 18.2 Hz, $^{2}J_{HH}$ = 7.8 Hz, 1H, IrH *cis* to Py) ppm.

^{31}P{^{1}H} NMR (162 MHz, THF-d_8): δ 75.5 ppm.

^{13}C{^{1}H} NMR (101 MHz, THF-d_8): δ 176.7 (d, J_{CP} = 119 Hz, C-2 NHC), 166.6 (d, J_{CP} = 5 Hz, C_q arom), 158.9 (C_q arom), 150.4 (C_q arom), 138.5 (C_q arom), 137.8 (C_q arom), 136.7 (C_q arom), 136.2 (C_q arom), 135.9 (CH arom),

129.2 (CH arom), 128.4 (CH arom), 127.8 (2 CH arom), 127.2 (2 CH arom), 125.6 (CH arom), 120.9 (d, J_{CP} = 2 Hz, CH arom), 120.7 (d, J_{CP} = 7 Hz, CH arom), 120.0 (CH arom), 119.4 (d, J_{CP} = 3 Hz, CH arom), 76.8 (CHN), 75.4 (CHOIr), 39.6 (d, J_{CP} = 21 Hz, *C*(CH_3)), 36.8 (d, J_{CP} = 7 Hz, CH_2P), 31.9 (d, J_{CP} = 23 Hz, *C*(CH_3)), 30.6 (d, J_{CP} = 3 Hz, 3 C(*C*H_3)), 29.5 (d, J_{CP} = 5 Hz, 3 C(*C*H_3)), 21.0 (CH_3), 19.1 (CH_3), 18.2 (CH_3) ppm.

Complex 30b^{M}

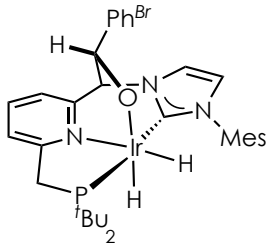

In a J.Young valved NMR tube, a solution of **22a** (0.010 g, 0.015 mmol) in THF-d_8 (0.5 mL) was treated with KHMDS (0.004 g, 0.020 mmol) and 4-bromobenzaldehyde (0.004 g, 0.022 mmol). The resulting solution was analyzed by NMR spectroscopy.

^{1}H NMR (500 MHz, THF-d_8): δ 7.78 (dd, $^{3}J_{HH}$ = 8.0 Hz, $^{3}J_{HH}$ = 8.0 Hz, 1H, H arom Py), 7.54 (d, $^{3}J_{HH}$ = 8.0 Hz, H arom Py), 7.44 (d, $^{3}J_{HH}$ = 8.1 Hz, H arom Py), 7.36 (d, $^{3}J_{HH}$ = 8.1 Hz, 2H, 2 H arom *p*-BrPh), 7.19 (d, $^{3}J_{HH}$ = 8.1 Hz, 2H, 2 H arom *p*-BrPh), 6.95 (s, 1H, H arom), 6.81 (s, 2H, 2 H arom), 6.66 (s, 1H, H arom), 5.62 (s, 1H, CHN), 4.87 (s, 1H, CHOIr), 3.61 (d, $^{2}J_{HH}$ = 15.6 Hz, $^{2}J_{HP}$ = 8.8 Hz, 1H, C*H*HP), 2.95 (dd, $^{2}J_{HH}$ = 15.6 Hz, $^{2}J_{HP}$ = 6.7 Hz, 1H, C*H*HP), 2.28 (s, 3H, CH_3), 2.18 (s, 3H, CH_3), 1.74 (s, 3H, CH_3), 1.22 (d, $^{3}J_{HP}$ = 12.1 Hz, 9H, C(CH_3)$_3$), 1.03 (d, $^{3}J_{HP}$ = 12.3 Hz, 9H, C(CH_3)$_3$), −19.35 (dd, $^{2}J_{HP}$ = 14.2 Hz, $^{2}J_{HH}$ = 7.8 Hz, 1H, IrH *trans* to Py), −24.56 (dd, $^{2}J_{HP}$ = 18.4 Hz, $^{2}J_{HH}$ = 7.8 Hz, 1H, IrH *cis* to Py) ppm.

^{31}P{^{1}H} NMR (202 MHz, THF-d_8): δ 75.6 ppm.

^{13}C{^{1}H} NMR (101 MHz, THF-d_8): δ 166.9 (d, J_{CP} = 4 Hz, C_q arom), 158.7 (C_q arom), 149.8 (C_q arom), 138.6 (C_q arom), 138.0 (C_q arom), 136.7 (C_q arom), 136.3 (C_q arom), 136.2 (CH arom), 130.4 (2 CH arom), 130.0 (2 CH

arom), 129.2 (CH arom), 128.6 (CH arom), 121.1 (m, 2 CH arom), 120.3 (CH arom), 120.0 (CH arom), 119.4 (C_q arom), 76.5 (CHN), 75.0 (CHOIr), 39.8 (d, J_{CP} = 21 Hz, *C*(CH_3)), 36.9 (d, J_{CP} = 7 Hz, CH_2P), 32.1 (d, J_{CP} = 23 Hz, *C*(CH_3)), 30.8 (d, J_{CP} = 3 Hz, 3 C(*C*H_3)), 29.6 (d, J_{CP} = 4 Hz, 3 C(*C*H_3)), 21.2 (CH_3), 19.2 (CH_3), 18.3 (CH_3) ppm. Signal of the C^2-NHC could not be detected.

I.3.8. Catalytic reactions

I.3.8.1. Hydrogenation reactions

Representative procedure for ketone hydrogenation

In a glovebox, a Fisher–Porter vessel was charged with a solution of complex **7a(Cl)** (2.0 mg, 2.5 μmol), KO^{t}Bu (2.7 mg, 37 μmol) and acetophenone (30 μL, 0.26 mmol) in 2-methyltetrahydrofuran (2.0 mL). The reactor was purged three times with H_2, and finally pressurized with 1 bar and heated to 60 ^{o}C. After 16 h, the reactor was slowly cooled down to room temperature, and depressurized. The reaction solution was evaporated, and conversion was determined by ^{1}H NMR spectroscopy using mesitylene as internal standard.

Representative procedure for ketone transfer hydrogenation

In a glovebox, a Schlenk flask was charged with a solution of complex **7a(Cl)** (1.0 mg, 1.2 μmol), KO^{t}Bu (2.1 mg, 18 μmol) and acetophenone (140 μL, 1.23 mmol) in 2-propanol (2.0 mL) and heated to 80 ^{o}C. After 16 h, the vessel was slowly cooled down to room temperature. The reaction solution was evaporated, and conversion was determined by ^{1}H NMR spectroscopy using mesitylene as internal standard.

Representative procedure for aldehyde hydrogenation

In a glovebox, a Fisher–Porter vessel was charged with a solution of complex **25a** (1.0 mg, 1.6 μmol) and benzaldehyde (162 μL, 1.6 mmol) in 2-methyltetrahydrofuran (0.8 mL). The reactor was purged three times with H_2, and finally pressurized with 4 bar. After 16 h, the reactor was

depressurized, the reaction solution was evaporated, and conversion was determined by ^{1}H NMR spectroscopy.

I.3.8.2. Hydroboration of CO_2

For the preparation of wet THF-d_8 solutions, commercial THF-d_8 (Eurisotop, <0.05% water) was dried with sodium–benzophenone–ketyl and distilled under argon. Known amounts of water were added to THF-d_8, and the water content in the prepared solutions was confirmed by ^{1}H NMR spectroscopy using hexamethylbenzene as internal standard.

Representative procedure for CO_2 hydroboration with HBcat

In a glovebox, a J.Young valved NMR tube was charged with a solution of **15a/15b** (1.6 mg, 2.3 μmol) and hexamethylbenzene (3.8 mg, 0.023 mmol) in THF-d_8 containing 0.2% of water (0.5 mL) (total water content: 5 mol%), and catecholborane (25 μL, 0.23 mmol) was added. The NMR tube was submitted to vacuum to remove the N_2 atmosphere, charged with CO_2 (2 bar) and heated to 30 ºC. Reaction progress was monitored by ^{1}H and ^{11}B NMR spectroscopies.

Representative procedure for CO_2 hydroboration with HBpin

In a glovebox, a J.Young valved NMR tube was charged with 300 μL of a freshly prepared 1.3 mM stock solution of **15a/15b** (0.4 μmol) in THF-d_8 containing 0.2% of water, hexamethylbenzene (3.8 mg, 0.023 mmol) and THF-d_8 (0.2 mL) containing 0.2% of water (total water content: 5 mol%). Pinacolborane (32 μL, 0.22 mmol) was added, and the NMR tube was

submitted to vacuum to remove the N_2 atmosphere, charged with CO_2 (1 bar) and heated to 30 ºC. Reaction progress was monitored by ^{1}H and ^{11}B NMR spectroscopies.

I.4. Bibliography

1) J. F. Hartwig, *Organotransition Metal Chemistry: From Bonding to Catalysis*, University Science Books, **2010**.

2) E. S. Wiedner, M. B. Chambers, C. L. Pitman, R. M. Bullock, A. J. M. Miller, A. M. Appel, *Chem. Rev.* **2016**, *116*, 8655.

3) (a) G. J. Kubas, D. M. Heinekey, *Physical Inorganic Chemistry: Reactions, Processes, and Applications*, ed. A. Bakac, John Wiley & Sons, **2010**, *Ch. 5*; (b) M. A. Esteruelas, A. M. López, M. Oliván, *Chem. Rev.* **2016**, *116*, 8770.

4) (a) G. J. Kubas, *Metal Dihydrogen and σ-Bond Complexes: Structure, Theory and Reactivity*; Kluwer, **2001**; (b) M. A. Esteruelas, L. A. Oro, *Chem. Rev.* **1998**, *98*, 577; (c) R. H. Crabtree, *Chem. Rev.* **2016**, *116*, 8750.

5) (a) P. G. Jessop, R. H. Morris, *Coord. Chem. Rev.* **1992**, *121*, 155; (b) D. M. Heinekey, W. J. Jr. Oldham, *Chem. Rev.* **1993**, *93*, 913.

6) (a) P. P. Deutsch, R. Eisenberg, *Chem. Rev.* **1988**, *88*, 1147; (b) L. Vaska, *Acc. Chem. Res.* **1968**, *1*, 335.

7) B. Rybtchinski, Y. Ben-David, D. Milstein, *Organometallics* **1997**, *16*, 3786.

8) J. M. Goldberg, S. D. T. Cherry, L. M. Guard, W. Kaminsky, K. I. Goldberg, D. M. Heinekey, *Organometallics* **2016**, *35*, 3546.

9) (a) A. Dedieu, A. Strich, *Inorg. Chem.* **1979**, *18*, 2940; (b) J.-Y. Saillard, R. Hoffmann, *J. Am. Chem. Soc.* **1984**, *106*, 2006.

10) S. M. Kloek, D. M. Heinekey, K. I. Goldberg, *Organometallics* **2006**, *25*, 3007.

11) F. Liu, A. S. Goldman, *Chem. Commun.* **1999**, 655.

12) J. J. Adams, N. Arulsamy, D. M. Roddick, *Organometallics* **2011**, *30*, 697.

13) S. Li, M. B. Hall, *Organometallics* **1999**, *18*, 5682.

14) T. T. Lekich, J. B. Gary, S. M. Bellows, T. R. Cundari, L. M. Guarda, D. M. Heinekey, *Dalton Trans.* **2018**, *47*, 16119

15) M. Findlater, W. H. Bernskoetter, M. Brookhart, *J. Am. Chem. Soc.* **2010**, *132*, 4534.

16) (a) M. D. Fryzuk, P. A. MacNeil, *Organometallics* **1983**, *2*, 682; (b) M. D. Fryzuk, P. A. MacNeil, S. J. Rettig, *Organometallics* **1985**, *4*, 1145; (c) M. D. Fryzuk, P. A. MacNeil, S. J. Rettig, *J. Am. Chem. Soc.* **1987**, *109*, 2803.

17) E. Ben-Ari, G. Leitus, L. J. M. Shimon, D. Milstein, *J. Am. Chem. Soc.* **2006**, *128*, 15390.

18) L. Schwartsburd, M. A. Iron, L. Konstantinovski, Y. Diskin-Posner, G. Leitus, L. J. W. Shimon, D. Milstein, *Organometallics* **2010**, *29*, 3817.

19) M. A. Iron, E. Ben-Ari, R. Cohen, D. Milstein, *Dalton Trans.* **2009**, 9433.

20) (a) R. Tanaka, M. Yamashita, K. Nozaki, *J. Am. Chem. Soc.* **2009**, *131*, 14168; (b) R. Tanaka, M. Yamashita, L. W. Chung, K. Morokuma, K. Nozaki, *Organometallics* **2011**, *30*, 6742.

21) (a) *Applied homogeneous catalysis with organometallic compounds*, 2nd Edn. B. Cornils, W. A. Herrmann (Eds.), VCH, **2002**; (b) *The handbook of homogeneous hydrogenation*, J. G. de Vries, C. J. Elsevier (Eds.), VCH, **2007**.

22) (a) *Iridium complexes in organic synthesis*, L. A. Oro, C. Claver (Eds.), VCH, **2009**; (b) *Iridium Catalysis*, P. G. Andersson (Ed.), Springer, **2011**.

23) D. Wang, D. Astruc, *Chem. Rev.* **2015**, *115*, 6621.

24) X. Chen, W. Jia, R. Guo, T. W. Graham, M. A. Gullons, K. Abdur-Rashid, *Dalton Trans.* **2009**, 1407.

25) Z. E. Clarke, P. T. Maragh, T. P. Dasgupta, D. G. Gusev, A. J. Lough, K. Abdur-Rashid, *Organometallics* **2006**, *25*, 4113.

26) P. A. Dub, T. Ikariya, *ACS Catal.* **2012**, *2*, 1718.

27) (a) J. Pritchard, G. A. Filonenko, R. van Putten, E. J. M. Hensen, E. A. Pidko, *Chem. Soc. Rev.* **2015**, *44*, 3808; (b) T. P. Brewster, N. M. Rezayee, Z. Culakova, M. S. Sanford, K. I. Goldberg, *ACS Catal.* **2016**, *6*, 3113.

28) K. Junge, B. Wendt, H. Jiao, M. Beller, *ChemCatChem* **2014**, *6*, 2810.

29) T. J. Schmeier, G. E. Dobereiner, R. H. Crabtree, N. Hazari, *J. Am. Chem. Soc.* **2011**, *133*, 9274.

30) (a) M. S. G. Ahlquist, *J. Mol. Catal. A: Chemical* **2010**, *324*, 3; (b) X. Yang, *ACS Catal.* **2011**, *1*, 849.

31) W. Li, J.-H. Xie, H. Lin, Q.-L. Zhou, *Green Chem.* **2012**, *14*, 2388.

32) Z. Yang, X. Wei, D. Liu, Y. Liu, M. Sugiya, T. Imamoto, W. Zhang, *J. Organomet. Chem.* **2015**, *791*, 41.

33) (a) M. Aresta, *Carbon Dioxide as Chemical Feedstock*, Wiley-VCH, **2010**; (b) Q. Liu, L. P. Wu, R. Jackstell, M. Beller, *Nat. Commun.* **2015**, *6*, 5933; (c) A. M. Appel, J. E. Bercaw, A. B. Bocarsly, H. Dobbek, D. L. DuBois, M. Dupuis, J. G. Ferry, E. Fujita, R. Hille, P. J. A. Kenis, C. A. Kerfeld, R. H. Morris, C. H. F. Peden, A. R. Portis, S. W. Ragsdale, T. B. Rauchfuss, J. N. H. Reek, L. C. Seefeldt, R. K. Thauer, G. L. Waldrop, *Chem. Rev.* **2013**, *113*, 6621; (d) Y. Li, X. Cui, K. Dong, K. Junge, M. Beller, *ACS Catal.* **2017**, *7*, 1077.

34) (a) J. Klankermayer, S. Wesselbaum, K. Beydoun, W. Leitner, *Angew. Chem. Int. Ed.* **2016**, *55*, 7296; (b) M. Aresta, A. Dibenedetto, A. Angelini, *Chem. Rev.* **2014**, *114*, 1709.

35) C. Chauvier, T. Cantat, *ACS Catal.* **2017**, *7*, 2107.

36) M. A. Benvenuto, *Industrial Chemistry*, De Gruyter, **2013**.

37) (a) Y.-N. Li, R. Ma, L.-N. He, Z.-F. Diao, *Catal. Sci. Technol.* **2014**, *4*, 1498; (b) W.-H. Wang, Y. Himeda, J. T. Muckerman, G. F. Manbeck, E. Fujita, *Chem. Rev.* **2015**, *115*, 12936; (c) W. Wang, S. Wang, X. Ma, J. Gong, *Chem. Soc. Rev.* **2011**, *40*, 3703.

38) F. J. Fernández-Álvarez, A. M. Aitani, L. A. Oro, *Catal. Sci. Technol.* **2014**, *4*, 611.

39) (a) C. C. Chong, R. Kinjo, *ACS Catal.* **2015**, *5*, 3238; (b) S. Bontemps, *Coord. Chem. Rev.* **2016**, *308*, 117.

40) A. Tlili, E. Blondiaux, X. Frogneux, T. Cantat, *Green Chem.* **2015**, *17*, 157.

41) (a) M.-A. Courtemanche, M.-A. Légaré, L. Maron, F.-G. Fontaine, *J. Am. Chem. Soc.* **2013**, *135*, 9326; (b) T. Wang, D. W. Stephan, *Chem. Eur. J.* **2014**, *20*, 3036; (c) Y. Yang, M. Xu, D. Song, *Chem. Commun.* **2015**, *51*, 11293; (d) A. Ramos, A. Antiñolo, F. Carrillo-Hermosilla, R. Fernández-Galán, A. Rodríguez-Diéguez, D. García-Vivó, *Chem. Commun.* **2018**, *54*, 4700; (e) S. C. Sau, R. Bhattacharjee, P. K. Vardhanapu, G. Vijaykumar, A. Datta, S. K. Mandal, *Angew. Chem. Int. Ed.* **2016**, *55*, 15147; (f) R. Declercq, G. Bouhadir, D. Bourissou, M.-A. Légaré, M.-A. Courtemanche, K. S. Nahi, N. Bouchard, F.-G. Fontaine, L. Maron, *ACS Catal.* **2015**, *5*, 2513; (g) M.-A. Courtemanche, M.-A. Légaré, L. Maron, F.-G. Fontaine, *J. Am. Chem. Soc.* **2014**, *136*, 10708; (h) C. Das Neves Gomes, E. Blondiaux, P.

Thuéry, T. Cantat, *Chem. Eur. J.* **2014**, *20*, 7098; (i) T. Wang, D. W. Stephan, *Chem. Commun.* **2014**, *50*, 7007; (j) A. Tlili, A. Voituriez, A. Marinetti, P. Thuéry, T. Cantat, *Chem. Commun.* **2016**, *52*, 7553; (k) N. von Wolff, G. Lefèvre, J.-C. Berthet, P. Thuéry, T. Cantat, *ACS Catal.* **2016**, *6*, 4526; (l) G. Tuci, A. Rossin, L. Luconi, C. Pham-Huu, S. Cicchi, H. Ba, G. Giambastiani, *Catal. Sci. Technol.* **2017**, *7*, 5833.

42) (a) M. D. Anker, M. Arrowsmith, P. Bellham, M. S. Hill, G. Kociok-Köhn, D. J. Liptrot, M. F. Mahon, C. Weetman, *Chem. Sci.* **2014**, *5*, 2826; (b) D. Mukherjee, S. Shirase, T. P. Spaniol, K. Mashima, J. Okuda, *Chem. Commun.* **2016**, *52*, 13155; (c) D. Mukherjee, H. Osseili, T. P. Spaniol, J. Okuda, *J. Am. Chem. Soc.* **2016**, *138*, 10790; (d) T. J. Hadlington, C. E. Kefalidis, L. Maron, C. Jones, *ACS Catal.* **2017**, *7*, 1853; (e) J. A. B. Abdalla, I. M. Riddlestone, R. Tirfoin, S. Aldridge, *Angew. Chem. Int. Ed.* **2015**, *54*, 5098.

43) M. J. Sgro, D. W. Stephan, *Angew. Chem. Int. Ed.* **2012**, *51*, 11343.

44) S. Bontemps, L. Vendier, S. Sabo-Etienne, *Angew. Chem. Int. Ed.* **2012**, *51*, 1671.

45) R. Pal, T. L. Groy, R. J. Trovitch, *Inorg. Chem.* **2015**, *54*, 7506.

46) (a) F. Huang, C. Zhang, J. Jiang, Z.-X. Wang, H. Guan, *Inorg. Chem.* **2011**, *50*, 3816; (b) F. Huang, Q. Wang, J. Guo, M. Wenb, Z.-X. Wang, *Dalton Trans.* **2018**, *47*, 4804; (c) M. R. Espinosa, D. J. Charboneau, A. Garcia de Oliveira, N. Hazari, *ACS Catal.* **2019**, *9*, 301.

47) S. Bontemps, L. Vendier, S. Sabo-Etienne, *J. Am. Chem. Soc.* **2014**, *136*, 4419.

48) T. Liu, W. Meng, Q.-Q. Ma, J. Zhang, H. Li, S. Li, Q. Zhao, X. Chen, *Dalton Trans.* **2017**, *46*, 4504.

49) Q.-Q. Ma, T. Liu, S. Li, J. Zhang, X. Chen, H. Guan, *Chem. Commun.* **2016**, *52,* 14262.

50) (a) S. Chakraborty, J. Zhang, J. A. Krause, H. Guan, *J. Am. Chem. Soc.* **2010**, *132*, 8872; (b) S. Chakraborty, J. Zhang, Y. J. Patel, J. A. Krause, H. Guan, *Inorg. Chem.* **2013**, *52*, 37; (c) S. Chakraborty, Y. J. Patel, J. A. Krause, H. Guan, *Polyhedron* **2012**, *32*, 30.

51) N. N. Wellala, H. T. Dong, J. A. Krause, H. Guan, *Organometallics* **2018**, *37*, 4031.

52) J. Zhang, J. Chang, T. Liu, B. Cao, Y. Ding, X. Chen, *Catalysts* **2018**, *8*, 508.

53) R. Shintani, K. Nozaki, *Organometallics* **2013**, *32*, 2459.

54) A. Burgun, R. S. Crees, M. L. Cole, C. J. Doonan, C. J. Sumby, *Chem. Commun.* **2014**, *50*, 11760.

55) S. Bagherzadeh, N. P. Mankad, *J. Am. Chem. Soc.* **2015**, *137*, 10898.

56) C. Koon Ng, J. Wu, T. S. Andy Hor, H.-K. Luo, *Chem. Commun.* **2016**, *52*, 11842.

57) H.-W. Suh, L. M. Guard, N. Hazari, *Chem. Sci.* **2014**, *5*, 3859.

58) L. J. Murphy, H. Hollenhorst, R. McDonald, M. Ferguson, M. D. Lumsden, L. Turculet, *Organometallics* **2017**, *36*, 3709.

59) G. Jin, C. G. Werncke, Y. Escudié, S. Sabo-Etienne, S. Bontemps, *J. Am. Chem. Soc.* **2015**, *137*, 9563.

60) M. Asay, D. Morales-Morales, *Dalton Trans.* **2015**, *44*, 17432.

61) X. Liu, P. Braunstein, *Inorg. Chem.* **2013**, *52*, 7367.

62) (a) T. Simler, A. A. Danopoulos, P. Braunstein, *Chem. Commun.* **2015**, *51*, 10699; (b) T. Simler, P. Braunstein, A. A. Danopoulos, *Chem. Commun.* **2016**, *52*, 2717; (c) T. Simler, L. Karmazin, C. Bailly, P. Braunstein, A. A. Danopoulos, *Organometallics* **2016**, *35*, 903; (d) T.

Simler, S. Choua, A. A. Danopoulos, P. Braunstein, *Dalton Trans.* **2018**, *47*, 7888.

63) R. S. Rowland, R. Taylor, *J. Phys. Chem.* **1996,** *100,* 7384.

64) (a) H. M. J. Wang, I. J. B. Lin, *Organometallics* **1998**, *17*, 972; (b) J. C. Garrison, W. J. Youngs, *Chem. Rev.* **2005**, *105*, 3978; (c) I. J. B. Lin, C. S. Vasam, *Coord. Chem. Rev.* **2007**, *251*, 642.

65) N. Selander, K. J. Szabó, *Chem. Rev.* **2011**, *111*, 2048.

66) (a) J. I. van der Vlugt, M. A. Siegler, M. Janssen, D. Vogt, A. L. Spek, *Organometallics* **2009**, *28*, 7025; (b) M. Feller, E. Ben-Ari, M. A. Iron, Y. Diskin-Posner, G. Leitus, L. J. W. Shimon, L. Konstantinovski, D. Milstein, *Inorg. Chem.* **2010**, *49*, 1615; (c) W. D. Bailey, W. Kaminsky, R. A. Kemp, K. I. Goldberg, *Organometallics* **2014**, *33*, 2503.

67) (a) M. Hernández-Juárez, M. Vaquero, E. Álvarez, V. Salazar, A. Suárez, *Dalton Trans.* **2013**, *42*, 351; (b) M. Hernández-Juárez, J. López-Serrano, P. Lara, J. P. Morales-Cerón, M. Vaquero, E. Álvarez, V. Salazar, A. Suárez, *Chem. Eur. J.* **2015**, *21*, 7540.

68) G. A. Silantyev, O. A. Filippov, S. Musa, D. Gelman, N. V. Belkova, K. Weisz, L. M. Epstein, E. S. Shubina, *Organometallics* **2014**, *33*, 5964.

69) (a) D. M. Roddick, D. Zargarian, *Inorg. Chim. Acta* **2014**, *422*, 251; (b) G. Mancano, M. J. Page, M. Bhadbhade, B. A. Messerle, *Inorg. Chem.* **2014**, *53*, 10159; (c) P. D. Newman, K. J. Cavell, A. J. Hallett, B. M. Kariuki, *Dalton Trans.* **2011**, *40*, 8807; (d) B. M. Kariuki, J. A. Platts, P. D. Newman, *Dalton Trans.* **2014**, *43*, 2971; (e) M. Iglesias, A. Iturmendi, P. J. Sanz Miguel, V. Polo, J. J. Pérez-Torrente, L. A. Oro, *Chem. Commun.* **2015**, *51*, 12431.

70) J. Sandström, *Dynamic NMR Spectroscopy*, Academic Press, **1982**. Chap. 6.

71) M. Feller, E. Ben-Ari, Y. Diskin-Posner, R. Carmieli, L. Weiner, D. Milstein, *J. Am. Chem. Soc.* **2015**, *137*, 4634.

72) J. Reedijk, *Chem. Soc. Rev.* **2013**, *42*, 1776.

73) For selected examples of ketone hydrogenation catalyzed by Ir complexes with proton-responsive ligands: (a) L. Dahlenburg, R. Götz, *Eur. J. Inorg. Chem.* **2004**, 888; (b) C. S. Letko, Z. M. Heiden, T. B. Rauchfuss, *Eur. J. Inorg. Chem.* **2009**, 4927; (c) J. E. D. Martins, M. Wills, *Tetrahedron* **2009**, *65*, 5782; (d) J.-H. Xie, X.-Y. Liu, J.-B. Xie, L.-X. Wang, Q.-L. Zhou, *Angew. Chem. Int. Ed.* **2011**, *50*, 7329; (e) W. W. N. O, A. J. Lough, R. H. Morris, *Organometallics* **2012**, *31*, 2152.

74) E. Ben-Ari, R. Cohen, M. Gandelman, L. J. W. Shimon, J. M. L. Martin, D. Milstein, *Organometallics* **2006**, *25*, 3190.

75) (a) L. Vaska, *Science* **1966**, *152*, 769; (b) A. V. Polukeev, O. F. Wendt, *Organometallics* **2015**, *34*, 4262.

76) (a) S. Gründemann, M. Albrecht, J. A. Loch, J. W. Faller, R. H. Crabtree, *Organometallics* **2001**, *20*, 5485; (b) J. R. Miecznikowski, S. Gründemann, M. Albrecht, C. Mégret, E. Clot, J. W. Faller, O. Eisenstein, R. H. Crabtree, *Dalton Trans.* **2003**, 831.

77) (a) K. Krogh-Jespersen, M. Czerw, K. Zhu, B. Singh, M. Kanzelberger, N. Darji, P. D. Achord, K. B. Renkema, A. S. Goldman, *J. Am. Chem. Soc.* **2002**, *124*, 10797; (b) I. Göttker-Schnetmann, P. S. White, M. Brookhart, *Organometallics* **2004**, *23*, 1766.

78) For the solid state structure of an analogous Ir(PNP*)(CO) complex: ref. 18.

79) T. Cheisson, A. Auffrant, *Dalton Trans.* **2016**, *45*, 2069.

80) A. Lang, J. Knizek, H. Nöth, S. Schur, M. Thomann, *Z. Anorg. Allg. Chem.* **1997**, *623*, 901.

81) (a) A. Dedieu, A. Strich, *Inorg. Chem.* **1979**, *18*, 2940; (b) J.-Y. Saillard, R. Hoffmann, *J. Am. Chem. Soc.* **1984**, *106*, 2006.

82) (a) J. A. Melanson, C. M. Vogels, A. Decken, S. A. Westcott, *Inorg. Chem. Commun.*, **2010**, *13*, 1396; (b) G. M. Lee, C. M. Vogels, A. Decken, S. A. Westcott, *Eur. J. Inorg. Chem.* **2011**, 2433; (c) S. A. Westcott, T. B. Marder, R. T. Baker, J. C. Calabrese, *Can. J. Chem.* **1993**, *71*, 930; (d) S. A. Westcott, H. P. Blom, T. B. Marder, R. T. Baker, *J. Am. Chem. Soc.* **1992**, *114*, 8863; (e) S. A. Westcott, H. P. Blom, T. B. Marder, R. T. Baker, J. C. Calabrese, *Inorg. Chem.* **1993**, *32*, 2175; (f) S. Lachaize, K. Essalah, V. Montiel-Palma, L. Vendier, B. Chaudret, J.-C. Barthelat, S. Sabo-Etienne, *Organometallics* **2005**, *24*, 2935; (g) W. Clegg, M. R. J. Elsegood, A. J. Scott, T. B. Marder, C. Dai, N. C. Norman, N. L. Pickett, E. G. Robins, *Acta Crystallogr. Sect. C: Cryst. Struct. Commun.* **1999**, *55*, 733; (h) S. A. Westcott, N. J. Taylor, T. B. Marder, R. T. Baker, N. J. Jones, J. C. Calabrese, *J. Chem. Soc., Chem. Commun*. **1991**, 304; (i) J. Knizek, H. Nöth, *Eur. J. Inorg. Chem.* **2011**, 1888; (j) S. Harder, J. Spielmann, *J. Organomet. Chem.* **2012**, *698*, 7.

83) (a) C. M. Crudden, Y. B. Hleba, A. C. Chen, *J. Am. Chem. Soc.* **2004**, *126*, 9200; (b) C. E. Tucker, J. Davidson, P. Knochel, *J. Org. Chem.* **1992**, *57*, 3482; (c) C. M. Crudden, D. Edwards, *Eur. J. Org. Chem.* **2003**, 4695; (d) I. Beletskaya, A. Pelter, *Tetrahedron* **1997**, *53*, 4957.

84) (a) J. Dale, *J. Chem. Soc.* **1961**, 922; (b) C. Kleeberg, A. G. Crawford, A. S. Batsanov, P. Hodgkinson, D. C. Apperley, M. S. Cheung, Z.

Lin, T. B. Marder, *J. Org. Chem.* **2012**, *77*, 785; (c) W. G. Henderson, M. J. How, G. R. Kennedy, E. F. Mooney, *Carbohydr. Res.* **1973**, *28*, 1; (d) H. Wu, J. M. Garcia, F. Haeffner, S. Radomkit, A. R. Zhugralin, A. H. Hoveyda, *J. Am. Chem. Soc.* **2015**, *137*, 10585.

85) A. Anaby, B. Butschke, Y. Ben-David, L. J. W. Shimon, G. Leitus, M. Feller, D. Milstein, *Organometallics* **2014**, *33*, 3716.

86) M. I. Webb, N. R. Halcovitch, E. G. Bowes, G. M. Lee, M. J. Geier, C. M. Vogels, T. O'Neill, H. Li, A. Flewelling, A. Decken, C. A. Gray, S. A. Westcott, *J. Heterocycl. Chem.* **2014**, *51*, 157.

87) (a) H. Braunschweig, M. Colling, *Coord. Chem. Rev.* **2001**, *223*, 1; (b) J. Zhu, Z. Lin, T. B. Marder, *Inorg. Chem.* **2005**, *44*, 9384.

88) M. Albrecht, *Chem. Rev.* **2010**, *110*, 576.

89) M. Hernández-Juárez, J. López-Serrano, P. González-Herrero, N. Rendón, E. Álvarez, M. Paneque, A. Suárez, *Chem. Commun.* **2018**, *54*, 3843.

90) (a) D. M. Heinekey, N. G. Payne, G. K. Schulte *J. Am. Chem. Soc.* **1988**, *110*, 2303; (b) D. M. Heinekey, J. M. Millar, T. F. Koetzle, N. G. Payne, K. W. Zilm, *J. Am. Chem. Soc.* **1990**, *112,* 909; (c) D. M. Heinekey, A. S. Hinkle, J. D. Close, *J. Am. Chem. Soc.* **1996**, *118,* 5353; (d) W. J. Oldham, A. S. Hinkle, D. M. Heinekey, *J. Am. Chem. Soc.* **1997**, *119,* 11028.

91) (a) G. J. Kubas *Metal Dihydrogen and σ-Bond Complexes. Structure, Theroy and Reactivity*, Kluwer Academic/Plenum Publishers, **2001**, *Chap. 5*; (b) R. H. Crabtree, *Acc. Chem. Res.* **1990**, *23*, 95.

92) D. G. Hamilton, R. H. Crabtree, *J. Am. Chem. Soc.* **1988**, *110*, 4126.

93) (a) X. Yang, M. B. Hall, *J. Am. Chem. Soc.* **2010**, *132*, 120; (b) J. Li, Y. Shiota, K. Yoshizawa, *J. Am. Chem. Soc.* **2009**, *131*, 13584.

94) For selected examples of aldehyde hydrogenation catalyzed by Ir complexes: (a) I. Cano, L. M. Martínez-Prieto, L. Vendier, P. W. N. M. van Leeuwen, *Catal. Sci. Technol.* **2018**, *8*, 221; (b) X. Wu, C. Corcoran, S. Yang, J. Xiao, *ChemSusChem* **2008**, *1*, 71; (c) M. G. Manas, J. Graeupner, L. J. Allen, G. E. Dobereiner, K. C. Rippy, N. Hazari, R. H. Crabtree, *Organometallics* **2013**, *32*, 4501.

95) (a) P. Gallezot, D. Richard, *Catal. Rev.: Sci. Eng.* **1998**, *40*, 81; (b) P. Mäki-Arvela, J. Hájek, T. Salmi, D. Y. Murzin, *Appl. Catal. A* **2005**, *292*, 1.

96) (a) C. Gunanathan, D. Milstein, *Acc. Chem. Res.* **2011**, *44*, 588; (b) R. Khusnutdinova, D. Milstein, *Angew. Chem. Int. Ed.* **2015**, *54*, 12236.

97) (a) J.-F. Riehl, Y. Jean, O. Eisenstein, M. Pélissier, *Organometallics* **1992**, *11*, 729; (b) M. Gupta, C. Hagen, W. C. Kaska, R. E. Cramer, C. M. Jensen, *J. Am. Chem. Soc.* **1997**, *119*, 840; (c) K. Krogh-Jespersen, M. Czerw, M. Kanzelberger, A. S. Goldman, *J. Chem. Inf. Comput. Sci.* **2001**, *41*, 56; (d) S. Niu, M. B. Hall, *J. Am. Chem. Soc.* **1999**, *121*, 3992.

98) A. V. Polukeev, R. Marcos, M. S. G. Ahlquist, O. F. Wendt, *Chem. Eur. J.* **2016**, *22*, 4078.

99) (a) M. Vogt, M. Gargir, M. A. Iron, Y. Diskin-Posner, Y. Ben-David, D. Milstein, *Chem. Eur. J.* **2012**, *18*, 9194; (b) C. A. Huff, J. W. Kampf, M. S. Sanford, *Organometallics* **2012**, *31*, 4643; (c) M. Montag, J. Zhang, D. Milstein, *J. Am. Chem. Soc.* **2012**, *134*, 10325; (d) C. A. Huff, J. W. Kampf, M. S. Sanford, *Chem. Commun.* **2013**, *49*, 7147; (e) C. A. Huff, M. S. Sanford, *ACS Catal.* **2013**, *3*, 2412; (f) G. A. Filonenko, M. P. Conley, C. Copéret, M. Lutz, E. J. M. Hensen, E. A. Pidko, *ACS Catal.* **2013**, *3*, 2522; (g) M. Vogt, A. Nerush, M. A. Iron, G.

Leitus, Y. Diskin-Posner, L. J. W. Shimon, Y. Ben-David, D. Milstein, *J. Am. Chem. Soc.* **2013**, *135*, 17004; (h) M. Vogt, A. Nerush, Y. Diskin-Posner, Y. Ben-David, D. Milstein, *Chem. Sci.* **2014**, *5*, 2043; (i) G. A. Filonenko, E. Cosimi, L. Lefort, M. P. Conley, C. Copéret, M. Lutz, E. J. M. Hensen, E. A. Pidko, *ACS Catal.* **2014**, *4*, 2667.

100) A. Kumar, M. Feller, Y. Ben-David, Y. Diskin-Posner, D. Milstein, *Chem. Commun.* **2018**, *54*, 5365.

101) R. Noyori, M. Yamakawa, S. Hashiguchi, *J. Org. Chem.* **2001**, *66*, 7931.

102) (a) J. C. M. Ritter; R. G. Bergman, *J. Am. Chem. Soc.* **1997**, *119*, 2580. (b) J. C. M. Ritter; R. G. Bergman, *J. Am. Chem. Soc.* **1998**, *120*, 6826.

103) (a) O. Blum, D. Milstein, *J. Organomet. Chem.* **2000**, *593−594*, 479; (b) C. M. Fafard, O. V. Ozerov, *Inorg. Chim. Acta* **2007**, *360*, 286; (c) N. A. Smythe, K. A. Grice, B. S. Williams, K. I. Goldberg, *Organometallics* **2009**, *28*, 277. (d) G. R. Fulmer, A. N. Herndon, W. Kaminsky, R. A. Kemp, K. I. Goldberg, *J. Am. Chem. Soc.* **2011**, *133*, 17713.

104) D. F. Shriver, M. A. Dredzon, *The Manipulation of Air-Sensitive Compounds*, 2nd Edition; Wiley-Interscience, **1986**.

105) D. D. Perrin, W. L. F. Armarego, *Purification of Laboratory Chemicals*, 2nd Edition; Pergamon Press, **1980**.

106) M. Rueping, R. M. Koenigs, R. Borrmann, J. Zoller, T. E. Weirich, J. Mayer, *Chem. Mater.* **2011**, *23*, 2008.

107) N. A. Yakelis, R. G. Bergman, *Organometallics* **2005,** *24,* 3579.

108) M. C. Perry, X. Cui, M. T. Powell, D.-R. Hou, J. H. Reibenspies, K. Burgess, *J. Am. Chem. Soc.* **2003**, *125*, 113.

Chapter II

Synthesis of Ru-CNN(H) complexes. Catalytic applications in hydrogenation and dehydrogenation of *N*-heterocycles

II.1. Introduction

Hydrogenation and acceptorless dehydrogenation are low environmental impact processes for the reduction of aromatic *N*-heterocycles to their corresponding saturated derivatives, and the oxidation of the latter products to the parent *N*-heteroarenes. These transformations are not only of synthetic interest but may also serve for the development of H_2-storage systems based on *N*-heteroarenes as organic hydrogen carriers.

In Chapter II, a series of Ru complexes stabilized with lutidine-derived pincer ligands incorporating a secondary amino group has been synthetized. As a consequence of the presence of two acidic functionalities, i.e. the lutidine methylenes and the NH moieties, it could be expected that these complexes might exhibit two modes of metal-ligand cooperation: pyridine aromatization/dearomatization and amine/amido interconversion. Additionally, the catalytic activity of these complexes for the reversible (de)hydrogenation of *N*-heterocycles has been examined, and preliminary mechanistic studies have been performed.

II.1.1. Catalytic applications of metal complexes based on multimodal proton-responsive ligands

Among the considerable diversity of ligands containing Brønsted acid/base functionalities, those incorporating amine[1] and lutidine donors[2] have provided highly active and selective catalysts for a broad variety of hydrogenation and dehydrogenation reactions. Since both metal-ligand cooperation (MLC) strategies, amine/amido interconversion and pyridine aromatization/dearomatization, have been proven successful, a further approach for the development of efficient catalysts might consist of the use of ligands containing two different proton-responsive modes. The underlying idea of this strategy is to allow the catalyst to choose the lowest energetically accessible MLC mode for each step of the catalytic cycle. While this approach has led in some cases to more efficient catalysts, mechanistic information regarding the action modes of these catalytic systems still remains scarce.

II.1.1.a. Ruthenium complexes

The Milstein group has synthetized ruthenium complexes incorporating lutidine-based tridentate PNN(H) ligands containing secondary amines as side donors (Figure 1).[3] These derivatives are active ester

[1] (a) B. Zhao, Z. Han, K. Ding, *Angew. Chem. Int. Ed.* **2013**, *52*, 4744; (b) T. Ikariya, *Bull. Chem. Soc. Jpn.* **2011**, *84*, 1.
[2] (a) J. L. van der Vlugt, J. N. H. Reek, *Angew. Chem. Int. Ed.* **2009**, *48*, 8832; (b) C. Gunanathan, D. Milstein, *Acc. Chem. Res.* **2011**, *44*, 588; (c) D. Milstein, *Phil. Trans. R. Soc. A* **2015**, *373*, 20140189.
[3] E. Fogler, J. A. Garg, P. Hu, G. Leitus, L. J. W. Shimon, D. Milstein, *Chem. Eur. J.* **2014**, *20*, 15727.

hydrogenation catalysts under very mild conditions (room temperature, 5 bar of H_2), and catalyze the dehydrogenative coupling of alcohols to esters at low temperatures (35 °C). Interestingly, reaction of a Ru-PNN(H) complex with 2.5 equiv of KH produced the formation of an enamino anionic Ru(II) species (Scheme 1). DFT calculations supported that the latter species is able to catalyze the dehydrogenative coupling of alcohols only involving the amine/amido metal-ligand cooperation mode.[4] The origin of this preference for amine/amido interconversion has been attributed to the conjugation effect of the amido group that stabilizes the dearomatized complex and diminishes the driving force of the aromatization/dearomatization mode.

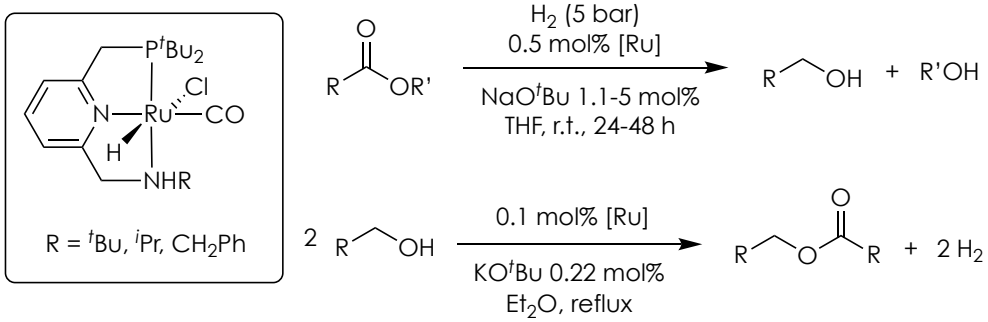

Figure 1. Hydrogenation of esters and dehydrogenation of alcohols catalyzed by Ru-PNN(H) complexes.

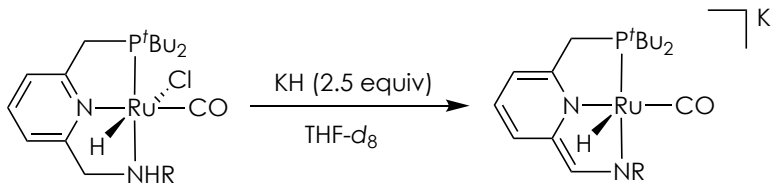

Scheme 1. Reactivity of a Ru-PNN(H) complex towards base.

[4] C. Hou, J. Jiang, Y. Li, C. Zhao, Z. Ke, *ACS Catal.* **2017**, *7*, 786.

Aiming to develop H_2-storage systems, Milstein and co-workers have investigated the reversible dehydrogenation of 2-aminoethanol (AE) to a cyclic dipeptide (glycine anhydride, GA) and linear polypeptides using ruthenium catalysts containing lutidine-derived PNN ligands, in which the N-arm is either a hemilabile diethylamino group or a proton-responsive NH functionality (Figure 2).[5] Mixtures of glycine anhydride and linear polypeptides were hydrogenated to 2-aminoethanol and 2-amino-*N*-(2-hydroxyethyl)acetamide (AA) with similar catalytic activities by both complexes in the presence of base. On the contrary, slightly higher conversions were achieved in the dehydrogenation reaction upon using the Ru-PNN(H) precursor. More importantly, repetitive cycles of H_2 release/recharge were conducted using the Ru-PNN(H) complex without adding new catalyst loadings.

[5] P. Hu, E. Fogler, Y. Diskin-Posner, M. A. Iron, D. Milstein, *Nat. Commun.* **2015**, *6*, 6859.

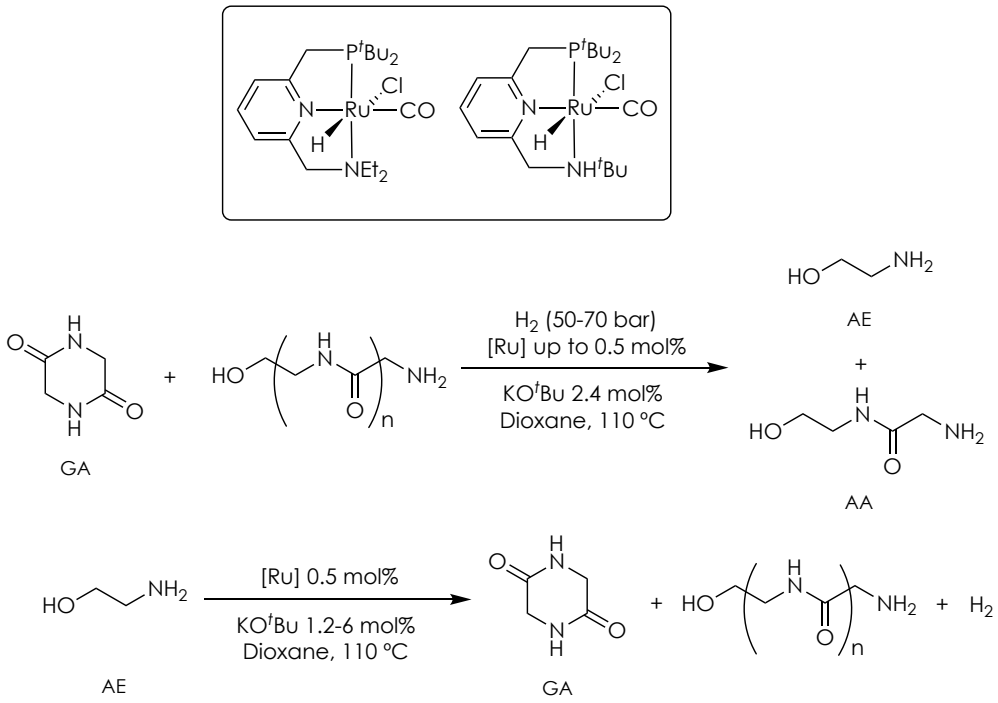

Figure 2. Hydrogenation of GA and dehydrogenation of AE with Ru-PNN complexes.

Furthermore, the same group has examined the hydrogenation of a variety of cyclic imides to diols and amines using ruthenium catalysts bearing lutidine-containing ligands (Figure 3).[6] The higher catalytic activities observed with a Ru-PNN(H) complex in comparison to catalysts based on other PNN ligands have been ascribed to the ability of the former derivative to exhibit both N(H)-M/N=M and lutidine aromatization/dearomatization MLC modes. Moreover, the high selectivity achieved for succinimide hydrogenation led to testing a hydrogen storage system based on the reversible hydrogenation of a bis-cyclic imide formed by the dehydrogenative coupling of 1,4-butanediol and ethylenediamine.

[6] A. Kumar, T. Janes , N. A. Espinosa-Jalapa, D. Milstein, *J. Am. Chem. Soc.* **2018**, *140*, 7453.

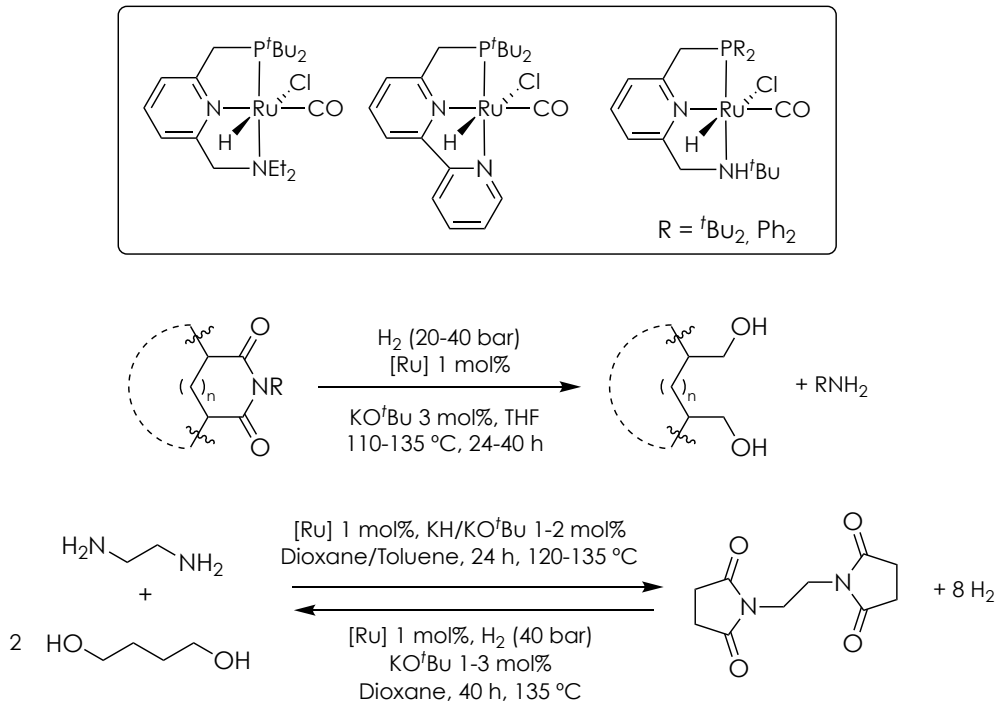

Figure 3. Hydrogenation of cyclic imides and dehydrogenation of diols in the presence of amines.

A ruthenium complex based on a tetradentate PN(H)NP ligand containing amine and lutidine fragments has been investigated by Zhang and coworkers (Figure 4).[7] This Ru-PN(H)NP complex in the presence of an alkoxide base was found particularly effective for the hydrogenation of esters at very low metal loadings (S/C = 10^4–10^5). For example, the hydrogenation of ethyl acetate was achieved under 50 bar of H_2 at 80 °C under solventless conditions with a TON of 80,000 and a TOF of 2,600 h^{-1}. This catalytic system has also exhibited a high activity in the hydrogenation of amides

[7] (a) X. Tan, Y. Wang, Y. Liu, F. Wang, L. Shi, K-H. Lee, Z. Lin, H. Lv, X. Zhang, *Org. Lett.* **2015**, *17*, 454; (b) F. Wang, X. Tan, H. Lv, X. Zhang, *Chem. Asian J.* **2016**, *11*, 2103.

under 50 bar of H_2 at 100 °C in the presence of KO^{t}Bu as base (Figure 4).[8] The reduction of challenging secondary and tertiary amides was achieved with wide functional group tolerance and TONs of up to 19,600.

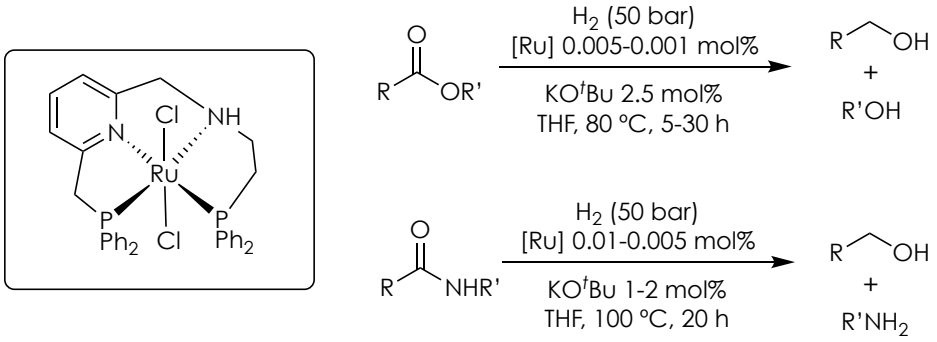

Figure 4. Hydrogenation of esters and amides using Ru-PN(H)NP complex.

Gao and coworkers have examined a series of Ru complexes with lutidine-derived pincer ligands incorporating NHC flanking groups in the hydrogenation of ethylene carbonate (Figure 5).[9] A Ru-CNN(H) complex provided very similar catalytic activities to that of structurally related Ru-CNC derivatives.

[8] L. Shi, X. Tan, J. Long, X. Xiong, S. Yang, P. Xue, H. Lv, X. Zhang, *Chem. Eur. J.* **2017**, *23*, 546.
[9] X. Wu, L. Ji, Y. Ji, E. H. M. Elageed, G. Gao, *Catal. Commun.* **2016**, *85*, 57.

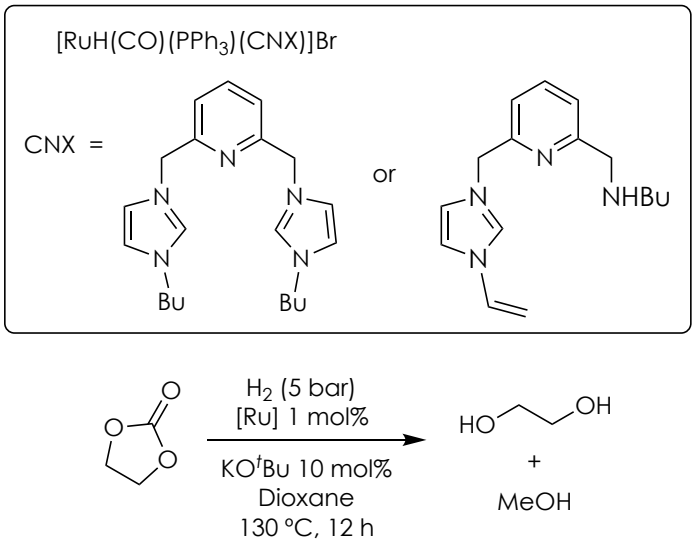

Figure 5. Hydrogenation of ethylene carbonate using Ru-CNC and Ru-CNN(H) complexes.

Finally, van der Vlugt *et al.* studied the application of a ruthenium complex based on an unsymmetrical PNN pincer ligand having both pyridine aromatization/dearomatization and 2-hydroxypyridine/pyridone MLC modes (Figure 6).[10] Selective deprotonation of the 2-hydroxypyridine functionality was observed upon reaction of this derivative with DBU or stronger bases (KO*t*Bu and KHMDS). The latter derivative was catalytically active in the base-free dehydrogenation of formic acid, as well as for the dehydrogenative coupling of alcohols, giving high conversions to different esters and outperforming the catalytic activity provided by Ru catalysts based on structurally related PNN ligands lacking the 2-hydroxypyridine fragment. DFT calculations suggest that the improved efficiency of this catalyst can be

[10] S. Y. de Boer, T. J. Korstanje, S. R. La Rooij, R. Kox, J. N. H. Reek, J. I. van der Vlugt, *Organometallics* **2017**, *36*, 1541.

ascribed to a more favorable H_2 release step that takes place through the reversible reactivity of the hydroxypyridine functionality.

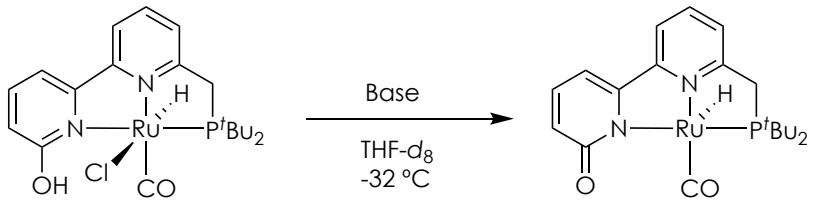

Figure 6. Deprotonation of the Ru-PNN complex reported by van der Vlugt and coworkers.

II.1.1.b. First-row metal complexes

Besides ruthenium complexes based on PNN(H) ligands, Milstein and co-workers studied the application of first-row metal derivatives, particularly of cobalt and manganese, incorporating these ligands in catalytic hydrogenation and dehydrogenation processes. While cobalt complexes based on lutidine-derived PNP and PNN ligands promoted the reduction of esters with H_2 in the presence of sub-stoichiometric amounts of $NaHBEt_3$ and KO^{t}Bu, a significant increase in the catalytic activity was found upon using a catalyst incorporating a secondary amino group (Figure 7).[11] Interestingly, activated esters such as trifluoroacetates and aryl esters could not be reduced with this catalytic system since only hydrogenation of enolizable derivatives was accomplished. Hence, based on the observed reactivity, a mechanism involving an ester enolate intermediate was proposed.

[11] D. Srimani, A. Mukherjee, A. F. G. Goldberg, G. Leitus, Y. Diskin-Posner, L. J. W. Shimon, Y. Ben-David, D. Milstein, *Angew. Chem. Int. Ed.* **2015**, *54*, 12357.

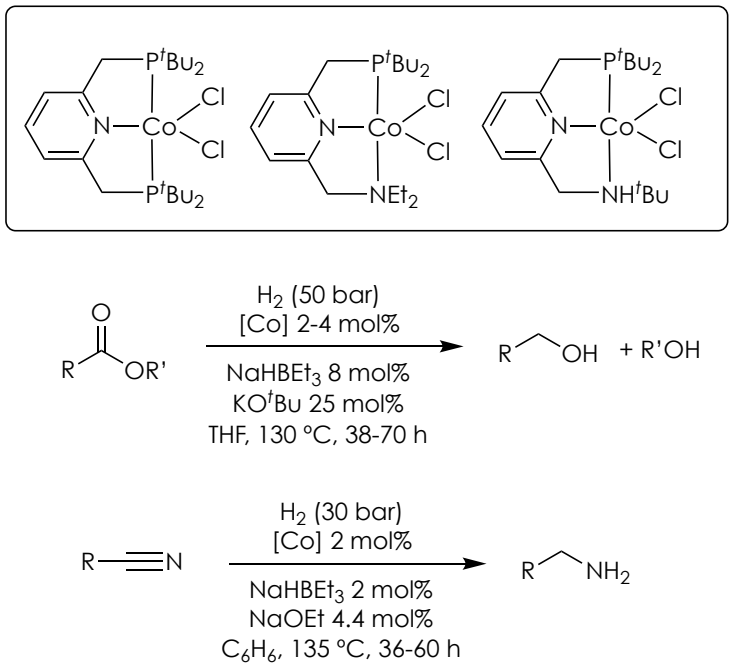

Figure 7. Hydrogenation of esters and nitriles using a Co-PNN(H) complex.

Similarly, the Co-PNN(H) derivatives also catalyzes the hydrogenation of (hetero)aromatic, benzylic, and aliphatic nitriles to the corresponding primary amines (Figure 7).[12] As before, this catalyst was found superior to related cobalt complexes based on lutidine-derived PNP and PNN ligands both in terms of conversion and selectivity towards the formation of the amine products.

Furthermore, the same Co-PNN(H) complex was employed as catalyst for the dehydrogenative couplings of diols and amines to give *N*-substituted pyrroles,[13] and of 1,2-diaminobenzenes and alcohols to yield benzimidazoles

[12] A. Mukherjee, D. Srimani, S. Chakraborty, Y. Ben-David, D. Milstein, *J. Am. Chem. Soc.* **2015**, *137*, 8888.
[13] P. Daw, S. Chakraborty, J. A. Garg, Y. Ben-David, D. Milstein, *Angew. Chem. Int. Ed.* **2016**, *55*, 14373.

(Figure 8).[14] In these processes, this complex was found superior to the related cobalt complexes incorporating PNP and PNN ligands.

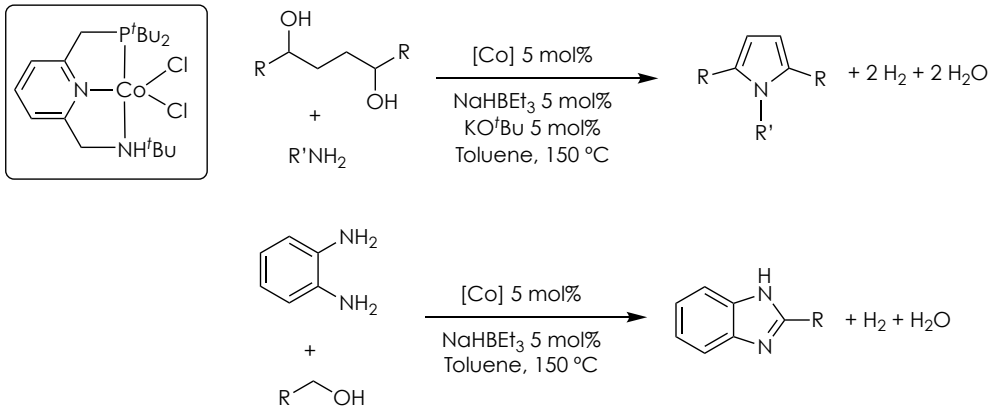

Figure 8. Synthesis of pyrroles and benzimidazoles using a Co-PNN(H) complex.

Manganese complexes based on lutidine-derived PNN(H) pincers are also active catalysts in hydrogenation reactions. A Mn-PNN(H) derivative catalyzed the reduction of a series of esters at 100 °C under 20 bar of H_2 in the presence of KH providing, in most cases, quantitative conversions to the corresponding alcohols (Figure 9).[15] Similarly, this complex is also able to efficiently promote the hydrogenation of organic carbonates.[16] Interestingly, deprotonation of the Mn-PNN(H) complex with base yielded a manganese amido complex, which reversibly activates H_2 by a ligand-assisted process and catalyzes the hydrogenation of esters under base free conditions. Therefore, although the ligand incorporates two proton-responsive functionalities, preliminary mechanistic studies only support a MLC mode based on amine deprotonation.

---

[14] P. Daw, Y. Ben-David, D. Milstein, *ACS Catal.* **2017**, *7*, 7456.
[15] N. A. Espinosa-Jalapa, A. Nerush, L. J. W. Shimon, G. Leitus, L. Avram, Y. Ben-David, D. Milstein, *Chem. Eur. J.* **2017**, *23*, 5934.
[16] A. Kumar, T. Janes, N. A. Espinosa-Jalapa, D. Milstein, *Angew. Chem. Int. Ed.* **2018**, *57*, 12076.

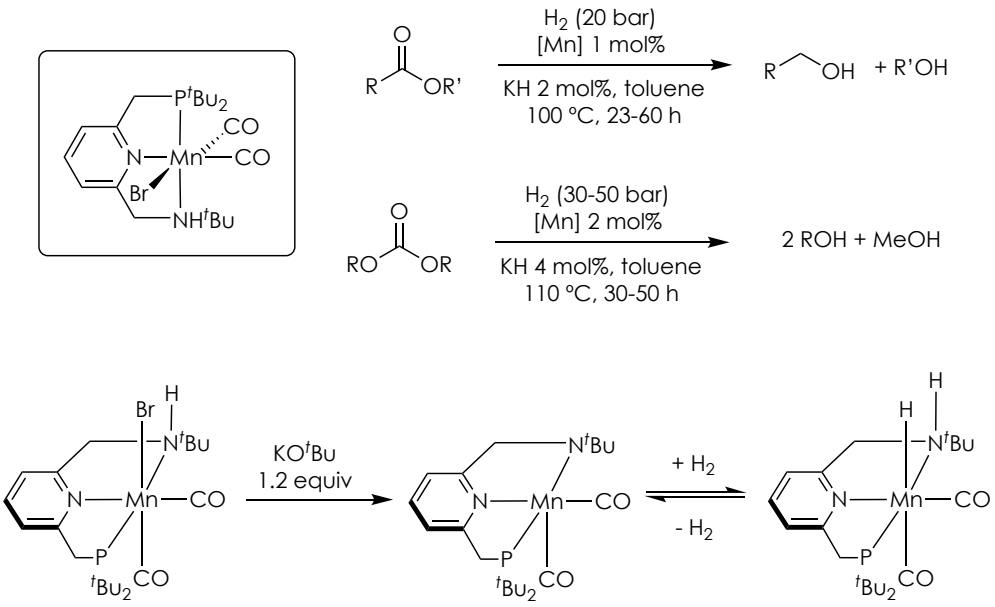

Figure 9. Mn-PNN(H) catalyst for the hydrogenation of esters and carbonates.

Furthermore, Mn-PNN(H) complexes have been employed for the synthesis of amides by dehydrogenative coupling of alcohols with amines,[17] and of cyclic imides by the reaction of diols and amines with H_2 release (Figure 10).[18] A deprotonated Mn-PNN complex incorporating a diethylamino group was found ineffective for both types of processes, further hinting at the importance of the presence of the N-H moiety in the ligand.

[17] A. Kumar, N. A. Espinosa-Jalapa, G. Leitus, Y. Diskin-Posner, L. Avram, D. Milstein, *Angew. Chem. Int. Ed.* **2017**, *56*, 14992.
[18] N. A. Espinosa-Jalapa, A. Kumar, G. Leitus, Y. Diskin-Posner, D. Milstein, *J. Am. Chem. Soc.* **2017**, *139*, 11722.

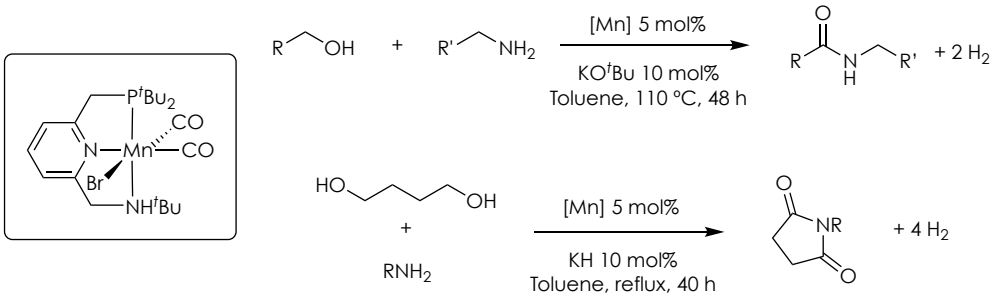

Figure 10. Dehydrogenative synthesis of amides and cyclic imides using a Mn-PNN(H) complex.

II.1.2. Acceptorless dehydrogenation of *N*-heterocycles

Saturated and unsaturated *N*-heterocycles are important building blocks for the synthesis of dyes, biologically active molecules, and ligands with applications in homogeneous catalysis.[19] At this respect, hydrogenation of *N*-heteroarenes is of paramount importance in industry,[20] where heterogeneous catalysts are usually preferred. However, significant efforts have been made for the development of efficient catalysts based on transition metal complexes,[21] mainly due to the higher selectivity, milder reaction conditions and easiness of mechanistic understanding usually associated to the homogeneous catalysts.

Likewise, oxidation of saturated *N*-heterocycles to their unsaturated counterparts is also of synthetic interest. From the perspective of Green Chemistry, the most efficient process for this transformation is the direct dehydrogenation of the substrate in the absence of a hydrogen acceptor. Since in these reactions free H_2 is released, these transformations are not only synthetically appealing but can also be potentially applied for the development of hydrogen storage systems based on the realization of cycles of hydrogenation and dehydrogenation of *N*-heterocycles.[22]

---

[19] L. D. Quin, J. Tyrell, *Fundamentals of Heterocyclic Chemistry: Importance in Nature and in the Synthesis of Pharmaceuticals*, Wiley, **2010**.

[20] (a) B. Chen, U. Dingerdissen, J. G. E. Krauter, H. G. J. Lansink-Rotgerink, K. Möbus, D. J. Ostgard, P. Panster, T. H. Riermeier, S. Seebald, T. Tacke, H. Trauthwein, *Appl. Catal. A: General* **2005**, *280*, 17; (b) H.-U. Blaser, C. Malan, B. Pugin, F. Spindler, H. Steiner, M. Studer, *Adv. Synth. Catal.* **2003**, *345*, 103.

[21] (a) Z. X. Giustra, J. S. Ishibashi, S. Y. Liu, *Coord. Chem. Rev.* **2016**, *314*, 134; (b) C. Bianchini, A. Meli, F. Vizza, *"Hydrogenation of Arenes and Heteroaromatics"* in *The Handbook of Homogeneous Hydrogenation* (J. G. de Vries, C. J. Elsevier, Eds.), *Vol. 1*, Chap. 16. Wiley-VCH, **2007**.

[22] (a) D. L. J. Broere, *Phys. Sci. Rev.* **2018**, *3*, 9; (b) R. H. Crabtree, *ACS Sustainable Chem. Eng.* **2017**, *5*, 4491; (c) P. Preuster, C. Papp, P. Wasserscheid, *Acc. Chem. Res.* **2017**, *50*, 74.

Dehydrogenation of cyclic hydrocarbons is highly endothermic; however, isolobal replacement of a CH_2 unit by NH have been shown to significantly reduce the endothermicity of H_2 release because of the weakening effect caused to a C—H bond by an adjacent nitrogen and the presence of a slightly weaker N—H bond in comparison to a C—H bond (Figure 11).[23] Consequently, in the presence of a catalyst, it can be expected that acceptorless dehydrogenation of *N*-heterocycles can be carried out under relatively mild heating.

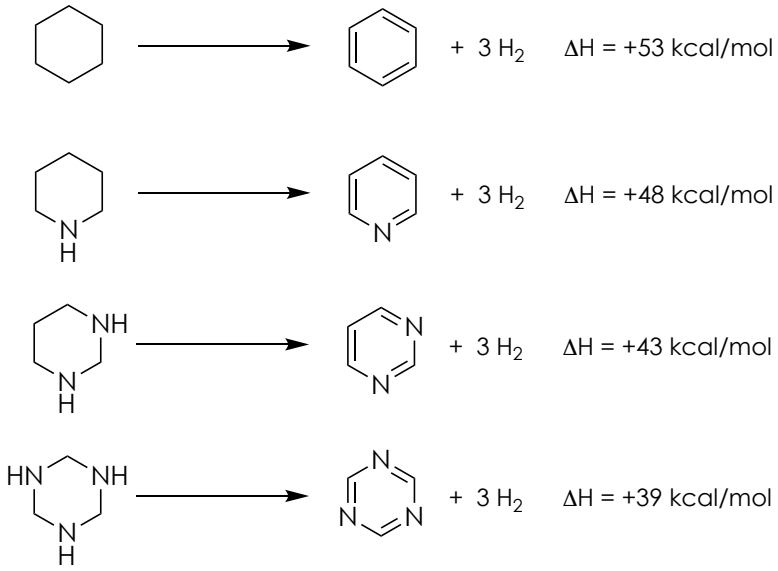

Figure 11. Effect of the replacement of CH_2 units by NH in the endothermicity of H_2 release (adapted from ref. 22a).

Although the principle of microscopic reversibility dictates that species able to catalyze the hydrogenation of a substrate should also be active for the reverse dehydrogenation process, the number of catalytic systems that

[23] (a) A. Moores, M. Poyatos, Y. Luo, R. H. Crabtree, *New J. Chem.* **2006**, *30*, 1675; (b) E. Clot, O. Eisenstein, R. H. Crabtree, *Chem. Commun.* **2007**, *22*, 2231; (c) R. H. Crabtree, *Energy Environ. Sci.* **2008**, *1*, 134.

promote both hydrogenation of *N*-heterocycles and acceptorless dehydrogenation of their reduced counterparts is scarce. A likely explanation to this resides in the still high endothermicity of the dehydrogenation process that requires robust catalysts that could operate under relatively harsh conditions. In fact, although the dehydrogenation of *N*-heterocycles has been reported using different homogeneous[24,25] as well as heterogeneous catalysts,[26] only very few catalytic systems are able to catalyze both processes.

Aiming to place the results of Section II.2. in context, ruthenium catalysts for the dehydrogenation of *N*-heterocycles, and systems based on transition metals for the reversible (de)hydrogenation of *N*-heteroarenes will be next reviewed.

II.1.2.a. Dehydrogenation of N-heterocycles with ruthenium catalysts

While ruthenium complexes have been examined in the dehydrogenation of nitrogen-containing heterocycles, their efficiency in the hydrogenation of the resulting unsaturated derivatives have usually not been explored. For example, some "classical" Ru hydrogenation catalysts, such as

[24] (a) M. A. Esteruelas, V. Lezaun, A. Martínez, M. Oliván, E. Oñate, *Organometallics* **2017**, *36*, 2996; (b) M. L. Buil, M. A. Esteruelas, M. P. Gay, M. Gómez-Gallego, A. I. Nicasio, E. Oñate, A. Santiago, M. A. Sierra, *Organometallics* **2018**, *37*, 603.
[25] (a) D. F. Brayton, C. M. Jensen, *Chem. Commun.* **2014**, *50*, 5987; (b) Z. Wang, I. Tonks, J. Belli, C. M. Jensen, *J. Organomet. Chem.* **2009**, *694*, 2854.
[26] For selected examples of heterogeneous catalysts for the reversible dehydrogenation of *N*-heterocycles: (a) C. Deraedt, R. Ye, W. T. Ralston, F. D. Toste, G. A. Somorjai, *J. Am. Chem. Soc.* **2017**, *139*, 18084; (b) S. K. Moromi, S. M. A. H. Siddiki, K. Kon, T. Toyao, K. Shimizu, *Catal. Today* **2017**, *281*, 507; (c) Y. Han, Z. Wang, R. Xu, W. Zhang, W. Chen, L. Zheng, J. Zhang, J. Luo, K. Wu, Y. Zhu, C. Chen, Q. Peng, Q. Liu, P. Hu, D. Wang, Y. Li, *Angew. Chem. Int. Ed.* **2018**, *57*, 11262; (d) J.-W. Zhang, D.-D. Li, G.-P. Lu, T. Deng, C. Cai, *ChemCatChem* **2018**, *10*, 4966.

$RuCl_2(PPh_3)_3$,[27] $RuH_2(CO)(PPh_3)_3$,[27c-d,28] $RuH_2(PPh_3)_4$,[27c-d,29] and the Shvo´s complex[30] have been found to promote the acceptorless dehydrogenation of 1,2,3,4-tetrahydroisoquinoline, 1,2,3,4-tetrahydroquinoline and indoline (Figure 12).[31,32] However, the catalytic performance of these catalysts in the hydrogenation of the corresponding *N*-heteroarenes has not been reported.

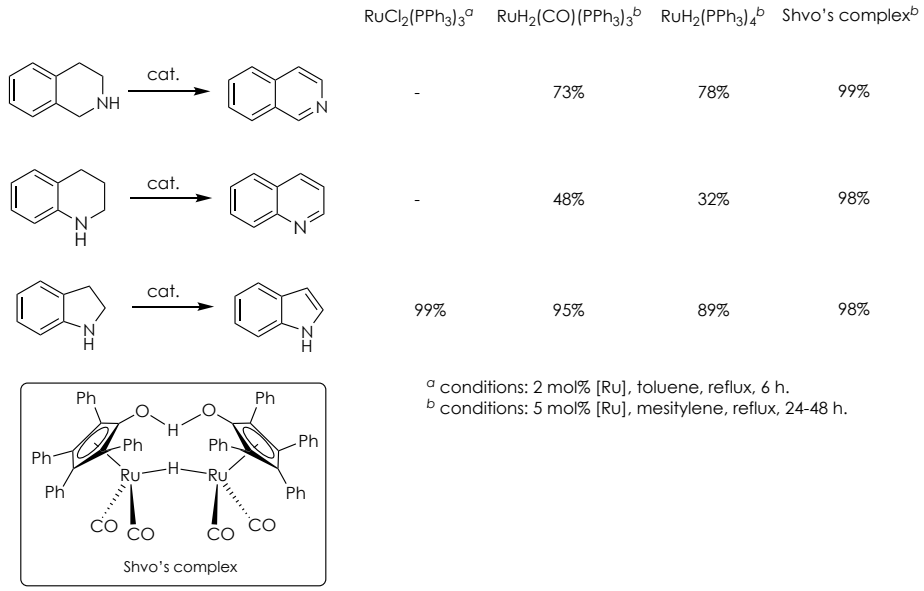

Figure 12. Dehydrogenation of *N*-heterocycles using Ru classical complexes.

---

[27] (a) Y. Takagi, S. Teratani, S. Takahashi, K. Tanaka, *J. Mol. Catal*. **1977**, *2*, 321; (b) S. R. Patil, R. V. Chaudhari, D. N. Sen, *J. Mol. Catal*. **1984**, *23*, 51; (c) R. A. Sánchez-Delgado, O. L. de Ochoa, *J. Organomet. Chem.* **1980**, *202*, 427; (d) R. A. Sánchez-Delgado, A. Andriollo, O. L. de Ochoa, T. Suárez, N. Valencia, *J. Organomet. Chem.* **1981**, *209*, 77; (e) J. F. Knifton, *Tetrahedron Lett.* **1975**, *26*, 2163; (f) J. F. Knifton, *J. Org. Chem.* **1975**, *40*, 519; (g) Y. Sasson, J. Blum, *J. Org. Chem.* **1975**, *40*, 1887; (h) J. Tsuji, H. Suzuki, *Chem. Lett.* **1977**, *6*, 1085.

[28] Z. Broucková, M. Czaková, M. Capka, *J. Mol. Catal.* **1985**, *30*, 241.

[29] (a) A. Toti, P. Frediani, A. Salvini, L. Rosi, C. Giolli, *J. Organomet. Chem.* **2005**, *690*, 3641; (b) A. Toti, P. Frediani, A. Salvini, L. Rosi, C. Giolli, C. Giannelli, *C. R. Chimie* **2004**, *7*, 769; (c) P. Frediani, V. Pistolesi, M. Frediani, L. Rosi, *Inorg. Chim. Acta* **2006**, *359*, 917; (d) S. Komiya, A. Yamamoto, *J. Organomet. Chem.* **1979**, *5*, 279.

[30] B. L. Conley, M. K. Pennington-Boggio, E. Boz, T. J. Williams, *Chem. Rev.* **2010,** *110,* 2294.

[31] Y. Tsuji, S. Kotachi,K. T. Huh, Y. Watanabe, *J. Org. Chem.* **1990**, *55*, 580.

[32] S. Muthaiah, S. H. Hong, *Adv. Synth. Catal.* **2012**, *354*, 3045.

The Blacquiere group compared the catalytic performance of $[Ru(Cp)(P_2N_2)(MeCN)]PF_6$ (Cp = cyclopentadienyl), containing a proton-responsive P_2N_2 ligand, and $[Ru(Cp)(dppp)(MeCN)]PF_6$ (dppp = $Ph_2PCH_2CH_2CH_2PPh_2$) in the dehydrogenation of five- and six-membered heterocycles (Figure 13).[33] Under the optimized catalytic conditions (3 mol% Ru, anisole at 110 °C), both catalysts dehydrogenated indoline with similar rates, although the Ru complex incorporating the proton-responsive P_2N_2 ligand significantly outperformed $[Ru(Cp)(dppp)(MeCN)]PF_6$ in the reaction of 2-methylindoline. On the contrary, both catalysts showed poor performances (<27% conv.) in the dehydrogenation of 1,2,3,4-tetrahydroquinoline.

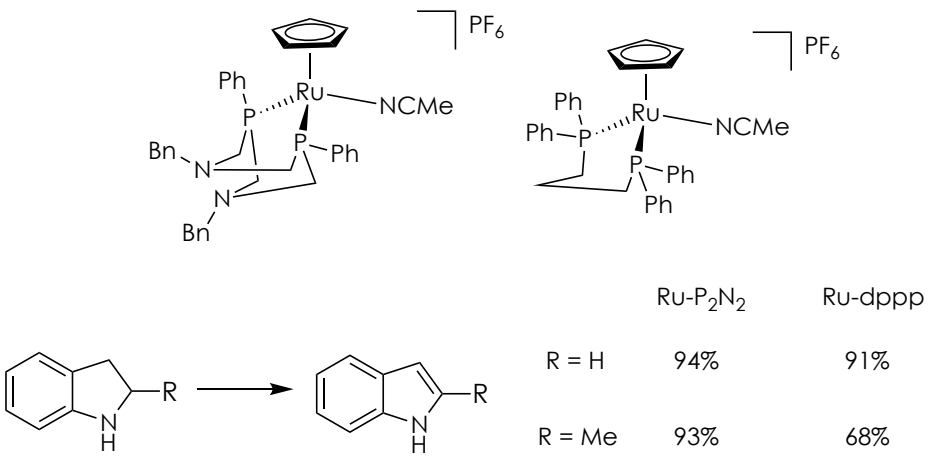

Figure 13. Dehydrogenation of *N*-heterocycles using $[Ru(Cp)(P_2N_2)(MeCN)]PF_6$ and $[Ru(Cp)(dppp)(MeCN)]PF_6$ complexes.

[33] J. M. Stubbs, R. J. Hazlehurst, P. D. Boyle, J. M. Blacquiere, *Organometallics* **2017**, *36*, 1692.

Recently, Yu and coworkers tested ruthenium complexes based on pyrazolyl-(2-indol-1-yl)-pyridine ligands for the oxidation of substituted tetrahydroquinolines, tetrahydroisoquinolines, terahydroquinoxalines and indolines (Figure 14).[34] These complexes provided high conversions in the dehydrogenation of a series of derivatives using 2.0 mol% catalyst loadings at 140 °C (*o*-xylene). Furthermore, this catalytic system was employed for the synthesis of *β*-carbolines that are derivatives of pharmaceutical interest.

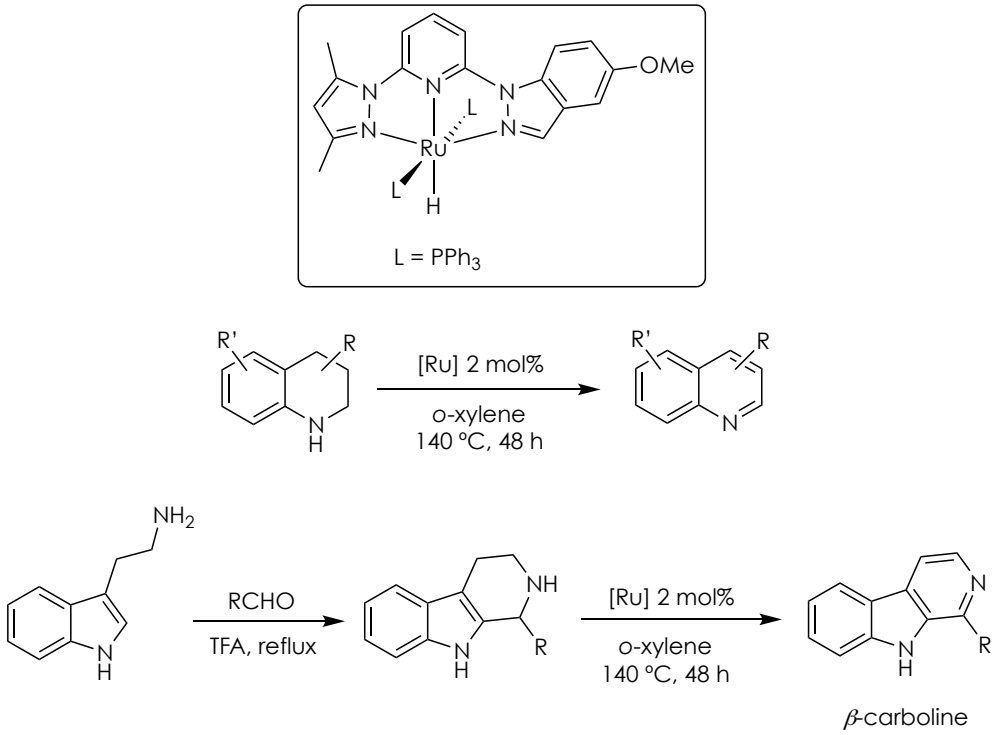

Figure 14. Dehydrogenation of *N*-heterocycles, and synthesis of *β*-carbolines, using the Ru complex reported by Yu and coworkers.

[34] Q. Wang, H. Chai, Z. Yu, *Organometallics* **2018**, *37*, 584.

Acceptorless dehydrogenation of indoline has also been investigated by the groups of Szymczak[35] and Mata[36] using Ru-NNN and arene Ru complexes incorporating NHC ligands, respectively (Figure 15). These catalysts quantitatively catalyzed the formation of indole under relatively mild conditions (100 °C, toluene) using catalyst loadings between 1-2 mol%.

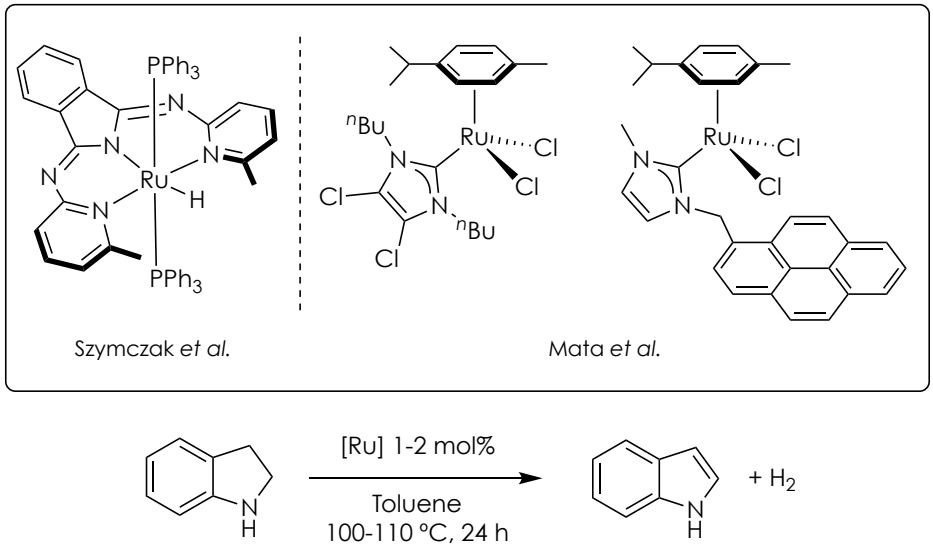

Figure 15. Dehydrogenation of indoline using the Ru complexes reported by the groups of Mata and Szymczak.

Finally, our group has reported the dehydrogenation of dihydrophenantridine using Ru complexes with facially coordinated CNC ligands as catalytic precursors. Upon using 1.0 mol% of a Ru-CNC complex in the presence of KO^{t}Bu (10 mol%), dihydrophenantridine was oxidized to phenanthridine in 24 h with 94% conversion (Figure 16).[37] Besides, the same catalytic system was capable of hydrogenating phenantridine under 10 bar of

[35] K.-N. T. Tseng, A. M. Rizzi, N. K. Szymczak, *J. Am. Chem. Soc.* **2013**, *135*, 16352.
[36] D. Ventura-Espinosa, A. Marzá-Beltrán, J. A. Mata, *Chem. Eur. J.* **2016**, *22*, 17758.
[37] M. Hernández-Juárez, J. López-Serrano, P. Lara, J. P. Morales-Cerón, M. Vaquero, E. Álvarez, V. Salazar, A. Suárez, *Chem. Eur. J.* **2015**, *21*, 7540.

H_2 at 80 °C. Although the catalyst hydrogenated other *N*-heterocycles under similar reaction conditions, including quinoline, quinoxaline, acridine, 4,7-phenanthroline and benzo[h]quinoline, it showed a negligible catalytic activity in the dehydrogenation of their saturated *N*-heterocyclic counterparts.[38]

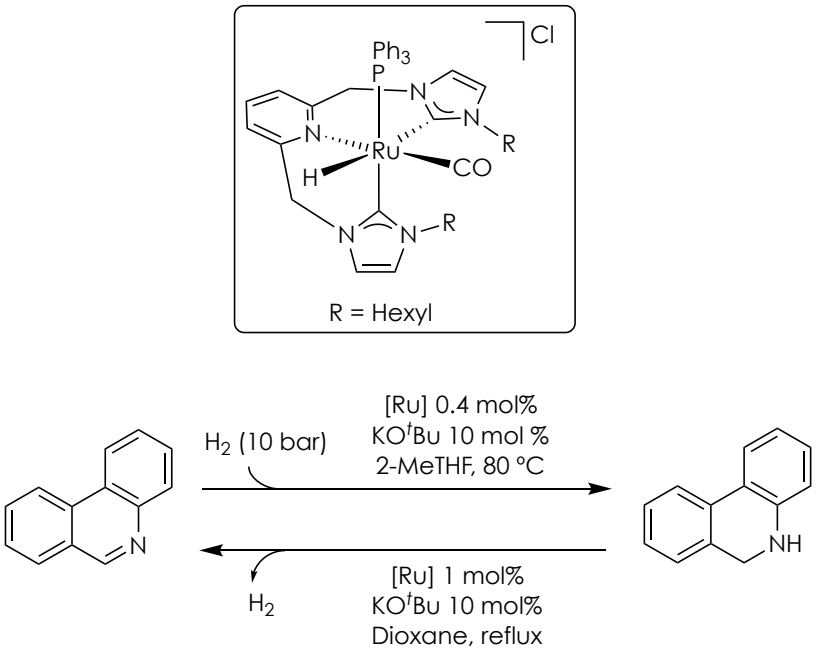

Figure 16. Reversible dehydrogenation of dihydrophenantridine using a Ru-CNC complex.

[38] J. Morales-Cerón, V. Salazar, A. Suárez. *Unpublished results.*

II.1.2.b. Reversible dehydrogenation of N-heterocycles catalyzed by transition metal complexes

In a seminal report, Fujita, Yamaguchi *et al.* reported the use of iridium complexes with pentamethylcyclopentadienyl (Cp*) and 2-pyridonate ligands for the dehydrogenation of 1,2,3,4-tetrahydroquinolines (Figure 17).[39] Hydrogen release from these substrates took place using 2 mol% catalyst in refluxing *p*-xylene. Furthermore, the same catalytic systems promoted the hydrogenation of quinolines under 1 bar of H_2 at 110 ^{o}C. Based on these results, the repetitive hydrogenation-dehydrogenation of 2-methylquinoline (H_2 gravimetric capacity: 2.7 wt%) was assayed with 5 mol% of catalyst. Up to five hydrogen storage/release cycles were performed with only a low erosion in the catalytic activity (100 to 98% conv.).

Interestingly, although experimental studies and DFT calculations have supported a ligand-assisted dehydrogenation process, the $[Cp^*Ir(Cl)(\mu\text{-}H)]_2$ complex, resulting from the protonation of the pyridonate ligand to 2-hydroxypyridine and subsequent decoordination, has been shown to be the active intermediate in the reduction reaction.[40]

[39] R. Yamaguchi, C. Ikeda, T. Takahashi, K. Fujita, *J. Am. Chem. Soc.* **2009**, *131*, 8410.
[40] (a) X. B. Zhang, Z. Xi, *Phys. Chem. Chem. Phys.* **2011**, *13*, 3997; (b) H. Li, J. Jiang, G. Lu, F. Huang, Z.-X. Wang, *Organometallics* **2011**, *30*, 3131.

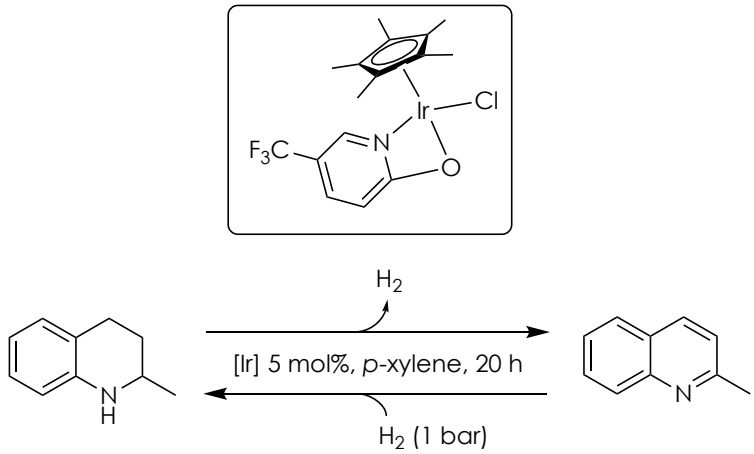

Figure 17. Dehydrogenation of 1,2,3,4-tetrahydroquinolines and hydrogenation of quinolines with the Cp*Ir complex reported by Fujita, Yamaguchi *et al.*

The same group has also carried out the perdehydrogenation of 2,6-dimethyldecahydro-1,5-naphthyridine, a fused saturated bicyclic compound, with release of five equivalents of H_2 per molecule catalyzed by Cp*Ir complexes with bipyridonate or 1,10-phenanthroline-2,6-dione ligands (Figure 18).[41] Using 5 mol% of catalyst, a mixture of the stereoisomers of 2,6-dimethyldecahydro-1,5-naphthyridine was dehydrogenatively oxidized with almost complete conversion in 20 h. These catalysts were also active in the perhydrogenation of 2,6-dimethyl-1,5-naphthyridine under 70 bar of H_2 at 130 ^{o}C. Sucessive hydrogenation of 2,6-dimethyl-1,5-naphthyridine and hydrogen release from the resulting hydrogen-rich products were accomplished under the optimized reaction conditions for the individual steps.

[41] K. Fujita, Y. Tanaka, M. Kobayashi, R. Yamaguchi, *J. Am. Chem. Soc.* **2014**, *136*, 4829.

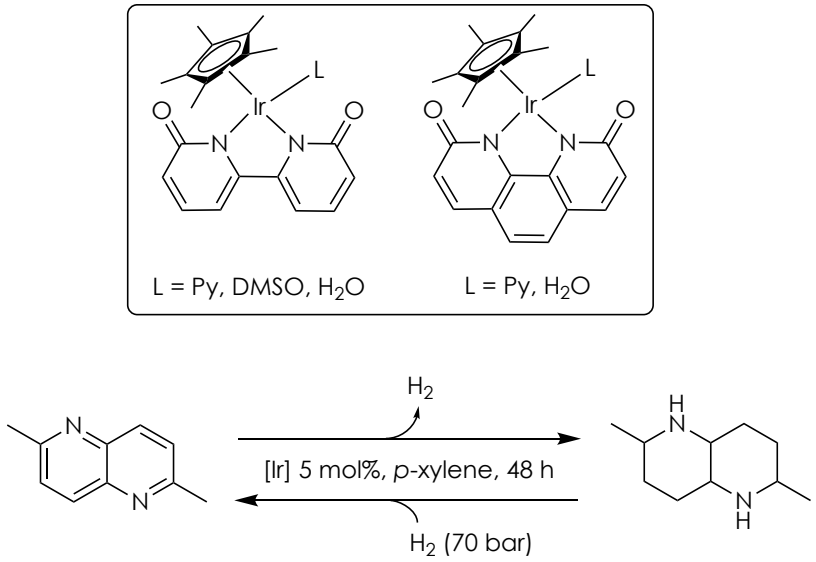

Figure 18. Dehydrogenation of 2,6-dimethyldecahydro-1,5-naphthyridine and hydrogenation of 2,6-dimethyl-1,5-naphthyridine with Cp*Ir complexes.

Fujita and coworkers reported the reversible transformation between 2,5-dimethylpyrazine and 2,5-dimethylpiperazine, which occurs by the uptake and evolution of three equivalents of hydrogen (Figure 19).[42] Up to four hydrogen release/recharge cycles were performed by using a Cp*Ir complex (1.0 mol%) accompanied of an excess of ligand 6,6´-dihydroxy-2,2´-bipyridine (2.0 mol%). The dehydrogenation step was carried out quantitatively at 110 ^{o}C in a *p*-xylene/H_2O solvent mixture; whereas, hydrogenation was accomplished after pressurization of the H_2-storage system with 15 bar of H_2.

[42] K. Fujita, T. Wada, T. Shiraishi, *Angew. Chem. Int. Ed.* **2017**, *56*, 10886.

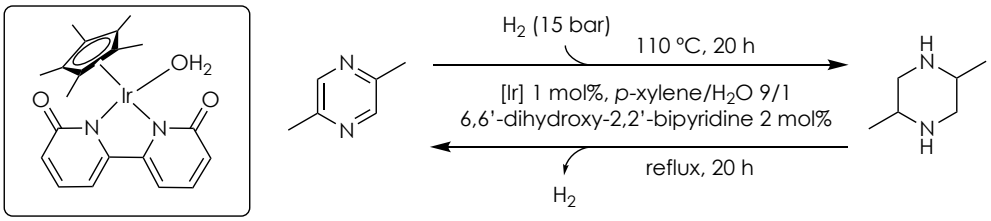

Figure 19. Dehydrogenation of 2,5-dimethylpiperazine and hydrogenation of 2,5-dimethylpyrazine with a Cp*Ir complex.

The Xiao group has explored cyclometallated Cp*Ir(N-C)Cl complexes derived from *N*-aryl ketimines in the dehydrogenation of different classes of *N*-heterocycles (Figure 20).[43] A range of tetrahydroquinolines, tetrahydroisoquinolines, 3,4-dihydroisoquinolines, indolines and tetrahydroquinoxalines were dehydrogenated with low loadings (0.1-1.0 mol%) of catalyst under relatively mild conditions in 2,2,2-trifluoroethanol (TFE) (78 °C). Moreover, this protocol was employed in the synthesis of two biologically active alkaloids, papaverine and harmine (Figure 21).

[43] J. Wu, D. Talwar, S. Johnston, M. Yan, J. Xiao, *Angew. Chem. Int. Ed.* **2013**, *52*, 6983.

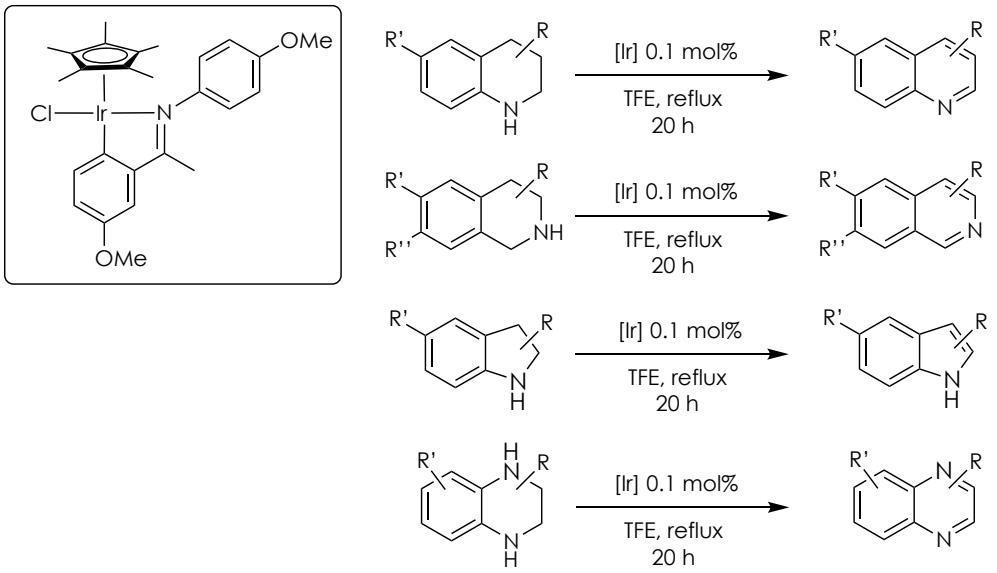

Figure 20. Dehydrogenation of *N*-heterocycles with a Cp*Ir complex.

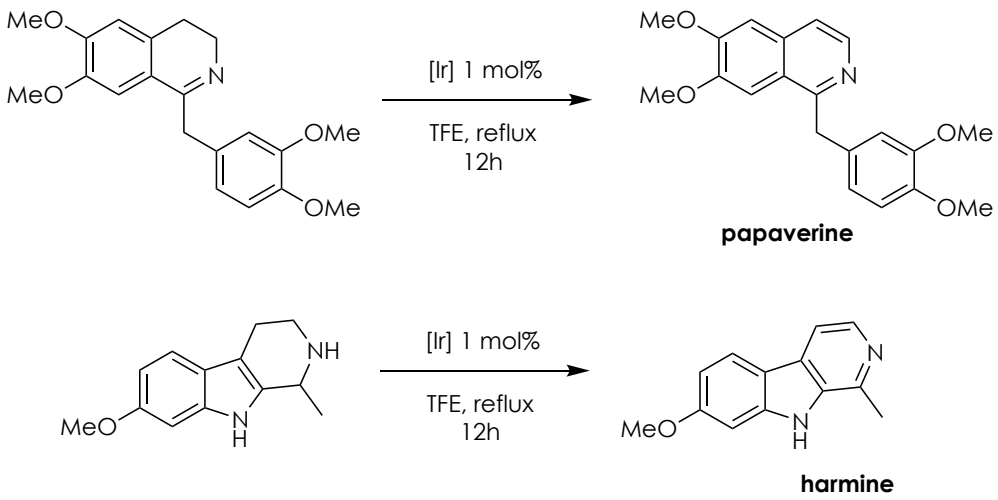

Figure 21. Synthetic applications of the dehydrogenation of *N*-heterocycles using the Cp*Ir complex reported by Xiao *et al.*

Furthermore, dehydrogenation/hydrogenation reversibility was demonstrated with the reduction of methylisoquinoline, which was carried out at 80 °C under 20 bar of H_2 using 1 mol% catalyst, and oxidation of 1,2,3,4-tetrahydromethylisoquinoline using 0.1 mol% catalyst in refluxing TFE (Figure 22). Interestingly, the use of related catalysts was also demonstrated in the reduction of other unsaturated *N*-heterocycles under mild conditions (1 bar H_2, r.t.).[44]

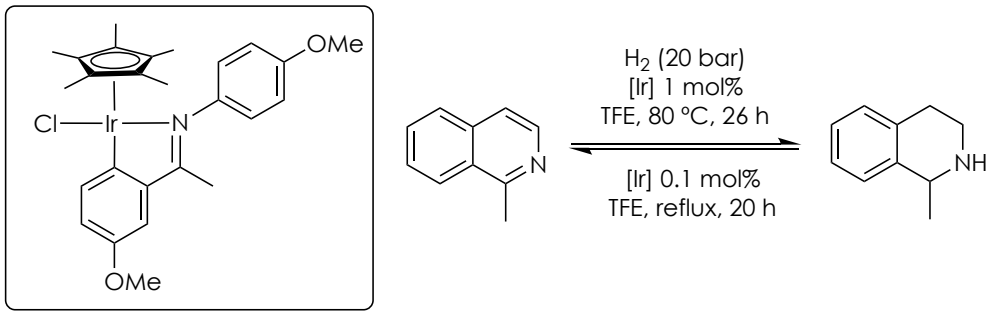

Figure 22. Reversible dehydrogenation/hydrogenation of methylisoquinoline with a Cp*Ir complex reported by Xiao *et al.*

Albrecht *et al.* examined a series of Cp*Ir complexes incorporating triazolylidene ligands in the hydrogenation of substituted quinolines using water as solvent. The reduction of quinoline to 1,2,3,4-tetrahydroquinoline was carried out quantitatively in 16 h under 5 bar of H_2 at 90 °C using a low catalyst loading (0.5 mol%) (Figure 23).[45] The same catalyst performed the dehydrogenation of tetrahydroquinoline with 90% conversion (2 mol%, 100 °C, H_2O).

[44] J. Wu, J. H. Barnard, Y. Zhang, D. Talwar, C. M. Robertson, J. Xiao, *Chem. Commun.* **2013**, *49*, 7052.
[45] Á. Vivancos, M. Beller, M. Albrecht, *ACS Catal.* **2018**, *8*, 17.

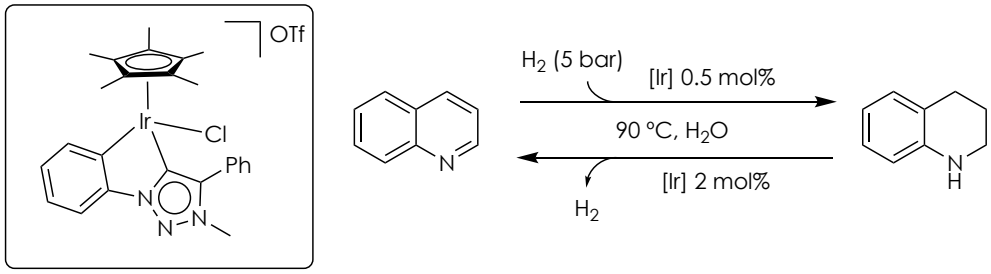

Figure 23. Dehydrogenation of 1,2,3,4-tetrahydroquinoline and hydrogenation of quinoline with the Cp*Ir complex reported by Albrecht *et al.*

Crabtree and coworkers have assayed different iridium catalysts, previously developed for the hydrogenation of *N*-heterocycles under mild conditions (1 bar H_2, 25 °C),[46] in the dehydrogenation of tetrahydroquinaldine (Figure 24).[47] These complexes were able to perform the dehydrogenation of this substrate using 5 mol% catalyst loadings at 135 °C (chlorobenzene), and the subsequent hydrogenation of quinaldine with 76-95% conversion.

[46] (a) G. E. Dobereiner, A. Nova, N. D. Schley, N. Hazari, S. J. Miller, O. Eisenstein, R. H. Crabtree, *J. Am. Chem. Soc.* **2011**, *133*, 7547; (b) M. G. Manas, J. Graeupner, L. J. Allen, G. E. Dobereiner, K. C. Rippy, N. Hazari, R. H. Crabtree, *Organometallics* **2013**, *32*, 4501.
[47] M. G. Manas, L. S. Sharninghausen, E. Lin, R. H. Crabtree, *J. Organomet. Chem.* **2015**, *792*, 184.

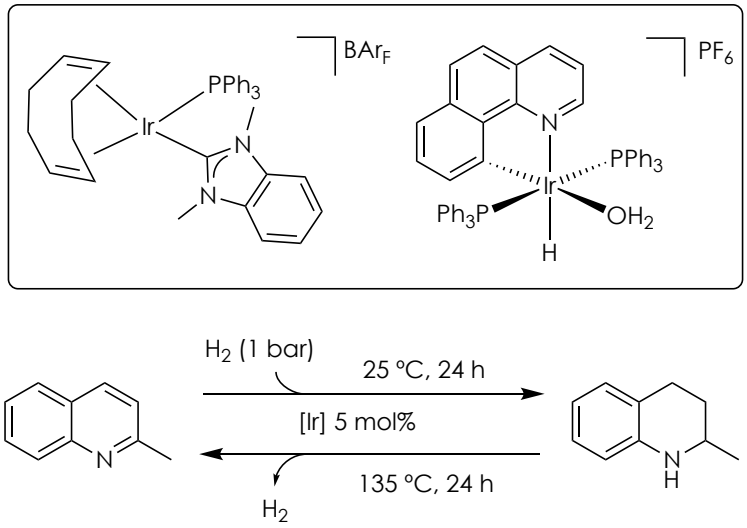

Figure 24. Dehydrogenation of 1,2,3,4-tetrahydroquinaldine and hydrogenation of quinaldine with Ir complexes.

Development of efficient hydrogenation/dehydrogenation catalysts based on earth-abundant, first-row transition metals has attracted significant attention in the last years.[48] In this vein, Jones and coworkers have studied the application of iron complexes containing proton-responsive bis(phosphino)amine PN(H)P ligands in the dehydrogenation and hydrogenation of a series of *N*-heterocycles (Figure 25).[49] The borohydride Fe complex provided significant levels of catalytic activity in the dehydrogenation reactions (3 mol%, 140 °C, xylene); whereas the bromo Fe-PN(H)P complex in combination with KO^{t}Bu efficiently catalyzed the

[48] (a) N. Gorgas, K. Kirchner, *Acc. Chem. Res.* **2018**, *51*, 1558; (b) N. Gorgas, K. Kirchner *"Well-defined Iron and Manganese Pincer Catalysts"* in *Pincer Compounds* (D. Morales-Morales, Ed.), Chap. 2. Elsevier, **2018**; (c) G. Bauer, K. Kirchner, *Angew. Chem. Int. Ed.* **2011**, *50*, 5798; (d) W. Liu, B. Sahoo, K. Junge, M. Beller, *Acc. Chem. Res.* **2018**, *51*, 1858; (e) F. Kallmeier, R. Kempe, *Angew. Chem. Int. Ed.* **2018**, *57*, 46; (f) T. Zell, R. Langer, *ChemCatChem* **2018**, *10*, 1930.

[49] S. Chakraborty, W. W. Brennessel, W. D. Jones, *J. Am. Chem. Soc.* **2014**, *136*, 8564.

hydrogenation of *N*-heterocycles (5-10 bar H_2, 80 °C, 3 mol% Fe, 10 mol% base). Mechanistic studies revealed that a pentacoordinated iron hydride species, containing a deprotonated PNP ligand, and a *trans*-dihydride intermediate were common intermediates for both processes.[50]

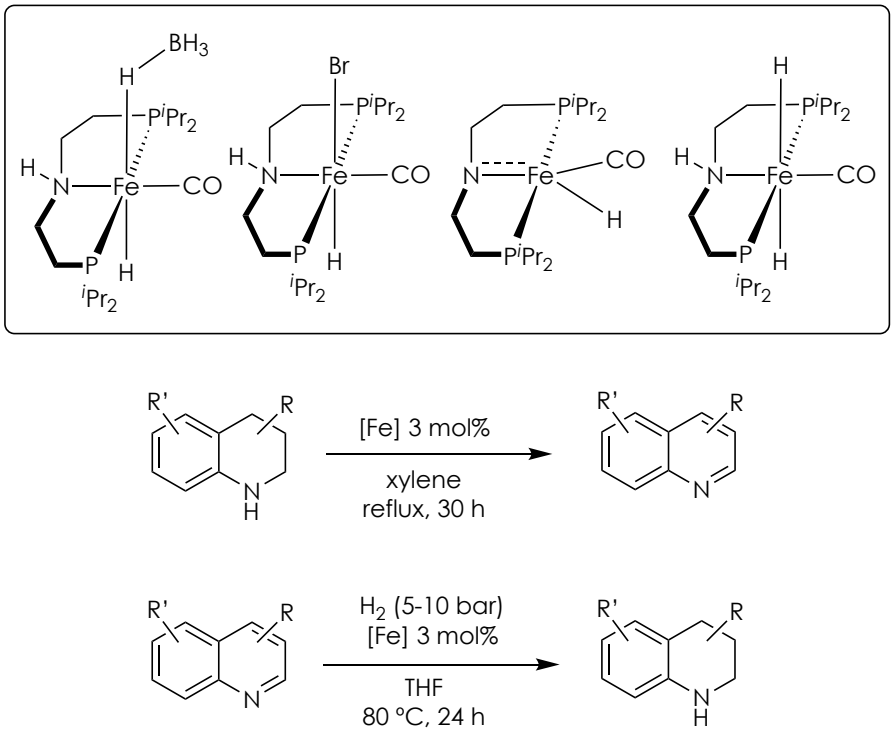

Figure 25. Dehydrogenation of *N*-heterocycles using Fe-PN(H)P complexes.

[50] (a) S. M. Bellows, S. Chakraborty, J. B. Gary, W. D. Jones, T. R. Cundari, *Inorg. Chem.* **2017**, *56*, 5519; (b) B. Sawatlon, P. Surawatanawong, *Dalton Trans.* **2016**, *45*, 14965.

Similarly, a cobalt complex based on a PN(H)P ligand was examined in the acceptorless dehydrogenation of *N*-heterocycles (Figure 26). [51] By using 10 mol% of catalyst in *p*-xylene at 150 ºC, a series of *N*-heterocycles, including six-membered tetrahydroquinoline and five-membered 2-methylindoline, were successfully dehydrogenated to produce the corresponding aromatic products with high conversions. Interestingly, a related complex based on a PN(Me)P ligand was inefficient in the oxidation of the *N*-heterocycles, pointing out to the participation of the ligand NH moiety in the catalytic process. On the other hand, the Co-PN(H)P complex was also found to efficiently catalyze the hydrogenation of *N*-heterocycles. However, in these reactions replacement of the NH function by a NMe group did not affect the hydrogenation activity.

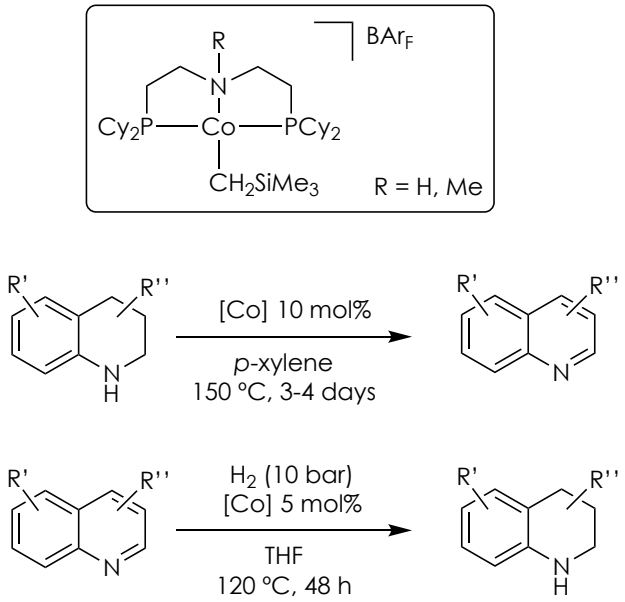

Figure 26. Dehydrogenation of *N*-heterocycles using the Co-PN(H)P complex.

[51] R. Xu, S. Chakraborty, H. Yuan, W. D. Jones, *ACS Catal.* **2015**, *5*, 6350.

II.2. Results and discussion

II.2.1. General considerations

As previously mentioned, two of the most representative types of proton-responsive pincer ligands are those based on M-amine/M-amido interconversion and lutidine reversible deprotonation. In Chapter II, we have aimed to combine both metal-ligand cooperation modes to develop efficient catalysts for the reversible hydrogenation of *N*-heterocycles. Particularly, new Ru complexes incorporating lutidine-derived pincer CNN(H) ligands containing a secondary amino side group have been synthetized (Figure 1). Moreover, these Ru-CNN(H) complexes have been examined in the hydrogenation and dehydrogenation of a series of *N*-heterocycles, and initial mechanistic studies have been performed.

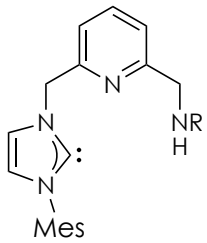

Figure 1. General structure of lutidine-derived CNN(H) ligands.

II.2.2. Synthesis of CNN(H) ligand-type precursors and Ag-CNN(H) complexes

Synthesis of imidazolium salts **2a-c** was effected by reaction of derivative **1a(Br)** with the corresponding primary amine RNH_2 (R = ^{t}Bu, CH_2Ph, Ph) (Scheme 1).[9] These compounds were obtained with moderate to good yields (60-90%) as white solids, and were characterized by NMR spectroscopy and high-resolution mass spectrometry. The ^{1}H NMR spectrum of **2a** presents the distinctive downfield signal appearing at 10.45 ppm expected for the imidazolium H-2 proton; whereas the resonances of the methylene CH_2-NHC and CH_2-NH bridges appear as singlets at 5.97 and 4.07 ppm, respectively, and that of the amine proton is exhibited at 5.22 ppm as a broad singlet. Similar NMR spectroscopic data were obtained for derivatives **2b** and **2c**.

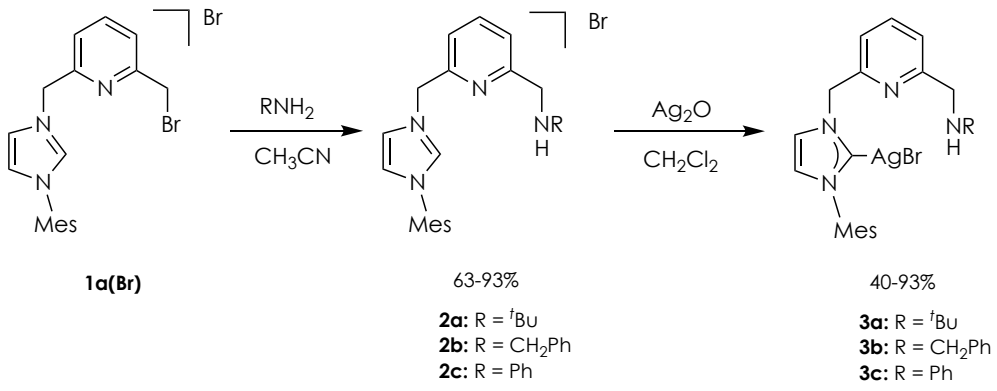

Scheme 1. Synthesis of CNN(H) ligand precursors **2**, and silver complexes **3**.

Treatment of the imidazolium salts **2a-c** with Ag_2O in CH_2Cl_2 allowed the isolation of the corresponding silver-carbene complexes **3a-c**, as inferred from the disappearance of the downfield signal of the imidazolium H-2 protons in the ^1H NMR spectra (Scheme 1). The silver complexes were characterized by NMR spectroscopy and elemental analysis. Their most relevant spectroscopic feature resides in the presence of a singlet resonance in the $^{13}C\{^1H\}$ NMR experiments at *ca.* 183 ppm attributable to the C-2 carbons of the NHC moieties.

II.2.3. Synthesis of Ru-CNN(H) complexes

Since the use of silver complexes as NHC transfer reagents for the synthesis of metal-NHC derivatives is well precedented[52] and have permitted the preparation of different ruthenium complexes incorporating pincer ligands with NHC donors,[37,53] the synthesis of Ru-CNN(H) complexes was sought by reaction of the silver derivatives **3** with an appropiate ruthenium precursor (Scheme 2). Addition of $RuHCl(CO)(PPh_3)_3$ to **3a** in THF at 55 ºC gave rise in the hydride region of the ^1H NMR spectrum of the reaction mixture to several resonances, which have been tentatively assigned to $[RuH(CNN(H))(CO)(PPh_3)]^+$ and RuHX(CNN(H))(CO) (X = Br, Cl) complexes (Figure 2). Aiming to obtain a single species, the mixture of complexes was treated with $NaBF_4$ and PPh_3 in CH_3CN, affording the isolation of complex **4a** in high yield (88%).[9] The ruthenium complexes **4b** and **4c** were prepared and isolated similarly.

---

[52] (a) H. M. J. Wang, I. J. B. Lin, *Organometallics* **1998**, *17*, 972; (b) J. C. Garrison, W. J. Youngs, *Chem. Rev.* **2005**, *105*, 3978; (c) I. J. B. Lin, C. S. Vasam, *Coord. Chem. Rev.* **2007**, *251*, 642.

[53] M. Hernández-Juárez, M. Vaquero, E. Álvarez, V. Salazar, A. Suárez, *Dalton Trans.* **2013**, *42*, 351.

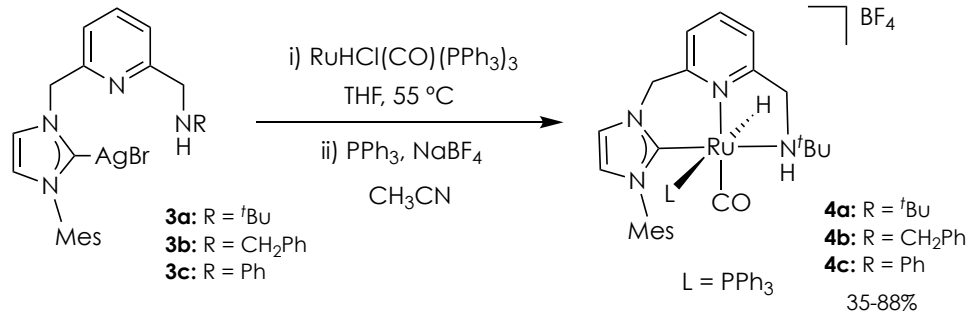

Scheme 2. Synthesis of ruthenium complexes **4a-c**.

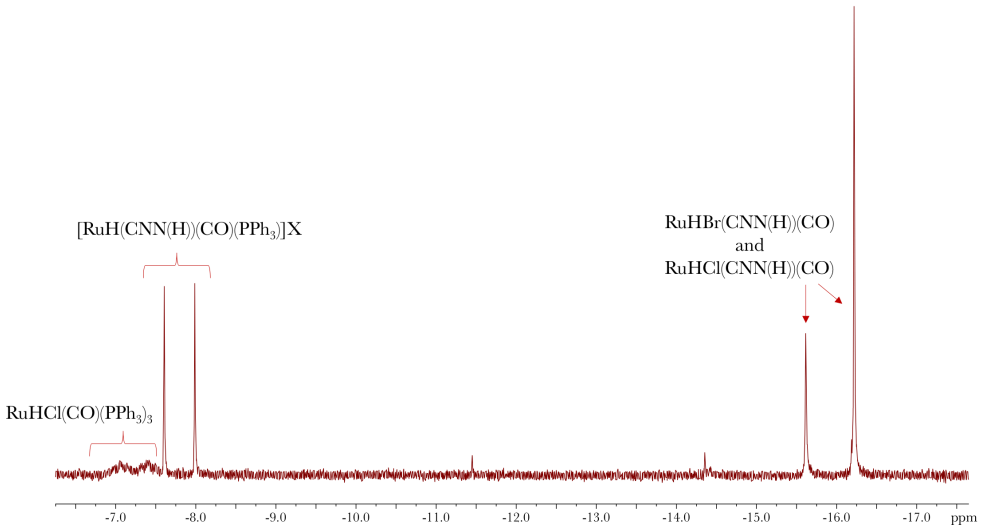

Figure 2. Hydride region of the ^{1}H NMR spectrum (300 MHz, CD_2Cl_2) of the reaction of $RuHCl(CO)(PPh_3)_3$ and **3a**.

Spectroscopic data of compounds **4** are in good agreement with their proposed structures, which have been further confirmed by X-ray diffraction studies carried out for complexes **4a** and **4b**. For example, in the hydride region, the ^{1}H NMR spectrum of **4a** shows a doublet resonance at −7.79 ppm with a large coupling constant of $^{2}J_{HP}$ = 114.0 Hz, evincing the *trans* arrangement of the hydrido and PPh_3 ligands (Figure 3, Table 1). In the same experiment, the resonance of the amine hydrogen appears at 2.71 ppm as a

broad doublet of doublet of doublet due to the coupling with the diastereotopic CH_2-N protons and the phosphorus atom ($^3J_{HH}$ = 12.2 Hz, $^3J_{HH}$ = 3.4 Hz, $^3J_{HP}$ = 3.4 Hz); whereas the methylene protons give rise to four different signals, two doublets appearing at 5.00 and 4.21 ppm ($^2J_{HH}$ = 15.6 Hz) corresponding to the CH_2-NHC bridge, and two doublets of doublets at 4.18 ($^2J_{HH}$ = 14.7 Hz, $^3J_{HH}$ = 3.7 Hz) and 3.95 ($^2J_{HH}$ = 14.2 Hz, $^3J_{HH}$ = 13.6 Hz) ppm caused by the CH_2N arm. Moreover, in the $^{13}C\{^1H\}$ NMR spectrum of **4a**, the presence of the coordinated CO was confirmed by the existence of a doublet resonance at 208.3 ppm (J_{CP} = 6 Hz), while the C-2 carbon atom of the NHC fragment causes a doublet at 185.2 ppm (J_{CP} = 5 Hz) (Table 2).

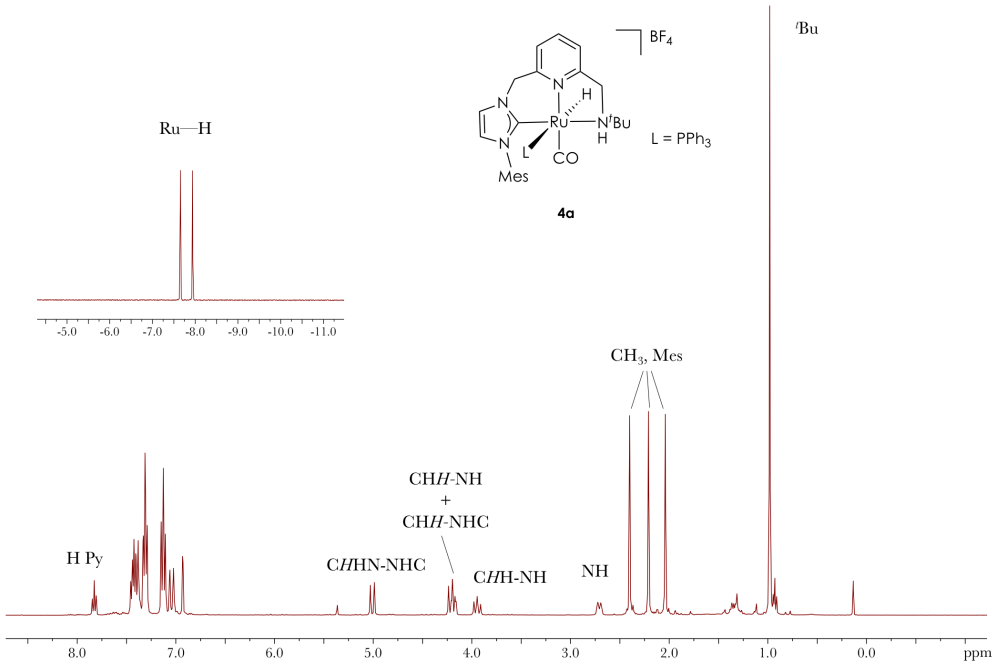

Figure 3. ^1H NMR spectrum (400 MHz, CD_2Cl_2) of complex **4a**.

Table 1. Selected ^{1}H NMR data of Ru-CNN(H) complexes **4**.[a]

[Ru]	δ (^{1}H)			
	Ru-H	C*H*H-NHC	C*H*H-NH	NH
4a	−7.79 (d) $^{2}J_{HP}$ = 114.0	5.00 (d) $^{2}J_{HH}$ = 16.1 4.21 (d) $^{2}J_{HH}$ = 15.6	4.18 (dd) $^{2}J_{HH}$ = 14.7 $^{3}J_{HH}$ = 3.7 3.95 (dd) $^{2}J_{HH}$ = 14.2 $^{3}J_{HH}$ = 12.6	2.71 (br ddd) $^{3}J_{HH}$ = 12.2 $^{3}J_{HH}$ = 3.4 $^{3}J_{HP}$ = 3.4
4b	−7.30 (d) $^{2}J_{HP}$ = 109.9	5.20 (d) $^{2}J_{HH}$ = 16.0 4.34 (d) $^{2}J_{HH}$ = 16.0	4.00 (overlapped) 3.83 (overlapped)	2.87 (br dd) $^{3}J_{HH}$ = 11.0 $^{3}J_{HH}$ = 11.0
4c	−7.05 (d) $^{2}J_{HP}$ = 110.7	5.15 (d) $^{2}J_{HH}$ = 15.6 4.40 (d) $^{2}J_{HH}$ = 15.6	4.54 (overlapped m, 2H)	4.54 (overlapped)

[a] NMR spectra registered in CD_2Cl_2 (400 MHz). Chemical shifts (δ) are given in ppm, and coupling constants (*J*) in Hz.

Table 2. Selected ^{13}C{^{1}H} NMR data of Ru-CNN(H) complexes **4**.[a]

[Ru]	δ (^{13}C)	
	C-2 NHC	CO
4a	185.2 (d) J_{CP} = 5	208.3 (d) J_{CP} = 6
4b	186.2 (d) J_{CP} = 5	206.8 (d) J_{CP} = 7
4c	185.8 (d) J_{CP} = 4	205.6 (d) J_{CP} = 7

[a] NMR spectra registered in CD_2Cl_2 (400 MHz). Chemical shifts (δ) are given in ppm, and coupling constants (*J*) in Hz.

To determine the differences in the donor strength of the different CNN(H) ligands, the CO stretching bands in the IR spectra of complexes **4** have been analyzed. Lower absorption energies were found for alkyl substituted Ru-CNN(H) complexes (**4a**: 1933 cm^{-1}; **4b**: 1936 cm^{-1}) in comparison to derivative **4c** that exhibits this band at 1958 cm^{-1}, evincing a higher basicity of the CNN(H) ligands of complexes **4a** and **4b**.

As mentioned above, the solid state structures of complexes **4a** and **4b** were studied by single crystal X-ray diffraction (Figures 4 and 5). These derivatives are isostructural and, therefore, only the structure of **4a** is next commented. Complex **4a** is comprised of a stereogenic Ru atom in an octahedral coordination geometry, with the carbene and amine fragments of the pincer disposed *trans* to each other (C_{NHC}-Ru-N_{amine} = 161.58(7)º), and the hydrido ligand coordinated *trans* to PPh_3 (P-Ru-H = 171.5º). The six-membered ring involving the NHC and pyridine donors adopts a boat-like conformation defined by a dihedral angle C(14)–N(3)–Ru(1)–C(1) of −27.4º; whereas the N_{Py}-Ru-N_{amine} chelate ring has an envelope conformation with a C(18)–N(3)–Ru(1)–N(4) torsion angle of −14.9º. These ring conformations cause the axial methylene hydrogen of the amine arm to be aligned with the hydrido ligand, albeit no short contact is evident, and the axial hydrogen of the CH_2-NHC bridge to lie parallel to the Ru-P bond, as also occurs with the N-H bond of the amine group. All the distances between the metal center and the donor atoms fall in the range of previously reported values.[3,54]

[54] (a) Y. Sun, C. Koehler, R. Tan, V. T. Annibale, D. Song, *Chem. Commun.* **2011**, *47*, 8349; (b) E. Fogler, E. Balaraman, Y. Ben-David, G. Leitus, L. J. W. Shimon, D. Milstein, *Organometallics* **2011**, *30*, 3826.

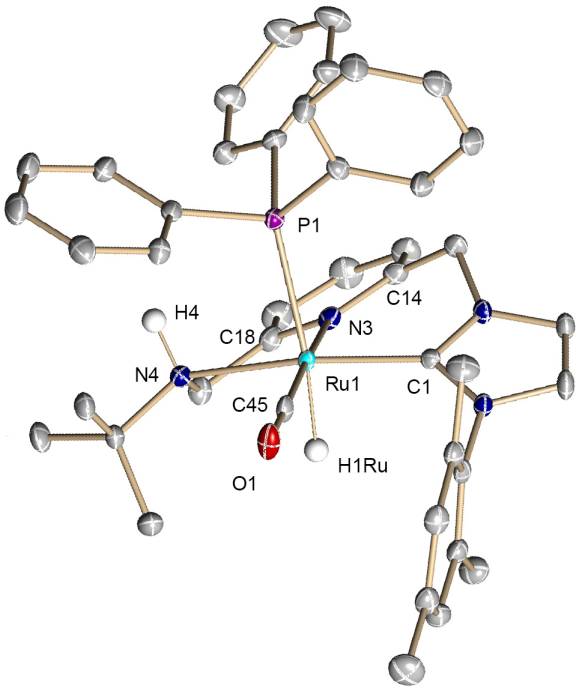

Bond lenghts (Å)		Angles (°)	
Ru(1)–C(1)	2.0196(19)	C(1)–Ru(1)–N(4)	161.58(7)
Ru(1)–N(3)	2.1367(18)	N(3)–Ru(1)–C(45)	172.84(8)
Ru(1)–N(4)	2.2716(17)	P(1)–Ru(1)–H(1)Ru	171.5
Ru(1)–H(1)Ru	1.5992	N(4)–Ru(1)–N(3)	77.97(7)
Ru(1)–C(45)	1.835(2)	C(1)–Ru(1)–C(45)	93.96(8)
Ru(1)–P(1)	2.4662(5)	C(1)–Ru(1)–N(3)	87.54(7)
		N(4)–Ru(1)–C(45)	99.08(8)

Figure 4. ORTEP drawing at 30% ellipsoid probability, and selected bond lengths (Å) and angles (°), of the cationic fragment of complex **4a**. Hydrogen atoms, except the hydrido ligand and the amine proton, and solvent molecules (CH_2Cl_2) have been omitted for clarity.

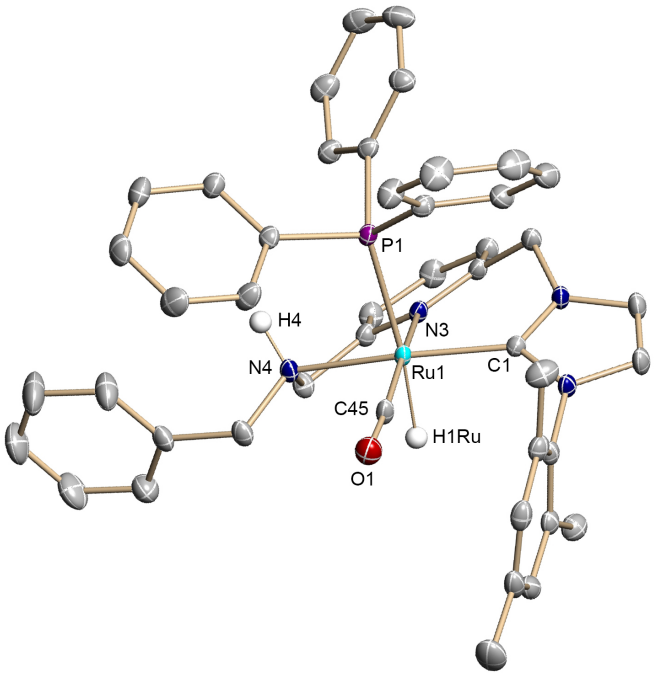

Bond lenghts (Å)		Angles (º)	
Ru(1)–C(1)	2.017(2)	C(1)–Ru(1)–N(4)	164.20(9)
Ru(1)–N(3)	2.1261(19)	N(3)–Ru(1)– C(45)	167.91(10)
Ru(1)–N(4)	2.201(2)	P(1)–Ru(1)–H(1)Ru	173.9(9)
Ru(1)–H(1)Ru	1.614(5)	N(4)–Ru(1)–N(3)	77.74(7)
Ru(1)–C(45)	1.838(2)	C(1)–Ru(1)–C(45)	95.24(10)
Ru(1)–P(1)	2.4368(6)	C(1)–Ru(1)–N(3)	88.71(8)
		N(4)–Ru(1)–C(45)	96.49(9)

Figure 5. ORTEP drawing at 30% ellipsoid probability, and selected bond lengths (Å) and angles (º), of the cationic fragment of complex **4b**. Hydrogen atoms, except the hydrido ligand and amine proton, and solvent molecules (MeOH) have been omitted for clarity.

II.2.4. Hydrogenation and dehydrogenation of *N*-heterocycles

II.2.4.a. Hydrogenation of N-heterocycles

To determine the applicability of the synthetized Ru-CNN(H) complexes as catalysts in the hydrogenation of *N*-heterocycles, derivatives **4a-c** were tested in the reduction of quinoxaline (**5a**) (Table 3). Under 4 bar of H_2, in 2-methyltetrahydrofuran at 80 °C, complex **4a** (0.5 mol%) in the presence of KO^{t}Bu (10 mol%) catalyzed the hydrogenation of **5a** to tetrahydroquinoxaline (**6a**) with full conversion after 6 h (entry 1). However, under the same conditions, complexes **4b** and **4c** were significantly less active than **4a** (entries 2 and 3). Also of interest, complex **7** (Figure 6),[54a] incorporating a diethylamino group, was found a poorer catalyst for this reaction (entry 4).

Table 3. Hydrogenation of *N*-heterocycles catalyzed by Ru-CNN(H) complexes.[a]

Entry	Substrate	Product	[Ru] (mol%)	T (°C)	Conv. (%) (time, h)
1	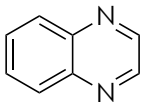 **5a**	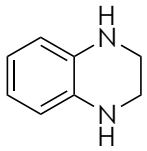 **6a**	**4a** (0.5)	80	>99 (6)
2			**4b** (0.5)	80	23 (6)
3			**4c** (0.5)	80	22 (6)
4			**7** (0.5)	80	12 (6)
5	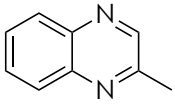 **5b**	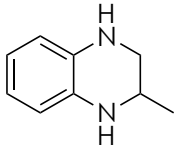 **6b**	**4a** (0.5)	80	>99 (24)

Table 3 (cont.). Hydrogenation of *N*-heterocycles catalyzed by Ru-CNN(H) complexes.[a]

Entry	Substrate	Product	[Ru] (mol%)	T (°C)	Conv. (%) (time, h)
6	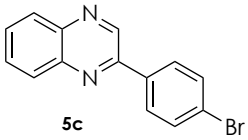 **5c**	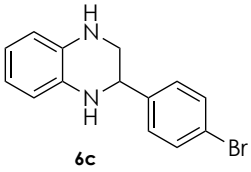 **6c**	**4a** (0.5)	95	88 (24)
7	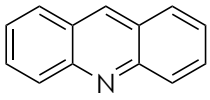 **5d**	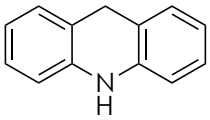 **6d**	**4a** (0.5)	80	98 (19)
8	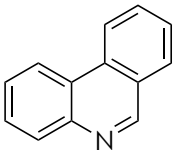 **5e**	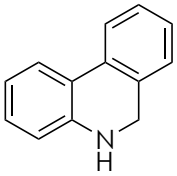 **6e**	**4a** (0.5)	80	92 (19)
9	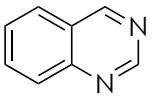 **5f**	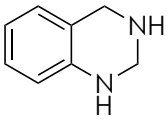 **6f**	**4a** (1.0)	95	98 (48)
10	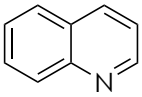 **5g**	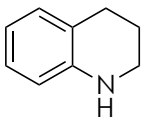 **6g**	**4a** (1.0)	95	>99 (48)
11	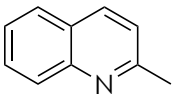 **5h**	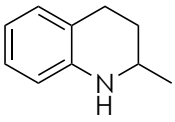 **6h**	**4a** (1.0)	95	95 (48)

Table 3 (cont.). Hydrogenation of *N*-heterocycles catalyzed by Ru-CNN(H) complexes.[a]

Entry	Substrate	Product	[Ru] (mol%)	T (°C)	Conv. (%) (time, h)
12	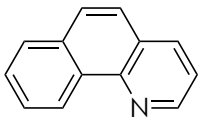 **5i**	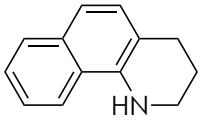 **6i**	**4a** (1.0)	95	97 (48)
13	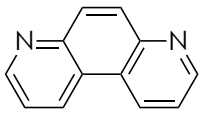 **5j**	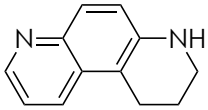 **6j**	**4a** (1.0)	95	>99 (24)
14[b]	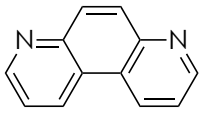 **5j**	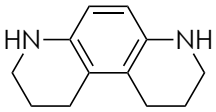 **6j'**	**4a** (1.0)	95	93 (72) (+ 7% **6j**)
15	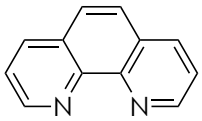 **5k**	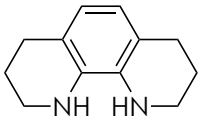 **6k**	**4a** (1.0)	85	0 (24)
16[b]	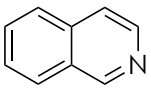 **5l**	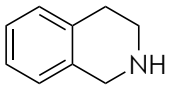 **6l**	**4a** (1.0)	95	74 (24)
17[b]	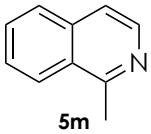 **5m**	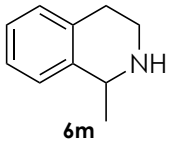 **6m**	**4a** (1.0)	95	0 (24)

[a] Reaction conditions, unless otherwise noted: 4 bar of H_2, 2-methyltetrahydrofuran, KO^{t}Bu (10 mol%). [S] = 0.24 M. Conversions were determined by ^{1}H NMR spectroscopy using mesitylene as internal standard. [b] 10 bar of H_2.

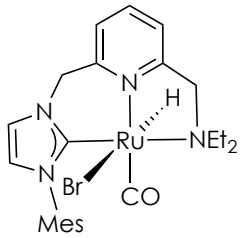

Figure 6. Complex **7**.

Based on these results, the hydrogenation of 2-substituted quinoxalines **5b** and **5c** was examined using complex **4a** (entries 5 and 6). These derivatives were reduced under the previous conditions with high conversions after 24 h.

Under the same reaction conditions, acridine (**5d**) and phenanthridine (**5e**) were hydrogenated with conversions higher than 92% in 19 h (entries 7 and 8). However, the reduction of other *N*-heterocycles, including quinazoline (**5f**), quinoline (**5g**), quinaldine (**5h**) and benzo[h]quinoline (**5i**), required higher catalyst loadings (1.0 mol%) and harsher reaction conditions (95 ^{o}C, 48 h) (entries 9-12).

Next, the reduction of 4,7-phenanthroline (**5j**), having two *N*-heterocyclic rings, was studied (entries 13 and 14). Under 4 bar of H_2, full hydrogenation of one of the *N*-containing rings was observed. Moreover, the hydrogenation of both *N*-heterocyclic rings was accomplished by increasing the H_2 pressure to 10 bar after a reaction time of 3 days. On the contrary, hydrogenation of the chelating 1,10-phenanthroline (**5k**) was not achieved (entry 15).

Hydrogenation of isoquinoline (**5l**) was also assayed, requiring 10 bar of H_2 to get acceptable conversions (entry 16). Alternatively, the reduction of 2-methylisoquinoline (**5m**) was not effected even under 10 bar of H_2 at 95 ^{o}C (entry 17).

II.2.4.b. Dehydrogenation of N-heterocycles

Taking into consideration the efficiency of complex **4a** in the hydrogenation of a series of *N*-heterocycles (Table 3), the catalytic performance of this derivative was tested in the reverse reactions, namely the dehydrogenation of the resulting hydrogenated heterocycles (Table 4). Initially, dehydrogenation of tetrahydroquinoxaline (**6a**) was performed using 4.0 mol% of **4a** and 15 mol% of KO^{t}Bu in 2-methyltetrahydrofuran at 85 ^{o}C, leading to complete formation of quinoxaline (**5a**) after 24 h (entry 1). However, these conditions were not appropriate for the dehydrogenation of **6b**, and more energetic reaction conditions (160 ^{o}C, *o*-xylene) and the influence of different bases were examined (entries 2-4). Using KHMDS as base did not improve the conversion in comparison to the the reaction with KO^{t}Bu, whereas NaH had a deleterious effect on the catalyst activity. Moreover, the oxidation of the 2-substituted tetrahydroquinoxaline **6c** using KO^{t}Bu as base was sluggish (entry 5).

Table 4. Dehydrogenation of *N*-heterocycles catalyzed by complex **4a**.[a]

Entry	Substrate	Product	Base	Conv. (%) (time, h)
1[b]	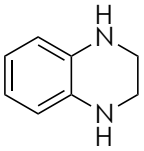 **6a**	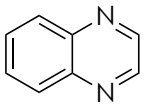 **5a**	KO*t*Bu	>99 (24)
2	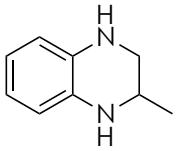 **6b**	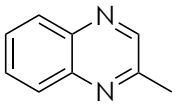 **5b**	KO*t*Bu	85 (24)
3			KHMDS	84 (24)
4			NaH	6 (24)
5	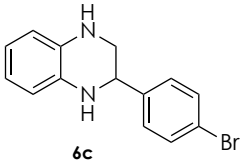 **6c**	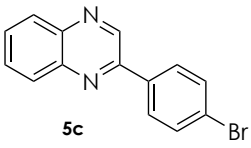 **5c**	KO*t*Bu	8 (24)
6	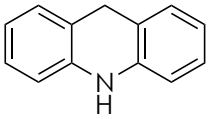 **6d**	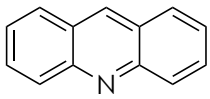 **5d**		50 (48)
7	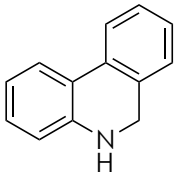 **6e**	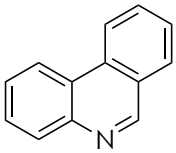 **5e**		94 (24)
8	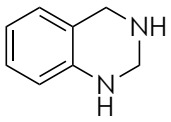 **6f**	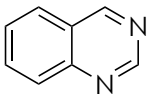 **5f**		>99 (24)

Table 4(cont.). Dehydrogenation of *N*-heterocycles catalyzed by complex **4a**.[a]

Entry	Substrate	Product	Base	Conv. (%) (time, h)
9	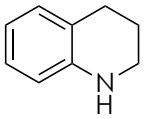 **6g**	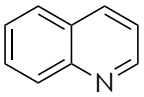 **5g**		47 (24) 50 (48)
10	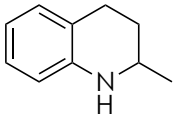 **6h**	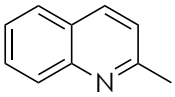 **5h**		16 (24) 27 (48)
11	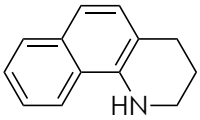 **6i**	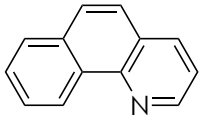 **5i**		84 (24)
12	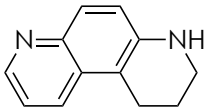 **6j**	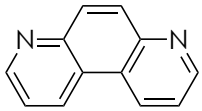 **5j**		51 (24) 74 (48)
13	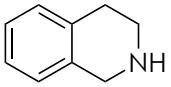 **6l**	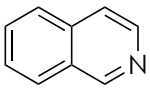 **5l**		27 (48)

[a] Reaction conditions, unless otherwise noted: *o*-xylene, 4.0 mol% **4a**, 160 °C, 15 mol% base. [S] = 0.12 M. Conversions were determined by ^{1}H NMR spectroscopy using mesitylene as internal standard. [b] 2-methyltetrahydrofuran, 85 °C. [S] = 0.06 M.

In addition to hydroquinoxalines, dehydrogenation of other classes of *N*-heterocycles was also tested. Dihydroacridine (**6d**) was oxidized under the conditions of Table 4, entry 2 with moderate catalytic activity (50% conversion after 48 h) (entry 6). Alternatively, the reactions of dihydrophenanthridine (**6e**) and tetrahydroquinazoline (**6f**) took place with conversions higher than 94% after 24 h (entries 7 and 8). Under the latter conditions, the dehydrogenation of tetrahydroquinoline (**6g**) and tetrahydroquinaldine (**6h**) proceeded with only low to moderate conversions, even increasing the reaction time from 24 to 48 h (entries 9 and 10). In contrast, hydrogen release from tetrahydrobenzoquinoline (**6i**) took place with 84% conversion after 24 h (entry 11). The oxidation of tetrahydro-4,7-phenanthroline (**6j**) yielded the corresponding dehydrogenated *N*-heterocycle with 51% conversion in 24 h, which was increased to 74% after 48 h (entry 12). Finally, the reaction of tetrahydroisoquinoline (**6l**) proceeded with low conversion even after 48 h (entry 13).

II.2.5. Reactivity of Ru-CNN(H) complexes towards bases and H_2. Mechanistic implications in the hydrogenation of *N*-heterocycles

In order to determine the ability of the CNN(H) ligands to participate in ligand-assisted processes, and to provide information regarding the species involved in the Ru-CNN(H) catalyzed reactions, deprotonation of the ruthenium complex **4a** was explored. Addition of 1.3 equiv of KO^{t}Bu to a clear solution of **4a** in THF-d_8 led to the instantaneous formation of a dark red solution of the deprotonated complex **8** (Scheme 3).[54] In the ^{1}H NMR spectrum, the hydrido ligand of **8** produces a slightly broad doublet at −7.64 ppm having a large coupling constant $^2J_{HP}$ of 140 Hz, indicative of the relative *trans* disposition of the phosphine and hydrido ligands (Figure 7). Moreover, selective deprotonation of the CH_2-NHC arm of **4a** was evident from the observation of a singlet signal at 4.38 ppm (integrating to 1H), corresponding to the methyne =CH-NHC bridge, and two doublets of doublets at 3.43 ($^2J_{HH}$ = 12.0 Hz, $^3J_{HH}$ = 12.0 Hz) and 3.09 ($^2J_{HH}$ = 11.3 Hz, $^3J_{HH}$ = 1.9 Hz) ppm, attributable to the methylene CH_2-NH moiety. Furthermore, the dearomatization of the pyridine fragment is manifested by the high-field shifted signals of the ring protons (5.08–6.09 ppm); whereas the proton of the NH donor group appears at 1.76 ppm overlapped with the solvent signal. The ^{13}C{^{1}H} NMR spectrum of **8** exhibits a singlet at 210.2 ppm for the CO ligand, while the resonance of the C-2 of the NHC moiety appears at 177.3 ppm. Finally, the coordination of the PPh_3 ligand is further manifested by the presence of a broad singlet at 16.0 ppm in the ^{31}P{^{1}H} NMR spectrum.

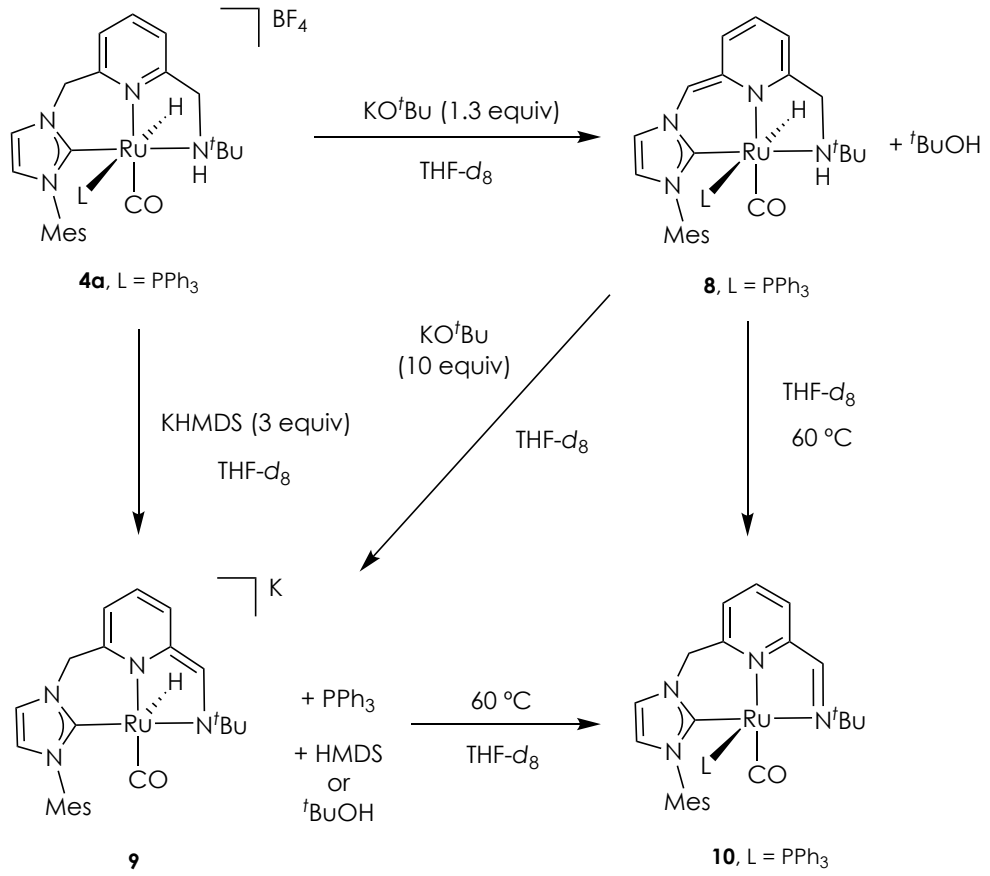

Scheme 3. Reactions of complex **4a** with bases yielding complexes **8**, **9** and **10**.

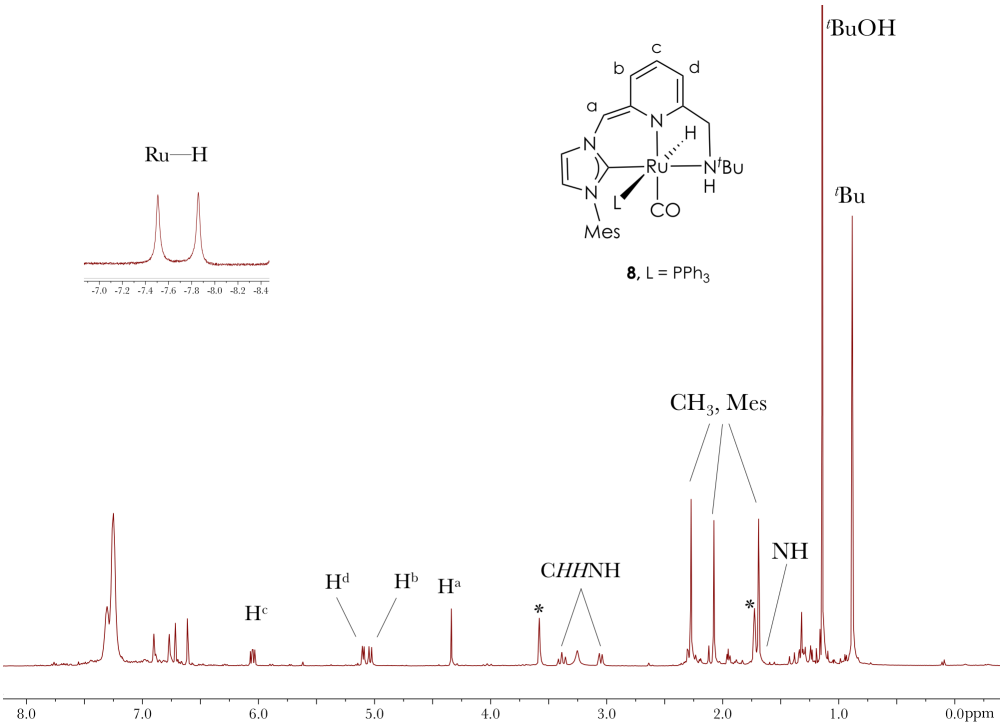

Figure 7. ^{1}H NMR spectrum (400 MHz) of the reaction of **4a** with KO^{t}Bu (1.3 equiv) in THF-d_8 to yield complex **8** (***** denotes residual THF).

Subsequent treatment of solutions in THF-d_8 of the *in situ* generated complex **8** with an excess of KO^{t}Bu (10 equiv), or of derivative **4a** with KHMDS (3.0 equiv), produced after 24 h a dark violet solution. NMR analysis of the sample indicated the formation of the anionic amido complex **9** (Scheme 3). In the ^{1}H NMR experiment of **9**, the enamino =CH-N^{t}Bu proton of the pincer ligand resonates at 6.69 ppm as a singlet, while the inequivalent methylene protons of the CH_2-NHC bridge appear as mutually coupled doublets at 4.83 and 4.56 ppm ($^{2}J_{HH}$ = 12.7 Hz) (Figure 8). As for complex **8**, the dearomatized central *N*-heterocycle produces upfield shifted resonances appearing in the range between 5.33 and 6.54 ppm. Moreover, the presence of the hydrido ligand is deduced by the existence of a singlet at

−17.09 ppm. Diagnostic signals in the $^{13}C\{^{1}H\}$ NMR spectrum of **9** include the resonances appearing at 213.7 ppm, corresponding to the CO ligand, and at 195.6 ppm due to the carbene carbon. In support of the proposed structure for complex **9**, it is worth mentioning a previous report of Milstein *et al.* on an analogous Ru(II) complex based on a deprotonated lutidine-derived PNN(H) ligand.[3]

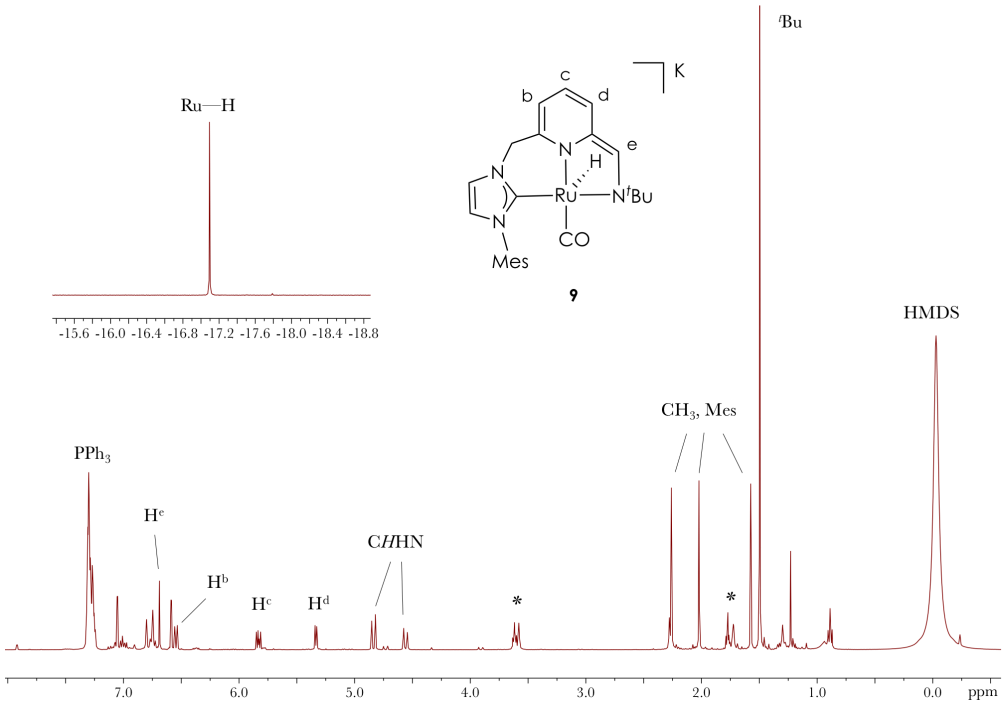

Figure 8. ^{1}H NMR spectrum (400 MHz, THF-d_8) of the reaction of **4a** with KHMDS (3.0 equiv) to yield complex **9** (* denotes residual THF).

Prolonged heating to 60 °C of solutions of the *in situ* formed complexes **8** or **9**, or mixtures thereof, produced the clean formation of a new species that has been spectroscopically characterized as the Ru(0) complex **10** (Scheme 3). ^{1}H NMR analysis of the resulting dark blue solution indicates the

presence of the imine moiety as deduced by the appearance of a doublet resonance at 7.92 ppm ($^4J_{HP}$ = 3.7 Hz) (Figure 9). Also, in this experiment, the geminal CH_2-NHC hydrogens appear as doublets at 4.74 and 3.91 ppm ($^2J_{HH}$ = 14 Hz). Moreover, phosphine coordination is manifested in the $^{31}P\{^1H\}$ NMR spectrum of **10** by the appareance of a singlet at 50.5 ppm. In the $^{13}C\{^1H\}$ NMR spectrum, the CO ligand and the C-2 carbene carbon cause doublet resonances at 216.1 (J_{CP} = 10 Hz) and 191.3 (J_{CP} = 7 Hz) ppm, respectively. Complex **10** can be regarded as derived from **8** by the formal loss of a H_2 molecule.

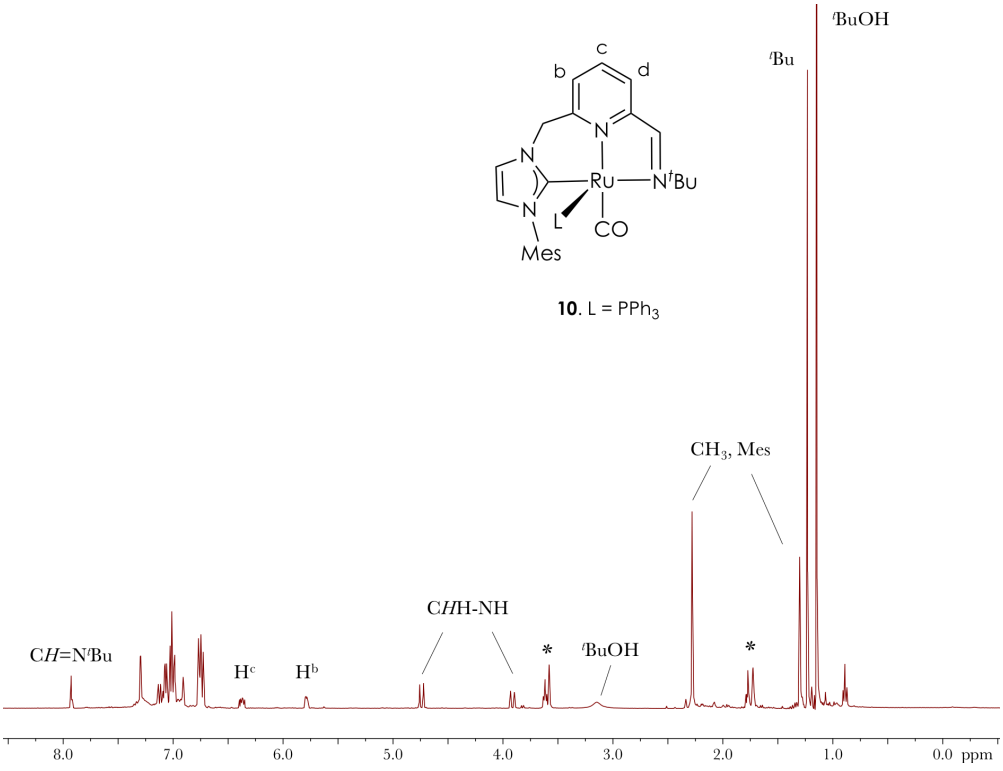

Figure 9. ^1H NMR spectrum (400 MHz, THF-d_8) of heated solution of the *in situ* formed complex **8** to yield **10** (* denotes residual THF).

In order to determine the likely formation of dihydride species from **8** and **9** potentially active in hydrogenation reactions, the reactivity of these complexes towards H_2 was examined by NMR spectroscopy. At room temperature, exposure to H_2 (3 bar) of THF-d_8 solutions of the *in situ* generated complexes **8** and **9** did not produce any observable change in the ^1H NMR experiments. On the contrary, pressurization of a solution of **8** with deuterium gas (3 bar) at room temperature led to complete H/D exchange of the hydrido ligand and the hydrogens of the methylene and methyne bridges after 1.5 h (Schemes 4). H/D scrambling of the NH could not be detected due to the overlap of the resonance with the solvent signal. Similarly, upon exposure of a THF-d_8 solution of **9** to D_2 (3 bar) at 60 °C for 24 h, partial incorporation of deuterium on the metal and into the methylene and methyne bridges was observed (Scheme 5). These observations are an indirect evidence of the ability of complexes **8** (after PPh_3 decoordination) and **9** to produce the reversible activation of H_2 in a ligand-assisted process or through the participation of an external base.

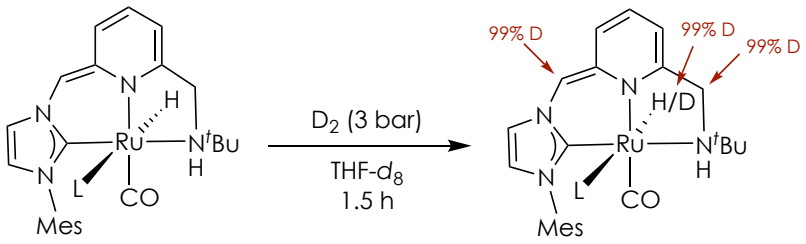

8, L = PPh_3 **8-*d***, L = PPh_3

Scheme 4. H/D scrambling in complex **8**, generated from **4a** and KO^{t}Bu (1.3 equiv), upon exposure to D_2 in THF-d_8.

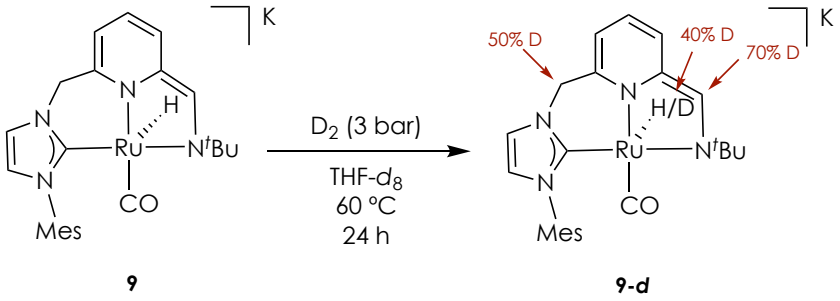

9 **9-*d***

Scheme 5. H/D scrambling in complex **9**, generated from **4a** and KHMDS (3.0 equiv), upon exposure to D_2 in THF-d_8.

Interestingly, pressurizing with H_2 solutions of the *in situ* formed complex **10** in THF-d_8 did not produce any noticeable change in the temperature range between –80 and 55 °C. Moreover, H/D exchange was not evidenced after pressurization of the same solutions with D_2 (3 bar) at 65 °C for 72 h. However, solutions containing complex **10** were found to hydrogenate 2-methylquinoxaline (10 equiv) at 65 °C (8 h), being **10** the only detectable metal species during the catalytic reaction. Furthermore, in a parallel experiment, addition of 2-methylquinoxaline (10 equiv) to a THF-d_8 solution of a 1:1 mixture of **8** and **9** produces the instantaneous formation of **10**. Subsequent pressurization with H_2 (3 bar) and heating to 65 °C of the resulting mixture brought about the hydrogenation of the *N*-containing heteroarene.

While more detailed mechanistic studies are required, the above results point out to **10** as the catalytic species in the reversible hydrogenation of *N*-heterocycles. This hypothesis implies a Ru(0)/Ru(II) catalytic cycle. Formation of carbonyl Ru(0) complexes has been shown to take place upon treatment of RuHCl(PXP)(CO) (PXP = diphosphine pincer ligand) with

strong bases,[55] and the resulting species were catalytically active in the hydrogenation of esters and the dehydrogenative coupling of alcohols. Moreover, Ru(0) complexes based on lutidine containing PNN ligands have been observed or proposed as intermediates in other unrelated metal mediated reactions.[56,57]

In our case, a plausible Ru(0)/Ru(II) mechanism for the hydrogenation of *N*-heterocycles might involve the initial decoordination of PPh_3 to form the zero-valent 16-electron complex **A** (Figure 10).[58] Subsequent oxidative addition of H_2 to **A** would yield the dihydride complex **B** capable of transfering H_2 to the substrate.[59] Since reaction of **10** with H_2 did not produce a measurable change, and **10** is the only observable species during the hydrogenation reactions, PPh_3 release from **10** to produce **A** must be significantly disfavored.

[55] (a) A. Anaby, M. Schelwies, J. Schwaben, F. Rominger, A. S. K. Hashmi, T. Schaub, *Organometallics* **2018**, *37*, 2193; (b) A. Eizawa, S. Nishimura, K. Arashiba, K. Nakajima, Y. Nishibayashi, *Organometallics* **2018**, *37*, 3086; (c) H. Salem, L. J. W. Shimon, Y. Diskin-Posner, G. Leitus, Y. Ben-David, D. Milstein, *Organometallics* **2009**, *28*, 4791; (d) M. A. Goni, E. Rosenberg, R. Gobetto, M. Chierotti, *J. Organomet. Chem.* **2017**, *845*, 213.
[56] S. Perdriau, M. Chang, E. Otten, H. J. Heeres, J. G. de Vries, *Chem. Eur. J.* **2014**, *20*, 15434.
[57] S. W. Kohl, L. Weiner, L. Schwartsburd, L. Konstantinovski, L. J. W. Shimon, Y. Ben-David, M. A. Iron, D. Milstein, *Science* **2009**, *324*, 74.
[58] M. J. Hanton, S. Tin, B. J. Boardman, P. Miller, *J. Mol. Catal. A: Chem.* **2011**, *346*, 70.
[59] (a) R. Osman, D. I. Pattison, R. N. Perutz, C. Bianchini, J. A. Casares, M. Peruzzini, *J. Am. Chem. Soc.* **1997**, *119*, 8459; (b) R. A. Diggle, S. A. Macgregor, M. K. Whittlesey, *Organometallics* **2004,** *23,* 1857.

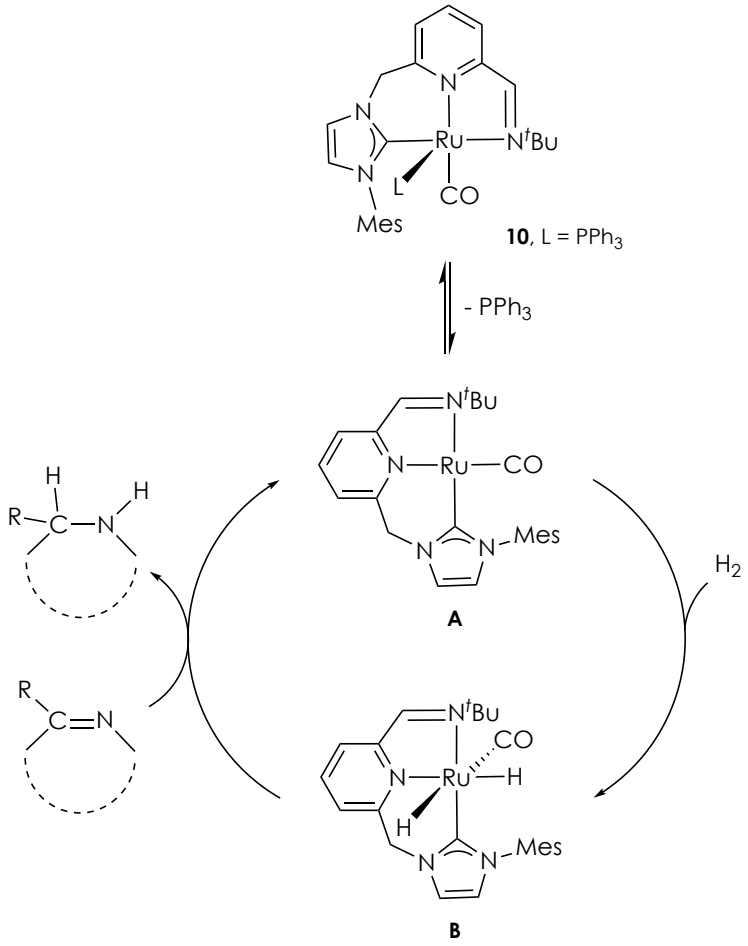

Figure 10. Plausible mechanism for the hydrogenation of *N*-heterocycles catalyzed by complex **10**.

II.3. Experimental procedures

II.3.1. General considerations

All reactions and manipulations were performed under nitrogen or argon atmosphere, either in a MBraun Unilab Pro glovebox or using standard Schlenk-type techniques.[60] All solvents were dried and distilled under nitrogen, using the following desiccants: sodium-benzophenone-ketyl for diethyl ether (Et_2O), tetrahydrofuran (THF) and 2-methyltetrahydrofuran (2-MeTHF); sodium for hexane, pentane, toluene and *o*-xylene; CaH_2 for dichloromethane (CH_2Cl_2) and acetonitrile (CH_3CN); and NaOMe for methanol (MeOH).[61] Microanalyses were performed by the Analytical Service of the Instituto de Investigaciones Químicas, using a Leco TruSpec Micro elemental analyzer. The NMR experiments were carried out on Bruker DPX-300, DRX-400, DRX-500 and Advance^{III}-400/R apparatus. The ^{1}H and ^{13}C spectra were referenced to external $SiMe_4$ using the residual proton peaks of the deuterated solvent as internal standards, while ^{31}P was referenced to external 85% H_3PO_4. Spectral assignments were made by routine one- and two-dimensional experiments, including ^{1}H-^{1}H COSY, ^{1}H-^{1}H NOESY, ^{1}H-^{13}C HSQC, ^{1}H-^{13}C HMBC and ^{31}P NMR spectroscopies. All NMR measurements were carried out at 25 °C. High resolution mass spectrometry (HRMS) data were obtained using a ThermoFisher QExactive mass spectrometer at the Analytical Services of the Universidad de Sevilla (CITIUS). ESI-MS experiments were carried out in a Bruker Esquire 6000 apparatus by the Mass Spectrometry Service of the Instituto de Investigaciones Químicas. Infrared spectra were recorded on a Bruker Tensor 27 spectrometer.

---

[60] D. F. Shriver, M. A. Dredzon, *The Manipulation of Air-Sensitive Compounds*, 2nd Edition; Wiley-Interscience, **1986**.
[61] D. D. Perrin, W. L. F. Armarego, *Purification of Laboratory Chemicals*, 2nd Edition; Pergamon Press, **1980**.

The following compounds were synthetized according to previously reported methods: 1-(2,4,6-trimethylphenyl)-1*H*-imidazole,[62] $RuHCl(CO)(PPh_3)_3$,[63] and $RuHBr(CNN^{Et})(CO)$ (**7**).[54a] All other reagents were purchased from commercial suppliers and used as received.

[62] M. C. Perry, X. Cui, M. T. Powell, D.-R. Hou, J. H. Reibenspies, K. Burgess, *J. Am. Chem. Soc.* **2003**, *125*, 113.
[63] N. Ahmad, J. J. Levison, S. D. Robinson, M. F. Uttley, E. R. Wonchoba, G. W. Parshall, *Inorg. Synth.* **1974**, *15*, 45.

II.3.2. Synthesis of imidazolium salts

1-[(6-(Bromomethyl)pyridin-2-yl)methyl]-3-mesityl-*1H*-imidazol-2-ium bromide, 1a(Br)

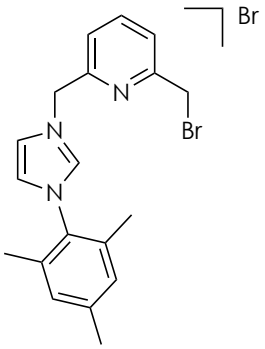

A solution of 1-mesityl-1*H*-imidazole (1.24 g, 6.6 mmol) and 2,6-bis(bromomethyl)pyridine (3.00 g, 11.3 mmol) in THF (30 mL) was stirred for 7 days. The resulting precipitate was filtered, washed with cold THF (2 × 10 mL) and hexane (2 × 10 mL) and dried under vacuum to yield a light brown solid (2.00 g, 67%). NMR spectra of the imidazolium salt **1a(Br)** are analogous to previously reported data.[54a,64]

^{1}H NMR (300 MHz, $CDCl_3$): δ 10.20 (s, 1H, H arom Imid), 8.20 (s, 1H, H arom Imid), 7.99 (d, $^3J_{HH}$ = 7.7 Hz, 1H, H arom Py), 7.80 (dd, $^3J_{HH}$ = 7.7 Hz, $^3J_{HH}$ = 7.7 Hz, 1H, H arom Py), 7.48 (d, $^3J_{HH}$ = 7.7 Hz, 1H, H arom Py), 7.20 (s, 1H, H arom Imid), 7.02 (s, 2H, H arom Mes), 6.25 (s, 2H, CH_2-Imid), 4.50 (s, 2H, CH_2Br), 2.42 (s, 3H, CH_3), 2.11 (s, 6H, 2 CH_3) ppm.

[64] C. del Pozo, M. Iglesias, F. Sanchez, *Organometallics* **2011**, *30*, 2180.

1-[(6-(*N-tert*-Butylaminomethyl)pyridin-2-yl)methyl]-3-mesityl-*1H*-imidazol-2-ium bromide, 2a

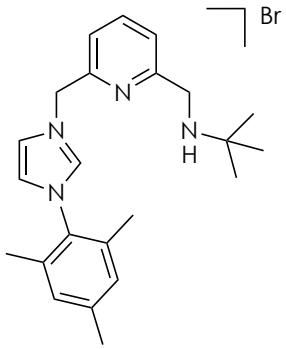

^{t}BuNH$_2$ (0.656 g, 8.98 mmol) was added to a solution of the imidazolium salt **1a(Br)** (0.810 g, 1.80 mmol) in CH_3CN (25 mL), and the resulting mixture was stirred overnight. The resulting mixture was filtered, and the solvent was evaporated under reduced pressure. The residue was washed with Et_2O (3 × 10 mL), dissolved in CH_2Cl_2 (10 mL), and treated with ScavengePore phenethyl diethylamine resin (3.50 g; 0.66 mmol/g loading). The solution was separated from the resin by filtration, brought to dryness and washed with Et_2O (3 × 10 mL). The treatment with the resin was repeated twice following the same steps. White solid (0.742 g, 93%).

^{1}H NMR (500 MHz, CD_2Cl_2): δ 10.45 (s, 1H, H arom Imid), 8.27 (s, 1H, H arom Imid), 7.77 (dd, $^3J_{HH}$ = 7.5 Hz, $^3J_{HH}$ = 7.5 Hz, 1H, H arom Py), 7.70 (d, $^3J_{HH}$ = 7.5 Hz, 1H, H arom Py), 7.53 (d, $^3J_{HH}$ = 7.5 Hz, 1H, H arom Py), 7.20 (s, 1H, H arom Imid), 7.08 (s, 2H, 2 H arom Mes), 5.97 (s, 2H, CH_2-Imid), 5.22 (br s, 1H, NH), 4.07 (s, 2H, CH_2NH), 2.39 (s, 3H, CH_3), 2.13 (s, 6H, 2 CH_3), 1.41 (s, 9H, C(CH_3)$_3$) ppm.

^{13}C{^{1}H} NMR (126 MHz, CD_2Cl_2): δ 156.3 (C_q arom), 152.0 (C_q arom),

141.2 (C_q arom), 138.5 (CH arom), 138.1 (CH arom), 134.4 (2 C_q arom), 130.9 (C_q arom), 129.7 (2 CH arom), 124.1 (CH arom), 123.3 (CH arom), 122.6 (CH arom), 122.6 (CH arom), 54.9 ($C(CH_3)_3$), 53.5 (overlapped with deuterated solvent signal, CH_2-Imid), 46.9 (CH_2NH), 27.1 ($C(CH_3)_3$), 20.8 (CH_3), 17.6 (2 CH_3) ppm.

HRMS (ESI): *m/z* calcd for $C_{23}H_{31}N_4$ $[(M-Br)^+]$: 363.2543; found: 363.2540.

1-[(6-(*N*-Benzylaminomethyl)pyridin-2-yl)methyl]-3-mesityl-*1H*-imidazol-2-ium bromide, 2b

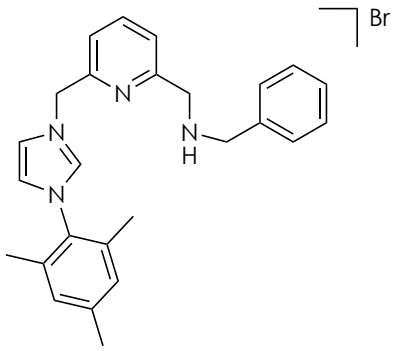

Benzylamine (0.143 g, 1.33 mmol) was added to a solution of the imidazolium salt **1a(Br)** (0.200 g, 0.44 mmol) in CH_3CN (12 mL), and the mixture was stirred overnight. The solvent was evaporated, and the residue was extracted with CH_2Cl_2 (2 × 10 mL). The solution was brought to dryness, and the residue was washed with Et_2O (2 × 10 mL) and pentane (2 × 10 mL) giving a white solid (0.133 g, 63%).[65]

^{1}H NMR (300 MHz, CD_2Cl_2): δ 10.30 (s, 1H, H arom Imid), 8.04 (s, 1H, H arom Imid), 7.76 (dd, $^3J_{HH}$ = 7.5 Hz, $^3J_{HH}$ = 7.5 Hz, 1H, H arom Py), 7.69 (d, $^3J_{HH}$ = 7.5 Hz, 1H, H arom Py), 7.41 (d, $^3J_{HH}$ = 7.2 Hz, 2H, 2 H arom CH_2Ph), 7.37 (d, $^3J_{HH}$ = 7.5 Hz, 1H, H arom Py), 7.30 (m, 3H, 3 H arom CH_2Ph), 7.13 (s, 1H, H arom Imid), 7.04 (s, 2H, 2 H arom Mes), 5.99 (s, 2H, CH_2-Imid), 3.92 (s, 2H, C*H*$_2$NH), 3.89 (s, 2H, C*H*$_2$NH), 2.64 (br s, 1H, NH), 2.36 (s, 3H, CH_3), 2.05 (s, 6H, 2 CH_3) ppm.

^{13}C{^{1}H} NMR (101 MHz, CD_2Cl_2): δ 159.4 (C_q arom), 152.4 (C_q arom), 141.7 (C_q arom), 138.9 (C_q arom), 138.7 (CH arom), 138.4 (CH arom), 134.8

[65] José Mª Gordón Pidal, *Trabajo Fin de Grado*. Universidad de Sevilla, **2017**.

(2 C_q arom), 131.2 (C_q arom), 130.1 (2 CH arom), 129.1 (2 CH arom), 128.8 (2 CH arom), 127.7 (CH arom), 124.1 (CH arom), 123.0 (CH arom), 122.9 (CH arom), 122.4 (CH arom), 54.2 (CH_2-Imid), 53.6 (CH_2NH), 53.1 (CH_2NH), 21.2 (CH_3), 17.8 (2 CH_3) ppm.

HRMS (ESI): *m/z* calcd for $C_{26}H_{29}N_4$ $[(M-Br)^+]$: 397.2392; found: 397.2387.

1-[(6-(*N*-Phenylaminomethyl)pyridin-2-yl)methyl]-3-mesityl-*1H*-imidazol-2-ium bromide, 2c

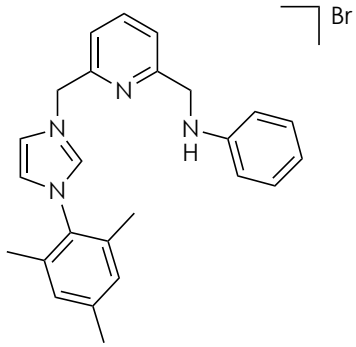

Aniline (0.433 g, 4.65 mmol) was added to a solution of the imidazolium salt **1a(Br)** (0.700 g, 1.55 mmol) in CH_3CN (15 mL), and the resulting mixture was stirred overnight. The mixture was filtered, and brought to dryness. The resulting residue was extracted with CH_2Cl_2 (2 × 10 mL), the solvent was evaporated under reduced pressure, and the solid was washed with Et_2O (2 × 10 mL) and pentane (2 × 10 mL). White solid (0.650 g, 90%).

^{1}H NMR (400 MHz, CD_2Cl_2): δ 10.29 (s, 1H, H arom Imid), 8.02 (s, 1H, H arom Imid), 7.73 (m, 2H, 2 H arom), 7.38 (d, $^3J_{HH}$ = 6.7 Hz, 1H, H arom Py), 7.14 (m, 3H, 3 H arom), 7.06 (s, 2H, 2 H arom Mes), 6.71 (m, 3H, 3 H arom), 6.07 (s, 2H, CH_2-Imid), 4.85 (br, 1H, NH), 4.44 (s, 2H, C*H*$_2$NH), 2.39 (s, 3H, CH_3), 2.09 (s, 6H, 2 CH_3) ppm.

^{13}C{^{1}H} NMR (101 MHz, CD_2Cl_2): δ 159.0 (C_q arom), 152.2 (C_q arom), 147.4 (C_q arom), 141.3 (C_q arom), 138.3 (CH arom), 138.1 (CH arom), 134.4 (2 C_q arom), 130.8 (C_q arom), 129.7 (2 CH arom), 129.1 (2 CH arom), 123.8 (CH arom), 122.6 (CH arom), 122.0 (CH arom), 121.9 (CH arom), 117.9

(CH arom), 113.4 (2 CH arom), 53.4 (overlapped with deuterated solvent signal, CH_2-Imid), 49.3 (CH_2NH), 20.8 (CH_3), 17.4 (2 CH_3) ppm.

HRMS (ESI): *m/z* calcd for $C_{25}H_{27}N_4$ $[(M-Br)^+]$: 383.2230; found: 383.2224.

II.3.3. Synthesis of Ag-CNN(H) complexes

Ag(CNN(H)^{tBu})Br (3a)

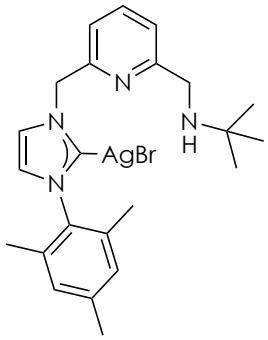

In the dark, dichloromethane (10 mL) was added to a mixture of **2a** (0.742 g, 1.35 mmol) and Ag_2O (0.250 g, 1.08 mmol). The resulting suspension was stirred overnight, filtered, and brought to dryness to give a light brown solid (0.861 g, 93%).

Anal. calcd (%) for $C_{23}H_{30}AgBrN_4$: C 50.2, H 5.5, N 10.2; found: C 50.4, H 5.2, N 9.8.

^{1}H NMR (400 MHz, CD_2Cl_2): δ 7.72 (dd, $^3J_{HH}$ = 7.5 Hz, $^3J_{HH}$ = 7.5 Hz, 1H, H arom Py), 7.39 (s, 1H, H arom NHC), 7.38 (d, $^3J_{HH}$ = 7.5 Hz, 1H, H arom Py), 7.12 (d, $^3J_{HH}$ = 7.5 Hz, 1H, H arom Py), 7.05 (s, 1H, H arom NHC), 7.05 (s, 2H, 2 H arom Mes), 5.53 (s, 2H, CH_2-NHC), 3.90 (br d, $^3J_{HH}$ = 4.7 Hz, 2H, CH_2NH), 2.40 (s, 3H, CH_3), 2.04 (s, 6H, 2 CH_3), 1.65 (br, 1H, NH), 1.19 (s, 9H, C(CH_3)$_3$) ppm.

^{13}C{^{1}H} NMR (101 MHz, CD_2Cl_2): δ 162.1 (C_q arom), 154.9 (C_q arom), 140.0 (C_q arom), 138.0 (CH arom), 136.0 (C_q arom), 135.3 (2 C_q arom), 129.7 (2 CH arom), 123.2 (CH arom), 122.4 (CH arom), 122.2 (CH arom),

120.1 (CH arom), 57.5 (CH_2-NHC), 50.9 ($C(CH_3)_3$), 48.8 (CH_2NH), 29.3 ($C(CH_3)_3$), 21.2 (CH_3), 17.9 (2 CH_3) ppm. Due to significant signal broadening, the chemical shift for the C-2 NHC carbon was determined from the ^{1}H-^{13}C HMBC experiment, appearing at 183.1 ppm.

Ag(CNN(H)^{Bn})Br (3b)

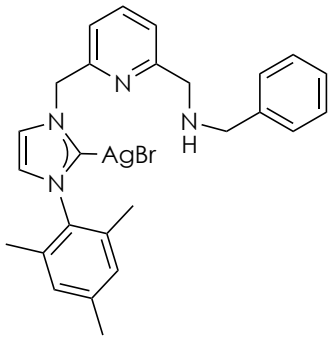

Silver complex **3b** was synthetized as described above for **3a** but using **2b**. Brown solid (0.065 g, 40%). Satisfactory elemental analysis for complex **3b** could not be obtained.

^{1}H NMR (400 MHz, CD_2Cl_2): δ 7.68 (dd, $^3J_{HH}$ = 7.6 Hz, $^3J_{HH}$ = 7.6 Hz, 1H, H arom Py), 7.35 (m, 3H, 3 H arom), 7.30 (m, 3H, 3 H arom), 7.25 (m, 1H, H arom), 7.08 (d, $^3J_{HH}$ = 7.6 Hz, 1H, H arom Py), 6.99 (m, 3H, 3 H arom), 5.45 (s, 2H, CH_2-NHC), 3.88 (br d, $^3J_{HH}$ = 6.5 Hz, 2H, CH_2NH), 3.81 (br d, $^3J_{HH}$ = 6.0 Hz, 2H, CH_2NH), 2.35 (s, 3H, CH_3), 2.15 (br m, 1H, NH), 1.95 (s, 6H, 2 CH_3) ppm.

DEPT ^{13}C NMR (101 MHz, CD_2Cl_2): δ 183.5 (br, C-2 NHC), 160.9 (C_q arom), 155.1 (C_q arom), 140.9 (C_q arom), 139.8 (C_q arom), 138.0 (CH arom), 135.9 (C_q arom), 135.2 (2 C_q arom), 129.6 (2 CH arom), 128.6 (2 CH arom), 128.5 (2 CH arom), 127.2 (CH arom), 123.2 (CH arom), 122.5 (CH arom), 122.1 (CH arom), 120.3 (CH arom), 57.3 (CH_2-NHC), 54.6 (CH_2NH), 53.7 (CH_2NH), 21.2 (CH_3), 17.8 (2 CH_3) ppm.

Ag(CNN(H)^{Ph})Br (3c)

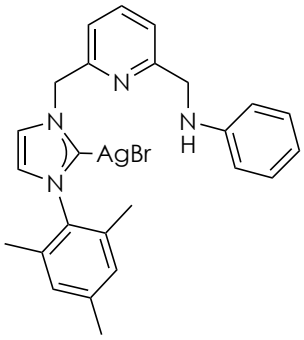

Silver complex **3c** was prepared as described above for **3a** but using **2c**. Brown solid (0.195 g, 79%).

Anal. calcd (%) for $C_{25}H_{26}AgBrN_4$: C 52.6, H 4.6, N 9.8; found: C 52.3, H 4.8, N 10.2.

^{1}H NMR (400 MHz, CD_2Cl_2): δ 7.71 (dd, $^3J_{HH}$ = 7.6 Hz, $^3J_{HH}$ = 7.6 Hz, 1H, H arom Py), 7.40 (d, $^3J_{HH}$ = 1.4 Hz, 1H, H arom NHC), 7.36 (d, $^3J_{HH}$ = 7.8 Hz, 1H, H arom Py), 7.16 (m, 3H, 3 H arom), 7.04 (m, 3H, 3 H arom), 6.70 (m, 3H, 3 H arom), 5.50 (s, 2H, CH_2-NHC), 5.01 (br t, $^3J_{HH}$ = 5.6 Hz, 1H, NH), 4.46 (br d, $^3J_{HH}$ = 5.6 Hz, 2H, CH_2NH), 2.40 (s, 3H, CH_3), 2.00 (s, 6H, 2 CH_3) ppm.

DEPT ^{13}C NMR (101 MHz, CD_2Cl_2): δ 183.6 (C-2 NHC), 159.4 (C_q arom), 155.0 (C_q arom), 148.3 (C_q arom), 139.8 (C_q arom), 138.1 (CH arom), 135.9 (C_q arom), 135.2 (2 C_q arom), 129.6 (2 CH arom), 129.5 (2 CH arom), 123.2 (CH arom), 122.5 (CH arom), 121.6 (CH arom), 120.5 (CH arom), 117.6 (CH arom), 113.2 (2 CH arom), 57.1 (CH_2-NHC), 49.2 (CH_2NH), 21.2 (CH_3), 17.8 (2 CH_3) ppm.

II.3.4. Synthesis of Ru-CNN(H) complexes

[RuH(CNN(H)^{tBu})(CO)(PPh$_3$)]BF$_4$ (4a)

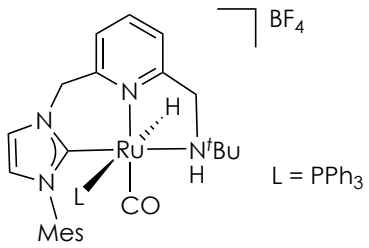

A suspension of **3a** (0.400 g, 0.73 mmol) and RuHCl(CO)(PPh$_3$)$_3$ (0.692 g, 0.73 mmol) in THF (30 mL) was heated to 55 ºC for 24 h. The solution was filtered, and the solvent was evaporated under reduced pressure. The resulting residue was extracted with MeOH (2 × 10 mL), solvent was removed and the obtained solid was dried under vacuum. To this solid PPh$_3$ (0.210 g, 0.80 mmol), NaBF$_4$ (0.087 g, 0.80 mmol) and CH$_3$CN (15 mL) were added, and the resulting mixture was stirred overnight. The solvent was evaporated, and the residue was extracted with CH_2Cl_2 (2 × 10 mL), precipitated by addition of toluene (10 mL) and washed with pentane (2 × 10 mL). Whitish solid (0.536 g, 88%). Crystals of **4a** suitable for X-ray diffraction analysis were grown from a saturated solution of the complex in CH_2Cl_2.

Anal. calcd (%) for $C_{42}H_{46}BF_4N_4OPRu$: C 59.9, H 5.5, N 6.7; found: C 59.8, H 5.3, N 6.8.

^{1}H NMR (400 MHz, CD_2Cl_2): δ 7.83 (dd, $^3J_{HH}$ = 7.7 Hz, $^3J_{HH}$ = 7.7 Hz, 1H, H arom Py), 7.42 (m, 5H, 3 H arom PPh$_3$ + 2 H arom Py), 7.38 (d, $^3J_{HH}$ = 1.9 Hz, 1H, H arom NHC), 7.31 (ddd, $^3J_{HH}$ = 7.4 Hz, $^3J_{HH}$ = 7.4 Hz, $^4J_{HP}$

= 1.2 Hz, 6H, 6 H arom PPh_3), 7.13 (dd, $^3J_{HH}$ = 8.0 Hz, $^3J_{HP}$ = 8.0 Hz, 6H, 6 H arom PPh_3), 7.06 (s, 1H, H arom Mes), 7.02 (s, 1H, H arom Mes), 6.93 (d, $^3J_{HH}$ = 1.9 Hz, 1H, H arom NHC), 5.00 (d, $^2J_{HH}$ = 16.1 Hz, 1H, C*H*H-NHC), 4.21 (d, $^2J_{HH}$ = 15.6 Hz, 1H, C*H*H-NHC), 4.18 (dd, $^2J_{HH}$ = 14.7 Hz, $^3J_{HH}$ = 3.7 Hz, 1H, C*H*HNH), 3.95 (dd, $^2J_{HH}$ = 14.2 Hz, $^3J_{HH}$ = 12.6 Hz, 1H, C*H*HNH), 2.71 (br ddd, $^3J_{HH}$ = 12.2 Hz, $^3J_{HH}$ = 3.4 Hz, $^3J_{HP}$ = 3.4 Hz, 1H, NH), 2.40 (s, 3H, CH_3), 2.21 (s, 3H, CH_3), 2.04 (s, 3H, CH_3), 0.98 (s, 9H, $C(CH_3)_3$), −7.79 (d, $^2J_{HP}$ = 114.0 Hz, 1H, RuH) ppm.

$^{31}P\{^1H\}$ NMR (121 MHz, CD_2Cl_2): δ 22.5 ppm.

$^{13}C\{^1H\}$ NMR (101 MHz, CD_2Cl_2): δ 208.3 (d, J_{CP} = 6 Hz, CO), 185.2 (d, J_{CP} = 5 Hz, C-2 NHC), 161.1 (C_q arom), 154.3 (C_q arom), 139.7 (C_q arom), 139.0 (CH arom), 137.2 (C_q arom), 136.6 (C_q arom), 136.6 (C_q arom), 134.6 (d, J_{CP} = 27 Hz, 3 C_q arom), 132.9 (d, J_{CP} = 11 Hz, 6 CH arom), 130.5 (3 CH arom), 129.6 (CH arom), 129.3 (CH arom), 129.3 (d, J_{CP} = 8 Hz, 6 CH arom), 123.9 (CH arom), 123.4 (CH arom), 123.2 (CH arom), 121.8 (CH arom), 57.8 ($C(CH_3)_3$), 55.5 (CH_2NH), 54.4 (CH_2-NHC), 28.4 ($C(CH_3)_3$), 21.2 (CH_3), 19.3 (CH_3), 19.1 (CH_3) ppm.

IR (Nujol): 1933 cm^{-1} (ν_{CO}).

[RuH(CNN(H)^{Bn})(CO)(PPh$_3$)]BF$_4$ (4b)

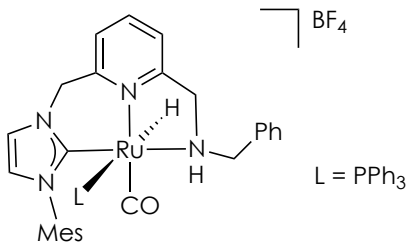

A suspension of **3b** (0.207 g, 0.35 mmol) and RuHCl(CO)(PPh$_3$)$_3$ (0.337 g, 0.35 mmol) in THF (15 mL) was heated to 55 °C for 24 h. The solution was filtered, and the solvent was evaporated under reduced pressure. The resulting residue was extracted with MeOH (2 × 10 mL), and the solvent was evaporated under vacuum. To the resulting solid, PPh$_3$ (0.102 g, 0.39 mmol), NaBF$_4$ (0.046 g, 0.43 mmol) and CH$_3$CN (8 mL) were added, and the mixture was stirred overnight. The solvent was evaporated, and the residue was extracted with CH$_2$Cl$_2$ (2 × 10 mL) and precipitated by addition of toluene. Crystallization from MeOH and subsequent washing with Et$_2$O (2 × 10 mL) of the complex yielded **4b** as a light brown solid (0.121 g, 39%). Crystals of **4b** suitable for X-ray diffraction analysis were grown from a saturated solution of the complex in MeOH.

Anal. calcd (%) for C$_{45}$H$_{44}$BF$_4$N$_4$OPRu: C 61.7, H 5.1, N 6.4; found: C 61.8, H 4.9, N 6.4.

^{1}H NMR (400 MHz, CD$_2$Cl$_2$): δ 7.83 (dd, $^3J_{HH}$ = 7.7 Hz, $^3J_{HH}$ = 7.7 Hz, 1H, H arom Py), 7.50 (d, $^3J_{HH}$ = 2.0 Hz, 1H, H arom NHC), 7.46 (m, 2H, 2 H arom), 7.40 (d, $^3J_{HH}$ = 7.7 Hz, 1H, H arom Py), 7.32 (m, 10 H, 10 H arom), 7.02 (s, 1H, H arom Mes), 6.92 (m, 7 H, 7 H arom), 6.88 (s, 1H, H arom Mes), 6.86 (d, $^3J_{HH}$ = 2.0 Hz, 1H, H arom NHC), 6.62 (m, 2H, 2 H

arom), 5.20 (d, $^{2}J_{HH}$ = 16.0 Hz, 1H, C*H*H-NHC), 4.34 (d, $^{2}J_{HH}$ = 16.0 Hz, 1H, C*H*H-NHC), 4.00 (m, 2H, Py-C*H*HNH + NC*H*HPh), 3.83 (m, 2H, Py-C*H*HNH + NC*H*HPh), 2.87 (br dd, $^{3}J_{HH}$ = 11.0 Hz, $^{3}J_{HH}$ = 11.0 Hz, 1H, NH), 2.33 (s, 3H, CH_3), 1.97 (s, 3H, CH_3), 1.85 (s, 3H, CH_3), −7.30 (d, $^{2}J_{HP}$ = 109.9 Hz, 1H, RuH) ppm.

$^{31}P\{^{1}H\}$ NMR (162 MHz, CD_2Cl_2): δ 24.5 ppm.

$^{13}C\{^{1}H\}$ NMR (101 MHz, CD_2Cl_2): δ 206.8 (d, J_{CP} = 7 Hz, CO), 186.2 (d, J_{CP} = 5 Hz, C-2 NHC), 159.9 (C_q arom), 154.9 (C_q arom), 139.5 (C_q arom), 139.1 (CH arom), 137.1 (C_q arom), 136.7 (2 C_q arom), 136.4 (C_q arom), 134.0 (d, J_{CP} = 28 Hz, 3 C_q arom), 132.9 (d, J_{CP} = 11 Hz, 6 CH arom), 130.8 (3 CH arom), 129.6 (m, 9 CH arom), 129.2 (CH arom), 129.1 (CH arom), 128.8 (2 CH arom), 124.9 (CH arom), 123.2 (CH arom), 123.0 (CH arom), 121.6 (CH arom), 63.0 (CH_2NH), 59.9 (CH_2NH), 54.5 (CH_2-NHC), 21.2 (CH_3), 19.2 (CH_3), 18.9 (CH_3) ppm.

IR (Nujol): 1936 cm^{-1} (ν_{CO}).

[RuH(CNN(H)^{Ph})(CO)(PPh$_3$)]BF$_4$ (4c)

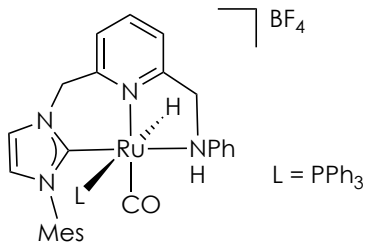

A suspension of **3c** (0.195 g, 0.34 mmol) and RuHCl(CO)(PPh$_3$)$_3$ (0.326 g, 0.34 mmol) in THF (12 mL) was heated to 55 ºC for 24 h. The solution was filtered, and the solvent was evaporated under reduced pressure. The resulting residue was extracted with MeOH (2 × 10 mL), solvent was removed and the obtained solid was dried under vacuum. To this solid PPh$_3$ (0.098 g, 0.38 mmol), NaBF$_4$ (0.045 g, 0.41 mmol) and CH$_3$CN (8 mL) were added, and the mixture was stirred overnight. The solvent was evaporated, and the residue was extracted with CH$_2$Cl$_2$ (2 × 10 mL) and precipitated with toluene (2 × 10 mL). Crystallization from MeOH and subsequent washing with Et$_2$O (2 × 10 mL) of the complex yielded **4c** as a light brown solid (0.104 g, 35%).

^{1}H NMR (400 MHz, CD$_2$Cl$_2$): δ 7.92 (dd, $^3J_{HH}$ = 7.7 Hz, $^3J_{HH}$ = 7.7 Hz, 1H, H arom Py), 7.50 (m, 2H, 2 H arom), 7.42 (m, 4H, 4 H arom), 7.24 (m, 8H, 8 H arom), 7.02 (s, 1H, H arom), 6.82 (m, 10H, 10 H arom), 6.76 (s, 1H, H arom), 5.15 (d, $^2J_{HH}$ = 15.6 Hz, 1H, C*H*H-NHC), 4.54 (m, 3H, 2 C*H*HNH + NH), 4.40 (d, $^2J_{HH}$ = 15.6 Hz, 1H, C*H*H-NHC), 2.29 (s, 3H, CH$_3$), 2.03 (s, 3H, CH$_3$), 1.78 (s, 3H, CH$_3$), −7.05 (d, $^2J_{HP}$ = 110.7 Hz, 1H, RuH) ppm.

^{31}P{^{1}H} NMR (162 MHz, CD$_2$Cl$_2$): δ 23.6 ppm.

$^{13}C\{^{1}H\}$ NMR (101 MHz, CD_2Cl_2): δ 205.6 (d, J_{CP} = 7 Hz, CO), 185.8 (d, J_{CP} = 4 Hz, C-2 NHC), 159.6 (C_q arom), 154.7 (C_q arom), 147.1 (C_q arom), 139.6 (C_q arom), 139.2 (CH arom), 137.0 (C_q arom), 136.6 (C_q arom), 136.4 (C_q arom), 133.6 (d, J_{CP} = 29 Hz, 3 C_q arom), 133.3 (d, J_{CP} = 11 Hz, 6 CH arom), 130.7 (3 CH arom), 129.5 (m, 9 CH arom), 129.1 (CH arom), 126.7 (CH arom), 124.7 (CH arom), 123.3 (CH arom), 123.1 (CH arom), 122.8 (2 CH arom), 122.0 (CH arom), 65.6 (CH_2NH), 54.6 (CH_2-NHC), 21.1 (CH_3), 19.1 (CH_3), 18.8 (CH_3) ppm.

IR (Nujol): 1958 cm^{-1} (ν_{CO}).

HRMS (ESI): *m/z* calcd for $C_{44}H_{42}N_4OPRu$ $[(M-BF_4)^+]$: 775.2140; found: 775.2133.

Complex 8

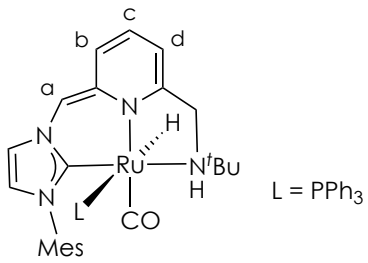

In a J.Young valved NMR tube, THF-d_8 (0.5 mL) was added to a mixture of **4a** (0.023 g, 0.027 mmol) and KO^{t}Bu (0.004 g, 0.035 mmol), giving rise to the immediate formation of a dark red solution. The resulting sample was analyzed by NMR spectroscopy. Attempted isolation of complex **8** was unsuccessful due to significant decomposition during work-up.

^{1}H NMR (400 MHz, THF-d_8): δ 7.32 (m, 15H, 15 H arom Ph), 6.94 (s, 1H, H arom Mes), 6.81 (s, 1H, H arom Mes), 6.75 (d, $^3J_{HH}$ = 1.9 Hz, 1H, H arom NHC), 6.65 (d, $^3J_{HH}$ = 1.9 Hz, 1H, H arom NHC), 6.09 (dd, $^3J_{HH}$ = 9.0 Hz, $^3J_{HH}$ = 6.1 Hz, 1H, H^c), 5.14 (d, $^3J_{HH}$ = 6.0 Hz, 1H, H^d), 5.08 (d, $^3J_{HH}$ = 9.0 Hz, 1H, H^b), 4.38 (s, 1H, H^a), 3.43 (dd, $^2J_{HH}$ = 12.0 Hz, $^3J_{HH}$ = 12.0 Hz, 1H, C*H*HNH), 3.09 (dd, $^2J_{HH}$ = 11.3 Hz, $^3J_{HH}$ = 1.9 Hz, 1H, C*H*HNH), 2.31 (s, 3H, CH_3), 2.12 (s, 3H, CH_3), 1.76 (overlapped with solvent signal, NH), 1.73 (s, 3H, CH_3), 0.93 (s, 9H, $C(CH_3)_3$), −7.64 (d, $^2J_{HP}$ = 140.2 Hz, 1H, RuH) ppm.

^{31}P{^{1}H} NMR (121 MHz, THF-d_8): δ 16.0 (br) ppm.

^{13}C{^{1}H} NMR (101 MHz, THF-d_8): δ 210.2 (CO), 177.3 (C-2 NHC), 155.7 (C_q arom), 143.0 (C_q arom), 137.9 (C_q arom), 137.7 (C_q arom), 137.6 (C_q arom), 137.4 (C_q arom), 133.6 (d, J_{CP} = 16 Hz, 6 CH arom PPh_3), 129.0 (m,

C^c + 10 CH arom + 3 C_q arom PPh_3), 120.8 (2 CH arom), 120.0 (CH arom), 111.8 (C^b), 96.8 (C^d), 90.9 (C^a), 55.6 ($C(CH_3)_3$), 54.7 (CH_2NH), 28.4 ($C(CH_3)_3$), 21.1 (CH_3), 19.2 (CH_3), 18.7 (CH_3) ppm.

Complex 9

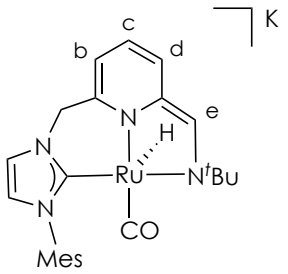

In a J.Young valved NMR tube, THF-d_8 (0.5 mL) was added to a mixture of **4a** (0.025 g, 0.030 mmol) and KHMDS (0.018 g, 0.090 mmol) giving rise initially to a dark red solution that gradually evolves to dark violet. The resulting solution was analyzed by NMR spectroscopy after 24 h. Attempted isolation of complex **9** was unsuccessful due to significant decomposition during work-up.

^{1}H NMR (400 MHz, THF-d_8): δ 7.05 (d, $^3J_{HH}$ = 2.0 Hz, 1H, H arom NHC), 6.80 (s, 1H, H arom Mes), 6.74 (s, 1H, H arom Mes), 6.69 (s, 1H, H^e), 6.59 (d, $^3J_{HH}$ = 2.0 Hz, 1H, H arom NHC), 6.54 (d, $^3J_{HH}$ = 8.9 Hz, 1H, H^b), 5.83 (dd, $^3J_{HH}$ = 8.9 Hz, $^3J_{HH}$ = 5.7 Hz, 1H, H^c), 5.33 (d, $^3J_{HH}$ = 5.7 Hz, 1H, H^d), 4.83 (d, $^2J_{HH}$ = 12.7 Hz, 1H, C*H*H-NHC), 4.56 (d, $^2J_{HH}$ = 12.7 Hz, 1H, C*H*H-NHC), 2.26 (s, 3H, CH_3), 2.02 (s, 3H, CH_3), 1.57 (s, 3H, CH_3), 1.50 (s, 9H, C(CH_3)$_3$), −17.09 (s, 1H, RuH) ppm.

^{13}C{^{1}H} NMR (101 MHz, THF-d_8): δ 213.7 (CO), 195.6 (C-2 NHC), 150.2 (C_q arom), 138.7 (C_q arom), 137.3 (C_q arom), 137.2 (C_q arom), 137.0 (C_q arom), 135.0 (C_q arom), 128.7 (2 CH arom), 120.4 (2 CH arom), 119.3 (C^b), 117.6 (C^e), 116.7 (C^c), 95.9 (C^d), 59.6 (*C*(CH_3)$_3$), 57.6 (CH_2-NHC), 35.9 (C(*C*H_3)$_3$), 21.1 (CH_3), 20.5 (CH_3), 18.4 (CH_3) ppm.

Complex 10

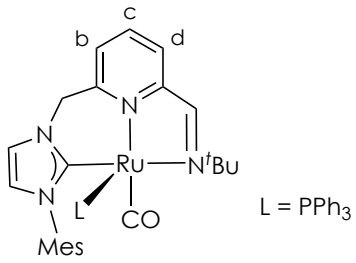

In a J.Young valved NMR tube, THF-d_8 (0.5 mL) was added to a mixture of **4a** (0.022 g, 0.026 mmol) and KO^{t}Bu (0.0038 g, 0.034 mmol) forming a dark red solution. Heating the resulting mixture to 60 °C for 24 h produced a dark blue solution that was analyzed by NMR spectroscopy. Attempted isolation of **10** was unsuccessful due to decomposition of the complex during work-up.

^{1}H NMR (400 MHz, THF-d_8): δ 7.92 (d, $^4J_{HP}$ = 3.7 Hz, 1H, C*H*=N^{t}Bu), 7.30 (d, $^3J_{HH}$ = 2.0 Hz, 1H, H arom NHC), 7.12 (d, $^3J_{HH}$ = 8.5 Hz, 1H, H^d), 7.07 (m, 3H, 3 H arom PPh$_3$), 7.00 (m, 7H, 6 H arom PPh$_3$ + H arom NHC), 6.91 (s, 1H, H arom Mes), 6.75 (m, 7H, 6 H arom PPh$_3$ + H arom Mes), 6.37 (ddd, $^3J_{HH}$ = 8.5 Hz, $^3J_{HH}$ = 6.4 Hz, $^6J_{HP}$ = 4.3 Hz, 1H, H^c), 5.79 (dd, $^3J_{HH}$ = 6.4 Hz, $^5J_{HP}$ = 3.1 Hz, 1H, H^b), 4.74 (d, $^2J_{HH}$ = 14.0 Hz, 1H, C*H*H-NHC), 3.91 (d, $^2J_{HH}$ = 13.9 Hz, 1H, C*H*H-NHC), 2.28 (s, 6H, 2 CH$_3$), 1.30 (s, 3H, CH$_3$), 1.23 (s, 9H, C(CH$_3$)$_3$) ppm.

^{31}P{^{1}H} NMR (162 MHz, THF-d_8): δ 50.5 ppm.

^{13}C{^{1}H} NMR (101 MHz, THF-d_8): δ 216.1 (d, J_{CP} = 10 Hz, CO), 191.3 (d, J_{CP} = 7 Hz, C-2 NHC), 148.1 (C$_q$ arom), 143.1 (C$_q$ arom), 139.8 (d, J_{CP} = 34 Hz, 3 C$_q$ arom), 138.6 (C$_q$ arom), 138.3 (C$_q$ arom), 137.0 (C$_q$ arom), 136.7

(C_q arom), 132.9 (d, J_{CP} = 11 Hz, 6 CH arom PPh_3), 131.8 (d, J_{CP} = 3 Hz, *C*H=N^{t}Bu), 129.4 (CH arom), 129.3 (CH arom), 128.1 (3 CH arom PPh_3), 127.8 (d, J_{CP} = 9 Hz, 6 CH arom PPh_3), 123.5 (CH arom), 122.8 (d, J_{CP} = 5 Hz, C^d), 121.6 (CH arom), 119.6 (d, J_{CP} = 4 Hz, C^c), 107.5 (C^b), 63.1 (d, J_{CP} = 4 Hz, *C*(CH_3)$_3$), 56.4 (CH_2-NHC), 33.9 (d, J_{CP} = 3 Hz, C(*C*H_3)$_3$), 21.0 (CH_3), 20.3 (CH_3), 19.0 (CH_3) ppm.

II.3.5. Catalytic reactions

Representative procedure for the hydrogenation of *N*-heterocycles

In a glovebox, a Fischer–Porter vessel was charged with a solution of complex **4a** (1.0 mg, 1.2 μmol), KO^{t}Bu (1.3 mg, 12 μmol) and quinoxaline (0.031 g, 0.24 mmol) in 2-methyltetrahydrofuran (1.0 mL). The reactor was purged three times with H_2, and finally pressurized to 4 bar and heated to 80 ^{o}C. After 6 h, the reactor was slowly cooled down to room temperature and depressurized. The reaction solution was evaporated, and conversion was determined by ^{1}H NMR spectroscopy using mesitylene as internal standard.

Representative procedure for the dehydrogenation of *N*-heterocycles

In a glovebox, a Schlenk tube was charged with a solution of complex **4a** (4.0 mg, 4.7 μmol), KO^{t}Bu (8.0 mg, 71 μmol) and tetrahydroquinoxaline (17.6 mg, 119 μmol) in 2-MeTHF (1.0 mL). A reflux condenser was adapted to the Schlenk tube, and the solution was heated to 85 ^{o}C under N_2. After 24 h, the reaction solution was evaporated, and conversion was determined by ^{1}H NMR spectroscopy using mesitylene as internal standard.

II.4. Bibliography

1) (a) B. Zhao, Z. Han, K. Ding, *Angew. Chem. Int. Ed.* **2013**, *52*, 4744; (b) T. Ikariya, *Bull. Chem. Soc. Jpn.* **2011**, *84*, 1.

2) (a) J. L. van der Vlugt, J. N. H. Reek, *Angew. Chem. Int. Ed.* **2009**, *48*, 8832; (b) C. Gunanathan, D. Milstein, *Acc. Chem. Res.* **2011**, *44*, 588; (c) D. Milstein, *Phil. Trans. R. Soc. A* **2015**, *373*, 20140189.

3) E. Fogler, J. A. Garg, P. Hu, G. Leitus, L. J. W. Shimon, D. Milstein, *Chem. Eur. J.* **2014**, *20*, 15727.

4) C. Hou, J. Jiang, Y. Li, C. Zhao, Z. Ke, *ACS Catal.* **2017**, *7*, 786.

5) P. Hu, E. Fogler, Y. Diskin-Posner, M. A. Iron, D. Milstein, *Nat. Commun.* **2015**, *6*, 6859.

6) A. Kumar, T. Janes , N. A. Espinosa-Jalapa, D. Milstein, *J. Am. Chem. Soc.* **2018**, *140*, 7453.

7) (a) X. Tan, Y. Wang, Y. Liu, F. Wang, L. Shi, K-H. Lee, Z. Lin, H. Lv, X. Zhang, *Org. Lett.* **2015**, *17*, 454; (b) F. Wang, X. Tan, H. Lv, X. Zhang, *Chem. Asian J.* **2016**, *11*, 2103.

8) L. Shi, X. Tan, J. Long, X. Xiong, S. Yang, P. Xue, H. Lv, X. Zhang, *Chem. Eur. J.* **2017**, *23*, 546.

9) X. Wu, L. Ji, Y. Ji, E. H. M. Elageed, G. Gao, *Catal. Commun.* **2016**, *85,* 57.

10) S. Y. de Boer, T. J. Korstanje, S. R. La Rooij, R. Kox, J. N. H. Reek, J. I. van der Vlugt, *Organometallics* **2017**, *36*, 1541.

11) D. Srimani, A. Mukherjee, A. F. G. Goldberg, G. Leitus, Y. Diskin-Posner, L. J. W. Shimon, Y. Ben-David, D. Milstein, *Angew. Chem. Int. Ed.* **2015**, *54*, 12357.

12) A. Mukherjee, D. Srimani, S. Chakraborty, Y. Ben-David, D. Milstein, *J. Am. Chem. Soc.* **2015**, *137*, 8888.

13) P. Daw, S. Chakraborty, J. A. Garg, Y. Ben-David, D. Milstein, *Angew. Chem. Int. Ed.* **2016**, *55*, 14373.

14) P. Daw, Y. Ben-David, D. Milstein, *ACS Catal.* **2017**, *7*, 7456.

15) N. A. Espinosa-Jalapa, A. Nerush, L. J. W. Shimon, G. Leitus, L. Avram, Y. Ben-David, D. Milstein, *Chem. Eur. J.* **2017**, *23*, 5934.

16) A. Kumar, T. Janes, N. A. Espinosa-Jalapa, D. Milstein, *Angew. Chem. Int. Ed.* **2018**, *57*, 12076.

17) A. Kumar, N. A. Espinosa-Jalapa, G. Leitus, Y. Diskin-Posner, L. Avram, D. Milstein, *Angew. Chem. Int. Ed.* **2017**, *56*, 14992.

18) N. A. Espinosa-Jalapa, A. Kumar, G. Leitus, Y. Diskin-Posner, D. Milstein, *J. Am. Chem. Soc.* **2017**, *139*, 11722.

19) L. D. Quin, J. Tyrell, *Fundamentals of Heterocyclic Chemistry: Importance in Nature and in the Synthesis of Pharmaceuticals*, Wiley, **2010**.

20) (a) B. Chen, U. Dingerdissen, J. G. E. Krauter, H. G. J. Lansink-Rotgerink, K. Möbus, D. J. Ostgard, P. Panster, T. H. Riermeier, S. Seebald, T. Tacke, H. Trauthwein, *Appl. Catal. A: General* **2005**, *280*, 17; (b) H.-U. Blaser, C. Malan, B. Pugin, F. Spindler, H. Steiner, M. Studer, *Adv. Synth. Catal.* **2003**, *345*, 103.

21) (a) Z. X. Giustra, J. S. Ishibashi, S. Y. Liu, *Coord. Chem. Rev.* **2016**, *314*, 134; (b) C. Bianchini, A. Meli, F. Vizza, *"Hydrogenation of Arenes and Heteroaromatics"* in *The Handbook of Homogeneous Hydrogenation* (J. G. de Vries, C. J. Elsevier, Eds.), *Vol. 1*, Chap. 16. Wiley-VCH, **2007**.

22) (a) D. L. J. Broere, *Phys. Sci. Rev.* **2018**, *3*, 9; (b) R. H. Crabtree, *ACS Sustainable Chem. Eng.* **2017**, *5*, 4491; (c) P. Preuster, C. Papp, P. Wasserscheid, *Acc. Chem. Res.* **2017**, *50*, 74.

23) (a) A. Moores, M. Poyatos, Y. Luo, R. H. Crabtree, *New J. Chem.* **2006**, *30*, 1675; (b) E. Clot, O. Eisenstein, R. H. Crabtree, *Chem.*

Commun. **2007**, *22*, 2231; (c) R. H. Crabtree, *Energy Environ. Sci.* **2008**, *1*, 134.

24) (a) M. A. Esteruelas, V. Lezaun, A. Martínez, M. Oliván, E. Oñate, *Organometallics* **2017**, *36*, 2996; (b) M. L. Buil, M. A. Esteruelas, M. P. Gay, M. Gómez-Gallego, A. I. Nicasio, E. Oñate, A. Santiago, M. A. Sierra, *Organometallics* **2018**, *37*, 603.

25) (a) D. F. Brayton, C. M. Jensen, *Chem. Commun.* **2014**, *50*, 5987; (b) Z. Wang, I. Tonks, J. Belli, C. M. Jensen, *J. Organomet. Chem.* **2009**, *694*, 2854.

26) For selected examples of heterogeneous catalysts for the reversible dehydrogenation of *N*-heterocycles: (a) C. Deraedt, R. Ye, W. T. Ralston, F. D. Toste, G. A. Somorjai, *J. Am. Chem. Soc.* **2017**, *139*, 18084; (b) S. K. Moromi, S. M. A. H. Siddiki, K. Kon, T. Toyao, K. Shimizu, *Catal. Today* **2017**, *281*, 507; (c) Y. Han, Z. Wang, R. Xu, W. Zhang, W. Chen, L. Zheng, J. Zhang, J. Luo, K. Wu, Y. Zhu, C. Chen, Q. Peng, Q. Liu, P. Hu, D. Wang, Y. Li, *Angew. Chem. Int. Ed.* **2018**, *57*, 11262; (d) J.-W. Zhang, D.-D. Li, G.-P. Lu, T. Deng, C. Cai, *ChemCatChem* **2018**, *10*, 4966.

27) (a) Y. Takagi, S. Teratani, S. Takahashi, K. Tanaka, *J. Mol. Catal.* **1977**, *2*, 321; (b) S. R. Patil, R. V. Chaudhari, D. N. Sen, *J. Mol. Catal.* **1984**, *23*, 51; (c) R. A. Sánchez-Delgado, O. L. de Ochoa, *J. Organomet. Chem.* **1980**, *202*, 427; (d) R. A. Sánchez-Delgado, A. Andriollo, O. L. de Ochoa, T. Suárez, N. Valencia, *J. Organomet. Chem.* **1981**, *209*, 77; (e) J. F. Knifton, *Tetrahedron Lett.* **1975**, *26*, 2163; (f) J. F. Knifton, *J. Org. Chem.* **1975**, *40*, 519; (g) Y. Sasson, J. Blum, *J. Org. Chem.* **1975**, *40*, 1887; (h) J. Tsuji, H. Suzuki, *Chem. Lett.* **1977**, *6*, 1085.

28) Z. Broucková, M. Czaková, M. Capka, *J. Mol. Catal.* **1985**, *30*, 241.

29) (a) A. Toti, P. Frediani, A. Salvini, L. Rosi, C. Giolli, *J. Organomet. Chem.* **2005**, *690*, 3641; (b) A. Toti, P. Frediani, A. Salvini, L. Rosi, C. Giolli, C. Giannelli, *C. R. Chimie* **2004**, *7*, 769; (c) P. Frediani, V. Pistolesi, M. Frediani, L. Rosi, *Inorg. Chim. Acta* **2006**, *359*, 917; (d) S. Komiya, A. Yamamoto, *J. Organomet. Chem.* **1979**, *5*, 279.

30) B. L. Conley, M. K. Pennington-Boggio, E. Boz, T. J. Williams, *Chem. Rev.* **2010,** *110,* 2294.

31) Y. Tsuji, S. Kotachi,K. T. Huh, Y. Watanabe, *J. Org. Chem.* **1990**, *55*, 580.

32) S. Muthaiah, S. H. Hong, *Adv. Synth. Catal.* **2012**, *354*, 3045.

33) J. M. Stubbs, R. J. Hazlehurst, P. D. Boyle, J. M. Blacquiere, *Organometallics* **2017**, *36*, 1692.

34) Q. Wang, H. Chai, Z. Yu, *Organometallics* **2018**, *37*, 584.

35) K.-N. T. Tseng, A. M. Rizzi, N. K. Szymczak, *J. Am. Chem. Soc.* **2013**, *135*, 16352.

36) D. Ventura-Espinosa, A. Marzá-Beltrán, J. A. Mata, *Chem. Eur. J.* **2016**, *22*, 17758.

37) M. Hernández-Juárez, J. López-Serrano, P. Lara, J. P. Morales-Cerón, M. Vaquero, E. Álvarez, V. Salazar, A. Suárez, *Chem. Eur. J.* **2015**, *21*, 7540.

38) J. Morales-Cerón, V. Salazar, A. Suárez. *Unpublished results.*

39) R. Yamaguchi, C. Ikeda, T. Takahashi, K. Fujita, *J. Am. Chem. Soc.* **2009**, *131*, 8410.

40) (a) X. B. Zhang, Z. Xi, *Phys. Chem. Chem. Phys.* **2011**, *13*, 3997; (b) H. Li, J. Jiang, G. Lu, F. Huang, Z.-X. Wang, *Organometallics* **2011**, *30*, 3131.

41) K. Fujita, Y. Tanaka, M. Kobayashi, R. Yamaguchi, *J. Am. Chem. Soc.* **2014**, *136*, 4829.

42) K. Fujita, T. Wada, T. Shiraishi, *Angew. Chem. Int. Ed.* **2017**, *56*, 10886.

43) J. Wu, D. Talwar, S. Johnston, M. Yan, J. Xiao, *Angew. Chem. Int. Ed.* **2013**, *52*, 6983.

44) J. Wu, J. H. Barnard, Y. Zhang, D. Talwar, C. M. Robertson, J. Xiao, *Chem. Commun.* **2013**, *49*, 7052.

45) Á. Vivancos, M. Beller, M. Albrecht, *ACS Catal.* **2018**, *8*, 17.

46) (a) G. E. Dobereiner, A. Nova, N. D. Schley, N. Hazari, S. J. Miller, O. Eisenstein, R. H. Crabtree, *J. Am. Chem. Soc.* **2011**, *133*, 7547; (b) M. G. Manas, J. Graeupner, L. J. Allen, G. E. Dobereiner, K. C. Rippy, N. Hazari, R. H. Crabtree, *Organometallics* **2013**, *32*, 4501.

47) M. G. Manas, L. S. Sharninghausen, E. Lin, R. H. Crabtree, *J. Organomet. Chem.* **2015**, *792*, 184.

48) (a) N. Gorgas, K. Kirchner, *Acc. Chem. Res.* **2018**, *51*, 1558; (b) N. Gorgas, K. Kirchner *"Well-defined Iron and Manganese Pincer Catalysts"* in *Pincer Compounds* (D. Morales-Morales, Ed.), Chap. 2. Elsevier, **2018**; (c) G. Bauer, K. Kirchner, *Angew. Chem. Int. Ed.* **2011**, *50*, 5798; (d) W. Liu, B. Sahoo, K. Junge, M. Beller, *Acc. Chem. Res.* **2018**, *51*, 1858; (e) F. Kallmeier, R. Kempe, *Angew. Chem. Int. Ed.* **2018**, *57*, 46; (f) T. Zell, R. Langer, *ChemCatChem* **2018**, *10*, 1930.

49) S. Chakraborty, W. W. Brennessel, W. D. Jones, *J. Am. Chem. Soc.* **2014**, *136*, 8564.

50) (a) S. M. Bellows, S. Chakraborty, J. B. Gary, W. D. Jones, T. R. Cundari, *Inorg. Chem.* **2017**, *56*, 5519; (b) B. Sawatlon, P. Surawatanawong, *Dalton Trans.* **2016**, *45*, 14965.

51) R. Xu, S. Chakraborty, H. Yuan, W. D. Jones, *ACS Catal.* **2015**, *5*, 6350.

52) (a) H. M. J. Wang, I. J. B. Lin, *Organometallics* **1998**, *17*, 972; (b) J. C. Garrison, W. J. Youngs, *Chem. Rev.* **2005**, *105*, 3978; (c) I. J. B. Lin, C. S. Vasam, *Coord. Chem. Rev.* **2007**, *251*, 642.

53) M. Hernández-Juárez, M. Vaquero, E. Álvarez, V. Salazar, A. Suárez, *Dalton Trans.* **2013**, *42*, 351.

54) (a) Y. Sun, C. Koehler, R. Tan, V. T. Annibale, D. Song, *Chem. Commun.* **2011**, *47*, 8349; (b) E. Fogler, E. Balaraman, Y. Ben-David, G. Leitus, L. J. W. Shimon, D. Milstein, *Organometallics* **2011**, *30*, 3826.

55) (a) A. Anaby, M. Schelwies, J. Schwaben, F. Rominger, A. S. K. Hashmi, T. Schaub, *Organometallics* **2018**, *37*, 2193; (b) A. Eizawa, S. Nishimura, K. Arashiba, K. Nakajima, Y. Nishibayashi, *Organometallics* **2018**, *37*, 3086; (c) H. Salem, L. J. W. Shimon, Y. Diskin-Posner, G. Leitus, Y. Ben-David, D. Milstein, *Organometallics* **2009**, *28*, 4791; (d) M. A. Goni, E. Rosenberg, R. Gobetto, M. Chierotti, *J. Organomet. Chem.* **2017**, *845*, 213.

56) S. Perdriau, M. Chang, E. Otten, H. J. Heeres, J. G. de Vries, *Chem. Eur. J.* **2014**, *20*, 15434.

57) S. W. Kohl, L. Weiner, L. Schwartsburd, L. Konstantinovski, L. J. W. Shimon, Y. Ben-David, M. A. Iron, D. Milstein, *Science* **2009**, *324*, 74.

58) M. J. Hanton, S. Tin, B. J. Boardman, P. Miller, *J. Mol. Catal. A: Chem.* **2011**, *346*, 70.

59) (a) R. Osman, D. I. Pattison, R. N. Perutz, C. Bianchini, J. A. Casares, M. Peruzzini, *J. Am. Chem. Soc.* **1997**, *119,* 8459; (b) R. A. Diggle, S. A. Macgregor, M. K. Whittlesey, *Organometallics* **2004,** *23,* 1857.

60) D. F. Shriver, M. A. Dredzon, *The Manipulation of Air-Sensitive Compounds*, 2nd Edition; Wiley-Interscience, **1986**.

61) D. D. Perrin, W. L. F. Armarego, *Purification of Laboratory Chemicals*, 2nd Edition; Pergamon Press, **1980**.

62) M. C. Perry, X. Cui, M. T. Powell, D.-R. Hou, J. H. Reibenspies, K. Burgess, *J. Am. Chem. Soc.* **2003**, *125*, 113.

63) N. Ahmad, J. J. Levison, S. D. Robinson, M. F. Uttley, E. R. Wonchoba, G. W. Parshall, *Inorg. Synth.* **1974**, *15*, 45.

64) C. del Pozo, M. Iglesias, F. Sanchez, *Organometallics* **2011**, *30*, 2180.

65) José Mª Gordón Pidal, *Trabajo Fin de Grado*. Universidad de Sevilla, **2017**.

Conclusions

1. A series of lutidine-derived CNP (C = *N*-heterocyclic carbene, P = phosphine) pincer-type ligand precursors has been prepared, and used in the synthesis of Pd and Ir complexes. Structural studies of these complexes have shown a considerable ability of the CNP ligands to adopt different coordination modes as a consequence of the flexibility of the six-membered Py–M–NHC chelate ring. Thus, both *fac* and *mer* coordination of the pincer ligand in five- and six-coordinated Ir–CNP complexes have been observed.

2. The M-CNP (M = Pd, Ir) complexes react with bases leading to the deprotonation of either the CH_2-NHC or the CH_2-P methylene bridge that is accompanied of the dearomatization of the pyridine central ring of the CNP ligand. Deprotonated Ir-CNP***** derivatives are able to activate H_2 in a ligand-assisted process providing hydride species that are catalytically active in the (transfer) hydrogenation of ketones in the presence of base (Ir-CNP^{Ph} complexes), and in the chemoselective reduction of aldehydes with H_2 (Ir-CNP^{tBu} complexes).

3. The deprotonated carbonyl Ir-CNP***** complexes **15a** and **15b** are efficient catalytic precursors for the selective hydroboration of CO_2 to methoxy- (with catecholborane) and formoxyborane (with pinacolborane). In these processes, a significant influence of the presence of small amounts of water on the rate of the catalytic reactions has been observed. Thus, TOF values of up to 58 h^{-1} in the reduction of CO_2 to methoxyborane with HBcat, and up to 1245 h^{-1} in the hydroboration to the formate level using HBpin have been achieved after optimization of the water content of the reactions. Moreover, NMR spectroscopy and MS analyses of the catalytic reactions have shown the formation, as the sole observable species, of Ir-CNP derivatives resulting from the oxidative addition of the hydroborane to $[Ir(CNP)(CO)][B(R_2)_2]$ (R_2 =

catechol, pinacol) complexes. Control experiments, however, have ruled out a significant participation of these species in the hydroboration reactions.

4. The synthesis of Ru complexes **4** incorporating lutidine-derived CNN(H) pincer ligands (C = *N*-heterocyclic carbene, N(H) = secondary amine) that have two potentially metal-ligand cooperation modes have been accomplished using Ag-CNN(H) complexes (**3**) as carbene transfer reagents. Use of Ru-CNN(H) complexes **4** in the presence of base lead to catalytically active species in the hydrogenation of a series of diverse *N*-heteroarenes and in the acceptorless dehydrogenation of the corresponding saturated *N*-heterocycles.

5. The acid-base reactivity of the Ru-CNN(H) complex **4a** has been explored. Addition of base (KHMDS or KO^{t}Bu) to solutions of **4a** produces the deprotonation of the methylene bridges as well as of the amino donor group, leading to the formation of mono- (complex **8**) and di-deprotonated (complex **9**) ruthenium species. Moreover, heating of these solutions provides the formal Ru(0) complex **10**. Control experiments suggest that this Ru(0) species is directly involved in the catalytic hydrogenation of *N*-heterocycles.